Winegrowing Futures

Final report

Theme 3

Multiseasonal impacts on vine productivity and grape composition











The National Wine and Grape Industry Centre is a research centre within Charles Sturt University in alliance with the Department of Primary Industries NSW and the NSW Wine Industry Association

Contents

Abstract 1

Summary 1

Background 2

Aims 3

Experiments 4

Experiment 3.1 Seasonal vine nutrient dynamics and distribution of Shiraz 4
Materials and methods 4
Results and discussion 5

Experiment 3.2 Vine nutrient reserves, rootstocks and root dynamics 9
Materials and methods 9
Results and discussion 11

Experiment 3.3 Vineyard inputs and leaf removal on vine reserves and root dynamics 17
Materials and methods 17
Results and discussion 18

Experiment 3.4 Timing of N application and water stress on shoot and berry development 24
Materials and methods 24
Results and discussion 25

Experiment 3.5 The net carbon balance in relation to growth and biomass accumulation of *Vitis vinifera* cv. Semillon vines 28
Materials and methods 28
Results and discussion 29

Experiment 3.6 Effects of fruiting on vegetative growth and development can be traced back to events at or before budbreak 34
Materials and methods 34
Results and discussion 35

Experiment 3.7 Heat stress affects flowering, berry growth, sugar accumulation, and photosynthesis 42
Materials and methods 42
Results and discussion 43

Experiment 3.8 Shoot architecture, growth and development dynamics of *Vitis vinifera* cv. Semillon vines grown with and without shade 49
Materials and methods 49
Results and discussion 49

Experiment 3.9 Reductions in biomass accumulation, photosynthesis *in situ* and the net carbon balance are the costs of protecting *Vitis vinifera* cv. Semillon grapevines from heat stress 56
Materials and methods 56
Results and discussion 57

Experiment 3.10 Technetium scintigraphy in plants **66**
Materials and methods 66
Results and discussion 67
Experiment 3.11 Xylem connections between the bunch and leaves **75**
Materials and methods 75
Results and discussion 75
Experiment 3.12 Berry oxygen isotope ratios **81**
Materials and methods 81
Results and discussion 82
Experiment 3.13 Susceptibility to fruit splitting **86**
Materials and methods 86
Results and discussion 87
Outcomes/conclusions **95**
Technetium scintigraphy 97
Xylem connections between the bunch and leaves 97
Berry oxygen isotope ratios 98
Fruit split 98
Theme outcomes 99
Theme outputs 99
Theme milestones 99
Recommendations **100**
Appendices **102**
Appendix 1 Communication **102**
Appendix 2 Intellectual property **105**
Appendix 3 References **106**
Appendix 4 Staff **115**
Appendix 5 Other relevant material **116**
Appendix 6 Budget reconciliation **117**

THEME 3: Multiseasonal impacts on vine productivity and grape composition

Abstract

The outcomes of Theme 3 fall within three main categories. Firstly, the project enhanced our understanding of the nutrient and carbohydrate reserve dynamics on root growth and vine perenniality in order to better target vineyard management. Secondly, the project developed methods that improved our understanding of assimilate and water movement through vines and bunches. Finally, the project determined the effects of selected climatic influences, including heat stress, on vine and berry development and growth.

Summary

Research in this theme has improved our understanding of seasonal nutrient dynamics in the perennial structure and the allocation to different organs of grapevines. This work showed the seasonal nutrient requirement by the annual growth and the importance of the perennial structure to provide nutrients to the early canopy development and, to a lesser extent to the reproductive development. The intra-seasonal changes have been assessed in two Shiraz trials, indicating the variation of the nutrient reserve pool between years. In addition, the work suggests that the nutrient reserves differ between rootstocks and can be altered by water and N supply. The relationship between root dynamics, nutrient accumulation and vine reserves was inconclusive and this requires further research.

Furthermore, findings have identified future research directions and a proportion of the data can be utilised for further work. These existing data on nutrient acquisition and reserve mobilisation can be utilised to enhance the timing and amounts of nutrient application, with the potential of integration into a grapevine model. However, the importance of nutrient supply from uptake or storage for early canopy growth and the acquisition of nutrients during berry development on berry composition will require further experimentation.

The project has further determined the importance of the roots as a storage organ, with its accumulated nutrients showing significant seasonal changes and between seasons. These dynamics are driven by the partitioning of the grapevine and the root environment, with factors such as soil temperature, water and nutrient supply. The understanding of the response of grapevines in relation to nutrient acquisition to the range of vine root environments relevant to current and future climatic trends is crucial. The predicted climatic changes will be reflected in the above and below ground environment and is important to understand the nutrition equitation and utilisation under various conditions for sustainable grape production. The future research on nutrition needs to integrate the soil processes, since they strongly contribute to the availability of nutrients for vine development and ultimately for the characteristics of grapes produced from a particular vineyard in a wine region.

The research undertaken in this study has demonstrated in one grapevine variety that the vine is unable to protect itself from regularly occurring heat events and vineyard intervention is needed to protect the flowers and berries from the heat. While hydrocooling may provide a solution in some locations, it may not be feasible where water is in short supply and/or expensive. Similarly, the infrastructure for hydrocooling required may also be expensive. However, the value of the crop will be a key determinant of the value of this protection method and wider discussion of this research is warranted. This is a potential priority area for extension, particularly to develop a case study to examine the economics of hydrocooling and potential application in vineyards.

Other practical solutions include interrow planting and a detailed study of the temperature profile in vineyards with and without interrow planting is required. The recent development of infrared radiometers used in this research to monitor canopy temperatures are ideal for a study of the temperature profile in the vineyard.

The theme has demonstrated that scintigraphy is an excellent tool for research into xylem transport through grapevines Because it is non-destructive, scintigraphy provides significantly improved data quality in a more efficient and reproducible manner for the exploration of time-related changes in plants. Currently accessibility to equipment and expertise are

factors limiting the wide-spread use of scintigraphy in plant physiology research, however this will be gradually overcome as gamma cameras are placed into plant research facilities.

Experiments using dye and pertechnetate ($^{99m}TcO_4^-$) revealed that bunches bearing unripe berries have strong xylem connections with primary leaves located on the same side of the shoot as the bunch. These connections are also strong with secondary shoots arising from axillary buds on the same side of the stem as the bunch. This research is one of the first to identify functional xylem connections between the grapevine bunch and lateral shoots, a phenomenon that likely affects the development of the bunch. This necessitates modification of current models predicting nutrient exchange between the shoots and bunches of the grapevine. Further research on the nutrient storing cells at nodes within shoots is warranted to understand how and when nutrients are released to the bunch.

The analysis of oxygen isotopes in organic matter ($\delta^{18}O_{OM}$) should be considered a potential tool for identifying the relative contribution of root carbohydrate reserves and current photosynthesis to dry matter accumulation in organs such as the pre-veraison grape bunch. The $\delta^{18}O_{OM}$ values of berries at physiological maturity, expressed relative to the same value early in the ripening period (i.e. $\delta^{18}O_{OM}$), should be explored as a proxy measure for between-cultivar comparisons of leaf stomatal conductance. To underpin the application of the technique, future research should confirm the oxygen isotopic composition of important carbohydrate pools, such as sugars hydrolysed from root starch, synthesised by leaves and accumulated by grape berries.

The decrease in susceptibility of Shiraz berries to splitting was found to diminish after about 100 days after anthesis and this can likely be applied to other seed grape varieties. When predicting the likelihood of splitting, all other factors being equal, early ripening cultivars are expected to become less susceptible to splitting before later ripening ones. Importantly, our study indicated that bunch age (days after the onset of ripening) is a more reliable indicator of susceptibility to splitting than berry ripeness per se, as determined by soluble solids concentration.

Background

This theme addresses physiological stresses that have a lasting influence on variability of grapevine yields and berry quality over several seasons. The research team will focus on the role of nutrients and assimilates on root dynamics and grape yield and also on the impacts of heat stress on berry composition. Research into the vascular transport processes will underpin both approaches aimed at managing variability in grape yield and composition.

Changes in nutrient and carbohydrate reserves over the growing season are important for vine growth and development. For grapevines, root and wood reserves are particularly required for early canopy development. Soil conditions, especially water and soil temperatures, impact on mobilising these reserves for translocation to the aerial parts of vines. Messages from roots and movement of reserves are both transported by the vascular system, and therefore, directly influence the resource allocation across the vine. Uptake of nutrients (macro and micro) and accumulation of carbohydrate reserves in a growing season are also influenced by internal (source–sink relationships) and external (climate, management) factors and both impact in the current season and on the next year's vine performance (perenniality). This performance dictates not only vine vigour but also reproductive capacity, final yield and grape composition.

Grower observations suggest heat during grape maturation cause sugar accumulation to stop in berries of Semillon, Shiraz and some other varieties. This is indicated by the berries becoming flaccid and bunches having retarded ripening between veraison and harvest. Berry size and composition are likely to be affected. Both are dependent on flow of water, nutrients and assimilates from the vine to the bunch. Continuity of vascular connections is, therefore, crucial for sugar transport into the bunch. The impact of heat and other stresses on these processes remains relatively unknown. Vines also appear to be slow to recover, suggesting the heat stress affects the whole vine possibly through the vascular transport processes. This also suggests impacts of heat stress could persist across several seasons through effects on nutrient and carbohydrate reserve accumulation.

The transport of the nutrients and assimilates around the vine and to the bunch are crucial processes supporting berry and vine growth. Phloem and xylem tissues supply assimilates and nutrients to

sinks with different demands during vine and bunch development. Understanding the communication between the processes of reserve mobilisation, assimilate production and nutrient acquisition is limited. This is an important knowledge gap because resource allocation drives the development of the different parts of the vine. A greater understanding of these physiological processes will improve ability to manage seasonal and annual variability in yield and berry composition and ultimately wine flavours.

Overall this theme will, therefore, lead to more consistent and stable grape production throughout Australia.

Aims

The aims of this theme were to:

1. Enhance understanding of the nutrient and carbohydrate reserve dynamics on root growth and vine perenniality.
2. Determine effects of selected climatic influences on vine and berry development and growth.
3. Improve knowledge of assimilate and water movement through vines and bunches.
4. Optimise targeting of vineyard nutrient applications, and ameliorate environmental stresses to enhance vine performance and improve berry composition.

Experiment		Aim/s Addressed
3.5.1	Seasonal vine nutrient dynamics and distribution of Shiraz	1 and 4
3.5.2	Vine nutrient reserves, rootstocks and root dynamics	1 and 4
3.5.3	Vineyard inputs and leaf removal on vine reserves and root dynamics	1 and 4
3.5.4	Timing of N application and water stress on shoot and berry development	4
3.5.5	The net carbon balance in relation to growth and biomass accumulation of *Vitis vinifera* cv. Semillon vines	2
3.5.6	Effects of fruiting on vegetative growth and development can be traced back to events at or before budbreak.	2
3.5.7	Heat stress affects flowering, berry growth, sugar accumulation, and photosynthesis	2
3.5.8	Shoot architecture, growth and development dynamics of *Vitis vinifera* cv. Semillon vines grown with and without shade	2
3.5.9	Reductions in biomass accumulation, photosynthesis *in situ* and the net carbon balance are the costs of protecting *Vitis vinifera* cv. Semillon grapevines from heat stress.	1 and 2
3.5.10	Technetium scintigraphy in plants	3
3.5.11	Xylem connections between the bunch and leaves	3
3.5.12	Berry oxygen isotope ratios	3
3.5.13	Susceptibility to fruit splitting	3

Experiments

Experiment 3.1
Seasonal vine nutrient dynamics and distribution of Shiraz

Materials and methods

The nutrient reserves in grapevine perennial structure perform a critical role in supplying grapevine with nutrients under conditions of insufficient nutrient uptake by the roots. The seasonal changes in these reserves largely depend on the developmental stage and the associated growth requirements of grapevines. These stored reserves are influenced by environmental conditions and certain vineyard management practices, such as production levels, water supply and canopy status, these stored resources contribute to the productivity level within and between seasons.

The grapevine stores a substantial amount of nutrients in the perennial structure after leaf fall, for N the amounts can vary between 10–75 g vine^{-1} (Löhnertz *et al.* 1989, Treeby and Weatley 2006), being influenced by environmental and management factors. Other Macro nutrients are not often reported on, with K and Ca present in similar ranges per vine and P and Mg are present in a few grams in Pinot Noir (Schreiner *et al.* 2006). In the warmer climates a substantial amount of N is taken up after harvest and provides 60% of the stored N for the following season (Condradie 1992), although the majority of nutrients is taken up from bloom and veraison, except P is taken up predominantly prior bloom (Schreiner *et al.* 2006). The stored of N together (and carbohydrate) reserves are required to support shoot growth in the following spring (Conradie 1992; Zapata *et al.* 2004), other nutrients could be equally important for the next season's growth (Tromp 1983). However, the different mobility of each nutrient determines the accumulation and mobilisation from the perennial structure.

This section of the project was aimed to assess the nutrient uptake and portioning of nutrition in a major wine variety grown in Australia. For this purpose whole vines were excavated numerous times over the growing season to determine the key uptake periods of the nutrients and to understand some of the mobilisation patterns during a season. Such a study has previously not being undertaken on winegrapes in Australia and could provide further information for the optimisation of fertiliser application for vine productivity and grape composition. The work was undertaken in conjunction with staff and resources from a recently completed project focusing on grapevine carbohydrate dynamics, allowing to investigate both nutrient and carbohydrate reserve dynamics.

Site details

The own-rooted Shiraz grapevines (clone PT23) utilised for the trial was located at the Charles Sturt University vineyard (35°03'38"S, 147°21'50"E). Wagga Wagga is a hot and semi-arid area with a mean January temperature of 24°C and average annual rainfall of 572 mm. The Shiraz vines were planted in 1998, trained to a single bilateral cordon, mechanically pruned (with a hand clean up) and harvested. Vine and row spacing is 2 and 3 m respectively. The vineyard is drip irrigated, in the 2007–08 season the vineyard received approximately 3.5 ML ha^{-1} of irrigation or rainfall, and carried a yield of 14.6 t ha^{-1}.

Vine excavations

The trunk circumference of all vines in the 1.1 ha trial area were measured during winter in 2007, and 44 uniformly sized vines were selected allowing 11 excavation dates with four replicates. The excavation began prior to bud-burst (21 August, 2007) and the last one was after leaf-fall (29 May, 2008); nine dates in between were 20 September, 17 October, 14 November, 13 December, 9 January, 6 February, 3 March, 2 and 30 April. The procedure at each excavation was as follows: the above ground section the vine was cut off and separated into different parts, with the number of tissues varying with the destructive harvest dates. Prior to bud-burst this was trunk, cordon, cordon arm and spurs and after leaf fall also canes, while during the season shoots, leaves and inflorescences/bunches were also separated. All of the wood was cut into smaller pieces, representative sub-samples collected, and washed. The procedure for the annual tissues was similar, but did not require the cutting into small pieces in all occasions. The sub-samples were then freeze dried for later analysis, and the dry weight recorded. The remaining wood and annual tissue was oven dried at 70°C, and the dry weight also recorded, with various tissues requiring different length of time for the drying process.

The below ground section of the vines were obtained on the same day, when wood samples were collected. The area allocated to each vine (6 m^2) was marked out and than excavated with a backhoe to a depth

of 80 to 100 cm (*Figure 3.1*). Deeper excavation was prevented due to high density sub-soils and the size of machinery and only the occasional root was detected below the excavation depth. After each excavation the majority of large roots and the rootstock were immediately collected and placed in a cool room. Over the next three days the soil from the four vine excavation sites was manually sieved through 10 x 10 mm mesh to remove all remaining roots. All of the roots from each vine were then separated into three size classes which corresponded approximately to the diameter range of the main structural roots (large >7 mm), secondary roots (medium 3 to 7 mm), and tertiary roots (small <3 mm). On the basis of random measurements made after the roots from each vine were separated, the average diameter in each class 10.7, 4.0 and 1.1 mm, respectively. The method of excavation did not allow to include any of the new seasons fine root growth, as these were either too fine to be caught in the sieve, or too delicate to survive the excavation process. After separation into the three size categories, the roots were sub-sampled and dried as described for the wood.

Nutrient analysis

For the nutrient analysis the tissue samples were ground trough a 0.12 mm using a heavy duty cutting mill (Retsch ZM2000, Haan, Germany), and then an ultra-centrifugal mill (Retsch ZM100). Total N was determined on a 50 mg subsample with a VarioMAX combustion analyser (Elementar, Hanau, Germany), and other nutrients with an inductively coupled plasma-optical emission spectrometer (ICP-OES) (ARL 3580B, Applied Research Laboratories, Ecublens, Switzerland) on a 300–400 mg sub-sample.

Results and discussion

The information collected during this trial has created a significant data set on whole vine nutrient concentrations and content, and together with association of growth and biomass accumulation, photosynthesis, canopy light interception, and berry development data, will provide a basis for ongoing work on vine nutrition and vine carbon balance. For this report the concentration and content of six macro nutrition for perennial tissues at all eleven excavation dates are presented (*Figure 3.2 and 3.3*). As being expected the seasonal changes of nutrients are both concentrations and amounts a most pronounced in the annual parts of vine. The inflorescences/



Figure 3.1 Beginning and progressed excavation of a Shiraz grapevine in the CSU vineyard (August 2007) to determine whole vine nutrient reserve distribution in the perennial structure.

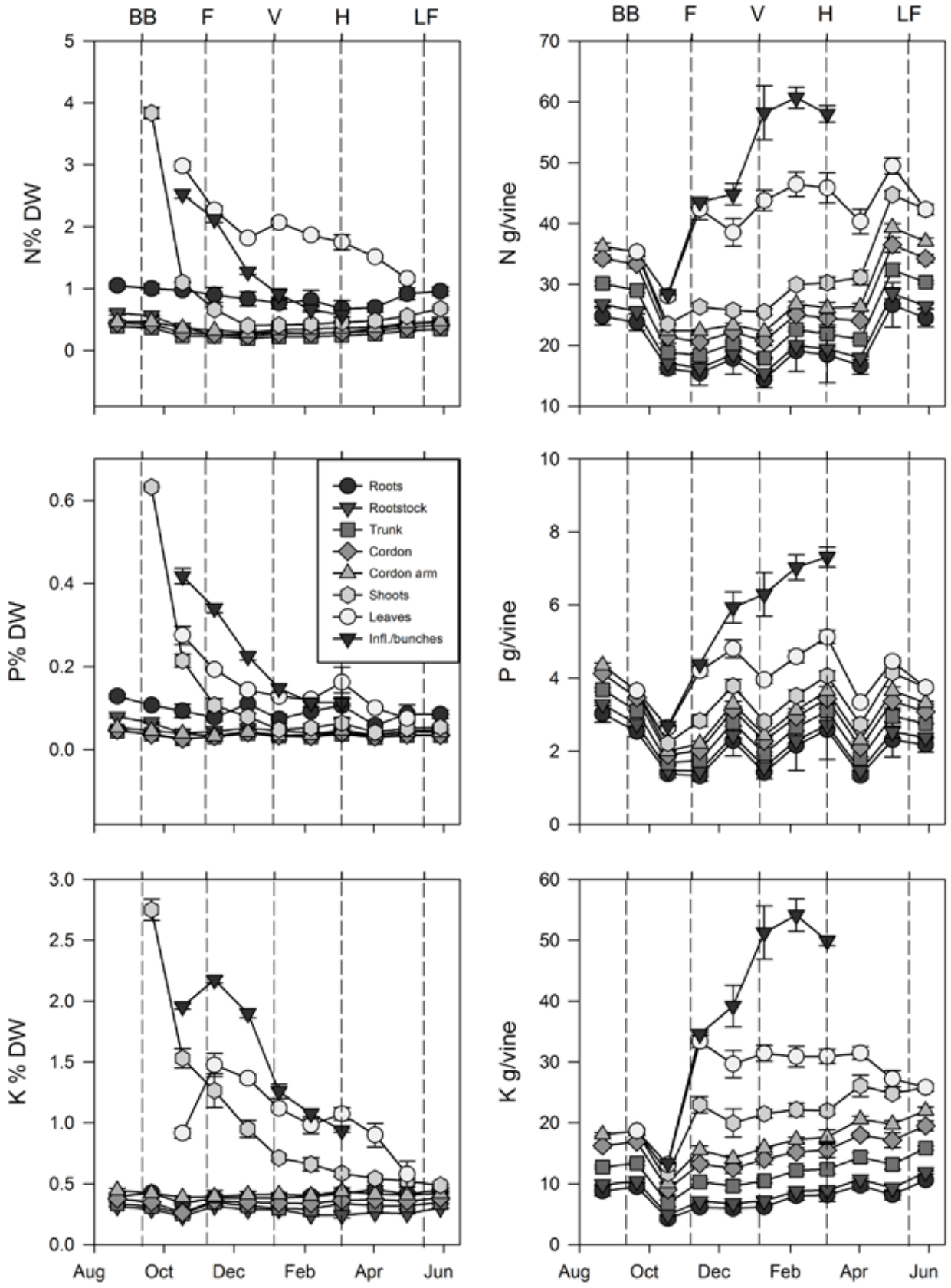


Figure 3.2 Seasonal changes in N, P and K concentrations (left) and contents (right) in the different parts of Shiraz grapevines during the 2007–08 season. The key developmental stages are indicated for bud-break (BB), flowering (F), veraison (V), harvest (H) and leaf-fall (LF). Standard errors are indicated as bars below and above the mean.

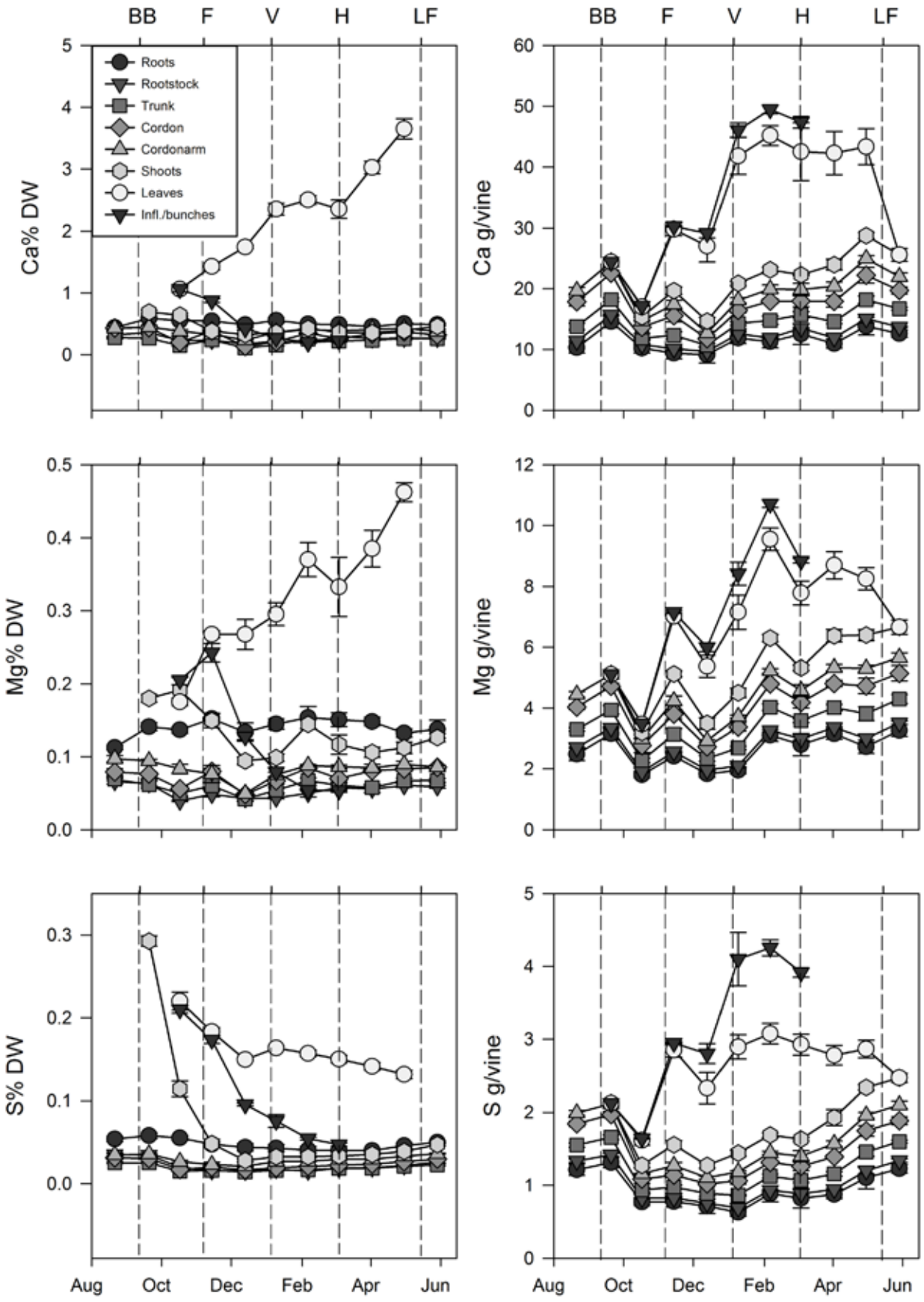


Figure 3.3 Seasonal changes in Ca, Mg and S concentrations (left) and contents (right) in the different parts of Shiraz grapevines during the 2007–08 season. The key developmental stages are indicated for bud-break (BB), flowering (F), veraison (V), harvest (H) and leaf-fall (LF). Standard errors are indicated as bars below and above the mean.

bunches show a decline in all nutrients, while the amounts per vine creases towards harvest. However, leaf concentrations decline also during the season for four nutrients, with Mg and Ca increasing until leaf-fall. Therefore the amounts of these nutrients are highest after harvest, while for the other nutrients occurring pre-harvest. All nutrient concentrations in shoots decline rapidly until flowering or veraison, with Ca only minor changes occur in the shoots. Content per vine is highest for NPK around bloom, while for the other thee nutrients the maximum is reached prior leaf-fall. The concentration changes of the perennial structure are relatively small, with decline in spring and replenishment during the season. However, the total amount of macro nutrients changes sustainably during the growing season, with 50% or more allocated to the below ground reserve sections of the vine early and late in the season. These results indicated the enormous buffer capacity of the perennial structure, providing the annual organs with sufficient nutrients when the supply is limited. The vines total nutrient content is highest prior harvest, being highest for N 60 g and lowest for S with about 4 g vine^{-1}, being 100 and 6.5 kg S ha^{-1}, respectively. For most nutrients more than half is located in the annual organs, with the majority in the leaves except for K, therefore the removal of this nutrient is the highest from the vineyard system.

Seasonal nutrient concentrations

The concentrations of N are generally the highest compared to the other nutrients. The annual organs starting with high concentrations in spring, with the leaves 2.5% and inflorescences with 3%, only the emerging buds are higher with nearly 4% DW. Both bunches at harvest and leaves prior leaf-fall declined to about 1% DW, shoots regain N concentration at the end of the season and finish with an N concentration of 0.7% DW. Both below and above ground parts decline during the season, the concentrations are at least double in the roots and the other section of the perennial structure. At the end of the season the concentration largely regain the levels prior bud-burst. The changes for both perennial and annual sections are similar for P and K, while this is only for the reserve tissues for K, Ca an Mg as well. However, the concentrations vary with K and Ca slightly below 0.5% DW, Mg concentrations are below 0.1% and S below 0.5% DW. The K concentrations are highest shortly after bloom for both bunches and leaves, with 2.2% and 1.5% respectively. At harvest the concentrations have declined to 1% in the bunches and just over 0.5% in the leaves prior leaf-fall. The concentration changes of P and S decline from early spring towards the end of the season similar to N, but as much lower levels. In contrast the nutrients Ca and Mg increase substantially in the leaves, Ca from 1 to 3.7% and Mg from 0.18 to 0.46%. While the Ca concentration is highest in the inflorescence with 1.5%, Mg has the concentration peak with 0.25% into the bunches after flowering. The decline in spring of nutrient concentration in the perennial structure indicates the mobilisation from theses tissues for the support of the annual growth and development, while the accumulation of Ca and Mg in the leaves indicates the poor redistribution of the nutrients into the perennial structure. Both observations are more demonstrated in the dynamic of nutrient content on whole vine basis.

Nutrient accumulation

During the gowning season the grape accumulates considerable nutrients in the growth, which is supplied mostly from new nutrient acquisition, but also from reserves located in the roots and the wood. N The N reserves in this study are 36 g vine prior bud burst, which is about half on other work reported from Australia on Sultana (Wheatly and Treeby 2006) but similar to research undertaken on Pinot Noir in Oregon (Schreiner *et al.* 2006) or on Concorde (Pradubsuk and Devonport 2010). The N content of the perennial structure declines considerable until around flowering, with a sharp increase only after harvest. In this study the decline of N between bud-burst and flowering in the root and wood tissues appear to have been at least half been mobilised for growing new roots, which we were mostly not able to collect during the destructive harvests. The majority of the N uptake was occurring four weeks before flowering and four week before veraison, with another significant uptake taken four weeks after harvest. The decline in N directly after harvest might be again the fine roots we could not account for. At harvest the annual growth contains more than half the N of the vine, with grapes being 12 g vine^{-1} or 20 kg N ha^{-1}. Most of the annual N is in the leaves and the least is in the shoots, both amounts will be available to the vine after decomposition after leaf-fall and pruning. However, the findings indicate that some of the N in the leaves has been already moved into the shoots and the perennial structure as reported in earlier studies (Conradie 1981). The N in the crop is usually removed from the vineyard system and needs to be replaced by fertiliser or appropriate cover crops.

All nutrients show a pattern of decline and replenishment in the root sand wood tissues and most nutrients are taken up mostly in the four weeks prior flowering and bloom. Mg is also strongly accumulated four weeks after veraison, while P is taken predominantly taken up and accumulated four weeks before and after flowering. Both these nutrients are also further accumulated in the post-harvest period, Mg in the first weeks after harvest and P in the later part, both following a decline prior to this accumulation. The amounts of nutrients allocated to the perennial structure and annual parts varies between the nutrients, but most important is the removal by the crop being highest for K with 19 g vine, followed by Ca with 4.8 g, P with 2.2 g, S and Mg with about one gram each. Re-mobilisation from the leaves in to the perennial structure and shoots appears not be taken place for Ca, but also for Mg. Both have been described as taken up after harvest, but the accumulated nutrients are lost to the vine by leaf fall. As for N the nutrients remaining in the leaves and shoots are recycled in the vineyard system over time after leaf-fall and pruning.

Conclusion

This research was undertaken on 12-year-old own rooted Shiraz grapevines excavated from an irrigated hot climate vineyard shows the nutrient concentrations and content over a growing season for all macro nutrients. The study demonstrated the decline of nutrient in the root and wood tissue, the utilisation of these mobilised nutrients for the annual growth and development and the replenishment towards the end of the season. The amount accumulated during the growing season at harvest is most pronounced for K, Ca and N with a range between 22 and 32 g per vine, while for the nutrients P, Mg and S the amount is between 2 and 6 g. However, further accumulation occurs after harvest in the annual and perennial structure for more or less for all macro nutrients. This is a period to replenish the reserve tissue to the level of the start of the season, indicating that the total uptake is higher than just the amount accumulated at harvest. The main periods of nutrient uptake are four weeks before flowering and also before veraison, with P having a uptake four weeks before and after bloom, while Mg is significantly taken up also four weeks after veraison. The reason behind this difference in uptake is not clear at this point of time, but the increase in P accumulation after bloom is in the developing bunch, while for Mg this accumulation is dominantly in the roots. However the accumulation pattern indicates that nutrient supply is important generally prior to bloom and veraison for the annual parts and after harvest to replenish the reserves if required. The following section will assist in understanding the nutrient dynamics over a longer period, since this excavation experiment was only conducted over one season due to the significant resources required.

Experiment 3.2
Vine nutrient reserves, rootstocks and root dynamics

Materials and methods

Vine nutrient reserves are altered by the uptake of nutrients by the roots, which vary throughout the growing season and between rootstocks. These differ in the extent of their root systems and therefore their access to nutrients in the soil. In addition, rootstocks influence the biomass and carbohydrate allocation between roots and the rest of the vine.

The uptake of nitrogen and other nutrients varies between rootstocks (May 2004) and the response in N uptake to the amounts of N applied to a vineyard differs (Holzapfel and Treeby 2007). The variation in mineral uptake by rootstocks can directly influence the nutrient status of the scion; being reflected in the petiole and berry concentrations of N, K and other minerals (Holzapfel and Treeby 2007; Whiting 2004). Vines grafted on certain rootstocks with the highest concentration of nitrogenous compounds in leaves and fruit also have generally the greatest growth (Kliewer 1991). The effect of high scion vigor is usually strongly correlated with high yield and a more extensive root system (Roberts and Blazer 1993). This rootstock effect on scion growth and yield can be greater than the effects of N fertilization (Wolf and Pool 1988). Rootstocks can also alter the N concentration in the roots and canes (Williams and Smith 1991), total carbohydrate content of their roots and the biomass partitioning of the vine (Smith 2004; Sommer and Clingeleffer 1996).

Nutrient uptake varies during the growing season concurrent with root growth activity, which is generally high when the growth demands from other parts of the vine is low, such as shoots and grapes. Nutrient reserves in the permanent structure are highest in winter (Conradie 1980, 1981), but can be influenced by cropping levels (Balasubrahmanyam *et al.* 1978), vineyard management and environmental conditions. The stored N is important because early demand in spring cannot be guaranteed by root

uptake (Zapata *et al.* 2004), other minerals such as P and K could be equally important (Sánchez-Alonso and Lachica 1987). Generally, there are two main periods of nutrient uptake, the first being after rapid shoot elongation ceases and the second after harvest (Van Zyl 1984). This leads to further uptake of N and other nutrients during the post-harvest period, significantly contributing to the vines mineral reserves for the next season (Bates *et al.* 2002; Conradie 2005). During these two most efficacious periods of nutrient uptake excess carbon supply is available to the roots.

Carbohydrate reserves also vary between parts of the vine; roots have been reported to have much higher levels than other parts of the perennial structure (Uys and Orffler 1983). The carbohydrate content is highest in winter (Sommer and Clingeleffer 1996) and the majority is stored as starch with the sugars consisting mostly of glucose, fructose and sucrose (Jones *et al.* 1999). As with nutrient reserves, the stored carbohydrates are important for early shoot development, with a mobilization maximum at the six to eight leaf stage (Yang and Hori 1979). With fruit set, the berry starts to become the major sink and after veraison a dominant sink (Koblet 1969). The mobilization of reserves from the permanent structure only occurs if supply of assimilates to the fruit is insufficient due to stress conditions (Candolfi-Vasconcelos *et al.* 1994), or if the crop load is beyond the capacity of the vine (Balasubrahmanyam *et al.* 1978). Storage of assimilates for future requirements in the following seasons (Miller *et al.* 1997) and the supply of carbohydrates to root growth (Candolfi-Vasconcelos *et al.* 1994) are also important carbon-requiring processes.

Root growth is most pronounced in two periods during the growing season; between bloom and veraison and after harvest. The first flush of root growth peaks between bloom and veraison (Van Zyl 1984) with nutrient demand of vines also increases during this period. In the irrigated, warmer grape growing regions the photosynthetic activity after harvest is important for the second major flush of roots (Van Zyl 1984) and for further nutrient uptake (Bates *et al.* 2002; Conradie 1980, 1981). Recent work has shown that root growth activity can vary between seasons, pruning systems and water supply (Comas *et al.* 2005). Minimal pruned vines showed earlier root production compared to heavily pruned vines, indicating a strong link between carbohydrate availability and root growth. The carbohydrate movement to the roots is high during the root growth flushes. Limited nutrient availability conditions can initiate further root growth, requiring more carbohydrates. The process of nutrient uptake can also increase under such conditions and would require further energy inputs for nutrient uptake (Lambers *et al.* 1995). Soil nutrient availability and demand from other parts of the vine for assimilates can determine the carbohydrate allocation to the roots.

This work is being conducted to investigate the influence of rootstocks on nutrient and carbohydrate reserves, and to determine the seasonal root activity of Shiraz grafted onto different rootstocks. The study attempts to assess links between nutrient and carbohydrates reserves and root activity of different rootstocks.

Vineyard and vines

The study was conducted in a Shiraz vineyard over the 2007–08 growing season, located at the CSU Winery, Wagga Wagga, NSW Australia. Wagga Wagga is a hot and semi-arid area with a mean daily January temperature of 24°C and average annual rainfall of 572 mm. The Shiraz vines and rootstocks were planted on red Kandosol overlaying coarse granite in 1998 with 3 m row spacing and 2 m between vines. In the following spring (early December) the scion Shiraz was chip grafted on the different rootstocks, including Shiraz on own roots. The drip irrigated vines were trained to a single bilateral cordon, and spur pruned by hand following mechanical pre-pruning. For this work, four two-vine replicates of own-rooted Shiraz (*V. vinifera*) and the three rootstocks Ramsey (*V. champinii*), Schwarzmann (*V. riparia* x *V. rupestris*) and Ruggeri 140 (*V. berlandieri* x *V. rupestris*) were used.

Nutrient analysis

Wood samples consisting of cordon and trunk were taken as drillings four times during the year (bud-burst, flowering, veraison and harvest); root samples were taken at the same time by collecting roots with a diameter of approximately 5 mm. The tissue samples were dried at 70°C and ground through a 0.12 mm sieve (Retsch ZM100, Retch GmbH, Haan, Germany). Total N content of the tissues was determined with a total combustion gas chromatograph using a 50 mg sub-sample (Vario Macro, Elementar, Hanau, Germany). The other macro nutrient (P, K, Ca, Mg and S) analysis was undertaken with an inductively coupled plasma optical emission spectrometer (ICP-

OES) (ARL 3580B, Applied Research Laboratories, Ecublens, Switzerland) on a 300–400 mg sub-sample.

Carbohydrate analysis

For analysis of non-structural carbohydrates a 20 mg sub-sample of each tissue above was weighed, and soluble sugars extracted with 80% ethanol at 80°C. The concentration of sugars were determined with enzyme assays (MEGAZYME International Ireland Ltd, Bray, Ireland) and a plate reader at 340 nm (μQuant, Bio-Tek Instruments Inc., Vermont, USA). After extracting soluble sugars with 80% ethanol the remaining starch in the wood and root samples were solubilised with dimethyl sulphoxide. Starch concentrations were determined by colorimetric assay for released glucose after enzymatic digestion with α-amylase and amylglucosidase (MEGAZYME International Ireland Ltd, Bray, Ireland). The released glucose concentrations were determined at 510 nm using the same plate reader as above. The concentrations of sugars and starch were used to calculate the total concentration of carbohydrate reserves in the root and wood tissues.

Root activity

A minirhizotron system was used to allow frequent root observation during the growing season of the major part of the root-zone. For this non-destructive method two polycarbonate tubes (1 m length) were installed in the vine row at a 30° angle in each plot shortly after harvest in 2007 for miniature camera system access (Bartz Technology, Santa Barbara, CA, USA). A number of images (50) throughout the length of the tube were taken every second week during the growing season from end of August to end of May to a soil depth of 60 cm, during winter the images were collected every four weeks. The total length of white roots was calculated for each tube using specifically designed software (Rootfly) to determine seasonal root activity (*Figure 3.4*).

Data analysis

The data were compiled and manipulated in Excel 2003 and further analysed using the graphic program Sigma Plot (Version 11.0). The statistical analysis was conducted using Genstat, Release 11.1 (Rothhamsted Experimental Station, Harpenden, Herts, United Kingdom). Analysis of variance and Fisher's LSD test was used to interpret differences in means at $P < 0.05$.

Results and discussion

The performance of Shiraz on the three rootstocks (Ramsey, Schwarzmann and Ruggeri 140) and own roots was similar, although Ruggeri 140 had the lower yield and Shiraz the highest with the pruning weights being the reverse. However, differences were observed for N and carbohydrate reserves at key staged in the perennial structure (roots, wood), other nutrients determined at bud-break were also influenced by the rootstock. The monitored root dynamics showed seasonal and intra-seasonal variation with some indication of rootstock influence.

Nutrients

The nutrient concentrations were much higher in the root tissue than in the wood, and the differences between rootstocks were also more pronounced in the root tissues (*Table 3.1*). At bud-burst 2007 own rooted Shiraz had the lowest wood N concentrations, while Ruggeri 140 was highest and the other rootstocks in between. Significant differences in the scion wood tissues were also present for Mg, Ramsey and Ruggeri 140 had significantly higher concentration than own rooted Shiraz or grafted onto Schwarzmann. The patterns for these two levels was similar in the roots, with other difference present for P, K, Ca and S.



Figure 3.4 Taking root images of a Shiraz grapevine in the CSU vineyard to determine seasonal root activity (left) and Rootfly software used for root image analysis (right)

Ramsey was highest in P, Ca and S. Shiraz roots had the highest K concentration and lowest in Ca and P, while the roots of Schwarzmann was the lowest in K, Mg and S levels. Root and wood tissue concentrations of N, Ca, Mg and S were generally highest in Ramsey. However, at the beginning of seasons 2008 and 2009 the differences in root mineral concentrations were less pronounced, with the most consistent being the highest Mg levels in the roots of Ramsey and highest K levels in own rooted Shiraz. The rootstock influence on N levels in the root and wood tissues was also demonstrated by Williams and Smith (1991). The results indicate that rootstocks can supply the scion with different amounts of N and other nutrients, but the amounts in the roots vary between seasons. In addition, the variable accumulation of all macro elements in roots, can assist the nutrient requirements for the scion (except Ca), when nutrient uptake is low early in the growing season. The general decline in N reserves is demonstrated for all rootstocks, falling from budburst to harvest to about half (*Figure 3.5*). This decline in N concentration varies between rootstock and seasons. For instance in 2007–08 own rooted Shiraz has reached its lowest N level already at version, while the other three rootstocks at harvest. In comparisons the differences between rootstocks and the seasonal changes of N concentrations in the wood tissue are generally much less pronounced. However,

Table 3.1 Nutrient concentrations in root and wood tissues of own rooted Shiraz and three rootstocks in the Riverina at bud-burst of three seasons.

		Tissue concentration (% DW)					
		N	**P**	**K**	**Ca**	**Mg**	**S**
				2007			
Wood	Own roots	0.320 c	0.037	0.350	0.278	0.069 b	0.026
	Ramsey	0.370 bc	0.040	0.380	0.263	0.082 a	0.027
	Schwarzmann	0.400 b	0.038	0.360	0.258	0.066 b	0.025
	Ruggeri 140	0.580 a	0.039	0.373	0.258	0.079 a	0.027
		***	ns	ns	ns	*	ns
Roots	Own roots	1.010 c	0.158 b	0.580 a	0.445 d	0.238 b	0.091 b
	Ramsey	1.450 a	0.233 a	0.470 b	0.843 a	0.333 a	0.135 a
	Schwarzmann	1.210 bc	0.200 ab	0.390 c	0.593 c	0.175 c	0.084 b
	Ruggeri 140	1.410 ab	0.200 ab	0.553 a	0.775 b	0.235 b	0.134 a
		**	*	**	***	***	***
				2008			
Wood	Own roots	0.324 c	0.031	0.415	0.310 ab	0.078 b	0.021 c
	Ramsey	0.377 a	0.036	0.385	0.373 a	0.097 a	0.027 a
	Schwarzmann	0.322 c	0.034	0.410	0.250 b	0.075 b	0.022 bc
	Ruggeri 140	0.342 b	0.036	0.420	0.288 b	0.099 a	0.025 ab
		*	ns	ns	*	**	**
Roots	Own roots	0.877	0.102	0.520	0.358 b	0.181 b	0.056 c
	Ramsey	0.950	0.121	0.410	0.700 a	0.296 a	0.081 ab
	Schwarzmann	0.928	0.111	0.478	0.560 a	0.179 b	0.066 b
	Ruggeri 140	0.920	0.134	0.460	0.605 a	0.207 b	0.089 a
		ns	ns	ns	**	*	*
				2009			
Wood	Own roots	0.155	0.031	0.478	0.228	0.075	0.023
	Ramsey	0.189	0.028	0.353	0.182	0.073	0.019
	Schwarzmann	0.165	0.029	0.403	0.183	0.060	0.018
	Ruggeri 140	0.202	0.029	0.368	0.208	0.073	0.020
		ns	ns	ns	ns	ns	ns
Roots	Own roots	1.098	0.116	0.588 a	0.428	0.165 b	0.058
	Ramsey	1.065	0.131	0.380 b	0.765	0.283 a	0.075
	Schwarzmann	0.943	0.110	0.373 b	0.528	0.134 b	0.054
	Ruggeri 140	0.879	0.127	0.320 b	0.543	0.122 b	0.055
		ns	ns	***	ns	***	ns

Means separated within columns using Fisher's LSD test. Different letters indicate a significant difference (p=0.05).
*, **, ***, and ns indicate significance at p ≤0.05, ≤0.01, ≤0.001), and not significant, respectively.

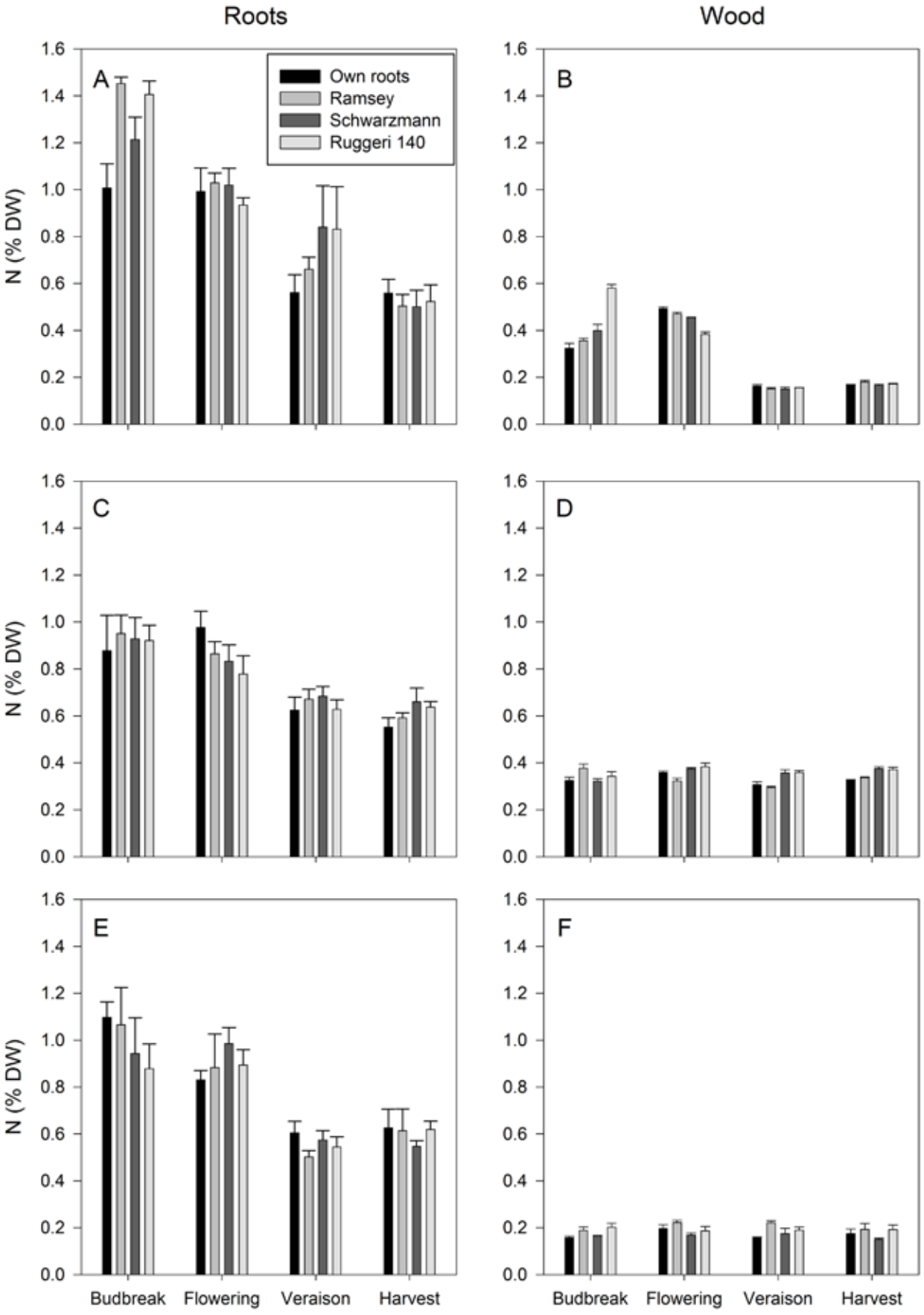


Figure 3.5 N concentrations in root (left) and wood tissue (right) of own rooted Shiraz and three rootstocks in the Riverina from three seasons (2007–08: A and B; 2008–09: C and D; 2009–10: E and F). Standard errors are indicated as bars above the mean.

the intra-seasonal concentrations vary more, being about half in 2009–10 compared to the other two seasons at bud-break and flowering. This indicates that the root N reserves (and other nutrients) and to lesser extend wood reserves are utilized for the annual development of the grapevines. Then both nutrients and carbohydrate reserves are particularly required for supporting early vine growth in early spring.

Carbohydrates

The carbohydrate concentrations in the root and wood tissues are lowest at flowering, since resources rare required for the early canopy development. The carbohydrate levels are higher in the roots than in the wood in own rooted Shiraz, while this is different on vines grafted onto the tree rootstocks (*Figure 3.6*). Similar seasonal changes and higher root carbohydrate levels in own rooted vines compared to wood have been observed in previous studies (Smith and Holzapfel 2009). Own rooted Shiraz had the highest carbohydrate concentrations in the roots at bud-burst and Ramsey had the lowest. The scion carbohydrate levels differences altered by the different rootstocks were relatively small compared to the observations in the roots. This indicates that the influence of the rootstocks on scion reserve carbohydrate levels is relatively small, while large differences in reserve levels exist in the roots. Recent work has shown, that altered assimilate production or demand of carbohydrates impacts mostly on the root reserves (Smith and Holzapfel 2009), indicating that carbohydrates in the root tissue is more influenced by assimilate supply than wood tissue. However, the total amount carbohydrate reserves also depend on the size of the root system. The total carbohydrate content in Ramsey in pots has been shown to be less than half of that of Ruggeri 140 (Smith 2004). This suggests that the sink for assimilates is also much smaller than for the other rootstocks, with potential implications for vine reserve depletion in spring and early root development.

Root dynamics

The activity of the roots varied between rootstocks in multitude and during the season and between seasons. However, the higher activity in the 2007–08 season is likely due to the disturbance from the placement of the minirhizotrons (*Figure 3.7*). In the first season some activity was present before bud-burst, increasing towards flowering when it was highest. The activities generally declined towards veraison and further from harvest to leaf fall, with some slightly higher activity during the maturation and post-harvest period. The root dynamics in the following two seasons monitored was much lower, with some increases prior to flowering and veraison in 2008–09 and pre bud-break and post-harvest in 2009–10. Overall a distinctive peak was only observed around flowering in 2007–08 and under these conditions a distinctive peak of root activity after harvest was not present in any season, further root growth and nutrient uptake is seen as a common occurrence in vines growing in warmer climates with a post-harvest period (Mullins *et al*. 1992). The lack of a more substantial activity could be due to relatively low rainfall and dryer conditions for several years in the grape growing area the vines were growing. Some differences between rootstocks were present, with Ruggeri 140 generally having the highest root activity in the first two seasons. The higher root activity of Ruggeri 140 could be due to the lower yield level compared to the other rootstocks. Ramsey had higher activity prior to bud-break. These findings indicate that rootstocks could be an important factor in determining seasonal root dynamics. The influence of other factors such as pruning levels and water supply on root dynamics has been reported earlier (Comas *et al*. 2005). The higher root activity in Ramsey at the beginning of the season might be a contributing factor in the higher nutrient levels in the roots at bud-burst. The multitude of root activity could have been influenced by winter carbohydrate reserve levels and utilization in the roots early in the season and by crop load in the second part of the season.

Conclusions

The work shows the influence of the different rootstocks on stored scion N and Mg levels at bud-burst. However, in the roots of these rootstocks differences were more pronounced for the macro nutrients, but particularly for the carbohydrate concentrations. This suggested that rootstocks have a different capacity to supply the early growth with nutrients and carbohydrates, when production of assimilates and uptake of nutrients is low. Some of the observed differences could be due to the root dynamics, since Ramsey has high early root activity and the highest nutrient levels in the roots, while Ruggeri 140 had generally a higher activity during the season and showed elevated scion N and Mg. The differences in root dynamics and nutrient storage between rootstocks could have implications for the timing of fertilizer applications to a vineyard.

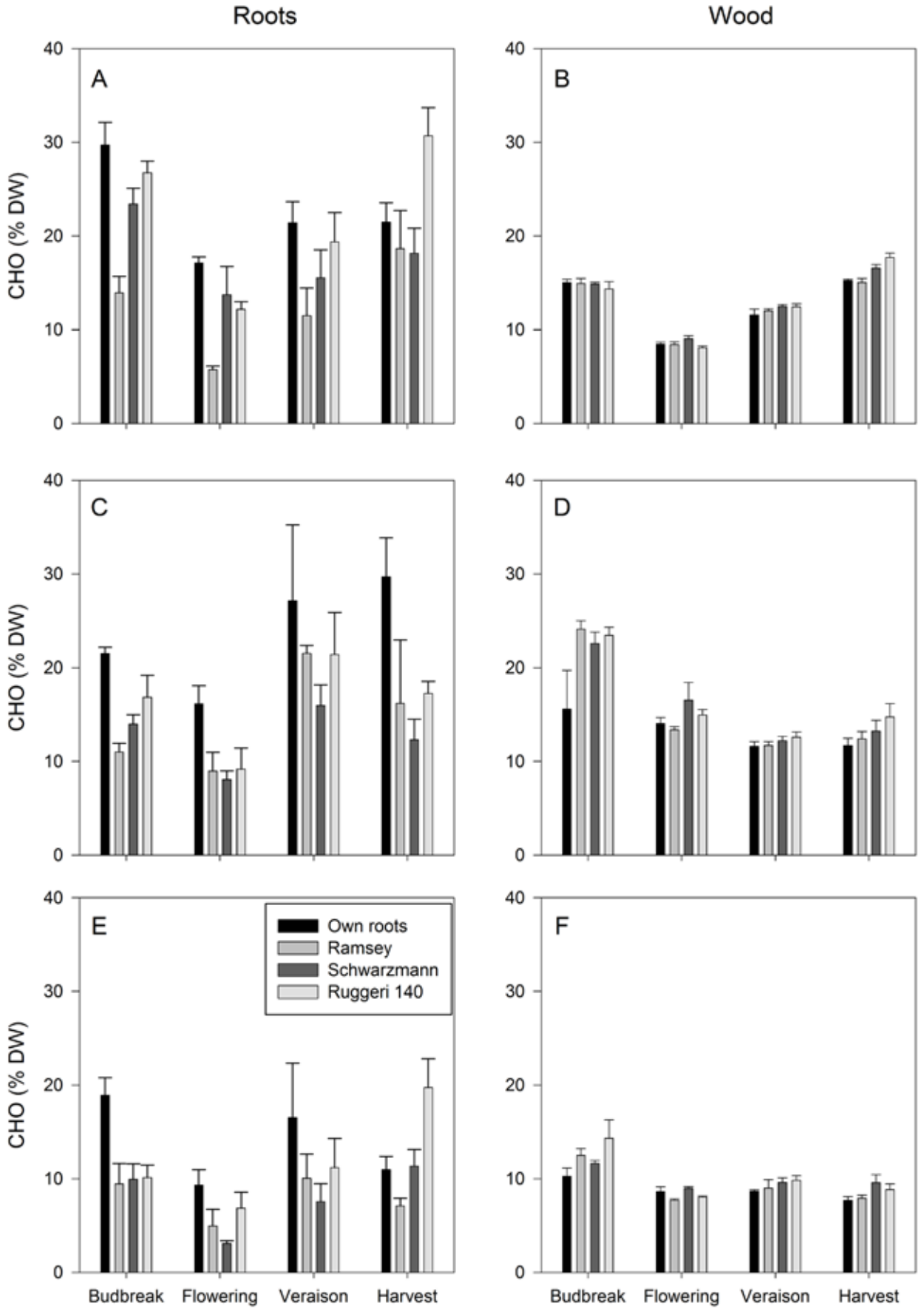


Figure 3.6 Total CHO concentrations in root (left) and wood tissue (right) of own rooted Shiraz and three rootstocks in the Riverina from three seasons (2007–08: A and B; 2008–09: C and D; 2009–10: E and F). Standard errors are indicated as bars above the mean.

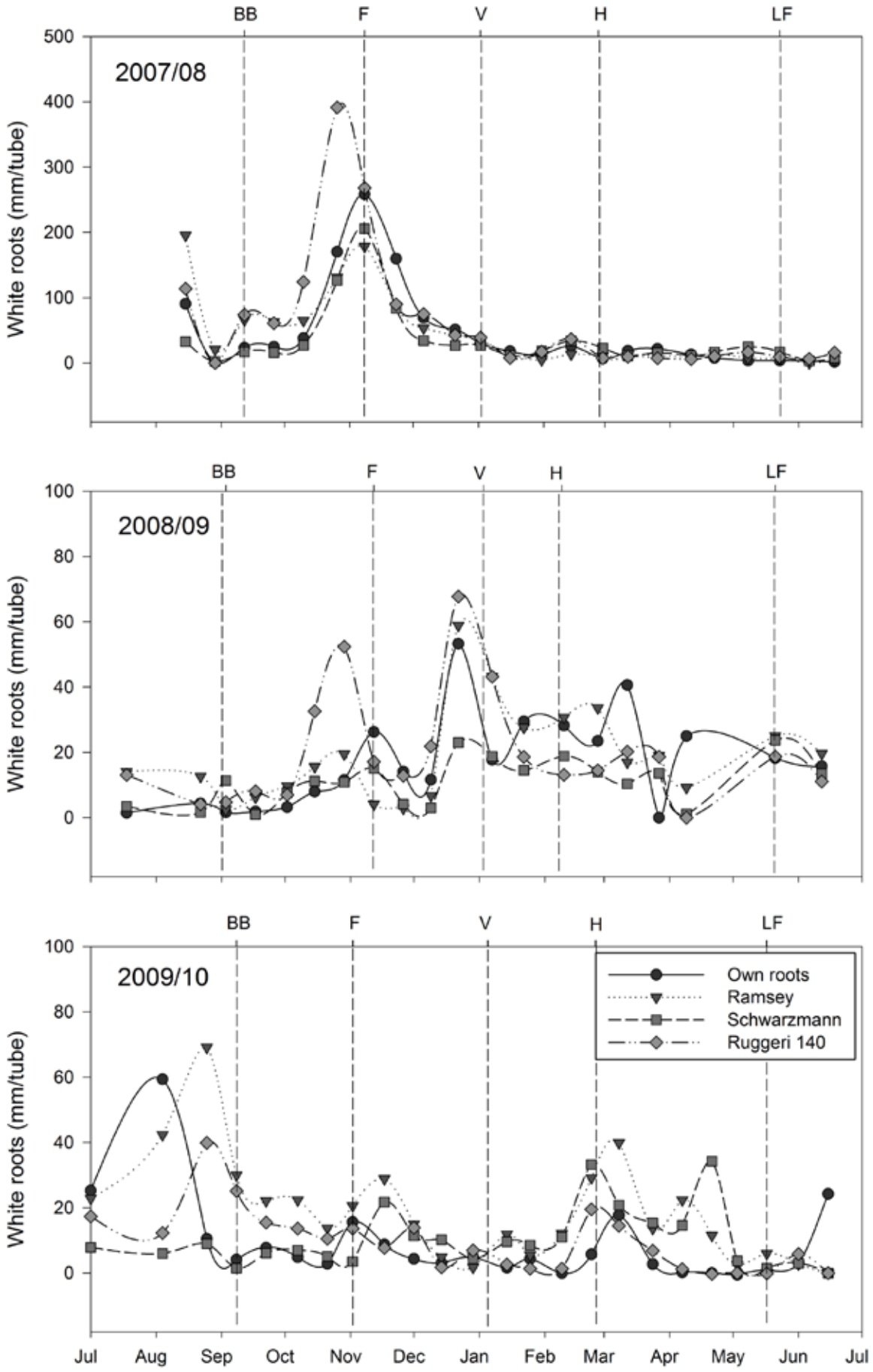


Figure 3.7 Root activity in own rooted Shiraz and three rootstocks in the Riverina during three growing seasons. The key developmental stages are indicated for bud-break (BB), flowering (F), veraison (V), harvest (H) and leaf-fall (LF).

Experiment 3.3
Vineyard inputs and leaf removal on vine reserves and root dynamics

Materials and methods

Vineyard management often impacts on vine nutrient and carbohydrate reserves of the perennial structure, by altering the nutrient and carbohydrate acquisition and the source-sink relationships of veins. The management practices together with the environmental conditions can alter root development during the season, differences have been particularly observed between different pruning systems and water supply situations.

Major inputs into the vineyard system are the supply of water and nutrients, N fertilizer being the most applied fertilizer. N can be applied either to the soil as granulate or through the irrigation water (fertigation), but also by foliar application, being less common due to the relative large amounts applied to the vineyard. Several studies have shown that the application of N increases vine N status (eg. Treeby and Wheatley 2006). Commonly N is applied between bloom and veraison, in this period the majority of the uptake takes place and the understanding is that main root growth activity occurs. Often N is applied after harvest, when another important uptake period can take place, particularly under the conditions in a warmer climate (Conradie 1980). Water supply is often used as vineyard management tool to manage vine growth and enhance grape composition in red varieties. This most common practice implementing a water stress between fruit-set and veraison is described as regulated deficit irrigation (RDI). Often water supply can be limited after harvest, impacting on the amount of carbohydrates stored in the perennial structure (Smith and Holzapfel 2009, Holzapfel *et al.* 2010). In contrast, it has been demonstrated that an increase of N concentration can occur in the roots after the implication of water stress (Holzapfel and Smith 2011). A reduction of leaf area reduces the production of assimilates and therefore the stored reserves in both wood and roots (Smith and Holzapfel 2009), but also the resources availability for the annual development of shoots and roots. The supply of the carbon is important for root respiration, root growth and nutrient uptake, all being energy requiring processes. The impact of carbohydrate supply on root activity or new root growth has been indicated by Comas *et al.* (2005), where minimal pruned vines showed earlier root production compared to heavily pruned vines.

This study was undertaken to understand the impact of carbohydrate, nutrient and water supply on vine reserves of nutrients and carbohydrates in the perennial structure. In addition, the aim was to investigate the impact of vineyard inputs and carbohydrate supply on root dynamics during the season. As indicated in the previous section, work attempts to assess links between nutrient and carbohydrates reserves and root activity.

Vineyard and treatments

The trial was conducted on a drip irrigated Shiraz vineyard (clone PT23) in the Riverina grape growing region, New South Wales, Australia. The Charles Sturt University vineyard was planted in 1998 on red Kandosol overlaying coarse granite (*Figure 3.8*). The mean January temperature at Wagga Wagga is 24°C with average annual rainfall of 572 mm, being a semi arid climate. The planting space of the own rooted Shiraz is 3 × 2 m vine to row spacing (1667 vines ha^{-1}), and were trained to a single bilateral cordon. The vines in the trial were spur pruned, with the trial conducted over three consecutive seasons (2008–09 to 2010–11). The treatment selection was based on practical



Figure 3.8 Shiraz field trial in the CSU vineyard (top) and taken root imaged during the season to determine seasonal root activity (bottom).

vineyard management practices, designed to alter nutrient and carbohydrate acquisition and therefore root development. Six treatments were applied to nine vines in a fully randomized block design. These comprised of a control (CON), a pre-flowering defoliation treatment (LS-E), reduced irrigation in the period post-fruit-set to veraison (RI-E), reduced irrigation from harvest to leaf-fall (RI-L), and pre-flowering N application to soil or to leaves in the rate of 40 kg ha^{-1} (AN-S and AN-L respectively). The foliar application was applied in three split application and the defoliation was undertaken three times in two weekly intervals in October to the first fully enfolded leaf of each shoot.

Root activity

As for the rootstocks described in the previous section a minirhizotron system to collect frequent images of the major part of the root-zone during the season (*Figure 3.8*) and less frequent over the winter period. For this purpose three polycarbonate tubes (1 m length) were installed in the vine row at a 30° angle in each plot shortly after harvest in 2008 (in the tree middle vines of a plot), allowing images to be taken of the rootzone with the miniature camera system (Bartz Technology, Santa Barbara, CA, USA). The length of white roots was determined in every image (50 per tube) and total length was calculated for each tube, covering a soil depth of 60 cm.

Sampling and analysis

Of the panel of each nine vine plot, four vines were used for monitoring nutrient and carbohydrate reserve concentrations by taking drillings of the perennial structure above ground and root sections. There were also two buffer vines and the tree middle vines of the plot were utilized for the study of the root dynamics described above. The sampling procedure and the analysis are described in detail in the pervious section. Briefly, the outer vines acted as buffers, while the two in the centre of the panel left undisturbed for root monitoring. Root and wood sampling were undertaken at bud burst, flowering, veraison, harvest and leaf-fall over three seasons. The tissue samples were dried at 70°C and ground through a 0.12 mm sieve, total N content of the tissues was determined with a N analyzer, while the other macro nutrient were determined with inductively coupled plasma optical emission spectrometer after digestion. The non-structural carbohydrates were determined enzymatically using a plate reader at 340 nm and 510 nm, determining soluble sugars and starch respectively. For data compiled in Excel 2003 and further analyzed using the graphic program Sigma plot (Version 11.0) and Genstat (Release 11.1).

Results and discussion

The Shiraz vineyard produced a yield of 14–15 t ha^{-1} in the first two seasons (2008–09 and 2009–10), while in the last season 2010–11 the yields were much lower due to disease pressure. The early leaf removal treatment (LS-E) showed the lowest yield in the two last seasons and always the lowest pruning weights. The reduced irrigation applied between fruit set and veraison (RI-E) showed the lowest yields in the first season, other treatment effects were less distinctive. The observed differences influenced by the various treatments for N were mostly in the root tissue, while carbohydrate reserves were also changed in the wood. The impact on other nutrients assessed at bud-break was less pronounced; the monitored root dynamics showed seasonal and intra-seasonal variation.

Nutrients

The reserve nutrients were higher in the root tissue than in the wood, with multitude varying between the six macro nutrients. For instance, N was about four times higher in the roots, while Ca was only slightly higher compared to the wood concentration (*Table 3.2* and *3.3*). Such differences could be due to mobility and the different requirements for the two parts of the vine. Generally, there was no significant impact of the treatments on reserve nutrient concentration, other than at bud-break 2010 for K concentrations of the roots, which was elevated by the LS-E and lowered by the AN-S. However, root N level was higher at bud-break 2009 and 2010, when N was either applied to the leaves or to the soil. The impact of both N application methods was also visible later in the season at flowering and veraison the 2009–10 and 2010–11 seasons (*Figure 3.9*). In contrast, the wood tissue N concentration appeared not to be influenced by N application, while the reduced irrigation treatments often reduced N concentrations in roots, but the effects were inconsistent between seasons.

The seasonal changes of N concentration (CON) between seasons in the roots were somewhat similar, being high early in the season and lower towards the end. In contrast, N wood levels were declining from bud-break to harvest in 2008–09; with minor difference between the key stages present in 2009–10 and the lowest concentrations present at flowering 2010. However, the concentrations varied between seasons for both tissues at bud-break, with

the 2009–10 season having lowest root and wood concentrations, less than 0.75% N and just over 0.16% N respectively. At veraison in this season the lowest root N was observed overall, (0.42% N), and in 2008–09 at the same stage the lowest wood reserve concentration was found (0.13% N). The results indicate the influence of fertilizer application on reserves, particularly in the roots, while the seasonal and intraseasonal variation could be due to differences in N uptake and requirements for annual growth. For instance, the 2009–10 season showed the highest yield and pruning weights of the three monitored seasons.

Carbohydrates

The carbohydrate concentrations varied between tissues, seasons and during the season as observed for N. Generally the concentrations were about double in the roots compared in the wood, showing the importance of the roots as a carbohydrate reserve pool (*Figure 3.10*). Root carbohydrate concentrations were highest at bud-break 2008 with about 40% and lowest at harvest 2010 with 12%. Similarly wood reserves are highest at bud-break in 2008 (13.5%), but lowest at flowering 2010 (7.6%). In the season 2008–09 and 2010–11 wood and root carbohydrate concentrations are lowest in bloom, while in the middle season in 2009–10. The most constant treatment effect was observed with the leaf removal treatment (LS-E) implemented prior to flowering, resulting generally in lower carbohydrate reserves in the roots and in the wood at flowering and even until harvest in the roots in the 2009–10 season. This treatment would have led to a substantial to reduction of assimilate production, limiting the availability for storage and annual growth, including new root growth.

Root dynamics

The observation of new white roots was much higher in the first season (2008–09), which was most likely due to the disturbance of the roots, initiating more root activity (*Figure 3.11*). In this season the root

Table 3.2 Nutrient concentrations in wood tissue of own rooted Shiraz at budbreak (2008, 2009, and 2010) influenced by early leaf removal (LS-E), reduced irrigation (RI-E, RI-L) and type of N fertilizer application (AN-L, AN-S) in the Riverina.

	Tissue concentration (% DW)					
	N	**P**	**K**	**Ca**	**Mg**	**S**
				2008		
CON	0.264	0.041	0.393	0.328	0.077	0.026
LS-E	0.244	0.039	0.383	0.333	0.080	0.025
RI-E	0.215	0.038	0.403	0.325	0.074	0.024
RI-L	0.220	0.040	0.433	0.348	0.080	0.026
AN-L	0.225	0.039	0.385	0.298	0.077	0.024
AN-S	0.270	0.040	0.365	0.338	0.078	0.025
	ns	ns	ns	ns	ns	ns
				2009		
CON	0.159	0.030	0.400	0.157	0.062	0.018
LS-E	0.172	0.029	0.405	0.150	0.064	0.017
RI-E	0.166	0.029	0.355	0.170	0.059	0.018
RI-L	0.165	0.029	0.363	0.189	0.060	0.018
AN-L	0.175	0.028	0.353	0.177	0.062	0.017
AN-S	0.196	0.030	0.358	0.190	0.067	0.019
	ns	ns	ns	ns	ns	ns
				2010		
CON	0.270	0.037	0.435	0.413	0.079	0.025
LS-E	0.271	0.033	0.398	0.450	0.085	0.024
RI-E	0.240	0.032	0.460	0.360	0.078	0.024
RI-L	0.255	0.035	0.410	0.433	0.084	0.024
AN-L	0.265	0.037	0.435	0.368	0.079	0.024
AN-S	0.270	0.035	0.395	0.375	0.078	0.025
	ns	ns	ns	ns	ns	ns

Means separated within columns using Fisher's LSD test. Different letters indicate a significant difference (p = 0.05). *, **, ***, and ns indicate significance at p ≤ 0.05, ≤ 0.01, ≤ 0.001), and not significant, respectively.

activity occurred mostly around bud-break and also flowering (CON), while there was no particular peak observed in the 2009–10 season. However, in the last season (2010–11) activity peaks were present around bud-break and between flowering and veraison. Such differences between seasons have been observed by others (Commas *et al.* 2005). Although the strong decline after the first year in the root activity, just after the minirhizothrons were inserted after harvest the season before, is similar to the previous section of the report on rootstocks. It appeared that in 2008–09 the AN-L treatment resulted in an activity peak between flowering and veraison, while the RI-E and LS-E treatments resulted in a peak around harvest. In the following 2009–10 season the LS-E treatment resulted in activity peaks prior to and after flowering and around veraison, while after harvest the irrigation (RI-E and RI-L) and the AN-L treatments the root activity was also elevated. In the last season (2010–11), most treatments (except LS-E and AN-S) showed activity around bud-burst, the LS-E treatment had the most pronounced activity peak around veraison, with no peak present between bud-break and flowering. Some less pronounced activity peaks were present after flowering to harvest in most treatments (except for AN-S and RI-E) in the last season of the field trial. The study showed some differences through the implemented treatments in root activity, the leaf removal treatment being the most constant in all three seasons. This could have contributed to alter supply of assimilates to the roots, indicated in the carbohydrate concentration. However, to further investigate the interaction between root dynamics, nutrient acquisition and carbohydrate supply more detailed studies should be undertaken.

Conclusions

This study was undertaken to investigate the impact of practical management strategies, such as irrigation or water supply on vine nutrient and carbohydrate reserves. The work showed the impact of N fertilizer application on N reserves, with two application

Table 3.3 Nutrient concentrations in root tissue of own rooted Shiraz at budbreak (2008, 2009, and 2010) influenced by early leaf removal (LS-E), reduced irrigation (RI-E, RI-L) and type of N fertilizer application (AN-L, AN-S) in the Riverina.

	Tissue concentration (% DW)					
	N	P	K	Ca	Mg	S
			2008			
CON	1.165	0.173	0.540	0.393	0.148	0.065
LS-E	1.164	0.187	0.598	0.425	0.149	0.065
RI-E	1.017	0.149	0.578	0.428	0.151	0.060
RI-L	1.026	0.142	0.573	0.393	0.152	0.069
AN-L	1.193	0.192	0.570	0.465	0.142	0.067
AN-S	1.167	0.189	0.575	0.463	0.160	0.072
	ns	ns	ns	ns	ns	ns
			2009			
CON	0.750	0.141	0.563	0.430	0.218	0.058
LS-E	0.766	0.127	0.465	0.443	0.176	0.054
RI-E	0.740	0.129	0.558	0.495	0.184	0.055
RI-L	0.784	0.124	0.538	0.498	0.181	0.053
AN-L	1.026	0.204	0.515	0.520	0.173	0.059
AN-S	1.059	0.186	0.535	0.463	0.180	0.064
	ns	ns	ns	ns	ns	ns
			2010			
CON	1.123	0.167	0.593 b	0.458	0.233	0.063
LS-E	1.005	0.181	0.770 a	0.440	0.220	0.067
RI-E	1.086	0.180	0.590 b	0.480	0.177	0.063
RI-L	1.040	0.150	0.563 b	0.415	0.207	0.061
AN-L	1.265	0.199	0.560 b	0.450	0.198	0.062
AN-S	1.386	0.173	0.488 c	0.413	0.153	0.065
	ns	ns	**	ns	ns	ns

Means separated within columns using Fisher's LSD test. Different letters indicate a significant difference (p=0.05).
*, **, ***, and ns indicate significance at p≤0.05, ≤0.01, ≤0.001), and not significant, respectively.

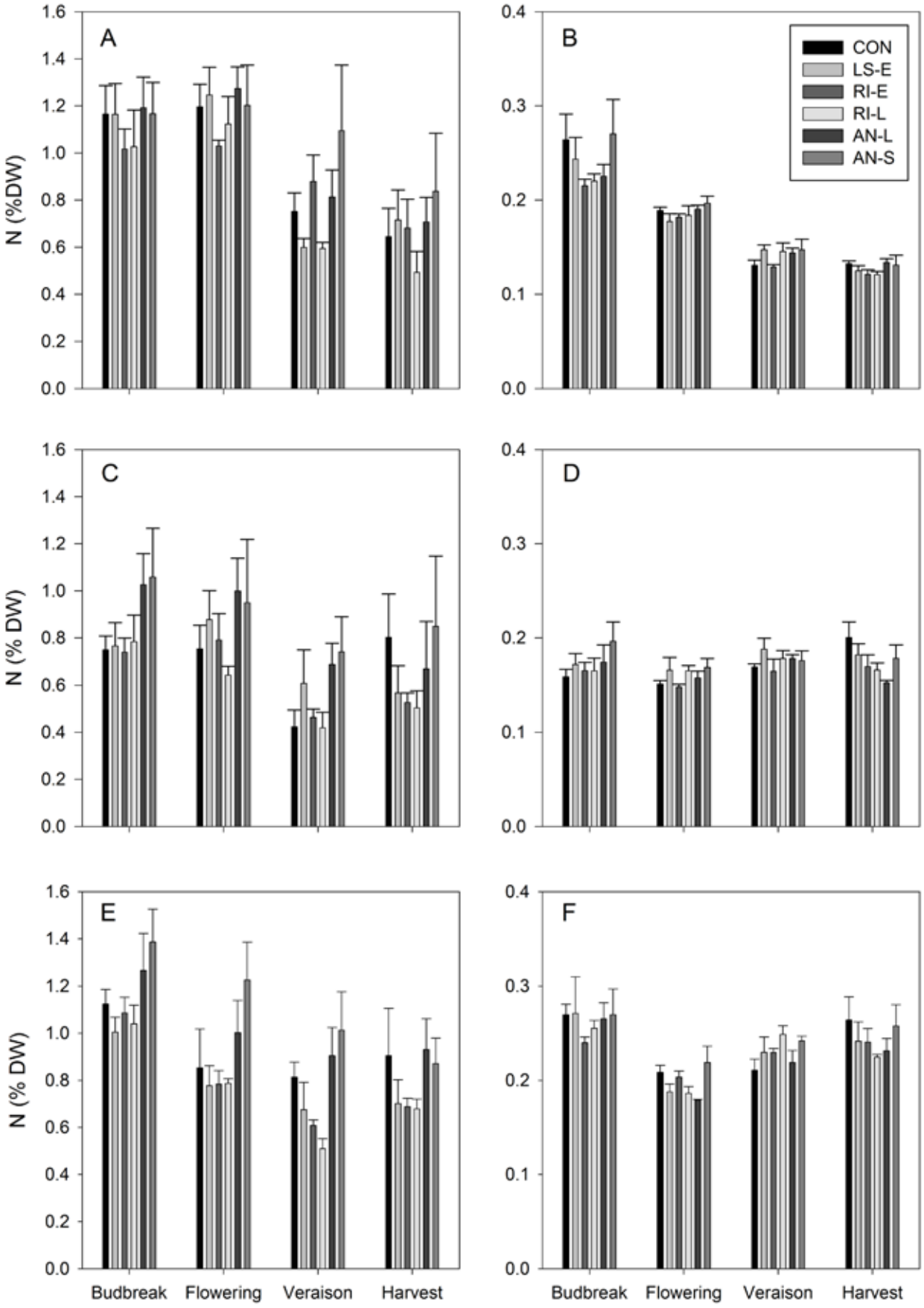


Figure 3.9 Total N concentrations in the perennial structure of Shiraz grapevines for three seasons (2008–09: A and B; 2009–10: C and D; 2010–11: E and F) influenced by early leaf removal, reduced irrigation and type of N fertiliser application. Standard errors are indicated as bars above the mean.

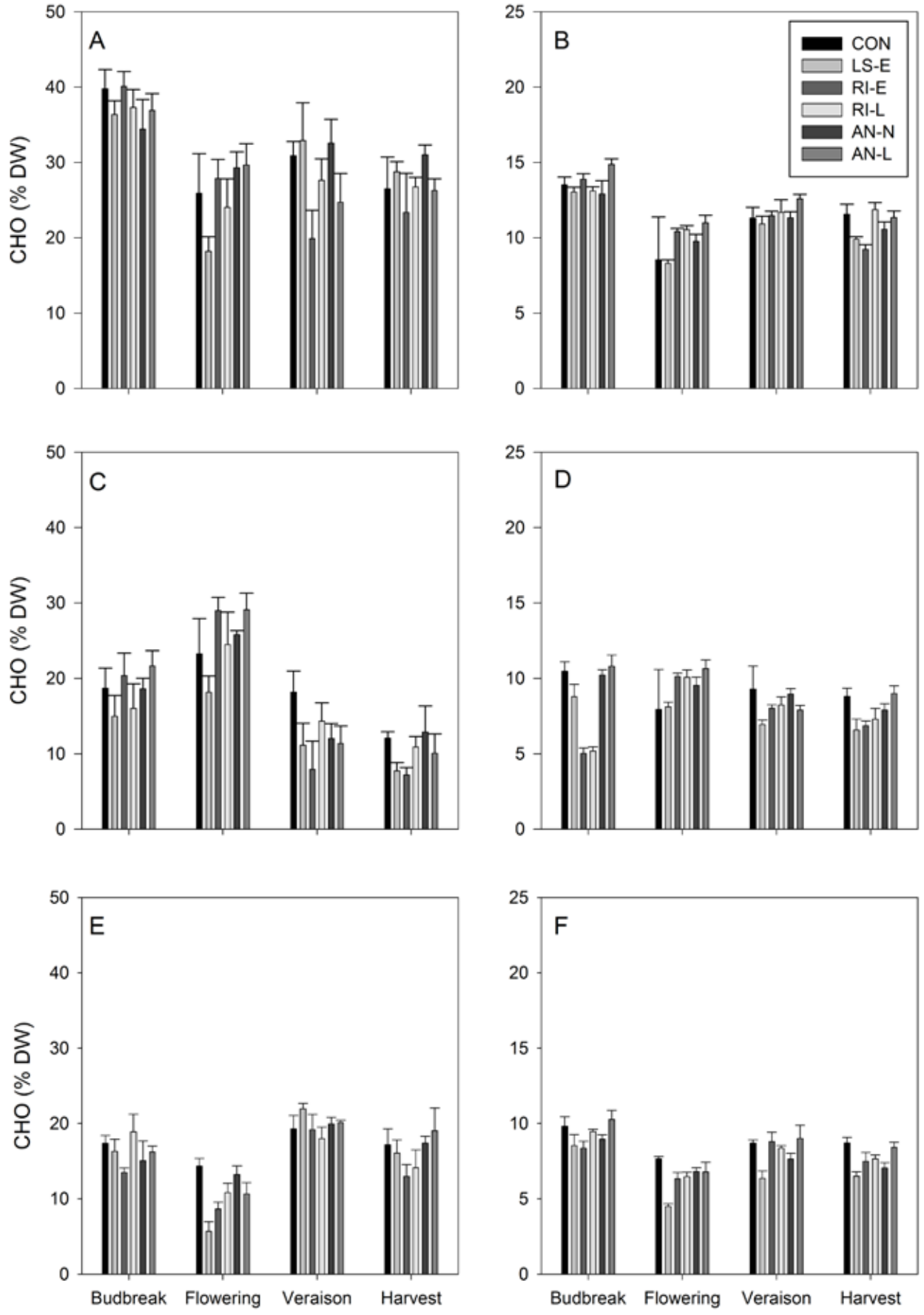


Figure 3.10 Total CHO concentrations in the perennial structure of Shiraz grapevines for three seasons (2008–09: A and B; 2009–10: C and D: 2010–11: E and F) influenced by early leaf removal, reduced irrigation and type of N fertiliser application. Standard errors are indicated as bars above the mean.

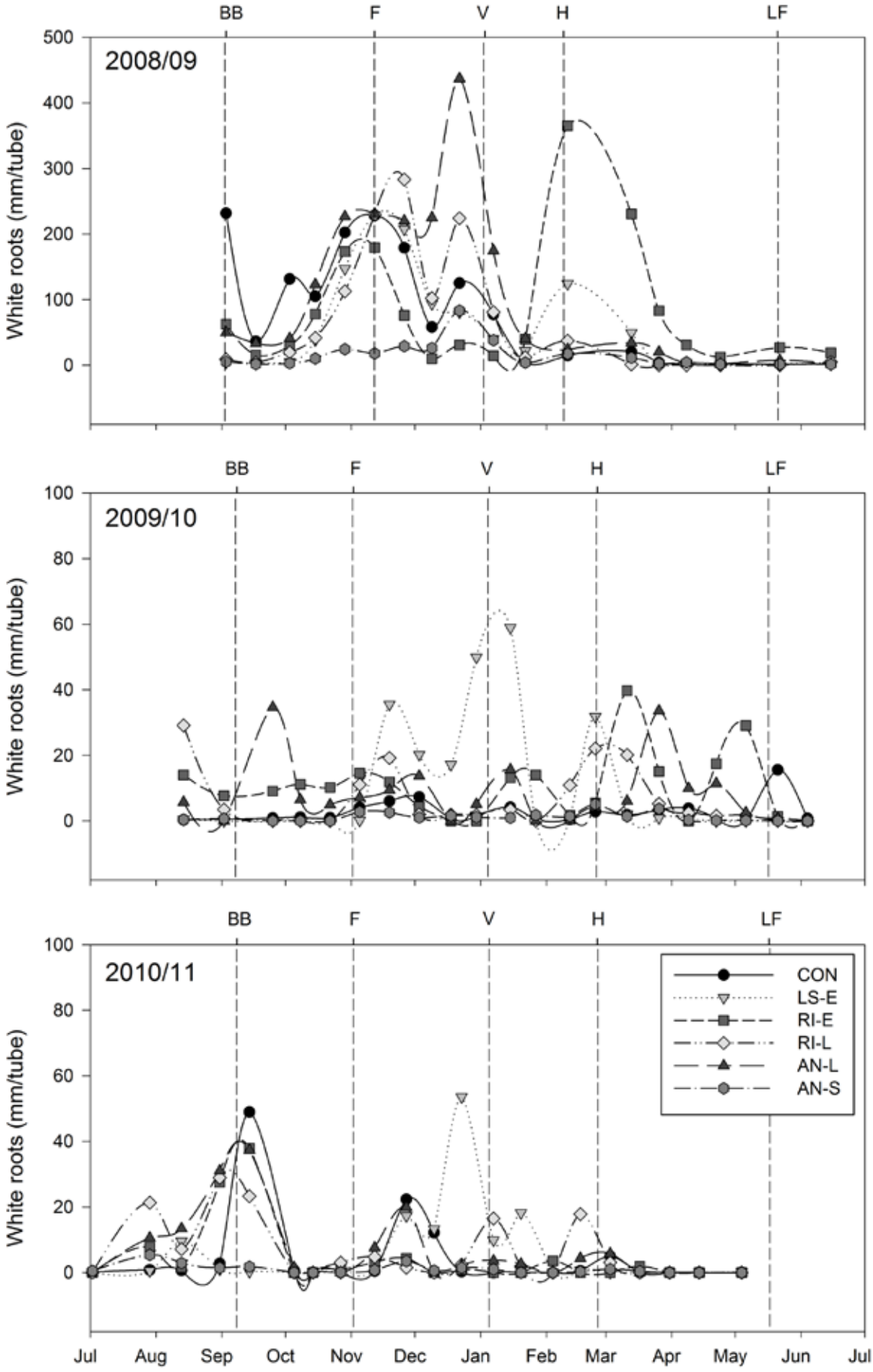


Figure 3.11 Root activity in own rooted Shiraz influenced by early leaf removal, reduced irrigation and type of N fertiliser application in the Riverina during three growing seasons. The key developmental stages are indicated for bud-break (BB), flowering (F), veraison (V), harvest (H) and leaf-fall (LF).

forms of N (foliar, soil) being similarly effective. The carbohydrate reserves were lowered substantially by leaf removal prior to flowering in root and wood tissues. However, the information provided by the use of minirhizothons in grapevines appears to be limited for details of root dynamics itself, which makes it difficult to study the relationship to nutrient uptake and carbohydrate supply and field conditions. The spring application of N fertilizer appears to be very effective not just for the annual growth, but also in elevating the N reserves required later during the season. Overall the work shows the importance of the supply of N and carbohydrate production on the reserves in the perennial structure within a season and between seasons.

Experiment 3.4
Timing of N application and water stress on shoot and berry development

Materials and methods

The uptake, storage and mobilization of N are important features of perennial crops like the grapevine, with the annual growth and development getting the N from either uptake or storage tissues. The amount of N moved to the berry during its development is critical for the amino-N content of the berry accumulated at harvest and therefore for the wine making process and the final wine composition.

Important N uptake periods are between bloom and veraison and after harvest, when most of the root growth is believed to take place (Conradie 1980). N fertilizer supply timing (and amount) in these periods alter the N directed towards the shoots and berries (Holzapfel and Treeby 2007), with an application between veraison and harvest resulting in higher berry N. We observed that most of the N is accumulated in the berries prior to veraison (see first section); while Schaller *et al.* (1990) found that the majority of the berry N is accumulated after veraison. This could be due to the different climatic conditions, since irrigation management has implications for berry amino N content (Wade *et al.* 2004). The understanding is that during berry maturation N uptake might slow or stop and redistribution from roots, shoots and leaves to bunches occurs (Conradie 1991a), being due to the limited N uptake (Keller 2010). However, the N moved to the berry is important for the amino-N concentration, being important for the fermentation processes. Must free primary amino N and ammonium are collectively referred to as yeast available N or YAN. Yeast typically need about 130 mg free primary amino N per L of must to complete a fermentation (Agenbach 1977). Low must N is associated with sluggish and stuck ferments (Ingledew and Kunkee 1985), while high N musts ferment too quickly (Monteiro and Bisson 1991). While N can be added in the winery in the form of di-ammonium-ortho-phosphate (DAP), the general view is that this addition is best only used for fine tuning the must, while the grape amino-N content should be optimized in the vineyard.

The work in the first section indicated that most of the N is accumulated from about fruit set to veraison. This research was undertaken with the intention to investigate the timing of supply of N during the berry development period under two water regimes on final N content. The aim was to provide a better understanding of the best timing of N application to enhance berry amino-N, and in which other parts of the vine the applied N is also allocated.

Plant material and treatments

Pot experiment was conducted in an outside bird-proof enclosure located at the National Wine and Grape Industry Centre, Charles Sturt University, Wagga Wagga (*Figure 3.12*). The five year-old Chardonnay vines were planted in 70 L pots and were filled with a standard premium potting mix which allowed for a water holding capacity of approximately of 8 L of plant available water per pot. Vines were trained to a single cordon and thinned to 12 shoots and one bunch per shoot (wherever possible). The shoots were vertically trained and were sprayed during all growing seasons to prevent mite and fungus infections. Prior to the treatment implementations all vines received initial 2 g N (3 November, 2010) as ammonium sulfate, with N-free Megamix. There were 4 replicates of each of the six N timing application (N1, N2, N3, N4, N5 and N6) and two water regimes (FI and HI), resulting in 12 treatment combinations. The water supply regimes implemented after fruit-set were fully irrigated and half irrigated (4 L and 2 L dripper), vines received four grams of N at each of the six application time. The first N amount was applied on 17 November, 2010 and the last of the six fortnightly applications was at the end of January 2011 (two weeks prior to harvest), each time eight vines received 4 g N. The N was applied as dissolved ammonium sulfate containing 10% of the stable isotope ^{15}N, the total of 6 g of N (2 g pre treatments and 4g treatment) was based on the prediction that each shoot will require





Figure 3.12 Potted chardonnay grapevines at the NWGIC prior harvest (early February 2011) to determine water supply and N application timing on berry N and allocation of other vine parts (left). Washed roots after the destructive harvest of the trial a few days later (right).

about 0.5 g N each. To maintain a good nutrient status for other minerals, N-free Megamix was applied, also every two week between the N applications, starting on 4 November, 2010.

Measurements and sampling

The influence of the two water supply regimes and the six timings of N supply on shoot and berry growth was determined at weekly intervals. For this purpose the length of six marked shoots per vine was measured once a week and 6 berries were also collected (starting shortly after fruit-set) from each vine for ^{15}N analysis (altering a one berry sample from a bunch between the six marked and six unmarked shoots). At veraison another lot of six berries was collected every week for amino-N determination. At harvest (9 February) an additional 25 berries were sampled and the yield was recorded from each vine, bunches were separated into bunch stems and berries. Each vine was than destructively harvested and separated into leaves, shoots, cordon arms, cordon (below last arm), trunk, rootstock (cut at soil level) and roots. Most of soil of rootstock and root system was removed prior washing, a sub sample of small (< 2 mm) and large roots (5–10 mm) were taken after washing. The fresh weight of all parts was determined prior to washing except the roots and the rootstock which were weighed after washing and air dying for about 18 hours. All parts were washed with phosphate free detergent and then rinsed with distilled water. The various parts were than placed into a drying oven at 60°C for several days and the dry weight was recorded. The drying time varied between the different tissues and was several weeks for the grapes. The destructive harvest was undertaken from 14–17 February, with one replicate of 12 vines processed per day and the last root fresh weight was determined on 18 February.

Soil moisture was determined twice weekly using a TDR system (Soil Moisture Systems), photosynthesis, transpiration and stomatal conductivity was measured with a similar frequency by utilizing LI6400 gas exchange system (Li-Cor Corporation, Lincoln, NE, USA). The chlorophyll index and water potential (pre-dawn) was determined once a week, using the chlorophyll meter (SPAD-502, Minolta Co., Ltd., Japan) and Scholander pressure chamber (ICT international, Armidale, NSW) respectively. The sub-samples were taken from all tissues then ground through a 0.12 mm sieve (Retsch ZM100, Retch GmbH, Haan, Germany) for analysis for non structural carbohydrates, total N and ^{15}N content. The samples were sent to the ANU Analytical Services for N determination and the non-structural carbohydrates will be determined using an enzymatic method (MEGAZYME International Ireland Ltd, Bray, Ireland). The amino-N will be determined by using HPLC methods for amino acids and ammonium, equipped with a fluorescence detector and conductivity detector respectively (Waters, Milford, MA, USA) respectively. The data from the measurements were compiled in Excel 2003 and further analyzed using the graphic program Sigma Plot (Version 11.0).

Results and discussion

The N uptake under different water regimes were reflected in plant water potential and chlorophyll index, responding to the water and application respectively. In addition, the vines responded to the vegetative and reproductive growth and development during the season and at the final assessment at harvest.

Physiological responses

The impact different irrigation treatments were observed in the more negative pre-dawn water potential shortly after implementation and became more pronounced after about a months, with differences of about 2 bar (*Figure 3.13A*). The differences between the N treatments were not reflected in the WP, despite the differences in canopy development. The differences between FI and HI became smaller closer to harvest, with -2.3 and -2.8 bar respectively. The chlorophyll index was commonly elevated after each timing of application, with the index increasing from flowering towards harvest, 20–25 and 27–32 respectively. The first application in the middle of November N1 resulted in 3–4 units more than any of treatments receiving N later (*Figure 3.13B*). The biggest increase was observed with N4, with increase of nearly 10 units in three weeks. It appeared that the application from veraison and thereafter and the most significant effect on chlorophyll content of the leaves, which could indicate a stronger uptake of the applied N or more N is allocated to the annual growth and development. However, further analysis is required from both the perennial structure and annual organs to provide further clarification. The irrigation influenced also the chlorophyll index and the HI treatment was slightly lower throughout berry development.

Shoot and berry development

The shoots growth responded clearly to the irrigation treatments, being observed shortly after implementation and with the difference relatively constant after two to three weeks (*Figure 3.14A*). The overall growth ceased two weeks prior veraison in middle of December. And the final length was 112 cm for FI and 93 cm for HI treatment. The N applied at the earliest time (N1) had the most impact on elevating shoot growth and final shoot size with 122 cm, while the last application N5 and N6 had the shortest shoots at harvest, with 92 and 94 cm respectively (*Figure 3.14B*). As observed for the two irrigation treatments, the shoot growth ceased about two weeks prior veraison, therefore the impact on

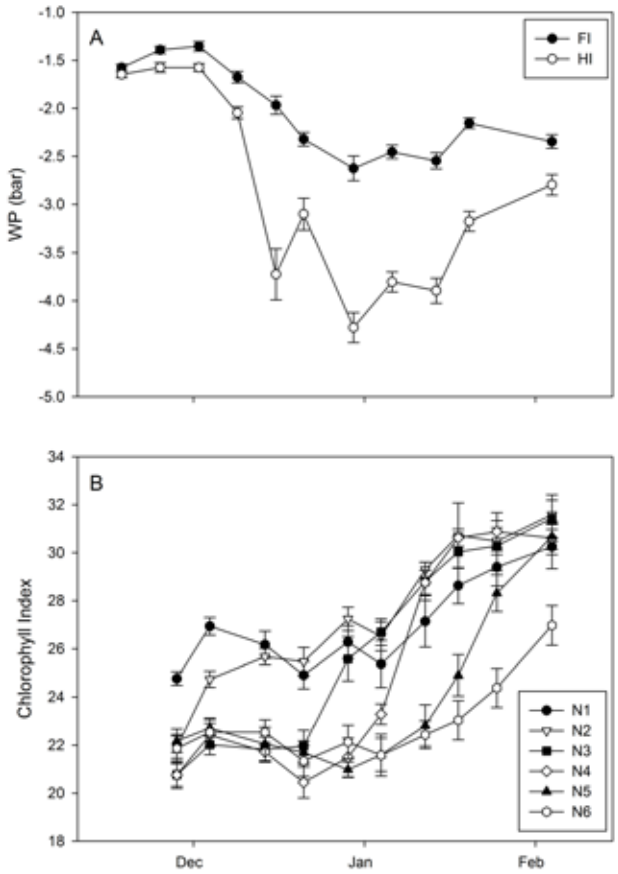


Figure 3.13 The impact of full (FI) and half (HI) irrigation treatments on dawn leaf-water potential (A) and six N application times (N1, N2, N3, N4, N5 and N6) on the chlorophyll index during berry development in potted Chardonnay vines (B). Standard errors are indicated as bars above and below the mean.

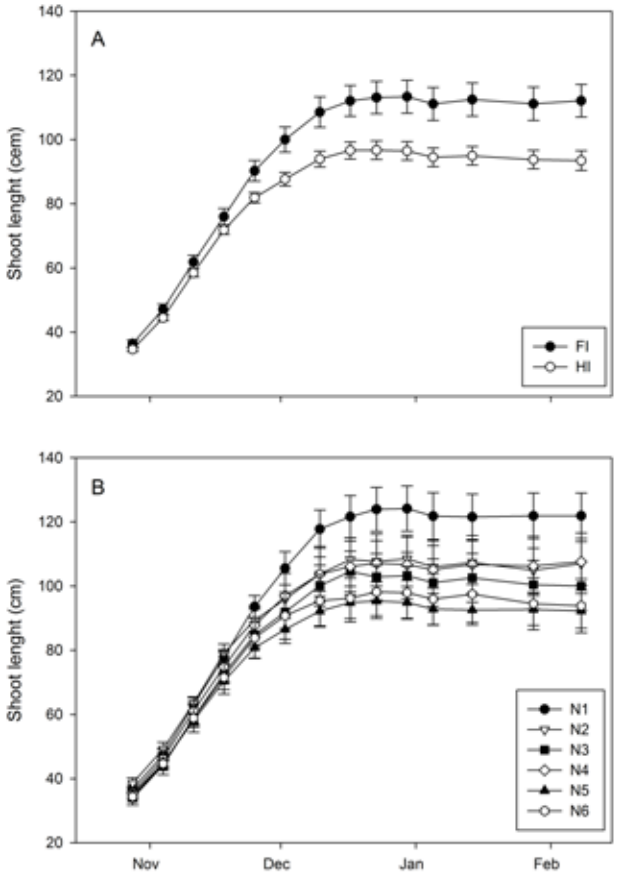


Figure 3.14 The impact of full (FI) and half (HI) irrigation treatments (A) and six N application times (N1, N2, N3, N4, N5 and N6) on shoot growth from fruit set to harvest in potted Chardonnay vines (B). Standard errors are indicated as bars above and below the mean.

shoot growth of the N application at the later times is minimal. A reduction in shoot growth by limited water and N supply is a common response, with the timing of N adding some new information, by indicating the point of time, when N application is less likely to enhance shoot growth. The berry weight measurements were only conducted on six berries through the development from fruit-set to harvest. The initial weight was around 0.2 g and at harvest around 1.2 g, with the weight final weight slightly lower in the HI treatment by 68 mg, the impact of the N treatment was insignificant (*Figure 3.15*). Consequentially, both yield and shoot weight (including leaves) was reduced by the HI treatment, by 23 and 27% respectively. The earliest N1 application led to the highest fruit yield and shoot weight (*Figure 3.16*). Water stress often reduces berry size and is commonly used to enhance fruit composition and limit shoot growth in red varieties. Application of N can elevate yield and enhance shoot growth, with the timing of N supply being crucial for the increase of both.

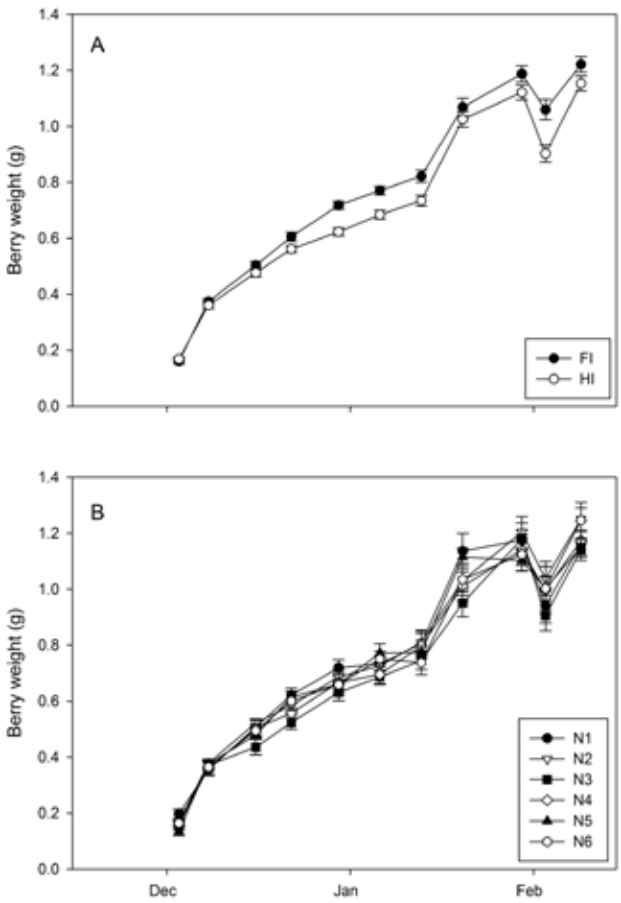


Figure 3.15 The impact of full (FI) and half (HI) irrigation treatments (A) and six N application times (N1, N2, N3, N4, N5 and N6) on berry weights during berry development in potted Chardonnay vines (B). Standard errors are indicated as bars above and below the mean.

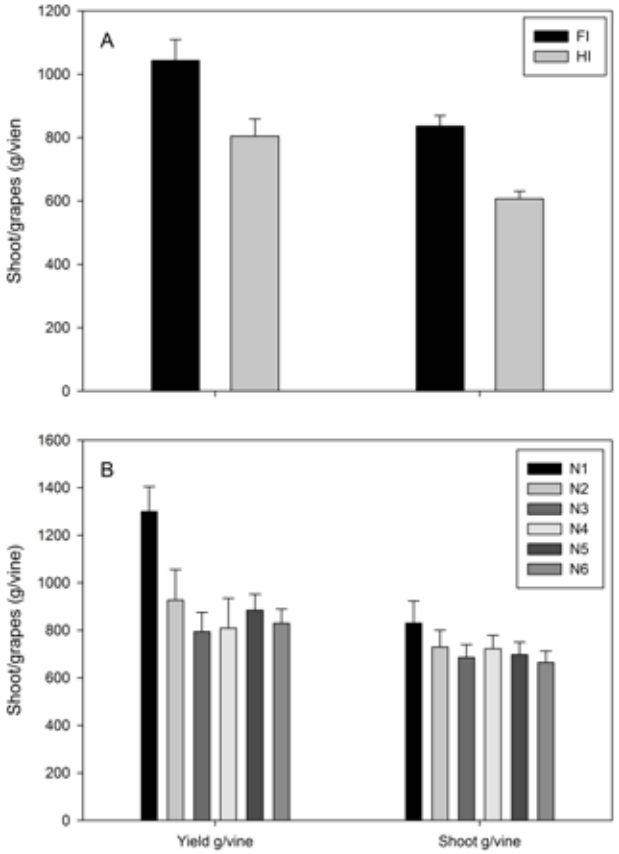


Figure 3.16 The impact of full (FI) and half (HI) irrigation treatments (A) and six N application times (N1, N2, N3, N4, N5 and N6) on grape yield and shoot weight (including leaves) at harvest in potted Chardonnay vines (B). Standard errors are indicated as bars above and below the mean.

Conclusions

The findings show that significant amount N is still taken up by the vine during grape maturation, being indicated by the chlorophyll content. The measurements also indicated that likely due to the reduced growth and size of the plants by the reduced irrigation, the chlorophyll index is higher. The timing of N application has been observed to be also important for shoot growth, being more pronounced with the earliest applications shortly after fruit-set. The annual components of the vine determined at harvest are higher with FI, but also with the N1 treatment. However, the partitioning of N between the annual and perennial section of the vines will be further assessed. The determination of the amino N will the most important part of this pot trial study, by indicating the best timing of N for grape composition.

As indicated above, at the time of this report not all analysis was completed (particularly for total $N/^{15}N$ and amino-N), since it was additional work not anticipated in the research program. However, it planned that most the remaining analysis will be

completed by the end of this year. This would provide further information of the allocation of N to the annual (shoots and grapes) and perennial organs (wood and trunk), and therefore to the overall project outcomes.

Experiment 3.5
The net carbon balance in relation to growth and biomass accumulation of *Vitis vinifera* cv. Semillon vines

Materials and methods

Plant material and growth conditions

Six potted Semillon (*Vitis vinifera* L.) vines (four year-old) on own roots were grown from prior to budbreak in a 6 m^3 controlled environment chamber (TH6000, Thermoline Scientific, Smithfield, Australia) for 150 days. The vines had previously been spur-pruned and were grown in 20 L pots in a sand, soil and fertiliser potting medium. Between 8 and 10 shoots developed and 4–6 on each vine were retained. Each shoot had an average of 1.8 bunches. The photon flux density PFD) was 800 μmol m^{-2} s^{-1} provided by an array of 4 x 1 kW High pressure discharge lamps (Powerstar HQI –T1000, Osram, Germany) and 8 x 20 W compact fluorescent lamps (cool white, Fairway, China) over a 12 h photoperiod. The day/night temperatures were 25/15 ±0.5°C and the corresponding vapour pressure deficits of the air were 1.0/0.6 ±0.1 kPa. The vines were watered regularly with an automated watering system and well supplied with nutrients.

Growth measurements

At 2–3 day intervals, leaf dimensions width and length) and stem lengths were measured on four fruiting shoots on each of the six vines. Leaves dimensions were measured from the time of appearance and continued until successive measurements indicated no further expansion was occurring. Shoot growth was terminated just after the 30th leaf had emerged by detaching the apical bud. All lateral shoots were removed from the main shoot as they appeared. Flowering occurred at 38 days after budbreak (DAB) and bunch growth was followed by regular length measurements. At harvest, determined by when the bunches reached maturity (25°Brix), the shoots were detached and the area of each leaf measured with a leaf area meter (LI3100, LiCor, Lincoln, Nebraska, USA) and leaves, stems and bunches oven-dried at 60°C for 2–3 weeks.

The measured leaf dimensions were converted to a leaf area through the product of length and width Sepúlveda and Kliewer 1983). Another linear relationship, (r^2 = 0.964, P<0.001) between leaf area and dry weight was determined from the destructively harvested leaves and used to estimate leaf biomass throughout the course of the experiment. A quadratic relationship (r^2 = 0.962 P<0.001) between stem dry weight and length was determined from the destructively harvested stems and used to estimate stem biomass throughout the growth stage.

At harvest, bunch dry weights were regressed against length (r^2 = 0.755, P<0.001) and then this relationship was used to convert the bunch length measurements over time to dry weights. For each vine, the cumulative bunch weights per shoot over time were calculated. All estimates of shoot area expansions and biomass accumulations were informally adjusted to ensure the estimated values matched those actually measured at harvest.

Net photosynthesis

At about 7–10 day intervals, net photosynthesis was measured on all leaves present and above about 30 mm in diameter on the selected shoot of each of the six vines. As the shoots grew, the expanding leaves were also measured, thus, up to 29 leaves of each shoot were measured on each occasion. An open gas exchange system and leaf chamber (LI-6400, LiCor, Lincoln, Nebraska, USA) was used with irradiance provided by the LED light source (6400 02B, LiCor). Measurements were conducted at a PFD of 900 μmol m^{-2} s^{-1} and a leaf temperature of 25°C.

Light and temperature photosynthetic responses were also determined for selected leaves using the LiCor gas exchange system and light and temperature control facilities.

Calculations of net carbon balance

For each vine and on each day of measurement, the mean total shoot leaf area was determined as the sum of all leaves present. The mean shoot cumulative leaf biomass for each vine was subsequently determined from the regression equations between leaf area and dry weight. Similarly, mean cumulative stem and bunch biomass for each vine was determined from the length of the stems and bunches each day. Total shoot biomass over the course of the experiment was then determined each day as the sum of the leaf, stem and bunch biomass. The data for leaves, stems

and bunches were then mathematically differentiated to determine the daily rate of carbon accumulated as biomass, assuming that 45% of the biomass was elemental carbon, over the whole growing period and then each mathematically integrated to give a sum total. Total shoot carbon accumulation was determined as the sum of leaves, stems and bunches.

For each vine and on each day of measurement, the net rate of photosynthesis was integrated over the day to obtain the net daily CO_2 fixation for each leaf, assuming the photosynthetic rates were generally constant throughout the day in the controlled environment conditions (Greer 1999; Greer and Wünsche 2003). The mean net daily CO_2 fixation per shoot for each vine was then determined as the product of the mean leaf area and photosynthesis for each leaf and accumulated over the number of leaves and leaf area present on the day of measurement. Rates of photosynthesis averaged over all leaves were about constant over the days of measurements not shown) thus assumed to be comparable between the days of measurement. Using a value for leaf respiration of 0.7 μmol CO_2 m^{-2} s^{-1}, obtained from light response data, net carbon acquisition for the developing shoot was then determined by summation over each day for each vine, taking into account the molecular fraction of carbon in CO_2 (Wullschleger *et al.* 1997; Greer *et al.* 2003). The net daily shoot carbon balance for each vine was then determined as the difference between the net daily carbon acquisition and the net daily carbon sequestration as biomass.

Results and discussion

An initial study into the heat impacts on Semillon vines using a single day 40°C event indicated no damage to any process had occurred and this included shoot growth, bunch growth, photosynthesis and the derived net carbon balance. However, as the carbon balance underpins the growth and development of the grapevine, it was decided to use these data to develop a basic understanding of grapevine performance in carefully controlled condition where fluctuations in environmental conditions are minimised, this ontogentical effects could be evaluated.

Shoot leaf and stem growth over time

In all cases, shoot leaf biomass (*Figure 3.17A*) increased over the growth stage in a sigmoid pattern, with growth completed at about 80 days after budbreak (DAB). Across all vines, the whole shoots at harvest averaged 13.4 ±0.1 g in leaf biomass. The duration of leaf biomass increasing from 20 to 80%

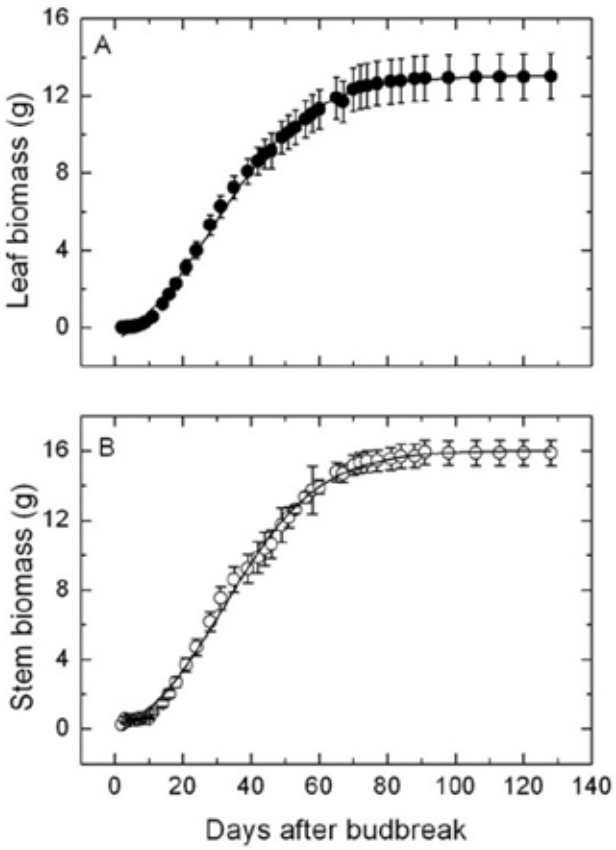


Figure 3.17 Accumulation of leaf biomass (A) and stem biomass (B) of shoots of Semillon vines over the course of the experiment from days after budbreak (Mean ±SE, N = 4-6). The data were averaged over all shoots on each vine. The lines are the best-fit to the Boltzmann sigmoid function fitted to the data in each case.

of the maximum was between 9 and 48 days, with the maximum rate of increase occurring at 28.9 ±0.8 DAB. The relative growth rate of leaf biomass accumulation over all vines averaged 0.27 ±0.03 g $g^{-1}d^{-1}$.

As with leaf weight accumulation, stem biomass for all vines also increased in a sigmoid pattern (*Figure 3.17B*), with growth being completed about 80 DAB. The duration for the biomass to increase from 20 to 80% of the maximum was from 13 to 51 days, with the maximum rate occurring at 32.4 ±0.7 DAB. Shoots averaged 16 ±0.7 g in dry weight and the relative growth rate of stem biomass accumulation averaged 0.35 ±0.04 g g^{-1} d^{-1} over all vines. Thus the dynamics of stem growth were slower than leaf growth but rates of biomass accumulation were higher in stems than in leaves.

These date showed there were some differences in the patterns of biomass accumulation between leaves and stems of Semillon vines, with the leaf growth pattern generally occurring sooner than the stem growth pattern as indicated by the times of

maximum expansion (28.9 ±0.8 *cf.* 32.4 ±0.8 days) by about four days overall. However, stem growth rates were significantly (P<0.01) higher than for leaves and overall accumulation of biomass was greater in the stems. By contrast, stem extension and shoot leaf area expansion of Semillon shoots both occurred significantly sooner than biomass accumulation, with maximum rates being reached 13 and 21 days after budbreak, respectively. These results demonstrate differences in the dynamics of growth and development of the Semillon vines.

Bunch growth

Bunch dry weight accumulation commenced shortly after fruit set and followed a curvilinear pattern (Figure 3.18) to reach an average of 42.5 ±6.1 g shoot^{-1} across all vines. There were on average 8 ±0.8 bunches vine^{-1} and individual bunches averaged 22.2 ±2.6 g dry matter (DM) although they were highly variable.

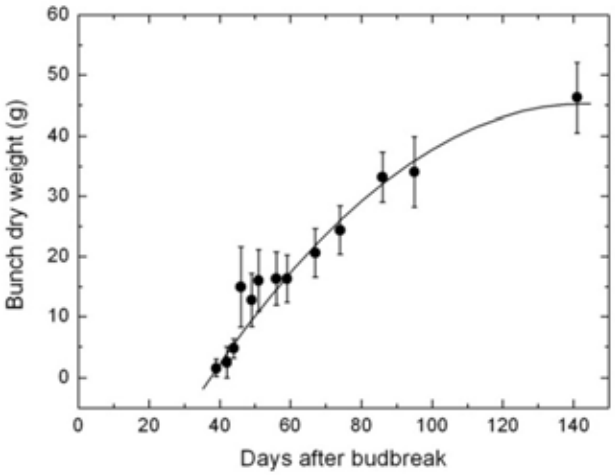


Figure 3.18 Bunch dry matter growth (Mean ±SE, N = 2-3) of Semillon vines as a function of time. The data were averaged over all bunches on each shoot. The line is the best fit to a sigmoid function fitted to all data.

Allocation of biomass

Biomass allocation (*Figure 3.19*) to both leaves and stems remained about equal throughout the growth period at about 50% each for the first 30 DAB. By then, the proportion of the total as leaves and stems declined progressively to about 25% as the allocation to the bunches gradually increased. At harvest, 21.6% of biomass was allocated to leaves, 23.9% to stems and 54.5% to bunches.

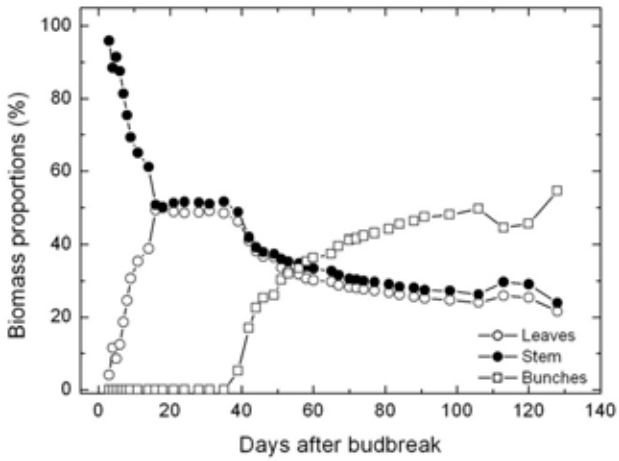


Figure 3.19 Changes in biomass distribution between leaves, stems and bunches (Mean ±SE, N = 6) throughout the course of the experiment for Semillon vines grown in a controlled environment. The data were averaged over all vines. Standard errors are smaller than the symbols in most cases.

Thus, bunches accumulated the most biomass once growth commenced. Leaves and stems both averaged about 20–25% of the total biomass while bunches averaged about 50%. Consistent with these data, mature field–grown Semillon vines allocated about 20% to leaves, 30% to stems and 50% to bunches (Greer *et al.* 2010). In general, these proportions are comparable with potted Pinot Noir vines although more biomass was allocated to leaves than stems in this variety (Petrie *et al.* 2000). In mature Sangiovese vines, proportions of biomass as stems and leaves both ranged between 29 and 36% while bunches were 26–39% of total above ground biomass (Palliotti *et al.* 2004). Chambourcin vines partitioned 67% of the biomass to bunches but only 7% to stems and 27% to leaves (Miller *et al.* 1997). Across a number of other varieties including Shiraz and Riesling, the proportion of leaf biomass at 50–60% consistently exceeded the proportion of stem biomass at 30–40% (Buttrose 1969), except that these vines were one year old vegetative cuttings. Thus, the allocation of biomass to leaves, stems and bunches clearly differed between varieties and also depended on the age of vines.

Photosynthesis

Photosynthesis along the shoot at selected times (*Figure 3.20A*) showed rates shortly after budbreak were highest in the early emerged leaves and progressively declined in young, recently emerged leaves. After flowering (*Figure 3.20B*), rates of net photosynthesis of the oldest few leaves had declined somewhat while the leaves around node 5–6 retained high rates at 10 μmol CO_2 m^{-2} s^{-1} and all other leaves except the very youngest had relatively similar rates, typically around 7.5 μmol CO_2 m^{-2} s^{-1}. This pattern persisted through canopy development (*Figure*

3.20C), with rates again ranging between 6 and 9 μmol CO_2 m^{-2} s^{-1}.

Over time, net photosynthesis of selected leaves (*Figure 3.21*) was highest in those leaves emerging first and generally lower with later emerging leaves. In each case, net photosynthesis increased to a maximum of about 12 μmol CO_2 m^{-2} s^{-1} for leaf 5 at about 20 DAB while for leaf 10, the maximum rate was about 8 μmol m^{-2} s^{-1} which occurred about 70 DAB. Maximum rates for leaves 15 and 20 were 7 and 6 μmol CO_2 m^{-2} s^{-1}, respectively and peaked at 60 and 70 DAB.

Throughout the day, average net photosynthesis varied between 6 and 8 μmol CO_2 m^{-2} s^{-1} (*Figure 3.22*) with no obvious pattern in accordance with the constant temperature, VPD and PFD conditions.

These results show net photosynthesis of the Semillon leaves was well within the range reported for other grape varieties (Poni and Giachino, 2000; Petrie *et al*. 2003). However, the pattern of net photosynthesis over time for individual Semillon leaves consistently showed a maximum being reached and then the rates declining, as also shown for Sultana (Kriedemann *et al*. 1970), Seyval (Edson *et al*. 1995) and Cabernet Sauvignon vines (Poni and Giachino 2000) This is a well established pattern for leaf photosynthesis (Flore and Lakso 1989). However, both the absolute maximum net photosynthesis in Semillon leaves and the time it occurred varied with leaf position, higher and earlier for proximally positioned leaves and lower and later for distally positioned leaves. The maximum rates also differed by about 2-fold between leaf 5 and leaf 20. Similar patterns in net photosynthesis along a shoot have been observed in Seyval grapevines (Edson *et al*. 1995), *Sassafras albidum* (De Soyza and Kincaid 1991) and *Actinidia deliciosa* shoots (Greer

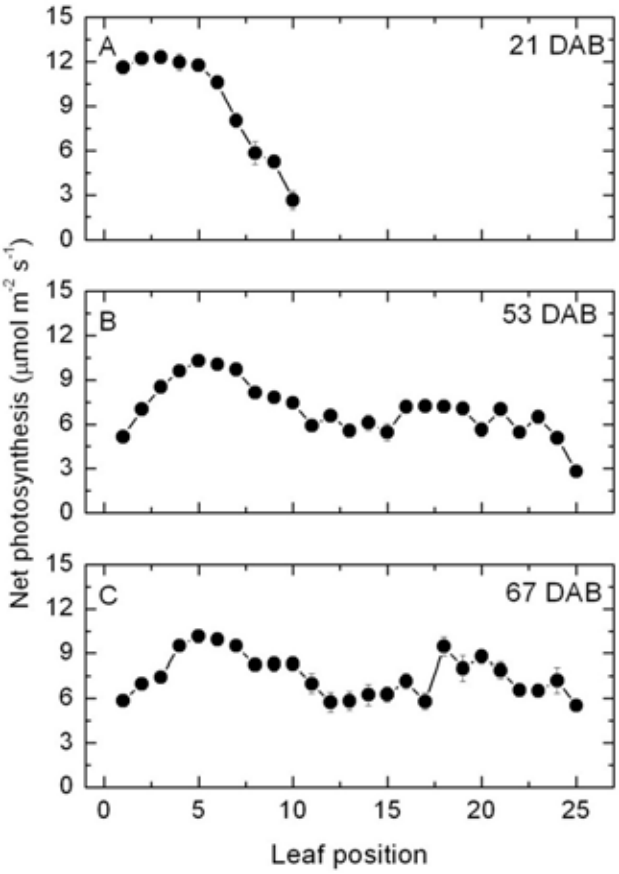


Figure 3.20 Mean rates of net photosynthesis (Mean ±SE, N = 6) of for leaves along the shoot at 21, 53 and 67 DAB during the growing season for Semillon vines grown in a controlled environment. These data were averaged over all vines.

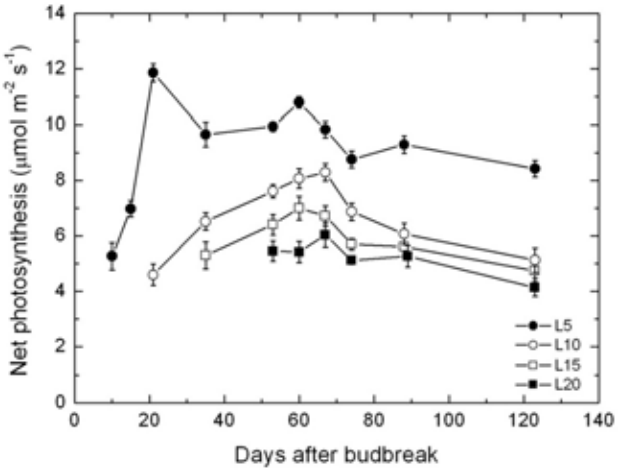


Figure 3.21 Mean rates of net photosynthesis (Mean ±SE, N = 6) of selected leaves as shown throughout the course of the experiment of Semillon vines grown in a controlled environment. L5 – L20 refer to the leaves at the indicated node positions. The data were averaged over all vines.

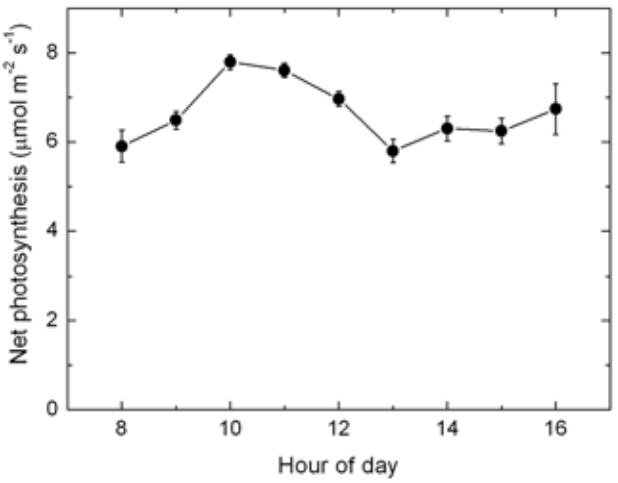


Figure 22 Mean rates of net photosynthesis (mean ±SE, n=30) throughout the course of a day for *Vitis vinifera* cv. Semillon vines grown in a controlled environment. The data were averaged over all leaves.

and Jeffares 1998). Thus, not only were the earliest emerging Semillon leaves the largest and the fastest to expand (Greer and Weston 2010*b*) but also the fastest to reach their maximum net photosynthetic rate, for example rates for leaves at nodes 1–2 for instance averaged 7.7 ±0.5 μmol CO_2 m^{-2} s^{-1} just 15 days after budbreak, respectively and also have the highest rates overall. Pinot noir leaves also reached 60% of maximum rates in just 15 to 20 days (Bertamini and Nedunchezhian 2003). These attributes are clearly an adaptation to maximise carbon acquisition after budbreak has occurred.

Despite these rapid rates of leaf expansion and net photosynthesis, the carbon acquisition that occurred in the first 10 DAB was almost negligible and most growth would have been supported by reserves (Loescher *et al.* 1990; Goffinet 2004). However, by 20 DAB and through to about 65 DAB, rates of carbon acquisition increased more or less continuously to a maximum rate of 0.8 g C $shoot^{-1}$ d^{-1}. This was coincident with and primarily driven by the canopy leaf area expansion. Thereafter, carbon acquisition rates declined slightly and this was probably also driven by the canopy not expanding further but also the reduction in rates of net photosynthesis. The total carbon fixed for the Semillon vines between budbreak and harvest was about 70 g C $shoot^{-1}$. This compares favourably well with that estimated at about 60 g C $shoot^{-1}$ for spur-pruned Riesling vines over the growing season (Downton and Grant 1992) but apparently lower than for a whole Sangiovese vine at 860 g C $vine^{-1}$ estimated from Palliotti *et al.* (2004). Daily carbon gain of Temperanillo vines was maximal at 7 g C $m^{-2}d^{-1}$ (Escalona *et al.* 2003) and for Riesling vines was maximal at 4.3 g C m^{-2} d^{-1} (Weyand and Schultz 2006). The comparable acquisition rate for the Semillon vines was 4 g C m^{-2} d^{-1}, thus well in keeping with other varieties. However, these rates of carbon acquisition for grapevines were markedly below that of *Actinidia deliciosa* shoots, which had maximum rates of about 5 g C $shoot^{-1}$ d^{-1} and fixed a total of 180 g C $shoot^{-1}$ (Greer and Jeffares 1998). However, the more than 10-fold greater leaf area of Actinidia vines compared to the Semillon vines probably also accounted in large part for the differences in carbon acquisition between the two species.

Net carbon balance

In spite of early increases in leaf area and high rates of net photosynthesis just after budbreak, the net rate of carbon acquisition was relatively slow to increase and remained negligible for about 10 DAB (*Figure 3.23A*). However, the rate increased rapidly after the initial delay and although there was some perturbation at about 40 DAB, the rate of carbon acquisition increased to a peak of 0.84 ±0.07 g $shoot^{-1}$ d^{-1} at 70 DAB. Thereafter, the rate declined by 25% to become relatively stable at 0.65 ±0.05 g $shoot^{-1}$ d^{-1} after 90 DAB. Over the entire growth period, on average, these Semillon vines acquired a net total of 69.5 g C $shoot^{-1}$.

By contrast, the rate of carbon sequestration as biomass increased very rapidly just after budbreak, without any notable lag, for about 20 days then increased more slowly to reach a peak of 0.49 ± 0.06 g $shoot^{-1}$ d^{-1} at about 40 DAB (*Figure 3.23B*). A steady decline in the rate of carbon sequestration occurred thereafter to reach a low rate, consistent with vines having essentially stopped growing. Over the growing period, 6.1 g C $shoot^{-1}$ was accumulated as leaves, 6.9 g C $shoot^{-1}$ as stems and 19.2 g C $shoot^{-1}$ as bunches giving the total carbon sequestered

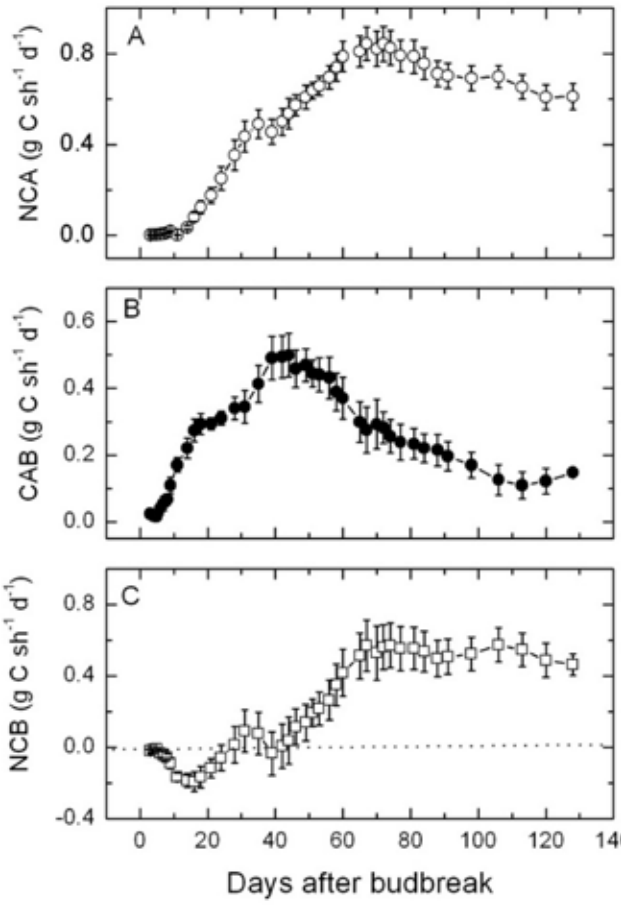


Figure 3.23 Changes in the net rates of carbon acquisition (A), carbon accumulated as biomass (B) and the carbon balance (C) of shoots of Semillon vines grown in a controlled environment Mean ±SE, N=6). The dotted line in C indicates where the carbon balance is zero. The data were averaged over all vines.

in biomass for these vines at 32.3 g shoot^{-1}. It was noteworthy that rate of carbon sequestration peaked some 30 days before the rate of carbon acquisition.

As a consequence of both the slow rate of acquisition and the high rate of carbon sequestration occurring in these vines just after budbreak, the net daily carbon balance became increasingly negative to a maximum of -0.19 ±0.05 g shoot^{-1} d^{-1}, at 16 DAB, indicating a net loss of carbon occurred from the shoots (*Figure 3.23C*). Thereafter, the carbon balance increased to become just positive at 28 DAB but a perturbation occurring around 40 DAB, caused the carbon balance to decrease and almost become negative again. This occurred about coincidentally with bunch growth commencing (cf. *Figure 3.18*) and perhaps indicative of the sudden shift in biomass allocation. Integration of these data over the first 42 days indicated nearly 2 g C shoot^{-1} in total were consumed in growth. After that, the carbon balance increased consistently to reach a maximum rate of 0.57 ±0.12 g shoot^{-1} d^{-1} at 74 DAB. In keeping with reduced acquisition in the later growth stage, the carbon balance rate also declined slightly. Integration of these data from 42 DAB until harvest indicated these vines produced a surplus of about 39 g C shoot^{-1}. In total then, over the whole growth period, a net gain of 37.2 g C shoot^{-1} occurred, in these Semillon vines. Presumably this was exported from the shoots to other sinks such as the roots.

From these results, it was apparent that carbon sequestration into biomass in the Semillon vines began with virtually no delay, most likely from the early stem extension. The rate of sequestration increased very rapidly to be about 0.3 g C shoot^{-1} d^{-1} at just over 20 DAB and maximal at about 0.5 g C shoot^{-1} d^{-1} after 40 DAB. The rate more or less declined continuously until about 100 DAB when there was only slow conversion of fixed carbon into biomass. This general pattern of rates increasing to a maximum and then declining also occurred in *Actinidia* vines grown at comparable temperatures (Greer and Jeffares 1998; Greer *et al*. 2003). The maxima between the two species were very different again, at about 2 and 0.5 g C shoot^{-1} for *Actinidia* and Semillon vines respectively. Riesling vines accumulated about 40 g C shoot^{-1} as new biomass over the whole growing season (Downton and Grant 1992) and the total for the Semillon vines was just over 32 g C shoot^{-1} and again apparently lower than for whole Sangiovese vines at 857 g C vine^{-1} estimated from Palliotti *et al*. (2004). By comparison, the total for *Actinidia* vines was 244 g C shoot^{-1} (Greer *et al*. 2003).

As a consequence of the initial delay in carbon acquisition but not in carbon sequestration, the Semillon shoots consumed carbon resources, presumably reserves, from outside of the shoot to meet the growth demand at least for a period after budbreak. Some 2 g C shoot^{-1} in total were consumed in the first 6 weeks of growth. This consumption of carbon conforms with results of Hansen (1971), who showed that the first 5–6 leaves of extension shoots of apple trees were entirely supported by imported carbon from reserve pools. The time for the net carbon balance to become positive was also comparable with that for *Actinidia* vines (Greer *et al*. 2003), walnut (Maillard *et al*. 1994) and other species Radoglou and Teskey 1997). Consistent with these data, Goffinet (2004) showed both xylem and phloem starch concentrations in Concord grapevines declined markedly from budbreak until about 25 DAB, as also shown for root starch in Merlot and Pinot Noir vines (Zapata *et al*. 2004), consistent with a period of reserve consumption and the net negative carbon balance of the shoots in the present study. Once a positive carbon balance occurred in Semillon vines, the rate of carbon accumulation increased linearly as in other species (Greer and Jeffares 1998). Overall from budbreak to harvest, the cost of growing shoots leaves and stems) was 9 and 10% of the fixed carbon and for the bunches was 28% and the balance of 53% the net surplus which amounted to 37 g C shoot^{-1}, was presumably exported from the shoots to other sinks such as the roots. Fruiting Riesling vines had an estimated surplus of 17 g C shoot^{-1} (Downton and Grant 1992) and *Actinidia* vines over 200 g C shoot^{-1} (Greer *et al*. 2003). Young apple trees had a surplus between carbon fixation and sequestration of 11 g, calculated from Procter *et al*. (1976). It was noteworthy that the carbon surplus in the Semillon vines nearly matched the total biomass allocated to the bunches and might imply more bunches could have been supported than were carried. However, given the importance of carbohydrate reserves in supporting spring growth, it seems likely that any surplus carbon would be readily allocated to these reserves.

Conclusions

The shoots of Semillon vines grown in a controlled environment accumulated approximately comparable amounts of biomass as leaves and stems and about twice as much biomass as bunches but invested 9,

10 and 28% of the available fixed and stored carbon, respectively, indicating reproductive growth was highly demanding of resources. Rates at which carbon was sequestered into biomass increased most rapidly within 20 DAB but lags in photosynthetic carbon acquisition lead to an initial deficit in the shoot carbon economy. About 2 g C shoot^{-1} of heterotrophically-supported growth from reserve carbohydrate pools was required to sustain early growth. Fully autotrophic growth, as indicated by increased rates of carbon acquisition and a positive carbon balance, occurred at about 40 DAB coincidentally with bunch growth commencing. Overall, despite the very high demand by bunches for carbon these shoots, nevertheless, had sufficient carbon to sustain all growth and achieved a 53% surplus, almost equal to the bunch biomass, and which may well have been exported to roots for storage.

Experiment 3.6
Effects of fruiting on vegetative growth and development can be traced back to events at or before budbreak

Materials and methods

Plant material and growth conditions

Nine DORmant Semillon grapevines on own roots were transferred to a growth chamber (TH6000, Thermoline Scientific, Smithfield, Australia) in early July (mid winter) for 150 days. Six of the vines flowered and produced bunches and the remaining three were vegetative (no flowers were produced). The five year old vines had previously been spur-pruned and were grown in 25 L pots containing potting media (soil, sand, and fertiliser). Between 8 and 10 shoots developed and 4-5 were retained on each vine. Each shoot on the fruiting vines had an average of 1.8 bunches. The vines were grown at a photon flux density (PFD) of 870 μmol m^{-2} s^{-1}, provided by 4 x 1 kW high pressure discharge lamps (Powerstar HQI–T1000, Osram, Munich, Germany) and 8 x 20 W commonly available compact fluorescent lamps over a 12 h photoperiod. The day/night temperature was 25/15 ±0.5°C and the corresponding vapour pressure deficit was 1.0/0.6 kPa. The vines were watered daily with an automatic system and well supplied with nutrients throughout.

Growth measurements

The length of each of four to five primary shoots per vine, the width and length dimensions of each leaf and the length of each internode on these shoots was measured at regular intervals (2-3 days) from the time when each metamer achieved about 10 mm in diameter or 5 mm in length. Shoot length was measured throughout the growth period but leaf and internode growth were measured until the maximum size was achieved, as indicated by no change in successive measurements. All lateral shoots that appeared on the shoots were removed. Growth was concluded at about the time in days after budbreak when approximately 30–32 leaves had emerged. Flowering occurred at 38 DAB and veraison at 101 DAB on the fruiting vines.

At the conclusion of the growth phase at 156 DAB, all shoots were detached just above the second node. Leaves were detached from each shoot and the leaf area measured (LI3000, LiCor Inc., Lincoln, Nebraska, USA). All internode lengths on each shoot and total shoot lengths were measured then all leaves and stems were oven-dried at 60°C for two weeks and dry weights of each leaf and stem determined. Total shoot leaf area expansion for each shoot on each vine was determined by integration of all leaves present on each day of measurement and shoot length extension determined by integration of internode lengths over each day of measurement.

Bud dissections

Five randomly chosen shoots each containing 4 buds from nodes 2 to 5 were collected from vineyard-grown Semillon vines when DORmant and cut into the individual buds. These were fixed into a solution containing 5% Formaldehyde (Sigma Chemical Co. St. Louis, Mo, USA) as a fixative, 5% Propionic acid Sigma Aldrich Pty. Ltd. Castle Hill, NSW, Australia) to permeate the cells to allow infiltration of solvents and resin and 50% Ethanol buffer to inhibit fungal growth. The buds were kept in this solution for 10 days and then were dried down with increasing gradients of ethanol from 60 to 90%, each at a minimum of two hours. For infiltration and embedding, the buds were submerged in Lecia Historesin (Leica Microsystems, Nusslock, Heidelberg, Germany) for two days to allow resin to infiltrate the cells of the bud. The resin was then poured off and replaced with fresh resin and allowed to infiltrate for another two days.

The buds were then embedded in a gelatine capsule by filling the capsule with a small quantity of resin, inserting the bud with the correct orientation,

topping up the capsule with resin and then capping the capsule. Each capsule was then placed in a 60°C oven overnight to allow the resin to polymerise. Buds were then sectioned with a Leica RM2265 rotary microtome (Leica Biosystems Melbourne Pty. Ltd, Mount Waverly, VIC, Australia). Sections were mounted on a slide using a drop of water and then fixed to the slide by placing on a heating plate until all water has evaporated. Each section was 5 µm thick and approximately every 7th section was mounted on a slide to be viewed.

For staining, the slides were place in a bath of toluidine blue (Proscitech, Thuringowa Central, QLD, Australia) at 0.1%, rinsed dried and then coverslipped using DPX Mountant 80% Xylene (Proscitech). Slides were observed and imaged under bright field using a Leica M165 FC Fluorescence microscope (Leica Biosystems Melbourne Pty. Ltd, Mount Waverly, VIC, Australia). Images were processed using the analySIS Lifescience Soft Imaging System (Gulfview Heights, SA, Australia).

Results and discussion

Leaf and internode growth patterns

Leaf growth followed a sigmoid pattern in each case (*Figure 3.24A*), with maximum leaf size decreasing with the node position along the shoot from the base. Leaves at node five were the largest at an average of 0.013 ±0.0017 m^2. Internode extension (*Figure 3.24B*) also followed a sigmoid pattern, again with the maximum size of internodes declining along the shoot from a maximum of 69.3 ±0.9 mm at node position six.

It was evident from this figure in directly comparing the leaves and internodes that internode growth was earlier and more rapid than leaf expansion at the same node, at least in the early emerging nodes

Leaf and internode appearance

Over all vines and shoots, budbreak occurred at 20 ±0.2 days after the vines were placed in the growth chamber. For vegetative vines, leaf appearance commenced within a day of budbreak (*Figure 3.25*) and the first 5 leaves emerged over 3–4 days at a rate of 1.4 ±0.2 leaves d^{-1}. Thereafter, successive leaves along the shoot to about node 19 appeared at a constant but nevertheless significantly (P<0.001) slower rate (0.44 ±0.02 leaves d^{-1}). From about node 20, there was a slight change in the rate of leaf appearance (0.35 ±0.04 leaves d^{-1}) though not significantly (P=0.11). For the fruiting vines, the first cohort of five leaves also appeared within a few days of each other (*Figure 3.25A*) and at a rate of 0.9 ±0.1 leaves d^{-1}. Thereafter, successive leaf appearance along the shoot occurred in two distinctive cohorts, centred at about node 19 and characterised by significantly (P<0.001) different rates of leaf appearance. The second cohort of leaves between nodes 6 and 19 appeared at a rate of 0.41 ±0.02 leaves d^{-1} thus similar to the rate of appearance of vegetative vines. For leaves in the third cohort beyond node 20, however, the rate of leaf appearance was significantly (P=0.040) slower at 0.31 ±0.03 leaves d^{-1}.

The patterns of internode appearance (*Figure 3.25B*) were similar to that of leaf appearance in that across the whole shoot, internodes appeared in a linear pattern within each cohort. The first cohort of internodes 1–5 appeared within 3–5 DAB in synchrony with appearance of each leaf at the same node. Rates of internode appearance for this cohort for either the fruiting or vegetative vines were not estimated because the regressions fitted to these data were not significant. By contrast, rates of internode appearance between nodes 6 and 19 were all highly significant

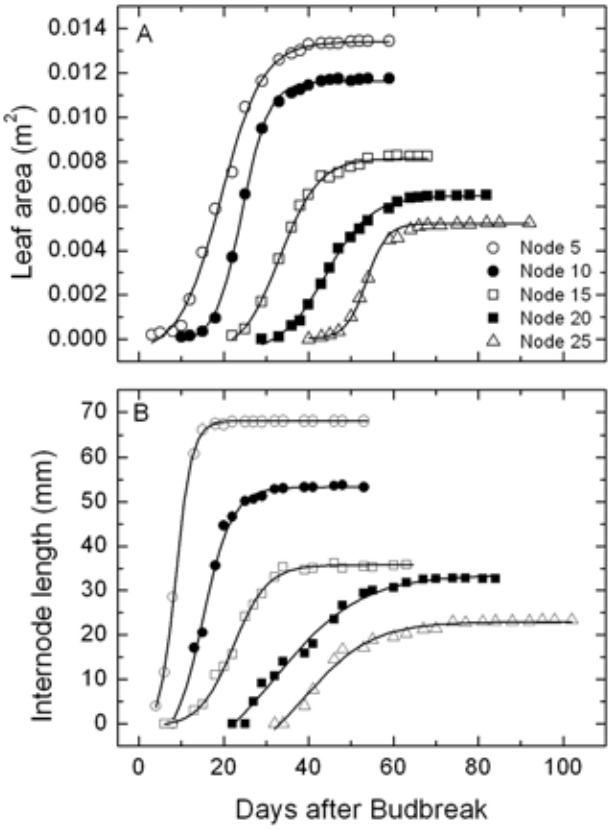


Figure 3.24 Leaf area expansion (A) and internode extension (B) over time after budbreak at selected node positions along a fruiting Semillon shoot as indicated with node 5 being at the proximal end of the shoot and node 25 at the distal end. The lines are the fit of the data to the Boltzmann sigmoid function in each case.

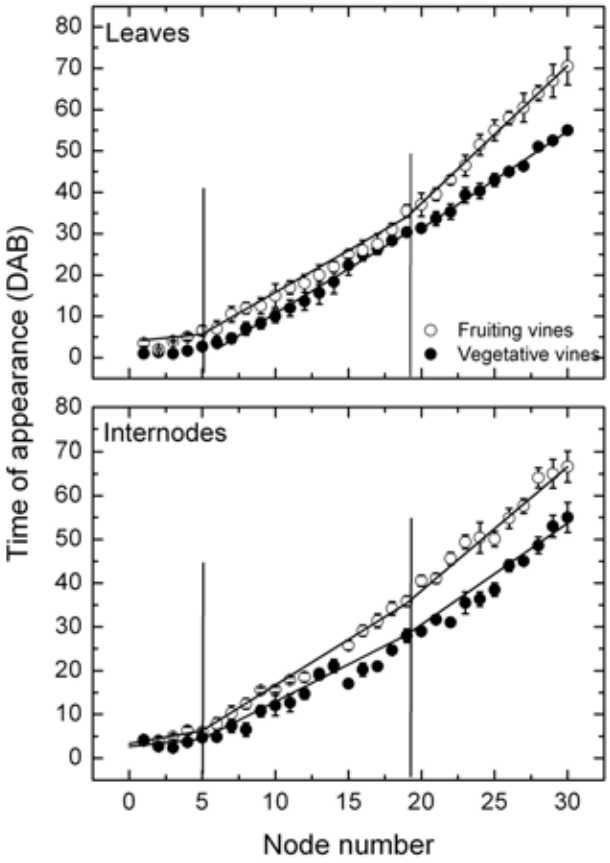


Figure 3.25 Leaf (A) and internode (B) appearance of vegetative and fruiting Semillon vines (Mean ±SE, n = 6 and n = 24, respectively) as a function of node position along the shoots. The vertical lines delineate the different zones characterised by changes in the rates of appearance. The other lines are fitted to the data by linear regression and are all highly significant ($P < 0.01$, $r2 = 0.9$) except for the fits to the data in the first zone nodes 1-5) which were not significant.

($P<0.0001$) at 0.28 ±0.01 and 0.54 ±0.03 internodes d^{-1} for fruiting and vegetative vines, respectively and these differences were significant ($P<0.0001$). Beyond node 20, the rates of internode appearance declined significantly ($P<0.001$) by 50–60% in both the fruiting and vegetative vines to 0.18 ±0.01 and 0.27 ±0.02 internodes d^{-1}, respectively. Again differences in rates of internode appearance between fruiting and vegetative vines were highly significant ($P<0.01$). Thus, rates of internode appearance were comparable with rates of leaf appearance for the cohort between 6 and 19 nodes but tended to be significantly ($P<0.01$) slower with the cohort of internodes beyond node 20.

Leaf and internode appearance of the Semillon grapevines grown in controlled conditions occurred at constant rates but could be resolved into at least three separate zones. The first zone was characterised by 5–6 leaves and internodes emerging more or less together as a cluster over a few days and was common to both the fruiting and vegetative vines. Each leaf and internode in this zone expanded to a markedly different size, more than tripling in size between the 1st and 3rd node. It was notable, however, that the largest leaves and internodes (nodes 5–6) in this zone on the fruiting vines were markedly smaller than comparable leaves on vegetative vines. This occurred despite floral morphogenesis not actually occurring for at least another month. However, these leaves and internodes were all preformed (May 2000; Gerrath *et al.* 2001) in the DORmant bud and it may be that their ontogenetic sizes were determined when the primordia were being formed. The presence of floral primordia in the bud may have competed with leaf primordia for allocation of carbon and hence the smaller sizes of leaf primordia. Buds are commonly most fruitful beyond node 4 (Sommer *et al.* 2000; Sanchez and Dokoozlian 2005) and consistent with this, for the Semillon vines, the average position for flowers/bunches to occur along the shoot was at the 4th node. It was at this position where differences in the size of leaves and internodes became apparent when comparing fruiting and vegetative vines.

The second zone of Semillon shoot development was characterised by both leaves and internodes of fruiting and vegetative vines emerging in a linear pattern but at a strikingly slower rate compared with the first zone metamers. Whereas rates of appearance in zone 1 were typically about 1–2 metamers every day, in Zone 2 this had declined to about one metamer every two days. Rates of leaf appearance in zone 2 were similar between vegetative and fruiting vines as has been also shown in Syrah and Grenache vines (Pallas *et al.* 2008). However, the Semillon leaves on the vegetative vines all emerged about 4–5 days earlier than comparable leaves on the fruiting vines. Likewise, the timing of internode appearance on vegetative vines was earlier than fruiting vines but because the rate of internode appearance on vegetative vines was significantly faster than for fruiting vines, the difference between them in time of internode appearance became increasingly different from about 4 to nearly 8 days from node 7 to 19. Thus, developmentally the 19th node on the vegetative vines produced a metamer 29 DAB whereas the same node on fruiting vines produced a metamer at the same position at 35 DAB.

On the basis of another change in rates of leaf and internode appearance occurring at or about node 19–20, a third zone of appearance was observed.

Again this was characterised by a linear pattern of leaf and internode appearance but also by another marked slowing of the rates of metamer appearance. Across both fruiting and vegetative vines and both leaves and internodes, rates of appearance in zone 3 declined about 30–40% compared with zone 2 to about one metamer appearing every four days. In this zone also, the time of appearance of leaves and internodes continued to become increasingly later in fruiting compared with vegetative vines, from about 9 days for node 20 to 14 days at node 30. Thus differences in development between fruiting and vegetative vines, first detected just after budbreak, continued to appreciate such that appearance at node 30 occurred at 55 DAB in the vegetative vines but not until 70 DAB in fruiting vines. Because flowering occurred at 38 DAB, that is around the time when nodes 20 to 21 where appearing, it might be tempting to suggest the presence of the third zone of appearance was attributable to a change in carbon demand by the developing flowers and bunches. Certainly this is a time in fruiting vines when carbon demand by the whole shoot increases dramatically (Greer and Sicard 2009). However, the rates of internode appearance on the vegetative vines declined markedly, by as much as 50%, between zones 2 and 3 while the comparable change occurring with leaf appearance rates (20%) was just non-significant.

The rates of leaf appearance for the Semillon vines in zone 2 and 3 were comparable with those reported for a range of varieties including Sultana, Shiraz and Riesling (Buttrose 1969), Cabernet Franc (Matthews *et al.* 1987), those estimated for Cabernet Sauvignon vines from Freeman and Kliewer (1984), Mataro (Moncur *et al.* 1989) and Grenache (Lebon *et al.* 2004). However, it has been proposed by Schultz (1992); Lebon *et al.* (2004) and Louarn *et al.* (2007) that rates of leaf appearance in grapevines, when based on a thermal time basis, were constant. The results of the present study with Semillon can only support this conclusion if a particular zone is considered because across the three zones of development, leaf and internode appearance rates differed markedly. While the present study was based on calendar time, in contrast with these other studies, it should be pointed out that thermal time in controlled environments accumulates as a linear function of calendar time and, therefore, the conclusions of the study were not dependent on the basis of determining the rates. Thus, rates of leaf and internode appearance in Semillon vines across the development of the whole shoot were not constant.

The conclusion that Semillon shoots have three distinct zones of shoot development has also been supported with results from Grenache and Syrah grapevines (Louarn *et al.* 2007). In these cultivars, the first two zones originated from preformed leaf primordia while the third zone originated from neoformed primordia. The bud dissection results for Semillon shoots are in accord with this conclusion. An identical pattern of development has also been demonstrated with *Actinidia deliciosa* vines (Seleznyova and Greer 2001).

It was notable that in the first two zones, Syrah shoots had 3 and 9 leaves and Grenache had 4 and 4 leaves, respectively (Louarn *et al.* 2007) compared with 5 and 14 in Semillon and 8 and 9 in *Actinidia* (Seleznyova and Greer 2001). These differences in numbers of leaves per zone may reflect varietal and species differences but perhaps also different methods of determining the number of metamers in the different studies. Several estimates put the number of preformed leaf primordia in DORmant buds of different *Vitis* cultivars, though not Semillon, at 12 (Mullins *et al.* 1992), no more than 10 (May 2000) and 8–11 (Pallas *et al.* 2008). By contrast, *Actinidia* vines have 17 performed leaf primordia (Seleznyova and Greer 2001). Our assessment of DORmant Semillon buds revealed 14–18 preformed leaf primordia occurred, which while more than estimates for other grapevine cultivars, accounted well for the total number of leaves in zones 1 and 2. Consistent with this, the number of preformed primordia in *Actinidia deliciosa* buds coincided directly with the boundary between zones 2 and 3 (Seleznyova and Greer 2001). Therefore, the explanation for three zones of shoot development in Semillon vines conforms to the conclusion that all metamers in zones 1 and 2 were preformed in the DORmant bud in the previous growing season while the leaves in zone 3 were neoformed from the shoot apical meristem in the present growing season.

Dynamics of leaf and internode development along the shoot

Timing of expansion From the Boltzmann function fitted to each leaf and internode, in a comparison of the timing of maximum extension (*Figure 3.26*) between leaves and internodes, internode extension occurred significantly earlier than leaf expansion for all nodes on the shoot, both for fruiting and vegetative vines. The regressions fitted to each cohort were all significant ($P<0.0001$) except for the internodes in zone 1 on the vegetative vines. The phyllochron

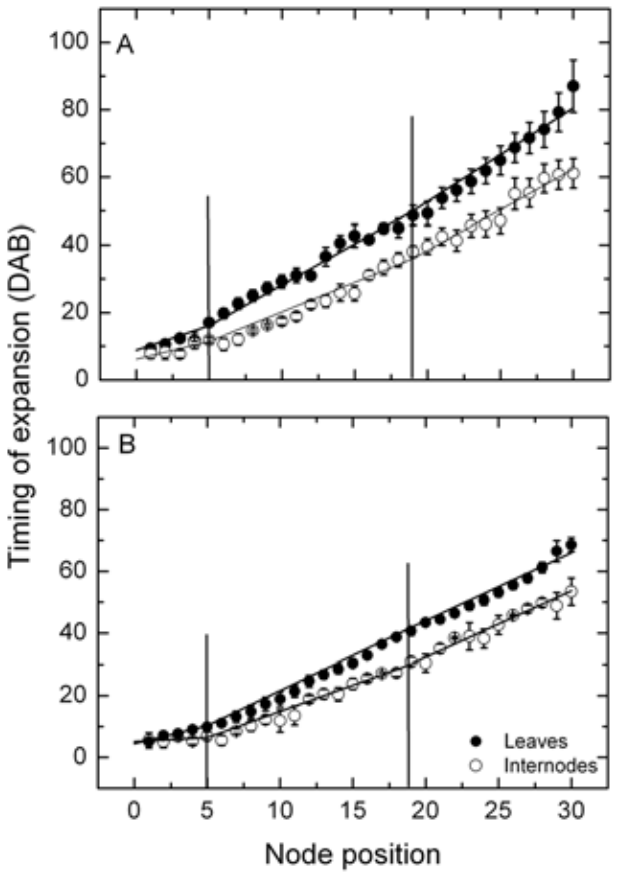


Figure 3.26 Timing of maximum leaf expansion and internode extension for vegetative (A) and fruiting shoots (B) as a function of node position along the Semillon shoots (Mean ±SE, n = 6 and n = 24, respectively). The timing of expansion to) was determined in each case as the midpoint of inflexion from the Boltzmann function fitted to each leaf or internode as it expanded. The lines are linear regressions fitted to these data.

(*Table 3.4*) for zone 1 leaves and internodes ranged between 1 and 2 days but these differences were not significant (P>0.05). For leaves in zone 2, the phyllochron was just over 2 days and for leaves in zone 3 was about 3 days and differences between vegetative and fruiting vines were highly significant (P<0.01) and the differences in phyllochron between zones 2 and 3 were also significant (P<0.05).

For internodes in both zone 2 and zone 3, the phyllochron was again about 2 days and although difference between vegetative and fruiting vines were significant (P<0.05), between zones there were no differences (P>0.05).

Duration of growth The duration of leaf growth was markedly different between fruiting and vegetative vines (*Figure 3.27A*), ranging from 6 to 13 days and 3 to 8 days, respectively. Across the three zones, for vegetative and fruiting vines, the duration averaged 3.6 ±0.2 and 7.7 ±0.4 days, 6.7 ±0.2 and 10.1 ±0.5 days and 7.7 ± 0.3 and 8.6 ±0.5 days for zones 1, 2 and 3, respectively. Thus leaf expansion was universally faster in vegetative vines than in fruiting vines.

Internode growth duration (*Figure 3.28B*) ranged for both fruiting and vegetative vines between about 1 and 15 days along the shoot. For each cohort, the duration for vegetative and fruiting vines averaged 1.3 ±0.5 and 3.9 ±0.8 days, 2.9 ±0.3 and 5.8 ±0.6 days and 8.5 ± 1.24 and 9.2 ±0.6 days for zones 1, 2 and 3 respectively. Vegetative vines again had faster internode extension than fruiting vines across the whole shoot. Furthermore, internode growth occurred over a shorter time span than leaf growth, typically by about 4 days across the whole shoot, except the last few distal internodes which were much slower to extend than the rest of the internodes.

The kinetic analysis of individual leaf and internode expansion patterns showed that on both the fruiting and vegetative Semillon vines, across all nodes, internode extension occurred before the subtending leaf expanded, even though both appeared more or less simultaneously. For example, the timing of maximum internode extension was on average, over the whole shoot, 8–10 days earlier than timing of maximum leaf expansion. However, there was a tendency for the early emerging leaves to expand just a few days behind the internodes whereas the later emerging leaves reached maximum expansion well after the internodes extended. Similarly, the duration

Table 3.4 The phyllochron (Mean ±SE, N=6, 26) determined from the slope coefficient of regressions fitted to the timing of maximum expansion for leaf and internode growth over the individual metamers on shoots of fruiting and vegetative Semillon vines shown in Figure 3.26. In all but one case, the regression lines were highly significant (P<0.001, r^2 =0.54–0.88).

		Zone 1	Zone 2	Zone 3
Metamer	**State**		**Days**	
Leaves	Vegetative	1.16 ± 0.18	2.33 ± 0.04	2.92 ± 0.14
	Fruiting	1.46 ± 0.27	2.41 ± 0.01	3.32 ± 0.43
Internodes	Vegetative	0.27 ± 0.43[1]	1.69 ± 0.07	1.79 ± 0.31
	Flowering	1.05 ± 0.43	1.90 ± 0.05	2.03 ± 0.32

[1] regression not significant

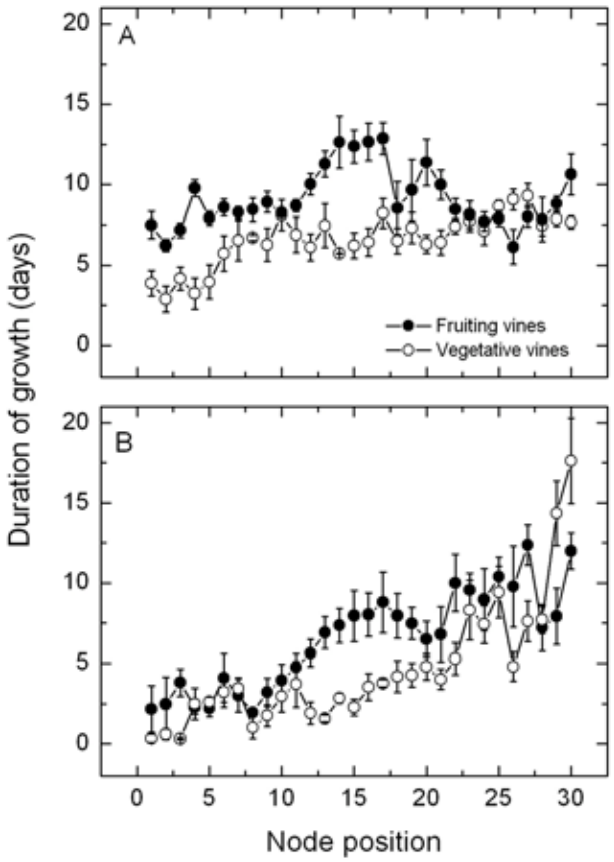


Figure 3.27. Duration of leaf expansion (A) and internode extension (B) for vegetative and fruiting shoots as indicated (Mean ±SE, n = 6 and n = 24, respectively) as a function of node position along the shoot of Semillon vines. The duration of expansion or extension was determined in each case from the Boltzmann function fitted to each leaf or internode as the time between when the leaf or internode changed from 20 to 80% of its full size.

of extension growth of the internodes was about 2–4 days shorter on average than was the duration of the subtending leaf expansion across the whole shoot.

Both the timing of maximum expansion and the duration of expansion of leaves and internodes were earlier and shorter, respectively, in vegetative than in fruiting vines. For example, the timing of maximum expansion rates of leaves on vegetative vines was, on average, 9 days earlier than for fruiting vines while for internode extension, the comparable difference was 6 days. Similarly, the duration of leaf growth of individual leaves along the shoot varied markedly between fruiting and vegetative vines, from a few days to well over 7 days earlier in the vegetative vines. Duration of internode growth was also longer in fruiting vines than vegetative vines but the differences were less than a few days overall. These data conformed to the earlier conclusion that vegetative vines developed faster and earlier than fruiting vines.

Final leaf and internode sizes along the shoot Fully expanded leaf areas were distributed in a highly consistent pattern (*Figure 3.28*) for both fruiting and vegetative vines. The leaf area of early-emerging leaves along the shoot increased rapidly such that the leaves at nodes 5-6 were the largest of all the Semillon grapevine leaves along the shoot at 0.012 ±0.0006 m^2 and 0.018 ±0.0007 m^2 for the fruiting and vegetative vines, respectively. In the fruiting vines, between node positions 6 and 30, leaf area declined in a generally consistent pattern along the shoot such that the later emerging leaves had fully expanded leaf sizes of only 30% of the largest leaves. For the vegetative vines, maximum leaf area between about nodes 8 and 21 was more or less constant. Beyond this, maximum leaf area declined in much the same way as for the fruiting vines. It was notable that across the whole

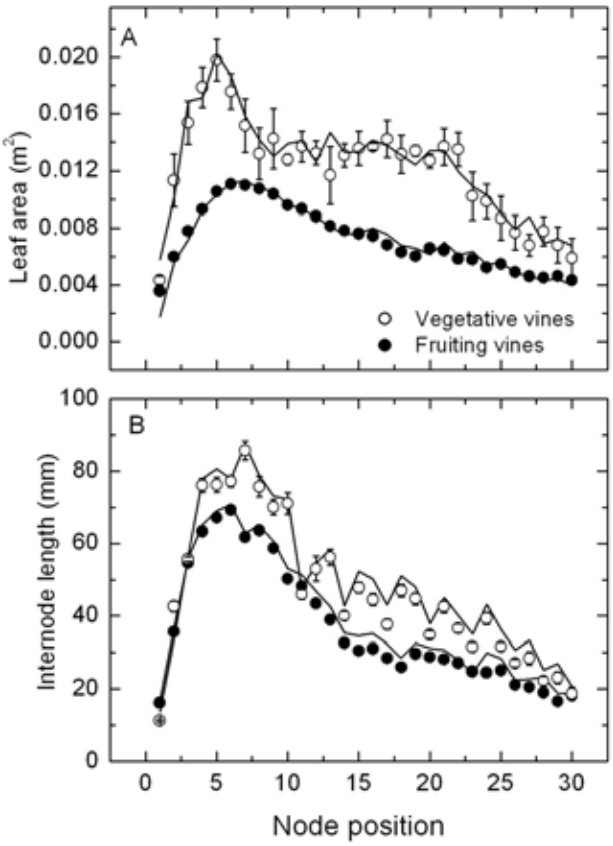


Figure 3.28 Maximum leaf area (A) and internode length (B) for vegetative and fruiting shoots (Mean ±SE, n=6 and n=24, respectively) as a function of node position along the Semillon shoots. The leaf areas were determined at the conclusion of the experiment when the shoots were destructively harvested. In all cases, the leaves were fully expanded and internodes fully extended. The lines shown are mean fitted lines derived from the Boltzmann sigmoid function (A max) applied to each leaf and internode and then averaged across all vines.

shoot, leaves of vegetative vines tended to be larger in size than those of fruiting vines.

The Boltzmann parameter A, for the upper asymptote of leaf area fitted to each leaf generally conformed well to the pattern of measured leaf area for both fruiting and vegetative vines, as shown in *Figure 3.28*. Fully expanded Internode lengths (*Figure 3.28A*) followed a pattern along the shoot that was generally consistent with that of the leaves in that early emerging internodes increased markedly to reach maximum lengths at node positions 6–7 of 85.7 ±2.5 and 69.3 ±0.9 mm for vegetative and fruiting vines respectively. However, internode length declined more or less consistently along the shoot in both vegetative and fruiting vines. Again fitting of the sigmoid function to internode extension showed the upper asymptote (A) fitted well with the actual internode lengths (*Figure 3.28B*).

Across the whole shoots, leaf area and internode lengths followed a similar pattern of distribution, initially increasing to positions 5–6 and then declining more or less continuously along the rest of the shoot. While there were differences between vegetative and fruiting vines, the pattern for both was comparable with other varieties including Riesling (Schultz 1992), Cabernet Sauvignon (Poni and Giachino 2000), Sultana (Sommer *et al.* 2000) Grenache (Lebon *et al.* 2004) and Tempranillo (Lopes and Pinto 2005) but not with potted vines of several varieties (Wample *et al.* 1987). The same pattern also occurred with other vines Greer and Jeffares 1998). Differences in leaf area size along the shoot in fruiting compared with vegetative vines as has also been shown in Pinot Noir shoots (Petrie *et al.* 2000).

Bud dissections

The number of preformed leaf primordia in DORmant buds of fruiting vines (*Figure 3.29*) varied across the shoots from 12 to 18 primordia with a maximum occurrence (31%) at 14 primordia (*Figure 3.30*). However, there was a somewhat bimodal pattern in the frequency distribution of numbers of leaf primordia in the Semillon buds with an additional maximum at 18 primordia in 23% of all buds. In fact, a sizable proportion (39%) of buds had greater than 15 leaf primordia in the DORmant buds.

Dynamics of shoot development

Leaf area For both fruiting and vegetative vines, shoot leaf area expanded in a sigmoidal pattern (*Figure 3.31A, B*) to reach a maximum at about 80 DAB. The total leaf area of the shoots of vegetative

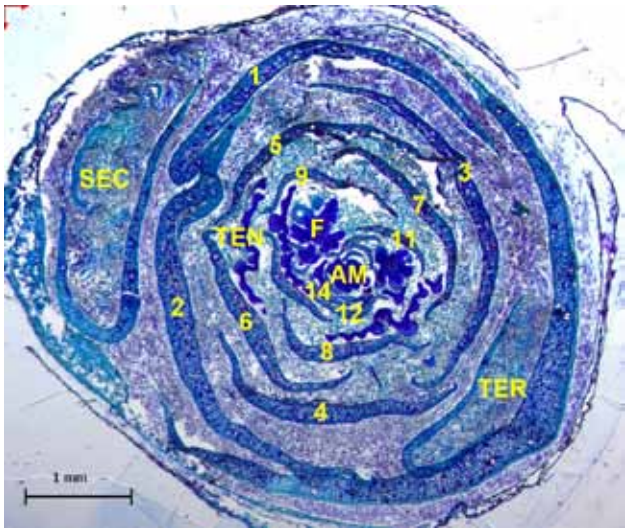


Figure 3.29 A transverse section of a DORmant Semillon bud showing the whorls of preformed leaf primordia. No floral structures were apparent but lateral branch primordia can be seen.

vines at 0.4 ±0.03 m^2 was twice as large as that for the fruiting vines (0.18 ±0.02 m^2). Rates of shoot leaf area expansion increased rapidly shortly after budbreak to reach a well defined maximum at about 20 DAB. For the vegetative vines, the maximum rate of shoot expansion was about 0.008 ±0.0003 m^2 d^{-1} while for the fruiting vines it was about 0.006 ±0.0009 m^2 d^{-1}.

Stem extension The pattern of stem extension followed that of canopy leaf area expansion in that stem growth also occurred in a sigmoidal pattern (*Figure 3.32A, B*) for both fruiting and vegetative vines. Final stem lengths of the vegetative vines exceeded that of the fruiting vines by about two-fold,

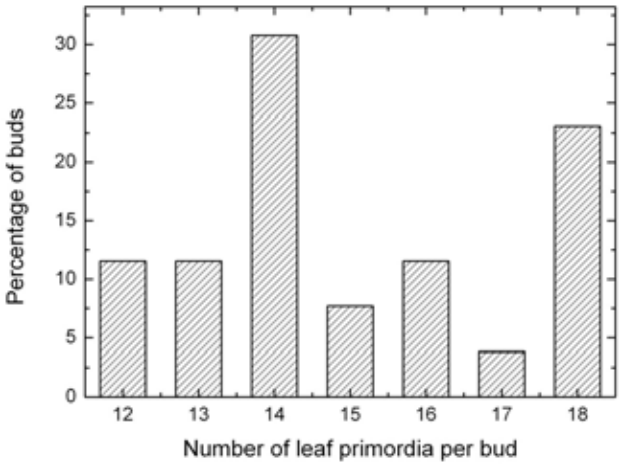


Figure 3.30 Percentage distribution of the number of DORmant Semillon buds that had between 12 and 18 preformed leaf primordia per bud. A total of 26 buds from 7 vines and 4 nodes were sectioned and examined microscopically to count leaf primordia numbers. There was no significant (P>0.05) effect of node position or vine differences in numbers of primordia per bud.

consistent with the greater canopy leaf area. Rates of stem extension increased rapidly immediately after budbreak and reached a maximum between 5 and 12 days after budbreak. However, the maximum rates were significantly ($P<0.001$) different with vegetative vines at 66 ±5 mm d^{-1} compared with 31 ±2 mm d^{-1} for the fruiting vines.

As shown in *Figure 3.31*, shoot leaf area development and stem extension both followed sigmoidal kinetics in fruiting and vegetative vines, with early rapid increases that reached a maximum stem length and leaf area about 60 and 80 days after budbreak, respectively. This pattern of shoot leaf area development has also been demonstrated in Sangiovese (Bindi *et al*. 1997), Cabernet Sauvignon (Poni and Giachino 2000) and Tempranillo vines (Lopes and Pinto 2005). Similar patterns of stem extension have also been reported for Cabernet Franc (Matthews *et al*. 1987) and Pinot Noir (Petrie *et al*. 2000) vines. As shown both for the Pinot Noir and Semillon vines, fruit growth had marked affects on both total leaf area and final stem length, reducing each by about 50%. Similarly, extension rates of Gewürztraminer vines increased when the crop was removed (Hardie and Martin 2000). By contrast, in Syrah and Grenache grapevines, differences in crop load had no effect on total leaf number, canopy area or stem length of the primary shoot (Pallas *et al*. 2008). For the Semillon vines, leaf area reduction could be ascribed to the altered dynamics of leaf development in the fruiting vines as outlined above. Likewise altered internode extension dynamics in response to fruiting would seem to account for reduced stem lengths in fruiting compared with vegetative vines.

Perhaps what was most surprising about the Semillon shoot development dynamics was how quickly the maximum rates of both leaf area expansion and stem extension were achieved. In both cases, these maxima occurred 12 to 20 DAB in the fruiting and vegetative vines. However, and in keeping with leaf and internode dynamics, the maximum rates of expansion and extension were higher in the vegetative vines compared to the fruiting vines. More importantly, the maximum rates occurred well

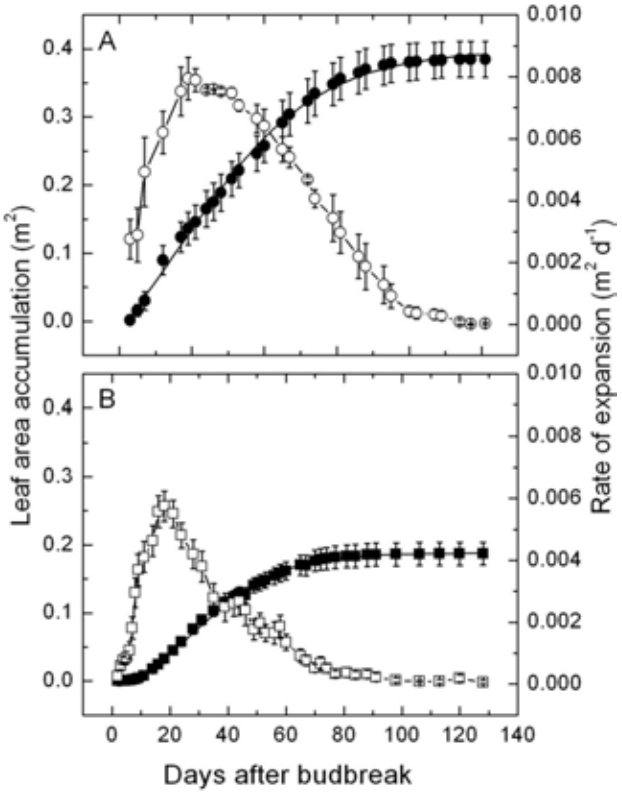


Figure 3.31 Shoot leaf area expansion (closed symbols) and the rates of shoot area expansion (open symbols) for Semillon shoots of vegetative (A) and fruiting vines (B), (Mean ±SE, n=6 and n=24, respectively) as a function of time after budbreak. Shoot leaf area was determined by summing the area of all leaves present on each stem on the respective days and the rates of expansion were determined by differentiation of these leaf areas over time for each shoot and then averaging over all vines.

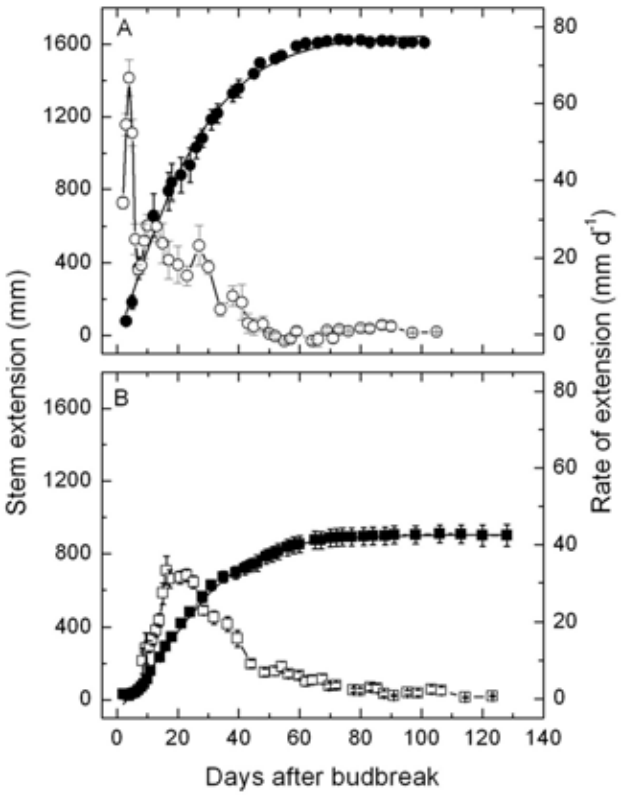


Figure 3.32 Stem extension (closed symbols) and the rates of stem extension (open symbols) of Semillon shoots of (A) vegetative and (B) fruiting vines Mean ±SE, n=6 and n=24, respectively) as a function of time after budbreak. The rates were determined by differentiating the stem extension data over time for each shoot and then averaging over all vines.

before flowering (38 DAB) in keeping with Smart and Coombe (1983) but contrary to Matthews *et al.* (1987), who showed in field-grown Cabernet Franc vines that the maximum rate of shoot elongation occurred two weeks after flowering. The period from budbreak to about flowering is a time when the vine growth was highly dependent on carbohydrate reserves (Goffinet 2004; Bennett *et al.* 2005) and when vines generally have a negative carbon balance (Greer and Jeffares 1998; Greer *et al.* 2003; Weyand and Schultz 2006; Greer and Sicard 2009).

Conclusions

Leaf and internode growth dynamics of Semillon grapevines revealed patterns of appearance and expansion that were highly dependent on shoot position, with earliest emerging metamers expanding at high rates over short durations and late emerging metamers slow to expand over a longer duration. Stem extension and shoot leaf area expansion also reached maximum rates early in the growing season when the vines were largely heterotrophic. Thus, early spring is an important period for grapevine shoot growth and development when vines invest much in establishing the canopy rapidly. Presumably, this accounts for the strong demand for carbohydrate reserves over this time. Even though flowering and subsequent fruit growth occurred much later indeed after about 22 leaves had emerged, effects on both individual leaves and internodes as well as on shoot dynamics were apparent immediately after budbreak, suggesting the effects of flowering on shoot development can be traced back to events at budbreak, if not before in the DORmant bud. The corollary to this, if vines had flowers removed at the time of flowering, patterns of leaf and internode development would not be different from the fruiting vine response.

Experiment 3.7
Heat stress affects flowering, berry growth, sugar accumulation, and photosynthesis

Materials and methods

Plant material and growth conditions

Three year old vines were grown in 25 L pots containing potting media (soil, sand, and fertiliser). In March (early autumn), 30 Semillon grapevines on own roots were transferred to a growth chamber (TH6000, Thermoline Scientific, Smithfield, Australia) for 6 weeks at a day/night temperature of 10/5°C to induce leaf fall and DORmancy. After this time, the day/night temperatures were increased to 25/15°C and the vines were grown for a further 105 days at a photon flux density (PFD) of 400 μmol m^{-2} s^{-1}, provided by 4 x 1 kW high pressure discharge lamps Powerstar HQI–T1000, Osram, Germany) and 4 x 20 W compact fluorescent lamps (Cool white, Fairway, China) over a 12 h photoperiod. The corresponding day/night vapour pressure deficits were 1.0/0.6 kPa. The vines were watered daily with an automatic system and well supplied with nutrients throughout. Between eight and ten shoots developed on each vine and four shoots were retained. Each vine had between five and eight bunches.

Heat treatments

At several stages throughout vine and berry development, namely flowering, fruit set, veraison and mid ripening, four vines were transferred to a second growth chamber which was set at all the same conditions as above except that the day/night temperatures were 40/25°C. On each occasion, the vines were treated for four days in this regime. Prior to the vines being exposed to the heat, the soil was well watered and soil water was maintained throughout the heat treatments at regular intervals. The vines were then returned to the growth conditions after the heat treatment. The vines were always transferred at the end of the day conditions at 25°C into the night treatment conditions at the same temperature to avoid any immediate heat shock. A similar group of plants were not exposed to the heat regime and used as controls.

Growth measurements

The length of 1–2 primary shoots per vine and the width and length dimensions of each leaf on these shoots were measured at regular intervals (2–3 days) from the time when the leaves were about 10 mm in diameter except when the vines were being heat treated. Time of appearance of leaves along the shoots was defined as the number of days after budbreak when each leaf attained 10 mm diameter. Shoot length was measured throughout the growth conditions but leaf growth was measured until maximum leaf size was achieved, as indicated by no change in successive measurements. All lateral shoots that appeared on the shoots were removed as they appeared. Growth was concluded at about the time when approximately 30– 35 leaves had emerged.

At the conclusion of the treatments all shoots were detached just above the second node and destructively harvested. Leaves were detached from each shoot and the leaf area measured (LI3000, LiCor Inc., Lincoln Nebraska, USA). Shoot lengths were measured and then all leaves and stems were oven-dried at 60°C for two weeks and then dry weights of each leaf and stem determined.

Flower and bunch analysis

On each shoot 1–3 inflorescences developed. Phenology, flowering, fruit set, berry development and veraison were followed using the E-L system (Coombe 1995) for each individual vine with visual observations. As flowering occurred, the length of the inflorescence was measured and this continued through fruit set with measurement of the bunch length until harvest. Berry diameter measurements with a microcaliper were conducted on three berries per bunch sampled at the top, middle and bottom of the bunch and these measurements continued through to just prior to harvest. Soluble solids were measured with a digital refractometer (PR-101, Atago, Tokyo, Japan) on three berries per bunch per vine (12–18 berries in total), sampled in the same locations as above, for each treatment and the fresh weight and diameter of three berries per bunch were also measured. At the stage when the soluble solids reached about 25°Brix, all bunches were harvested as above for yield determination and subsamples of berries taken for fresh weight, diameter and soluble solids concentration analysis. For those bunches exposed to the heat treatment, additional visual observations of flower survival and berry damage were made over several days following the heat regime.

Net photosynthesis

Immediately prior to and for several days after each vine was heat treated, gas exchange of leaves along a selected shoot of each vine was measured with an open gas exchange system (LI-6400, Licor Inc. Lincoln, Nebraska, USA). All measurements were conducted at a leaf temperature of 25°C and at the photon flux density of the growth conditions.

Carbon analysis

Net carbon acquisition on a shoot basis was determined from photosynthetic measurements of each leaf corrected for area, summed over all leaves and converted to carbon on the basis of the molecular fraction of carbon in CO_2 (Greer *et al*. 2003; Greer and Sicard 2009). The carbon content of the soluble solids of berries was determined on the assumption that the soluble fraction was mostly sugar (Coombe 1992) and based on the molecular fraction of carbon in glucose equivalents. Sugar content of the berries was determined from a linear relationship between sugar concentration and °Brix and corrected by the volume of the berry determined from berry diameter assuming the berry was spherical.

Results and discussion

Phenology and vegetative growth

Budbreak occurred on 29 May, flowering occurred 26 days later and fruit set an additional 5 days later. Veraison occurred 82 days after budbreak (DAB) and harvest occurred at 105 days after budbreak. Leaf appearance, patterns of leaf area distribution, cumulative leaf area and shoot growth (not shown) were all unaffected by the heat regime. Vegetative growth characteristics of these Semillon vines were, therefore, highly tolerant of such high temperatures, at least for short durations. By contrast, shoot growth rates of Chardonnay vines treated at 40°C were faster than untreated vines, whereas, the heat treatment decreased shoot growth rates of Chenin Blanc vines (Sepúlveda *et al*. 1986). Shoot growth rates of Pinot Noir and Carignane vines were also reduced by high temperatures (Kliewer 1977*a*) and similar affects occurred with Trebbiano Toscano vines (Ferrini *et al*. 1995). By contrast, Cabernet Sauvignon leaves were not visibly affected after exposure to 45oC (Morrell *et al*. 1997). Thus, there are varietal differences in vegetative growth responses to high temperature.

Flower and bunch growth

For the vines heat treated at the time of flowering, all flowers subsequently dropped off on those vines within a few weeks of the heat treatment and the flowers gained an overall length of 22 mm before abscising (*Figure 3.33*). For those bunches that were heat treated at all other times were significantly ($P<0.01$) longer at 85–90 mm but there were no statistical differences in bunch length between these latter heat treatments and the control vines. Thus, the heat event had marked effects on early reproductive growth only. Heat stress affects on reproductive growth has been studied in several varieties including Chardonnay and Chenin Blanc (Sepúlveda and Kliewer 1986*a*), Thompson Seedless and Napa Gamay (Matsui *et al*. 1986; 1991) and Cabernet Sauvignon, Pinot Noir, Carignane and Tokay (Kliewer 1977*a*). However, there was variation in sensitivity of the reproductive process to the heat. For example,

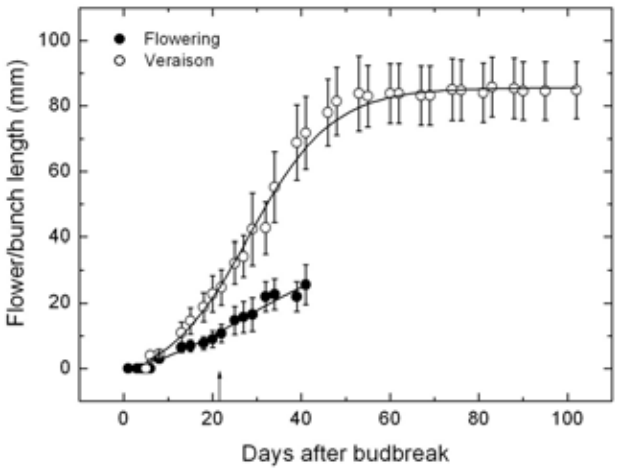


Figure 3.33 Development of the flower and bunch length (Mean ±SE, N=4–6) as a function of time from budbreak for Semillon vines grown in a controlled environment and exposed to a 40/25°C day/night temperature regime for 4 days at the flowering and veraison stages of reproductive development. The lines are the best fit to the Boltzmann sigmoid function.

Semillon flowering was extremely sensitive to high temperatures, with most inflorescences abscising within a few days of the heat treatment. Growth of the inflorescence was also impeded. Neither Alexander (1965) with Sultana vines nor Kliewer (1977*a*) with Pinot Noir and Carignane vines exposed to 40°C at flowering reported any affect of heat on flower abscission. By contrast, percentage fruit set and ovule fertility of the Pinot Noir and Carignane vines were markedly reduced by the heat stress (Kliewer 1977*a*). Although percentage fruit set was not determined in the present study, berry number per bunch and numbers of bunches per vine were not significantly different between Semillon vines heat treated at fruit set, veraison or mid ripening. This suggested fruit set *per se* was not affected by the heat treatment.

Berry growth

Individual berries on vines heat treated at fruit set appeared to grow relatively normally with a distinct double sigmoid growth pattern (*Figure 3.34*) and reached and overall size of 12–13 mm at harvest. By contrast, berries on vines heat treated at veraison did not exhibit the second growth increase and the berries stopped growing and even declined in size to about 9 mm at harvest. A similar effect was observed for vines treated at mid ripening in that growth was stopped after the heat event not shown). Control vines also had normal berry development, exhibiting the double sigmoid growth pattern and reached a maximum size of 13–14 mm.

In the later stages of berry development, berry fresh weight of control vines and those heat treated at fruit set remained more or less constant (*Figure 3.35*). For those vines exposed to the heat regime at veraison and mid ripening, fresh weight declined although only for the mid ripening treatment was the decline significant ($P<0.01$).

Thompson Seedless berry growth was also affected when vines were heat treated early in berry development and the double sigmoid growth pattern was also evident (Matsui *et al.* 1986). Similarly, berry volume of Cabernet Sauvignon grapevines was affected by exposure to high temperatures and the growth pattern was also retained (Kliewer 1977*a*). However, berries of Napa Gamay vines heat treated at veraison had markedly impaired diameter growth (Matsui *et al.* 1991), consistent with the Semillon vines. This suggests a general response to heat in grapevines is that berry growth is impeded markedly more when the heat events occur after veraison than before (see also Hale and Buttrose 1974).

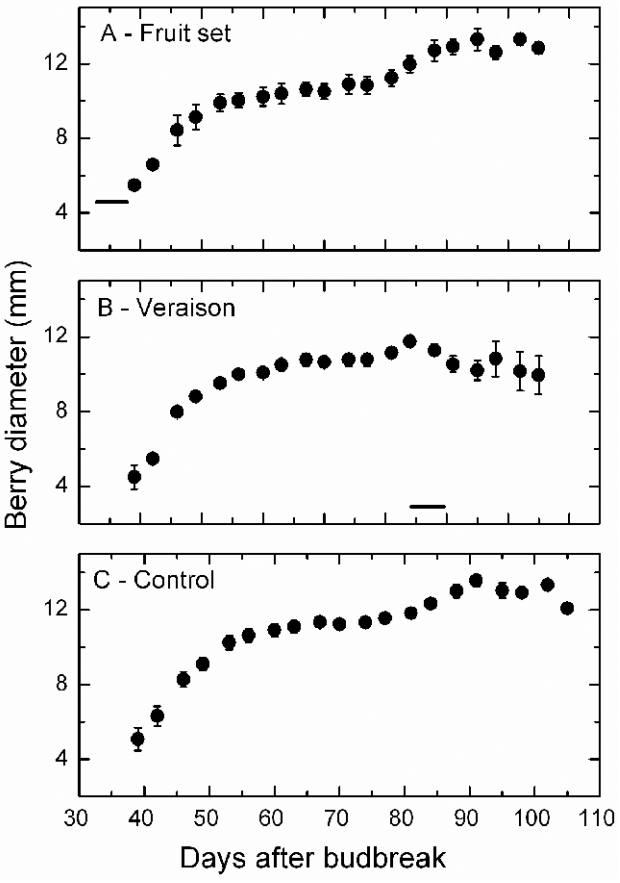


Figure 3.34 Changes in berry diameter (Mean ±SE, N=12–18) as a function of time after budbreak for Semillon vines grown in a controlled environment and exposed to a 40/25°C day/night temperature regime for 4 days. A, treated at fruit set; B, treated at veraison; and C, control vines. Bars indicate the times when the heat treatment was applied in each case.

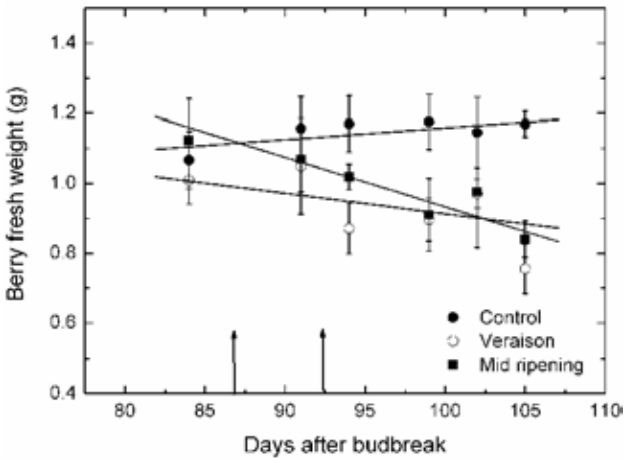


Figure 3.35 Changes in berry fresh weight (Mean ±SE, N=12–18) in the late stages of berry ripening for Semillon vines exposed to a 40/25°C day/night temperature regime for 4 days at veraison and at mid berry ripening. Other treatments are excluded for clarity only. The lines are linear regressions fitted to these data. The arrows point to when the heat was applied.

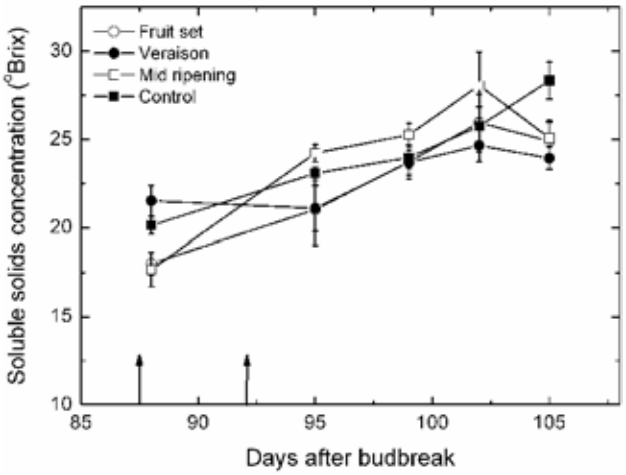


Figure 3.36 Changes in the soluble solids concentration mean ±SE, N=12–18) as a function of time after budbreak for Semillon vines exposed to a 40/25°C day/night temperature regime for 4 days at selected stages of reproductive development as indicated. Arrows indicate the times when the heat regime was applied except for the fruit set treatment which was applied at 31–35 DAB.

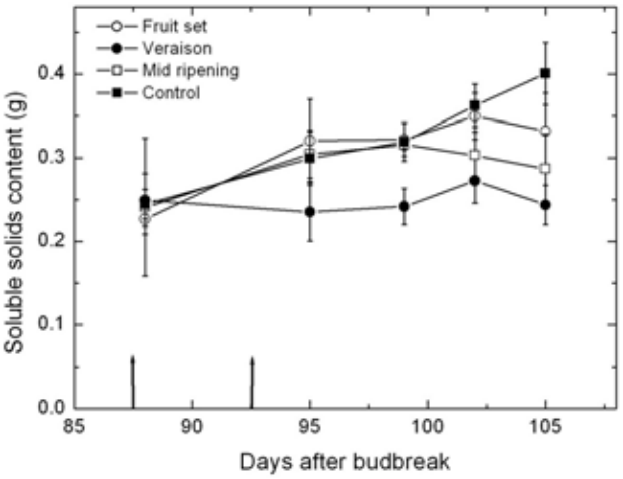


Figure 3.37 Changes in the estimated soluble solids content (Mean ±SE, N=12–18) as a function of time after budbreak for Semillon vines exposed to a 40/25°C day/night temperature regime for 4 days at selected stages of reproductive development as indicated. Arrows indicate the times when the heat regime was applied except for the fruit set treatment which was applied at 31–35 DAB.

Soluble solids accumulation

The sugar concentrations in the berries of vines heat treated at fruit set increased at a steady rate (*Figure 3.36*) to reach a maximum of 26°Brix at 102 DAB and then declined slightly. By contrast, sugar accumulation in berries on vines heat treated at veraison stopped for at least 8 days but then continued to reach a maximum of 25°Brix at 102 DAB and then also declined. For the vines heat treated at mid ripening, sugar accumulation slowed but did not stop and reached a maximum of 27°Brix at about 100 DAB before declining. Control vines also had a steady increase in sugar accumulation to a maximum of 27°Brix and, in contrast to the other bunches, continued to increase in soluble solids concentration. Because berry diameters changed dramatically through the late stages of ripening, berry volume changes also occurred and affected the sugar concentrations accordingly, and were determined to take berry volume changes into account.

This indicated (*Figure 3.37*) that sugar accumulation did stop for an extended period after heat was applied both at veraison and at mid ripening and subsequently declined by the time of harvest. For control vines and those treated at fruit set, berry sugar content increased at least to harvest but declined in the fruit set heat treated vines. Regression analysis indicated that for both the fruit set treated and control vines, the sugar content increased significantly in a linear pattern (r^2=0.95–0.99, P<0.01) at least up to 100 DAB, at rates of 7.8 ±1.8 and 8.7 ±1.5 mg berry^{-1} d^{-1}. Equivalent rates on a berry dry weight basis for both were 23 ±5 mg g(BDW)$^{-1}$ d^{-1} and on a glucose basis (40% carbon), the equivalent rate of carbon accumulation was 9.2 ±2 mg C g(BDW)$^{-1}$ d^{-1} The regressions for the veraison and mid ripened treated vines were not significant (P>0.05) thus, there was no measurable rate of carbon accumulation in the heat treated berries.

Kliewer (1977*b*) reported that Emperor grapes failed to increase soluble solids concentration beyond

10–13°Brix when vines were grown at 37/32°C. High temperatures also reduced sugar concentrations in Chardonnay (Sepúlveda and Kliewer 1986*a*) and Napa Gamay berries (Matsui *et al.* 1991). By contrast, sugar concentrations of both Cabernet Sauvignon and Tokay berries continued to increase after exposure to high temperatures (Kliewer 1977*a*) as was also observed with Shiraz berries (Soar *et al.* 2009). For the Semillon vines, there was also little evidence that heat prevented soluble solids from accumulating. The concentration of soluble solids did decline late in development in bunches from all heat treatments so was not a likely heat effect. However, concentration of sugars depends on berry size and, as shown above, this declined markedly after heat treatment. Thus, changes in concentration could be a product of changing berry volumes rather than increasing sugar uptake, *per se* as has been shown previously in Chardonnay berries (Sepúlveda *et al.* 1986).

Consistent with this, the sugar content of Semillon bunches at veraison did not increase after the heat treatment and actually declined at harvest. A similar pattern occurred with bunches heat treated at mid ripening. By contrast, both fruit set treated and control bunches increased in sugar content. These results clearly demonstrated that the heat severely impeded sugar flow into bunches, most strongly at veraison but also at the mid ripening stage of development of Semillon bunches.

Yield

The total yield per treatment averaged between 68 ±2 and 124 ±3 g for the vines treated from fruit set to mid ripening but for the control vines, the yield was significantly higher at 181 ±7 g (*Table 3.5*). Bunch numbers were not different except for the fruit set treatment but berry numbers per bunch were significantly higher for the control vines and accounted for the higher yield for these vines. It would appear that berry number was affected by all the heat treatments, consistent with a percentage of berries shrinking and abscising.

Table 3.5 Effect of the 40/25°C day/night temperature regime sustained over four days on bunch characteristics and yield (Mean ±SE, N=4–6) at selected stages of development of Semillon vines grown in a controlled environment. The flowering stage has been omitted because no bunches were retained after the temperature treatment. All vines were measured at 105 Days after budbreak, after the harvest.

Development Stage	Yield (g)	Number bunches	Number berries
Fruit set	68 ± 2	5	23 ± 5
Veraison	124 ± 3	8	32 ± 4
Mid ripening	84 ± 4	7	25 ± 6
Control	181 ± 7	8	40 ± 9
P	0.048	ns	ns

In general, berry characteristics at the destructive harvest of the vines reflected less effects of the heat regime at fruit set with berry fresh weight, diameter and sugar content all significantly higher than for vines treated at veraison and mid ripening (*Table 3.6*). Notably, soluble solids concentrations were not significant (P>0.05) at this stage even though the range was from 23.5 to 27.1°Brix.

Effect of the heat treatments on photosynthesis

Along the shoot, net photosynthesis varied markedly but with no consistent pattern (*Figure 3.38A*). One day after the heat regimes were applied at the time of veraison, net photosynthesis in almost leaves was reduced, with the average rates over all leaves reduced by 35%, however, 4 days later photosynthesis

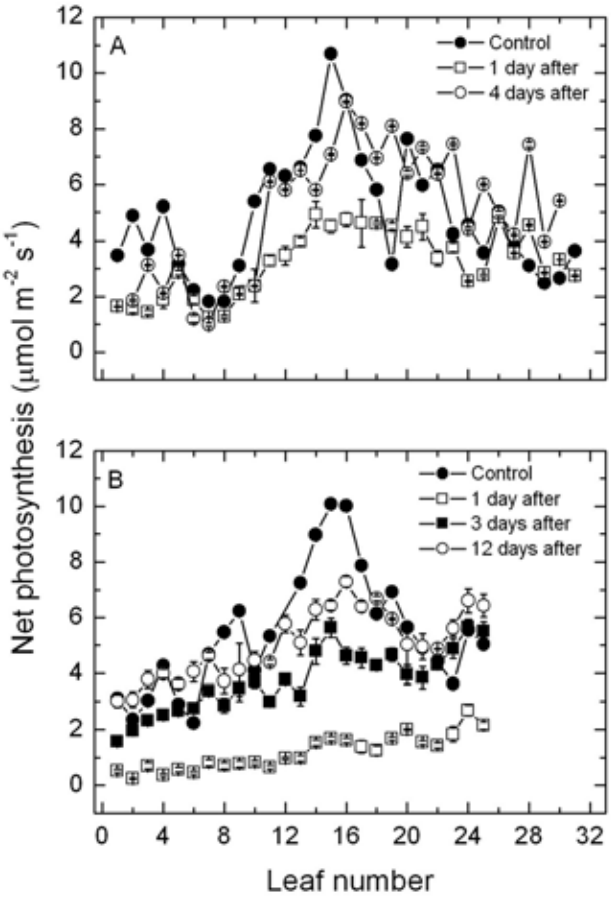


Figure 3.38 Changes in net photosynthesis (Mean ±SE, N=4) along the shoot of Semillon vines grown in a controlled environment and exposed to a 40/25°C day/night temperature regime for 4 days at veraison (A) and at mid ripening (B). Measurements were conducted just prior to and for several days after the heat treatment as indicated.

Table 3.6 Berry characteristics (Mean ±SE, N=40) at the time of the harvest 105 Days after budbreak) for Semillon vines exposed to a 4-day 40/25°C temperature regime at selected stages of development. There were no berries for the heat treatment at flowering so this stage has been omitted. Also shown is the probability of the data being statistically different.

Development stage	Berry fresh weight (g)	Berry diameter (mm)	Soluble solids (°Brix)	Sugar content (g)
Fruit set	1.04 ± 0.05	11.5 ± 0.2	27.1 ± 0.8	0.29 ± 0.01
Veraison	0.66 ± 0.05	9.9 ± 0.3	23.5 ± 0.7	0.23 ± 0.01
Mid ripening	0.86 ± 0.08	10.5 ± 0.4	24.9 ± 0.5	0.29 ± 0.01
Control	1.13 ± 0.04	13.6 ± 0.4	26.2 ± 0.5	0.35 ± 0.02
P	0.026	0.001	ns	0.0004

along the shoot had more or less recovered and the average rates were 5.2 ±0.4 μmol m^{-2} s^{-1}. Also shown is the effect of the heat regimes at mid ripening on net photosynthesis along the shoot (*Figure 3.38B*). Again net photosynthesis varied along the shoot with maximal rates occurring at node positions 14–16. However, one day after the heat treatment, photosynthesis along the shoot was severely reduced with rates at about 1.1 ±0.2 μmol m^{-2} s^{-1} but more affected towards the older leaves than the more recently emerged leaves. Although some recovery of photosynthesis occurred three days later it was not complete and even 12 days later there was still some leaf photosynthesis that had not fully recovered.

Thus it would appear that the photosynthetic response to the heat stress varied according to the stage of vine development, with more severe effects later in the season. This can be seen in Figure 3.39, where photosynthesis after vines were heat stressed early in development flowering) readily recovered with 2-3 days of the heat application. By contrast, vines heat treated later in development mid ripening) took upwards of 10 days to fully recover.

Stomatal conductance during the heat treatments (*Figure 3.40*) was affected in a similar way to photosynthesis with a significant ($P<0.01$) reduction immediately after the heat treatment and the recovery in conductance thereafter completed in 10 days. For each treatment, there was a significant linear relationship ($r^2=0.95$, $P<0.01$) between photosynthesis and stomatal conductance not shown).

The heat-induced impediment of sugar accumulation at veraison could be attributed to a number of reasons including restriction of phloem loading into the bunch, reduced transport of sugars to the bunch or reduced supply at the source. However, using ^{14}C as a tracer of photosynthate, (Sepúlveda *et al.* 1986*a*) concluded phloem transport was not affected by heat in Chardonnay vines. For other grape varieties (Ferrini *et al.* 1995), photosynthesis was significantly impaired after the heat stress, increasingly so at and after veraison, suggesting reduced supply was the problem. This is the time when sugar accumulation in bunches is maximal (Coombe 1992) and consequently there is a high demand for photosynthate. Although reallocation of ^{14}C to growing tips was observed in heat-treated Chardonnay vines (Sepúlveda *et al.* 1986*a*), as shown here Semillon vines had a sustained impairment

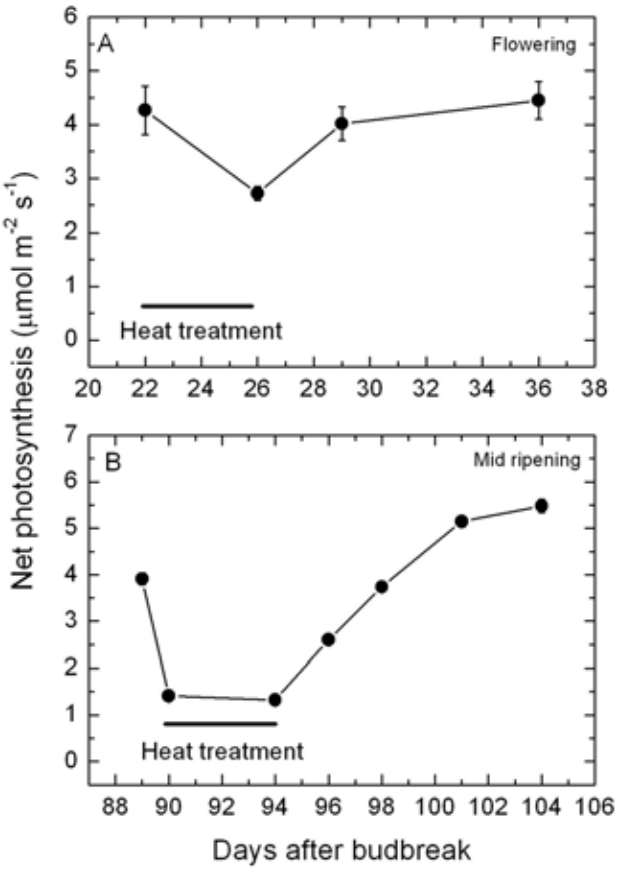


Figure 3.39 Changes in net photosynthesis (Mean, N=30–80) before and after exposure to a 40/25°C day/night temperature regime for 4 days and averaged over all leaves along the shoot of Semillon vines grown in a controlled environment. The heat treatment was applied at flowering (A) and mid ripening (B). The data were averaged over all leaves on the measured shoot for each vine in each treatment.

of leaf photosynthesis, taking 10–12 days after the heat treatment for full recovery. Stomatal limitation fully accounted for the change in photosynthesis, in keeping with Sepúlveda and Kliewer (1986*b*) and Matsui *et al*. (1991).

Net carbon acquisition

From veraison through to harvest, at each occasion of heat stress, the net carbon acquisition at the whole shoot declined by 76–56% (*Figure 3.41*) and in each case to about 4.0 ±1 mg g leaf dry weight (LDW)-1 d-1. It was notable, however, that the net carbon acquisition prior to or when photosynthesis recovered ranged from 15.0 ±3.3 mg g(LDW)$^{-1}$ d^{-1} at veraison to 19.4 ±1.5 mg g(LDW)$^{-1}$ d^{-1} at mid ripening then decreased by the time of harvest (not shown) to 10.6 ±1.7 mg g(LDW)$^{-1}$ d^{-1}). Thus supply of carbon was highest when the berries were expanding fastest between veraison and mid ripening and coincided with heat having the most marked effect on carbon supply. Thus during the berry expansion phase, about 10 mg g(BDW)$^{-1}$ d^{-1} of carbon is required to meet the berry needs in untreated vines. However, for at least 10 days after in those vines treated with heat, rates of carbon supply declined by as much as 60% and thus were not adequate to meet the carbon demand of the berries. Therefore, we can conclude that the impact of heat on the sugar accumulation process at veraison and at mid ripening can be traced right back to the impact of heat on the photosynthetic supply of sugar. The corollary of this conclusion was that heat had no affect on translocation (cf. Sepúlveda *et al*. 1986*a*) or on the loading of sugars into the berry but these need to be experimentally verified.

Conclusions

Semillon grapevine vegetative growth was tolerant of high temperatures but reproductive growth was a highly sensitive process. The impacts of the heat were dependent on stage of development, with the flowering process markedly affected while young developing berries largely unaffected. By contrast, berries reaching veraison were again very sensitive to the heat with rapid expansion growth strongly curtailed and sugar stopped from accumulating. However, a sustained impairment of leaf photosynthesis by the heat also occurred, affecting the supply of carbon available to meet the demand by the berries. Hence,

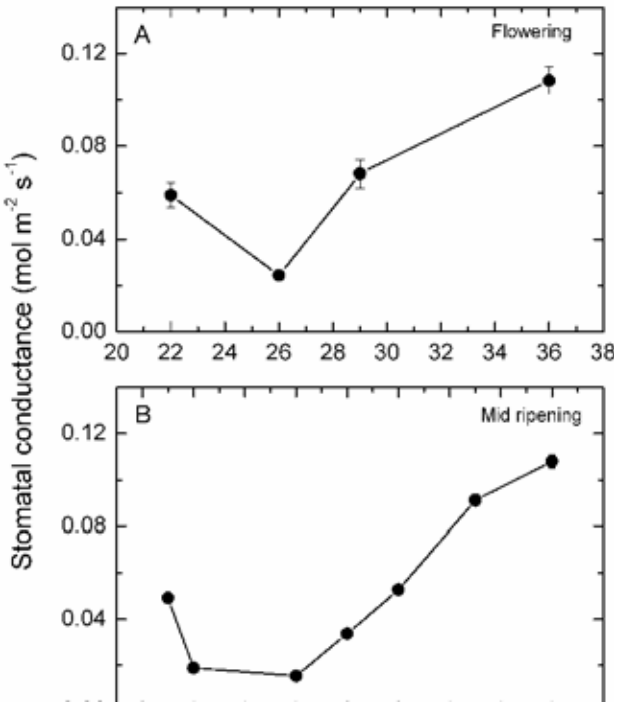


Figure 3.40 Changes in stomatal conductance (Mean ±SE, N=30–80) before and after exposure to a 40/25°C day/night temperature regime for 4 days and averaged over all leaves along the shoot of Semillon vines grown in a controlled environment. The heat treatment was applied at flowering (A) and mid ripening (B). The data were averaged over all leaves on the measured shoot for each vine in each treatment.

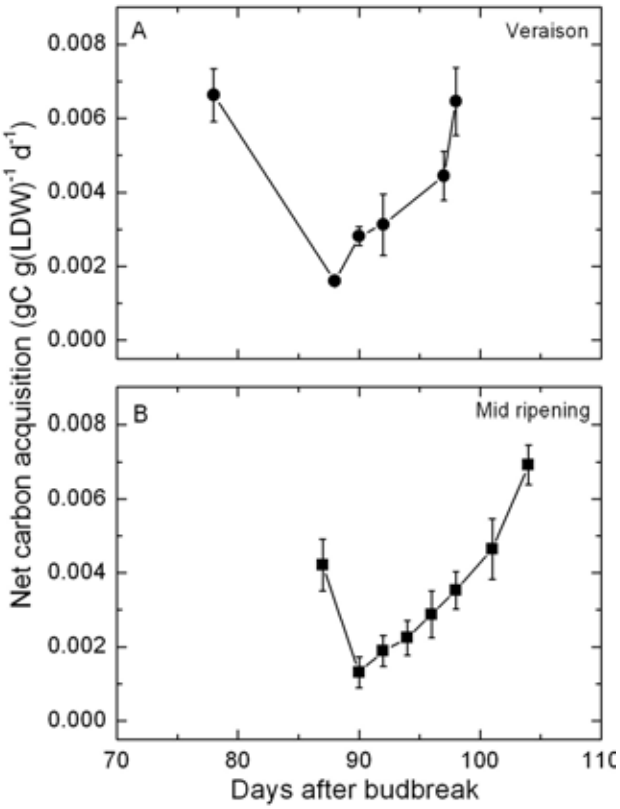


Figure 3.41 Changes in the net carbon acquisition (Mean ±SE, N=4) before and after exposure to a 40/25°C day/night temperature regime for 4 days for Semillon vines grown in a controlled environment. The heat treatment was applied at veraison (A) and mid ripening (B).

the failure of berries to accumulate sugar after high temperature events can be traced back to an impediment in sugar supply.

Experiment 3.8
Shoot architecture, growth and development dynamics of *Vitis vinifera* cv. Semillon vines grown with and without shade

Materials and methods

Plant material and growth conditions

This study was undertaken on a the same vineyard as above vineyard in the Riverina in NSW over three growing seasons from 2006–07 to 2008–09. The *Vitis vinifera* cv. Semillon (accession DA16162) vines were planted in 2003 from cuttings and grown on own roots. The rows were orientated north-south at 1.8 m spacing between vines and 3.5 m between the rows and the vines grown on a VSP trellis and spur pruned. The vines were drip irrigated with drippers at 0.6 m spacing and delivered 2.4 L h^{-1} for 12 h $week^{-1}$ until veraison when the irrigation was increased to 24 h $week^{-1}$. Nutrition was supplied through the dripper system. Budbreak occurred about the 25 September in each year and full bloom occurred in early-November and bunches harvested in early-February.

Shade cloth treatment

Neutral density shade cloth (70%) was placed over a whole panel of three vines. Wooden vertical poles and cross arms at each end of the panel were used to support the shade cloth 2.4 m above the ground. The shade cloth extended down each side of the panel by 1.2 m for some early morning-late afternoon cover. The whole experimental setup was replicated twice in the same row. The shade cloth was applied just prior to budbreak in each season and maintained until after harvest. For comparison, comparable panels without shade covering were used as controls. The shade cloth reduced the incident irradiance within the canopy, with photon flux densities typically less than 400 μmol m^{-2} s^{-1}. Canopy temperatures under the shade cloth were also lower by 3-5°C compared with air temperatures.

Temperatures and irradiance

Canopy temperatures on each side of one vine in each panel of each treatment were measured with infrared radiometers (IRRP, Apogee, Logan UT, USA) placed in the inter row space 30 cm from the vine and pointing at the canopy at about 1.2 m height. Each radiometer was logged CR1000, Campbell Scientific. Logan, UT, USA) and averaged over hourly intervals for each day of the trial. Screened air temperatures were also monitored throughout the growing season in the latter two seasons. Screened air and canopy temperatures and vapour pressure deficits in both the uncovered and covered vines were measured with a quantum sensor, (LI190, Licor Biosciences, Lincoln, NE, USA), combined humidity and temperature sensor (HPM50, Vaisala, Helsinki, Finland). All sensors were logged and averaged over hourly intervals throughout the growing season from mid-October to just beyond harvest. Irradiance was measured with a quantum sensor (QSO, Apogee, Logan, UT, USA) above the canopy and underneath the shade cloth.

Vine measurements

Shoot growth In the first two seasons, six shoots per vine per panel 3 vines, (18 shoots in total) were randomly chosen from both sides of the vine and shoot lengths measured at intervals throughout the growing season. In the third season, diameters of all leaves present on the six selected shoots were also measured, both in the width and length directions (see Greer and Weston 2010*b*) to assess leaf area development. Measurements were carried out from early in the growing season (October) until harvest (February). Only the main axis of shoot was measured in detail due to time constraints.

Internode and leaf area distribution Shortly after the grapes were harvested in each year, the selected shoots on each vine were destructively harvested and taken back to the laboratory. Leaves were removed and area of the individual leaves measured using a leaf area meter (LI3000, LiCor Inc. Lincoln, NEB, USA). Internode lengths along each shoot were measured in the first two seasons along with overall stem length.

Biomass After the destructive harvest and measurement, all components of the shoot including the laterals (leaves, stems and bunches) were dried at 60°C for two weeks and then weighed to determine biomass distribution.

Results and discussion

Canopy temperatures

Canopy temperatures of naturally exposed vines on both sides (*Figure 3.42*) were similar to air temperatures except that on the western side the canopy was often within ±2–3°C of air temperature

but when averaged over the whole growing season was 0.2°C below. However, the eastern side was commonly 1–2°C cooler and on average 0.5°C cooler than air temperature.

By contrast, shade cloth covering the vines had a marked effect on canopy temperatures (*Figure 3.43*), which were typically in the 15–25°C range on the western side but notably remained well below 40°C in midsummer. In fact, during the mid afternoon the canopy was commonly 4–6°C cooler than air temperature and when averaged over the whole growing season was 2.1°C cooler. A similar difference occurred with the eastern side of the canopy (*Figure 3.43B*) and, on average, was 1.6°C cooler than air temperature.

Covering Semillon vines in a vineyard with 70% shade cloth reduced the canopy temperatures on average by 3–5°C below the air temperature. This is well in keeping with many other studies (Cartechini and Palliotti 1995; Rana *et al*. 2004; Cohen *et al*. 2005; Lugassi-Ben-Hamo *et al*. 2010) that confirms shading reduces temperature in the canopy.

Shoot architecture

Numbers of nodes For the Semillon shoots, there were a variable number of nodes, ranging from as few as 7 and up to 45 nodes when the shoots were measured at harvest. On the basis of numbers of preformed primordia in Semillon buds (Greer and Weston 2010*b*), these shoots were divided into three classes (*Figure 3.44*); those with less than 15 nodes (short), those with less than 19 nodes (medium) and those longer than 19 nodes (long). The node number distribution effect was highly significant ($P<0.01$) but there was no difference statistically ($P>0.05$) between the exposed and shaded vines in distribution of node numbers. However, exposed vines had similar proportions of short and medium shoots (18–19%) whereas the shaded vines had twice as many medium shoots (33%) than short shoots (15%). Vines from both treatments had predominately long shoots; 63% of shoots on exposed vines and 52% on the shaded vines. Thus, there was a shift in node number distribution to more medium shoots in the shaded vines compared with exposed vines.

Vine architecture was, therefore, markedly affected by the presence of the shade, that is, the distribution of

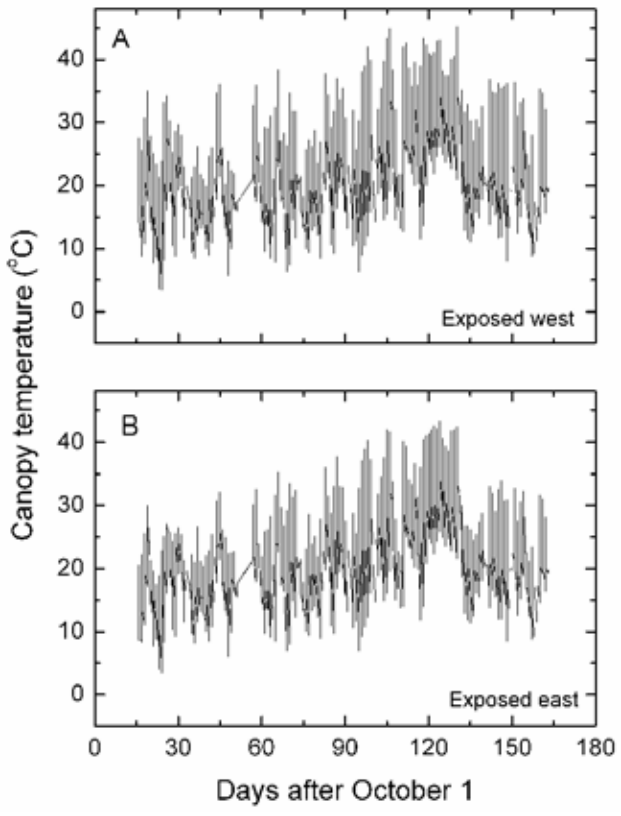


Figure 3.42 Averaged hourly canopy temperatures measured throughout each day of the 2008-09 growing season on the western (A) and eastern sides (B) of well exposed Semillon grapevines growing in a Riverina vineyard.

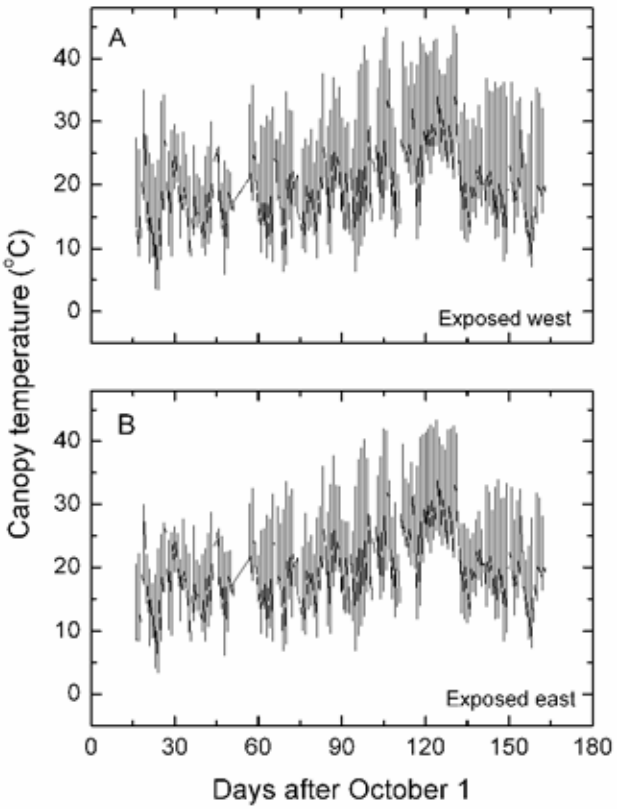


Figure 3.43 Averaged hourly canopy temperatures measured throughout each day of the 2008-09 growing season on the western (A) and eastern (B) sides of Semillon grapevines covered with 70% shade cloth and growing in a Riverina vineyard.

shoot types on each vine. Shoot type is dependent on the number of nodes on each shoot and the number can vary markedly. Node numbers are determined by two processes; expansion at or after budbreak of existing leaf primordia preformed in the dormant bud in the previous season and subsequent expansion of de novo primordial production by the shoot apical meristem in the current season (Seleznyova *et al.* 2002; Louarn *et al.* 2007; Spann *et al.* 2007; Greer and Weston 2010*b*). As shown earlier (*Figure 3.29* and *3.30*), the number of preformed primordia in Semillon buds is highly variable, from 12 to 19 but with distinct peaks at 14 and 18 primordia at frequencies of 30 and 22%, respectively. In addition, on the basis of actual shoot development, two zones of preformed primordial expansion could be recognised. All Semillon shoots have an initial cluster of 5–6 leaves that emerge together more or less as a single cohort over a few days. As has been shown in other vine species, shoot expansion can terminate after this cohort has expanded, generating short terminated shoots (Seleznyova and Greer 2001; Seleznyova *et al.* 2002). In other Semillon shoots, all the remaining preformed primordia will expand but again the growing tip may die after all these primordia have expanded and no new leaves added, thus generating medium length terminated shoots of varying lengths in the Semillon vines. The results of the earlier study suggest such Semillon shoots could be anywhere from 12 to 19 nodes long. In yet other shoots, new leaves are added to the existing expanded primordia by the shoot apical meristem and thus long non-terminating shoots with any number of nodes above 20 are created. A similar pattern of shoot architecture occurs in *Actinidia deliciosa* vines (Seleznyova *et al.* 2002), although the medium shoots are not variable in node number as occurs with Semillon.

Internode lengths The mean internode lengths along the shoot of each node class are shown in *Figure 3.45*. There was a highly significant interaction ($P<0.01$) between node class and treatment, indicative of more significant differences in internode lengths between the node number classes in the exposed vines than in the shaded vines. In all cases, maximum internode lengths typically occurred around node position 5–6 though internodes on long shoots of exposed vines were maximal at about node 15. In the short shoots, the longest internode lengths were on average 4.7 ±0.3 cm and thereafter the internodes declined consistently with increasing node number to less than 2 cm. For both medium and long shoots, the maximum internode length was spread broadly along the shoot, from node positions 5 to 10 but the maximum length increased from 5.0 ±0.3 cm in medium to 6.5 ±0.2 cm in long shoots. Internode lengths also declined consistently along the shoot in

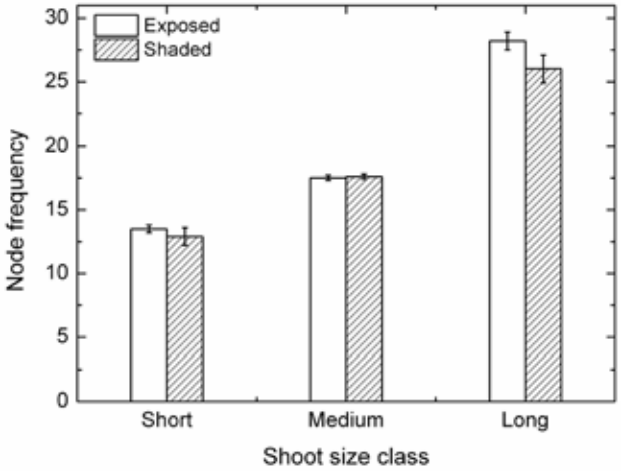


Figure 3.44 Frequency of nodes (Mean ±SE, N=24) in the different shoot types of Semillon vines grown in a Riverina vineyard either exposed to full sun or covered with 70% shade cloth. These data were averaged over two growing seasons from 2006–07 to 2007–08.

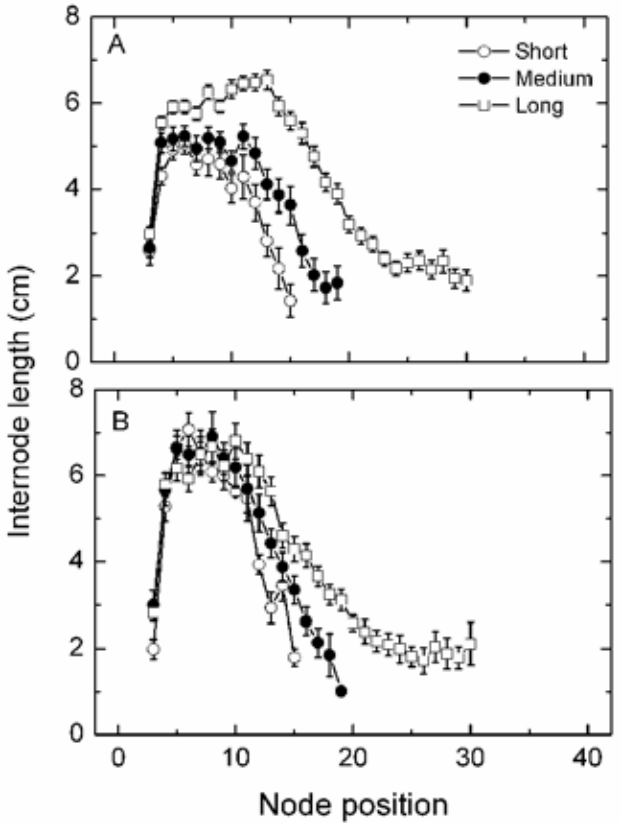


Figure 3.45 Internode lengths (Mean ±SE, N=12) along the stem at the different node positions on Semillon vines growing in a Riverina vineyard during the 2008-09 growing season and either exposed to full sun (A) or covered with 70% shade cloth (B) for the three types of shoots as indicated and measured at harvest. All internodes were fully expanded.

both medium and long shoots to about 1–1.5 cm. Internode lengths on fully exposed vines were, thus, markedly different in the long shoots at the basal node positions compared with short and medium shoots.

In contrast to the exposed vines, the shade treatment changed the pattern of internode size distribution along the shoots to much less clear differences between the three node number classes, particularly in the first 10 or so nodes. Here the maximum internode lengths all clustered around 6–6.5 cm, hence, there were longer internodes on shaded compared to exposed vines at comparable node positions. The pattern of declining internodes lengths in all shoots with increasing node number was evident in both shaded and exposed vines.

Stem growth Stems measured across the growing season were variable in length and could also be divided into the three size classes according to the number of nodes (*Figure 3.46*). Between these size classes, overall stem lengths were statistically different ($P<0.01$) but there was no statistical effect of the shade treatment on the stem lengths nor between seasons. Applying a kinetic analysis to these stem growth patterns over time indicated there were no significant ($P>0.05$) differences in either timing of stem extension or in the duration of stem growth between the different size classes. Similarly, there were no significant differences ($P>0.05$) in relative extension rates between the shoot size classes or between the treatments and overall the relative rate of extension averaged 2.23 ±0.85 mm d^{-1}. This suggests differences between the different shoots in length were due entirely to the number and length of the internodes and not to their ontogenetic growth pattern. Across all shoots, 12.5% were of short length, 26.4% were of medium length and 61.1% were long, thus, consistent with the distribution of node numbers.

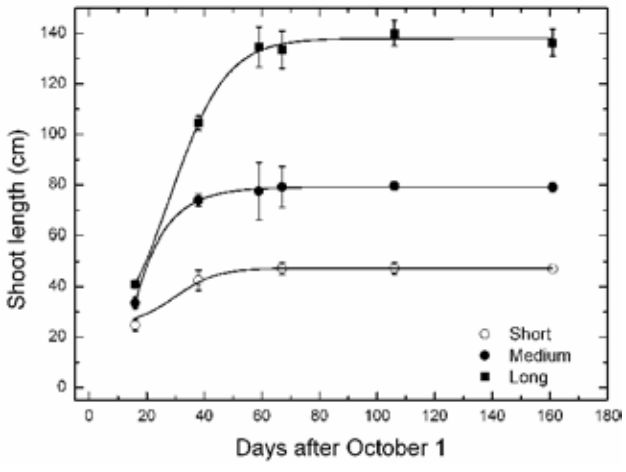


Figure 3.46 Shoot lengths (Mean ±SE, N=24) throughout the growing season of the different shoot types of Semillon vines grown in a Riverina vineyard. The data are averaged over two growing season from 2006–07 to 2007–08. The lines are the best fit to a sigmoid function.

Leaf area distribution along shoots In keeping with internode lengths, leaf area of fully expanded leaves along the shoot also varied with node number distribution (*Figure 3.47*). There was a highly significant interaction between the size class, treatment and node position ($P<0.001$) but seasonal effects were not significant. For exposed vines (*Figure 3.47A*), leaf areas along each of the different sized shoots were almost always significantly different; the smallest leaf areas on short shoots through to the largest leaf areas on long shoots. Thus, for each short shoot, the largest leaf was 0.0094 ±0.0015 m^2, for medium shoots was 0.0125 ±0.0018 m^2 and for long shoots, the largest leaf was 0.0158 ±0.0007 m^2 and these usually occurred at about node position 7. Across the whole shoot, the total leaf areas were, on average, 0.103 ±0.0005, 0.162 ±0.0007 and 0.324 ±0.0007 m^2 for short, medium and long shoots, respectively. The long shoots averaged 43 nodes in total.

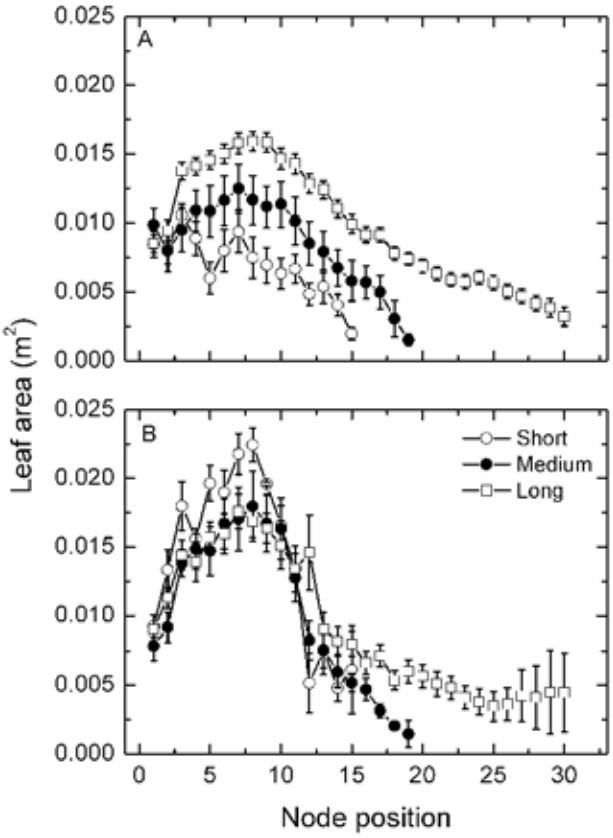


Figure 3.47 Leaf areas (Mean ±SE, N=12) along the stem at the different node positions on Semillon vines growing in a Riverina vineyard during the 2008-09 growing season and either exposed to full sun (A) or covered with 70% shade cloth (B) for the three types of shoots as indicated. All leaves were fully expanded.

For the shaded vines (*Figure 3.47B*), all leaf areas at each node up to about position 10 on all shoots were larger than the comparable leaf areas on the exposed vines. There were few differences between medium and long shoots in leaf areas and the largest leaves were 0.0180 ±0.0025 m^2 and 0.0175 ±0.0013 m^2, respectively, while in the short shoots leaves at positions 5–8 were the largest of all and reached 0.0224 ±0.0012 m^2. On the shaded vines, leaves beyond node position 10 were about the same in area as the leaves on the exposed vines. Overall leaf areas of the shaded vines averaged 0.212 ±0.0015 m^2, 0.196 ±0.0012 m^2 and 0.290 ±0.0008 m^2 for the short, medium and long shoots, respectively. Long shoots had an average of 33 nodes. Thus, exposed vines were largest in total area but only because of more nodes overall.

The three shoot types occurring in the present study differed in patterns of both internode length and leaf area distribution, suggesting differences in development between the shoot types. Short and medium shoot internodes of exposed vines both extended to similar lengths in the first five node cluster but long shoot internodes at comparable node positions were significantly longer. After appearance and extension of the next cohort of nodes, the internodes of medium shoots were significantly longer than those on the short shoots and this trend continued along the stem. However, the lengths of long shoot internodes were always much longer than those of the other shoot types. This distribution pattern was also repeated with the leaf areas along the shoot for the different types. Short shoots generally had the smallest leaves and long shoots the largest leaves. For long shoots, a similar leaf area pattern occurred with Grenache vines (Lebon *et al.* 2004) and for both internodes and leaf areas of Syrah and Grenache vines (Pallas *et al.* 2009). Unfortunately, it was not possible to collect internode or leaf expansion data over all the growing seasons of the present study and in the third season only leaf expansion data for long shoots were collected. Thus, the difference in internode lengths and leaf areas of the different shoot types might have occurred through different growth and development dynamics but otherwise there were no clear reasons for the differences.

The shade treatment clearly impacted on the internode length and leaf area distributions in the different shoot types but not consistently. For the internodes, there were no differences between the shoot types in overall lengths, however, they were all longer, at least in the first 10 nodes, than on exposed vines. Short shoots had the largest of all leaves in contrast to that on exposed shoots but the leaf areas of all shoot types were largest in the shaded vines. Thus, in shade conditions internodes extended and leaf areas expanded much more than in full sun conditions. This contrasts with maize plants in sun and shade conditions where internode lengths were markedly shorter in shade conditions (Fournier and Andrieu 2000). Similar results to the Semillon shoots were also recorded for the rainforest liana *Ipomoea phillomega* in shaded versus exposed conditions (Peńalosa 1983).

On the basis of these different shoot extension patterns, at least four shoot types may be observed in Semillon vines. Some very short shoots with no more than five leaves should occur. While such shoots were not explicitly observed in this study they do indeed occur in many varieties (S. Hackett *pers. comm.*). Short shoots with at least 14 nodes on average and medium shoots with 19 nodes on average as well as shoots with node numbers ranging from 20 to 45 occurred in the present study. In fact, the short and medium shoots both occur on the vines at frequencies of just under 20% while long shoots occur at over 60% of the total shoots per vine and, therefore, predominate. These data, therefore, confirm our hypothesis above. Interestingly, the shade cloth perturbed this pattern, with the frequency of short shoots dropping to about 15%, the medium shoots increasing in frequency to over 30% and long shoot frequency declining to about 50%. The fact that more medium shoots occurred largely at the expense of long shoots in shaded vines suggest termination of the apical meristem activity by sub apical tissue necrosis (Foster *et al.* 2007) may have increased, accounting for fewer long shoots, possibly from a carbohydrate limitation in these vines. Further work is needed to assess this hypothesis.

Leaf growth dynamics

The Boltzmann sigmoid function was fitted to the expansion of all leaves over time on each shoot of each vine and treatment and the fit (not shown) was statistically significant in all cases (r^2=0.98, P<0.001). The timing of maximum leaf expansion ascertained from fitting of the Boltzmann function to leaf expansion data revealed a significant difference between the exposed and shaded vines (Figure 3.48). Leaves in the initial cluster (1–5 nodes) all reached their midpoint of expansion about 26 days after budbreak in both treatments. Thereafter, the timing of expansion for individual leaves on exposed vines

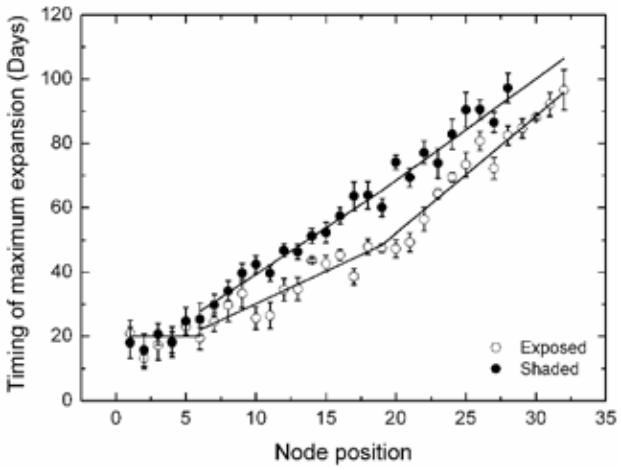


Figure 3.48 Timing of expansion (Mean ±SE, N=12) for each leaf along the stem for Semillon vines growing in a vineyard during the 2008–09 growing season and either exposed to full sun or covered with 70% shade cloth as indicated. The lines are linear regression fitted to each section of the data and were highly significant ($P<0.001$, $r^2=0.95$) except for the first five leaves where the line indicates the mean value.

increased in a linear pattern along the shoot, at least to about position 19, at a constant phyllochron of 2.39 ±0.34 days. Further along the shoot, the timing of expansion still increased in a linear pattern but at a significantly ($P<0.05$) higher phyllochron of 3.32 ±0.19 days. For the shaded vines it was noteworthy that the timing of expansion in all leaves was markedly later, on average by 13 (range 2–25) days. Furthermore, the linear regressions fitted to the timing of expansion for leaves along the shoot did not vary significantly around node 19 and along the whole shoot, timing of expansion could be described by a constant phyllochron of 2.99 ±0.09 days. This was significantly ($P<0.01$) longer than for exposed leaves up to position 19 but for leaves further along the shoot, the difference was not significant ($P<0.05$).

The times for the leaves along the shoot to achieve 20 and 80% expansion of full size (*Figure 3.49*) increased in a more or less linear pattern in all shoots, however, these times were again later for the shaded compared to the exposed vines. Perhaps of more importance, the difference, i.e. the duration of leaf expansion along the whole shoot of exposed vines averaged 16.7 ±1.0 days while for shaded vines, the duration of leaf expansion averaged 12.2 ±0.7 days and this difference was highly significant ($P<0.01$). Thus, while the shade treatment delayed the timing of leaf expansion, this appeared to be offset by faster leaf expansion in comparison with leaves on exposed vines.

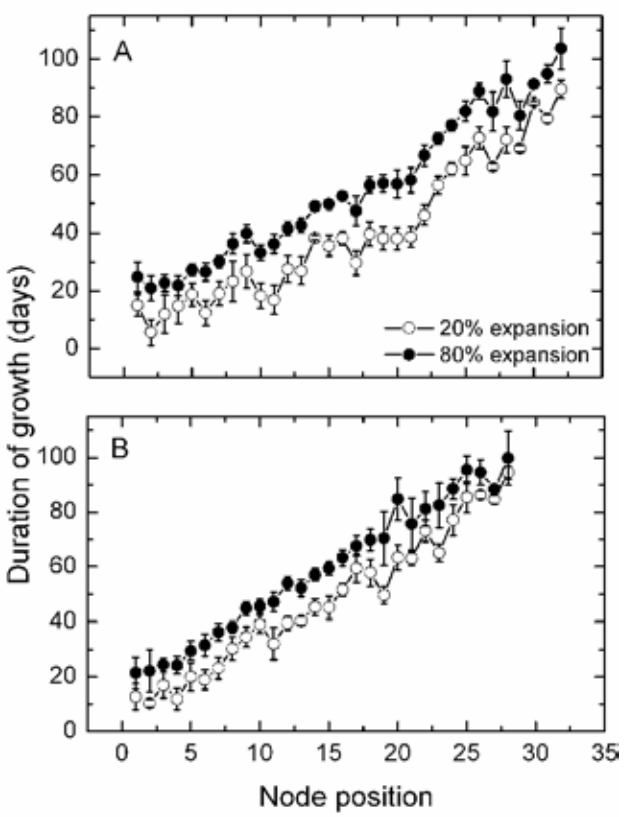


Figure 3.49 Times for leaf expansion (Mean ±SE, N=12) to reach 20 and 80% of the fully expanded size of each leaf along the stem of Semillon vines growing in a Riverina vineyard during the 2008–09 growing season and either exposed to full sun (A) or covered with 70% shade cloth (B). The difference between these two data sets indicates the duration of growth in each case.

The fully expanded area of each leaf along the shoot (*Figure 3.49*) determined from the Boltzmann function, initially increased over the first 6–7 nodes in both exposed and shaded vines and thereafter declined. While the largest leaves occurred at similar shoot positions, the area of these largest leaves was significantly ($P<0.01$) larger on shaded vines than on exposed vines by 50%. However, from about node 13, this difference was lost and all other leaves were more or less similar in final size for both treatments

Perhaps what was surprising was there were no treatment effects on the dynamics of stem extension of the different Semillon shoot types. Neither the timing of expansion nor the duration of extension was statistically different between the shoot types and shade had no effect as well. However, the final stem length was significantly different, thus confirming the shoot types do extend in length in accordance with the number of nodes. This contrasts with long and short shoots of Pistacia vera in that higher growth rates and greater duration of growth occurred in the long shoots (Spann *et al.* 2007).

By contrast with the stems, the detailed kinetic analysis of leaf expansion patterns revealed leaves of the shaded Semillon vines, at least those beyond the initial cluster, were generally later to develop than exposed vine leaves. This was shown by the delay in the timing of expansion of all leaves on the shaded vines compared with those on exposed vines. This delay reached upwards of 10 days and more. Delayed development of the shaded leaves was also evident by the times when leaf expansion reached 20% of full size, for example, leaves 9–11 were about 15 days behind while leaves 19–21 were nearly 24 days behind the exposed leaves at the comparable developmental stage. These data were perhaps indicative of delayed leaf appearance in the shaded vines, however, it was not possible to directly measure leaf appearance in this field study to confirm this. Nevertheless, we can conclude shading the vines caused developmental delays in leaf expansion and most probably also in internode extension. Fournier and Andrieu (2000) also observed delays in the timing of linear elongation of maize leaves in shade compared with sun conditions.

The shade treatment had another developmental effect on leaf expansion. It was apparent from the kinetic analysis of leaf development of leaves of exposed vines that three zones of development were apparent. A first zone of 5–6 nodes where the timing of expansion was more or less the same, a second zone to about position 19 where timing of expansion increased linearly along the shoot in a regular pattern and a third zone beyond where the timing of expansion, while linear, was at a much longer phyllochron or slower rate than the zone two leaf development. This pattern of development not only conforms to the origins of the different shoot types as outlined above but also exactly to the dynamic patterns of leaf and internode growth of potted Semillon vines (Greer and Weston 2010*b*). Shade appeared to alter this developmental pattern in the present study such that no discernable change in timing of expansion could be detected around nodes 19–20 as occurred with the exposed vines. As this pattern of shoot development has been shown to hold for potted vines in controlled growth conditions (Greer and Weston 2010*b*) and for vineyard conditions as well, it perhaps suggests ontogenetical control of shoot development occurred. This conclusion conforms to that for Actinidia deliciosa where shoot development under a range of condition was assessed (Greer and Jeffares 1998). More particularly, Greer (2001) showed shoot development in *Actinidia* was not affected by irradiance. Thus, it remains uncertain why shade should alter the pattern of shoot development in Semillon shoots.

Despite the delayed and altered development under shade, leaf expansion rates were markedly higher, as indicated by the shorter durations of expansion, compared with leaves on exposed vines. By contrast, shade increased duration of maple leaf expansion (Seiwa 1999). Shaded Semillon leaves were also consistently larger, at least up to node 12, compared with exposed leaves and the total shoot leaf area was also greater. Therefore, higher rates of expansion appear to have offset the delayed development shown here.

Biomass accumulation and leaf area

There were no significant interactions (P>0.05) between the shaded and exposed treatments and the growing seasons. However, there were highly significant effects of both growing season and treatment on shoot biomass (*Table 3.7*). Leaf, stem and bunch weights all varied significantly across the each of the three growing seasons but there was no consistent change. For example, bunch biomass

Table 3.7 Leaf, stem, bunch and total biomass (Mean ±SE, N=24) over each of the three years of the study and for the shaded vines and those exposed to full sun conditions. All data were collected from a destructive harvest of the shoots at the end of the growing season in each case. Note each value includes the main axes and all lateral branches. Also shown are the proportions of biomass for each of the three components and the probability of the differences being statistical significance ns, (P>0.05).

	Growing season				Treatment		
Dry weight	**2006–07**	**2007–08**	**2008–09**	**P**	**Exposed**	**Shaded**	**P**
Leaf (g)	15.4 ± 1.3	23.6 ± 1.2	19.5 ± 1.7	0.0001	22.3 ± 1.0	16.8 ± 1.3	0.0010
Stem (g)	12.9 ± 1.6	30.4 ± 1.5	32.7 ± 1.6	0.0001	26.3 ± 1.1	24.3 ± 1.6	ns
Bunch (g)	65.1 ± 3.4	54.0 ± 3.0	42.6 ± 3.0	0.0001	58.7 ± 2.1	49.1 ± 2.9	0.0093
Total (g)	93.4 ± 4.9	108.0 ± 4.4	96.1 ± 6.4	ns	110.0 ± 3.9	89.0 ± 4.9	0.0009
% Leaves	17.3 ± 1.1	21.9 ± 0.9	20.4 ± 1.4	0.0060	20.7 ± 0.8	19.1 ± 1.0	ns
% Stems	13.7 ± 1.2	27.7 ± 1.1	33.3 ± 1.6	0.0001	24.1 ± 0.9	25.8 ± 1.2	ns
% Bunch	66.9 ± 2.2	50.3 ± 1.9	46.1 ± 2.7	0.0001	56.1 ± 1.6	55.1 ± 2.1	ns

progressively declined while stem biomass increased. Notably, the total biomass of the shoots did not vary significantly over the different growing seasons.

By contrast, when averaged over the three growing seasons, leaf, bunch and the total biomass per shoot declined significantly in shaded compared with exposed vines by 20–25%. Stem biomass, however, did not vary significantly between shaded and exposed vines.

While the biomass allocated to bunches was the greatest and more or less similar allocations to leaves and stem occurred, there were significant changes in biomass allocation over the different growing seasons (*Table 3.7*). There was a marked tendency for biomass to be reallocated to leaves but more particularly to stems at the expanse of bunch biomass from the first through to the third growing season. By contrast, there were no effects of shading on biomass allocation with 20% allocated to leaves, 25% to stems and 55% to bunches.

Across all years, total shoot leaf area between shaded and exposed vines did not vary significantly (not shown) and averaged 0.296 ±0.021 m^2. However, specific leaf areas were significantly ($P<0.001$) higher for the shade leaves (0.0179 ±0.0003 $m^2\ g^{-1}$) compared with sun leaves (0.014 ±0.0002 $m^2\ g^{-1}$).

Shading reduced the irradiance that the Semillon vines were exposed to and, given the well established effect on reducing photosynthesis (Givnish 1988), there is an a priori expectation that dry matter accumulation would be impacted on by shading the vines. Certainly this is in keeping with many other studies (Cohen *et al.* 2005; Grassi and Minotti 2000; Guglielmini and Satorre 2002; Liu *et al.* 2007). In confirmation, averaged across all growing seasons, total biomass of the Semillon shoots declined about 20% in the shade and it was the decreases in both leaf and reproductive biomass that caused this reduction.

Conclusions

Covering Semillon vines in vineyard conditions with shade cloth reduced the canopy temperatures by about 5°C below air temperatures thus effectively reducing the vine exposure to high temperatures. The shade cloth also reduced irradiance by 70%, which in turn reduced shoot growth but not the proportional allocation of biomass. The shade also changed the shoot architecture towards a higher frequency of medium shoots and lower frequency of long shoots compared with exposed vines. Shoot development was also delayed by the shade but leaf expansion rates and fully expanded leaf areas increased possibly by way of compensation. The impact of these changes in development on the vine carbon balance is the focus of the next study.

Experiment 3.9
Reductions in biomass accumulation, photosynthesis *in situ* and the net carbon balance are the costs of protecting *Vitis vinifera* cv. Semillon grapevines from heat stress

Materials and methods

Plant material and treatment conditions

This study was undertaken on the same vineyard in the Riverina as above. New vines were selected for study in each growing season. Budbreak occurred in mid September, flowering in early-November and fruit set in mid-November. The shade treatment was the same as described above.

Vine measurements

Shoots Six shoots were randomly selected from each vine of each treatment (6 vines per treatment) from both the eastern and western sides of the canopies In each growing season. Lengths of each selected shoot were measured at about weekly intervals throughout the growing season. In the second season, leaf width and length dimensions of each leaf on two of the six shoots per vine were also measured at regular intervals to determine leaf area as the simple product of width and length (Sepúlveda and Kliewer 1983). Allometric relationships between stem length and dry matter and between leaf area and dry matter were applied to determine dry matter accumulation of stems and leaves across the growing season (Greer and Sicard 2009). All data were informally adjusted to ensure each stem or leaf dry weight estimation at the end of the growing season matching the actual weights measured at the destructive harvest by adjusting each value by the ratio of the measured weight to the estimated weight.

Bunches The length of each bunch on each of the six selected shoots on each vine were also measured at regular intervals after flowering. Using an allometric relationship between bunch length and dry matter (Greer and Sicard 2009), the changes in dry matter accumulation for each bunch over the growing season was determined. Again informal adjustments

occurred to ensure calculated determinations match the measured values at harvest. All bunches on the selected shoots of each vine were harvested about 12 February and taken to the laboratory and dried at 60°C for two weeks to determine dry matter content.

Harvest

Approximately one month later (mid-March), the selected shoots on each vine were destructively harvested and taken to the laboratory . Leaf areas were measured on all leaves using a leaf area meter (LI-3000, Li-Cor, Lincoln, NE, USA) then all stems and leaves were oven-dried at 60°C for two weeks to determine dry matter content.

Gas exchange

From about the time when individual leaves were about 35 mm in width, gas exchange was measured using an open gas exchange system (LCA4, Analytical development Company, Hoddeson, UK). All leaves on each of two of the selected shoots in each section were measured at about weekly intervals in all conditions except rainy days. These measurements commenced late in the growing season (early January) In the first season, but in the second growing season, measurements commenced on 9 October. All leaves on the selected shoots were measured sequentially along the shoot on each occasion, thus an increasing number of measurements were required as the shoots developed up to 30 leaves as the season progressed. All measurements were recorded during daylight hours from 9 am to 5 pm *in situ* at the prevailing orientation of each leaf on the shoot. The PFD and leaf temperatures were measured concurrently with a quantum sensor and thermister attached to the leaf cuvette of the gas exchange system and these reflected the leaf orientation in each case.

Net carbon balance

The total carbon fixed per shoot throughout the growing season was assessed by integrating the net rate of photosynthesis over the day, assuming the measured rates represented a daily value (Cartechini and Palliotti 1995; Edson *et al.* 1995). The net daily CO_2 fixation per shoot was determined as the product of the area of each leaf and it's attendant photosynthetic rate then summed over all the leaves present on the shoot of each day of the measurements. These values were then summed over all measurement days across the whole growing season. Rates of dark respiration of these leaves were determined separately and used in the daily accumulation of CO_2. Net carbon acquisition was then determined by taking into account the molecular fraction of carbon in carbon dioxide (Wullschleger *et al.* 1997; Greer *et al.* 2003).

The carbon accumulated as biomass was determined from the total biomass accumulated over the growing season for each shoot firstly by assuming that 45% of the biomass was elemental carbon (Walton and Fowke 1995). The product was then mathematically differentiated using Origin V8.1 software (OriginLab, Northampton, MA, USA) to determine the rate of carbon accumulation per day over the whole growing season for each shoot in each treatment. The net daily carbon balance was then determined as the mathematical difference between the rates of carbon acquisition and the rates of carbon sequestered as biomass for each shoot.

Results and discussion

Vine attributes

Across both growing seasons, there were no significant ($P>0.05$) differences in either the numbers of shoots set on the vines or the number of bunches per vine (*Table 3.8*) between the exposed and shaded treatments. However, there was a marked and significant ($P<0.05$) decrease in the number of shoots (20%) and bunches (30–40%) in the second growing season of the study compared with the first growing season. In both cases, an average of just over two bunches per shoot occurred in each treatment.

Table 3.8 Average numbers af shoots and bunches on each Semillon vine (Mean ±se, n=12) in the exposed and shaded treatments over the two growing seasons of the study. In each case, the shoot and buds numbers were set in the previous winter through the vineyard management.

Year	Treatment	Shoots vine^{-1}	Bunches vine^{-1}
2007–08	Exposed	30.7 ± 3.1	66.8 ± 7.2
	Shaded	33.7 ± 2.7	63.3 ± 4.1
2008–09	Exposed	25.3 ± 1.9	40.6 ± 3.9
	Shaded	26.5 ± 2.2	45.8 ± 5.9

Biomass accumulation

Across the whole growing season, stem and leaf biomass of each shoot accumulated in a curvilinear pattern (*Figure 3.51*) and reached a maximum about 80 days after budbreak (DAB). For the stems, there was no significant difference between exposed and shaded shoots in both seasons and the total stem biomass averaged (mean ±SE) 33 ±2.8 g. By contrast, leaf biomass accumulation was significantly ($P<0.01$) higher in exposed shoots compared with those in the shade (*Table 3.9*) and reached 28.5 ±1.3 g compared

with 20.1 ±0.9 g in the 2007-08 season and similar amounts in the 2008-09 growing season. Thus, allocation of biomass to stems in both cases was greater than to the leaves.

It was noteworthy that the total biomass accumulated over the growing season in a somewhat double sigmoid pattern (*Figure 3.51*). The first increase in total biomass occurred because of the biomass accumulation as leaves and stems and subsided as these stopped growing. Then the total biomass increased again in accordance with the development and growth of the bunches in the later half of the growing season. Thus, stem growth probably slowed in response to growth of the bunches. Because of significantly higher leaf and bunch biomass allocation in the exposed compared to the shaded vines the total biomass was also significantly ($P<0.01$) higher at about 200 ±12 g compared with 150 ±11 g (*Table 3.9*).

The biomass of bunches (*Figure 3.51*) greatly exceeded the allocation to the stems and leaves and over both seasons reached maximum dry weights of 130–140 ±10 g for the exposed vines and about 100 ±8 g for the shaded vines and these differences were statistically significant ($P<0.01$).

The dynamics of growth of the stems and leaves of the exposed vines were generally similar in that timing of maximum growth rates occurred around 33 DAB but the shoot leaf area extended over a longer time interval (14 days) compared with the stem extension (10 days). By contrast, shoot leaf area expansion of shaded vines was delayed in reaching maximum rates by nearly 6 days compared with stem extension but the duration of maximum growth was similar in each at about 10 days (*Figure 3.50*). Bunches reached their maximum growth some 70 DAB after the leaves and stems in both cases, but maximum growth rates of the bunches were maintained over 7 days, hence markedly shorter than for stems and leaves. Shade covering thus had no affect on bunch development.

These date show that shade covering over Semillon grapevines impacted on some of the components of biomass accumulation over the growing season. In particular, leaf and bunch biomass growth was significantly reduced but stem biomass was unaffected. The dynamic pattern of stem biomass accumulation in both treatments was also unaffected, reaching maximum rates at the same time. This suggested shade covering had no effect on stem growth and development. By contrast, the dynamic pattern of leaf biomass accumulation was significantly affected, with a marked delay in the shaded vines at achieving the

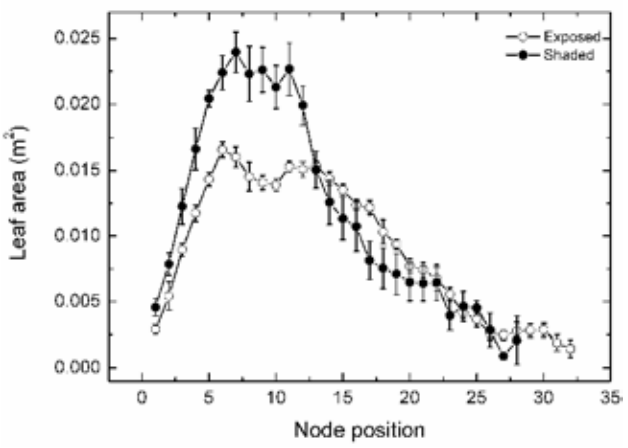


Figure 3.50 The maximum leaf area (Mean ±SE, N=12) along the long stems of Semillon vines growing in a Riverina vineyard during the 2008–09 growing season and either exposed to full sun or covered with 70% shade cloth, as indicated. Each value is estimated from the fitting of the sigmoid function to the expansion of individual leaves.

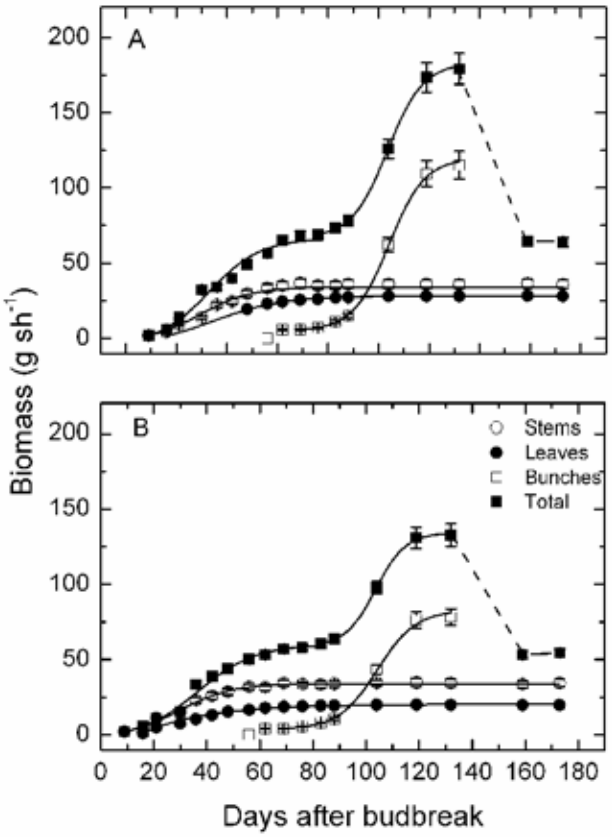


Figure 3.51 Changes in dry weight accumulation of leaves, stems and bunches and the total biomass as indicated (Mean ±se, n=18–36) of Semillon shoots across the growing season on vines grown in an irrigated vineyard without (A) and with shade covering (B) and averaged over two growing seasons. The lines are the Boltzmann sigmoid function fitted to the data. Also shown is the total biomass after harvest of the bunches. Flowering occurred on about 40 DAB and veraison about 90 DAB.

Table 3.9 Components of the total biomass (Mean ±se, n=12) per shoot at harvest of Semillon vines over two growing seasons and growing with and without shade covering as indicated. In all cases there were an average of 2.2 bunches per shoot.

Year	Treatment	Leaf biomass	Stem biomass (g)	Bunch biomass	Total biomass
2007-08	Exposed	28.5 ± 1.3	35.5 ± 3.6	132.5 ± 7.3	196.4 ± 15.9
	Shaded	20.6 ± 0.9	30.1 ± 4.2	98.2 ± 10.8	148.3 ± 12.7
2008-09	Exposed	28.1 ± 0.7	33.7 ± 3.5	150.1 ± 6.3	209.2 ± 8.8
	Shaded	19.1 ± 1.0	31.9 ± 2.9	107.6 ± 5.2	158.8 ± 6.5

maximum rates compared with the exposed vines. Perhaps of more significance, however, was that leaf biomass accumulation in both treatments initially commenced at about the same rate at a time when the vines were heterotrophic and dependent on carbon reserves in the roots to support this growth (Holzapfel *et al.* 2010). This suggests shade should have had no affect until the vines became fully autotrophic and dependent on current photosynthate for growth.

That bunch biomass accumulation was markedly affected by the shade covering was certainly consistent with the impact of shade on photosynthate production, given that bunch growth occurred when the vines were fully autotrophic. Over both seasons, some 25–40% lower biomass accumulation occurred in the shaded compared with exposed vines. It was evident that by the time the bunches commenced growth, vegetative growth of the shoots had all but stopped. Thus, there appeared to be little competition for carbon between the vegetative and reproductive growth, given the temporal separation in their development. Indeed, rates of bunch biomass accumulation were also markedly higher than occurred with the leaves and stems (cf. Flore and Lakso 1989) and a clear indication of the strength of the bunches as a carbon sink (Petrie *et al.* 2000).

Leaf area development

Budbreak occurred close to 25 September in both seasons and leaf measurements commenced within 15 days of budbreak. The pattern of leaf area along the shoot showed a regular quadratic shape (*Figure 3.52*) with leaf area of the first few leaves increasing dramatically to reach a maximum at positions 6 and 7 and then further along the shoot, leaf areas declined, in part because of recent leaf appearance. This same pattern was retained throughout the growing season but stretched out with the maximum leaf areas occurring in a broad peak between positions 6 and 11 and again, along the shoot, leaf areas declined.

It was noteworthy that the leaves along the shoots of shaded vines were generally larger in the peak positions at about 0.022 ±0.001 m^2 compared with comparable positions on the shoots of exposed vines where the leaves were about 0.015 ±0.007 m^2 and these differences were significant ($P<0.001$). However, at shoot positions beyond about node 12, shaded leaves tended to be smaller than comparable exposed leaves and this pattern persisted from mid to late season. Because all these leaves were relatively small, at least compared with those in peak nodal positions, they made little impact on the total shoot leaf area. For instance, for the shaded shoots, total leaf areas were 0.189 ±0.009, 0.302 ±0.016, and 0.312 ±0.018 m^2 at 42, 83 and 104 DAB whereas for the exposed vines, total leaf areas for the same times were 0.155 ±0.024, 0.278 ±0.036 and 0.289 ±0.037 m^2.

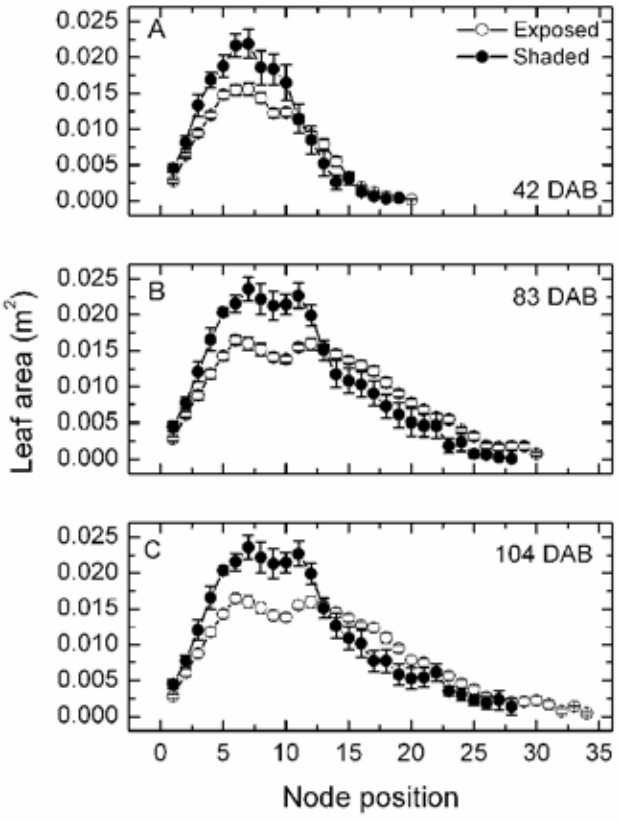


Figure 3.52 Leaf area distribution (Mean ±se, n=12) of Semillon leaves along the shoot at three different occassions (A–C) throughout the 2008-09 growing season on vines grown in an irrigated vineyard with and without shade covering as indicated. Flowering occurred about 42 DAB, veraison was near to 83 DAB and mid berry ripening occurred at 104 DAB.

These data show the vines in the shade also had much larger leaves, at least in the basal half of the shoot compared with those on exposed vines. This pattern of larger leaf sizes in the basal portion was apparent early in the growing season when the canopy leaf area was over 20% larger than in exposed vines. Later, the advantage in leaf area declined to under 10% in mid and late season, when a higher proportion of the leaves on shoots in both treatments were similar in size. These data are consistent with the well established leaf response to shade (Givnish 1988) in that generally leaf area increases while leaf thickness declines. The differences in leaf area occurring early in development are perhaps surprising as these Semillon leaves are largely preformed in the DORmant bud (Greer *et al*. 2010) and their size ontogentically determined (Greer and Jeffares 1998). However, from the current study, it would appear leaf expansion of preformed leaf primordia is perhaps more dependent on current photosynthate than previously considered and warrants investigation.

Photosynthesis

Along the shoot Rates of photosynthesis along the shoots initially showed a similar pattern to the leaf areas at 42 DAB (*Figure 3.53*), increasing from leaf 1 to a maximum at leaf 8 and thereafter the rates declined consistently between leaves 9 and 16 and probably reflected the incomplete development of these younger leaves. In the exposed vines, the maximum photosynthetic rate at this time was about 11.1 ±0.4 μmol (CO_2) m^{-2} s^{-1} and in the shaded vines it was about 7.6 ±0.7 μmol (CO_2) m^{-2} s^{-1} and this difference was significant ($P<0.01$). Integrating the photosynthetic rates across all leaves and taking the shoot leaf area into account at the time indicated the leaves on shoots in the shaded vines had 17% lower overall photosynthesis (12.8 ±0.5 cf. 15.4 ±0.7 μmol (CO_2) sh^{-1} s^{-1}) than the leaves on exposed vines.

Later in the growing season (83 DAB), differences in rates of photosynthesis between exposed and shaded leaves in the basal node positions (1–12) were not significant ($P>0.05$) but thereafter they were. Further along the shoot, rates of photosynthesis of the shaded leaves remained relatively low at about 5–6 μmol (CO_2) m^{-2} s^{-1} at least up to node position 18. By contrast, not only did the rates of photosynthesis of leaves further along the shoots of the exposed vines continued to increase between node positions 9 and 16 but the rates also increased to a higher maximum of 13.3 ±0.5 μmol (CO_2) m^{-2} s^{-1}. Beyond these nodal positions, the leaves of the exposed vines retained higher rates of photosynthesis across the shoot compared with the shaded shoots. This resulted in a 2.7-fold higher overall photosynthesis for the exposed shoots 58 ±0.5 μmol (CO_2) sh^{-1} s^{-1}) compared to the shaded shoots (21.8 ±0.2 μmol CO_2) sh^{-1} s^{-1}) when integrated over the whole shoot.

The pattern of changes in photosynthetic rates along the shoots was repeated at 104 DAB except that differences in the rates between leaves of exposed and shaded vines were small right up to nodal position 17 and only beyond this position were the rates of photosynthesis higher in the exposed than in the shaded leaves. However, rates of photosynthesis at this time were no higher than 10 μmol (CO_2) m^{-2} s^{-1} in all leaves of both treatments and markedly lower than earlier in the growing season. On this occasion, integration of photosynthesis across the shoots of the shaded vines (29.3 ±0.3 μmol (CO_2) sh^{-1} s^{-1}) was 32% lower than for the exposed vines (43.1 ±0.5 μmol (CO_2) sh^{-1} s^{-1}).

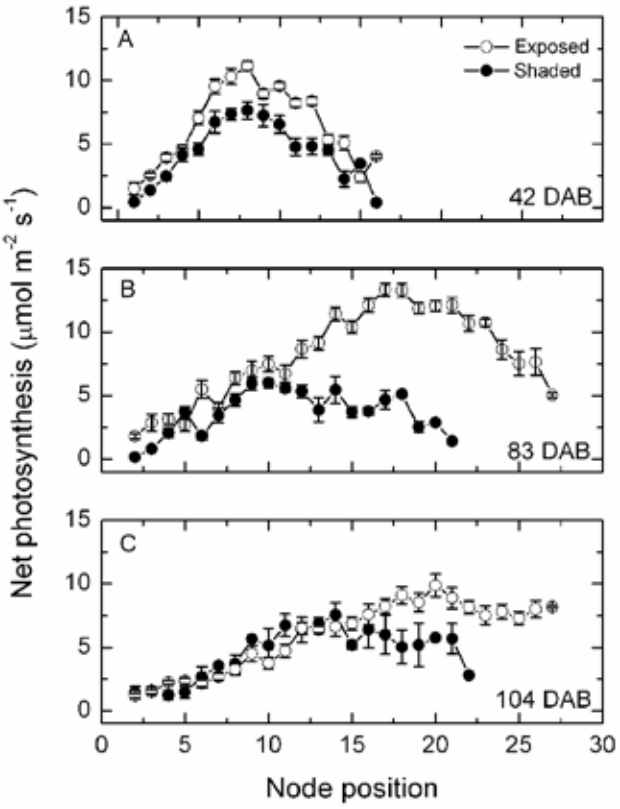


Figure 3.53 Changes in net photosynthesis)Mean ±se, n=8) of Semillon leaves along the shoot at three different occasions (A–C) throughout the 2008-09 growing season on vines grown in an irrigated vineyard with and without shade covering as indicated. Leaf temperatures averaged 25.5 and 23.4°C, 27.3 and 24.1°C and 31.6 and 30.9°C for the exposed and shaded leaves respectively on each occasion.

Across the whole growing season and averaged over all leaves, there were highly significant (P<0.001) effects of shade in both seasons on overall rates of photosynthesis with mean rates for the exposed vines ranging from 5.5 ±0.2 to 6.4 ±0.1 μmol (CO_2) m^{-2} s^{-1} in the two seasons while comparable rates for the shaded vines were 3.3 ±0.2 and 4.0 ±0.1 μmol (CO_2) m^{-2} s^{-1}.

In large part, differences in rates of photosynthesis between exposed and shaded leaves on each occasion of measurement were related to the PFD incident upon the leaves (*Figure 3.54*). For the shaded leaves, PFDs were typically less than 500 μmol (photons) m^{-2} s^{-1} whereas the exposed leaves experienced PFDs well above 1000 μmol (photons) m^{-2} s^{-1} except in the basal positions (nodes 1–7) of the shoot. However, the decline in photosynthetic rates along the shoot especially in the late emerging leaves was not necessarily related to the incident PFD but additionally to development of the leaf and gaining of photosynthetic competance, at least up to 83 DAB. Late in the season, the incident PFD appeared to drive leaf photosynthesis in all cases.

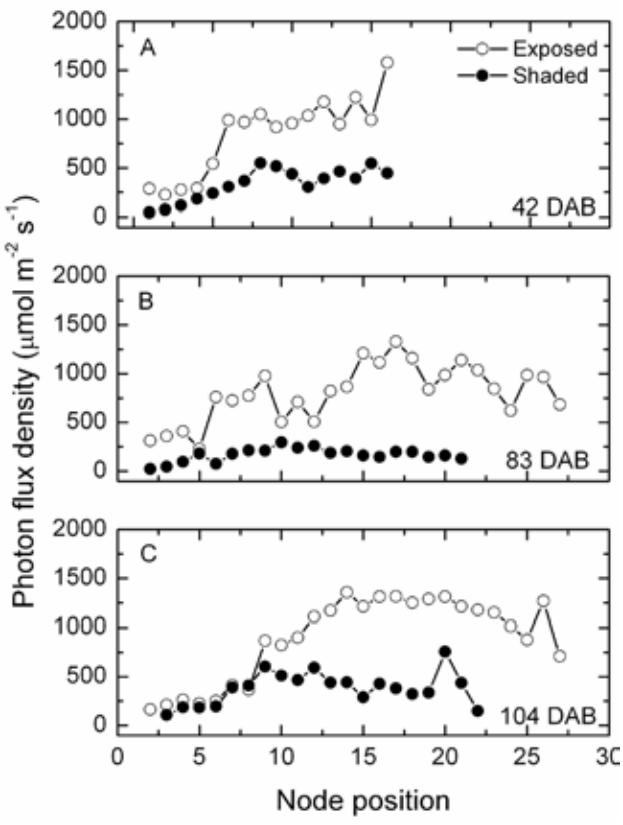


Figure 3.54 Changes in the incident photon flux density of Semillon leaves along the shoot at three different occasions throughout the 2008-09 growing season on vines grown in an irrigated vineyard with and without shade covering as indicated. Each value was measured simultaneously with gas exchange measurements.

Leaf photosynthetic rates over time There were clear differences in the maximum photosynthetic rates achieved by each leaf in the exposed vine treatment, with the maximum increasing successively between leaves 5 and 15; from 7.0 ±0.5 to about 10.3 ±0.8 and then to 13.4 ±0.5 μmol (CO_2) m^{-2} s^{-1} for leaves 5, 10 and 15 respectively (*Figure 3.55A*). By contrast, leaf 20 had a lower maximum rate than leaf 15. In all cases, however, leaf photosynthesis followed a regular pattern of increasing rates over the first few weeks to a peak rate and then declining markedly to lower but somewhat steady rates throughout the remaining growing season. Again, the steady state rate depended on leaf position, 2–3 μmol (CO_2) m^{-2} s^{-1} for leaf 5 to 5–6 μmol (CO_2) m^{-2} s^{-1} for leaves 15 and 20.

A similar pattern of changes in photosynthesis was evident for each leaf in the shaded vines (*Figure 3.55B*) except that differences in maximum rates between leaves 10 and 15 were not different while leaf 5 had then lowest maximum rate and leaf 20 had the highest maximum. However, in all cases, the maximum rates for the shaded vines (4.5–7.2 μmol (CO_2) m^{-2} s^{-1}) were lower than that for the exposed vines (7–14 μmol (CO_2) m^{-2} s^{-1}).

It is well established that shade plants have lower rates of light saturated photosynthesis than well exposed plants (Givnish 1988) and the photosynthetic light responses for the Semillon leaves conform with this conclusion. Also in keeping, the light saturation for the shaded leaves was below 600 μmol (photons) m^{-2} s^{-1} whereas it was more than double this for the exposed leaves. Further evidence for the impact of shade comes from the diurnal rates of photosynthesis. Similar photosynthetic responses between exposed and shaded plants have been reported for Sangiovese vines (Cartechini and Palliotti 1995) and *Picea abies* seedlings (Grassi and Minotta 2000). These shade responses of the Semillon leaves thus conform well to the generalised response to shade.

The rates of photosynthesis measured *in situ* at the native orientation of each leaf in the exposed and shaded treatments initially mirrored the pattern of leaf size along the shoot (see also Downton and Grant 1992; Poni and Giachino 2000) in the early part of the growing season (42 DAB) except that rates were significantly higher in the exposed compared to the shaded leaves. Most of these differences were clearly related to the incident PFDs within the canopy of each treatment (cf. *Figure 3.54*). However, some differences also pertained to the leaves, especially those emerging

late were still actively expanding and, therefore, not fully competent for maximum photosynthesis (Ho and Shaw 1977; Wullschleger and Oosterhuis 1990). This lack of photosynthetic competency was most apparent in mid season 83 DAB) when rates of photosynthesis in these same leaves (nodes 10–17) increased dramatically to over 10 μmol (CO_2) m^{-2} s^{-1} in exposed vines and at least up to 5 μmol (CO_2) m^{-2} s^{-1} in the shaded vines. It was also noteworthy that in spite of higher leaf areas in the shaded vines, the total CO_2 fixation per shoot, integrated over all leaves, was higher (15.4 to 58 μmol (CO_2) sh^{-1} s^{-1} at 42 and 83 DAB, respectively) in exposed than shaded vines (12.8 to 21.8 μmol (CO_2) sh^{-1} s^{-1}). A similar difference (43.1 cf. 29.3 μmol (CO_2) sh^{-1} s^{-1} for exposed and shaded vines) in total CO_2 fixation occurred late in the growing season (104 DAB). Thus, the shade covering had a considerable impact on the incident PFDs within the canopy and a flow-on effect on rates of photosynthesis, consistent with the photosynthetic light response of the shaded leaves. These results also conform well with the effect of shade on photosynthesis of Sangiovese leaves (Cartechini and Palliotti 1995) and Riesling leaves (Schultz *et al.* 1996).

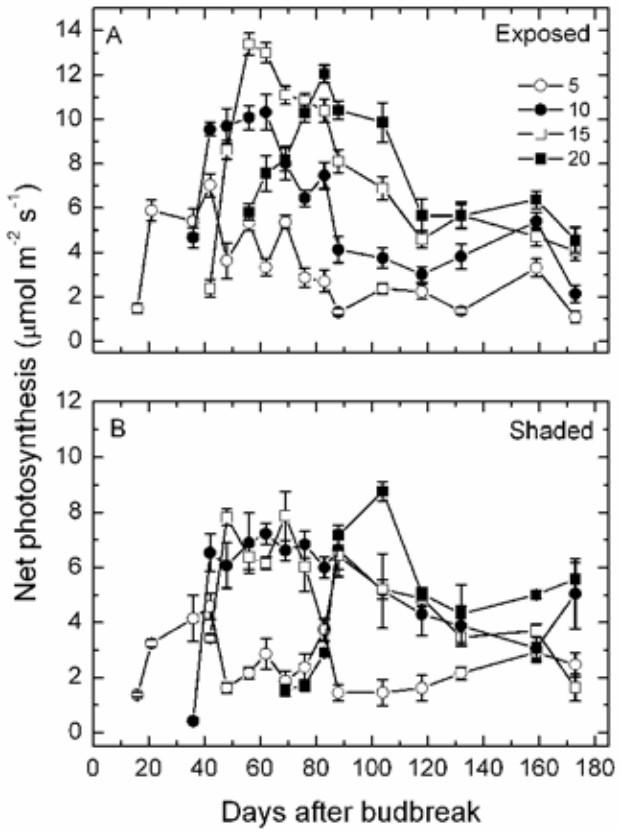


Figure 3.55 Changes in the net photosynthesis (Mean ±se, n=8) of selected leaves as indicated over the 2008-09 growing season on Semillon vines grown in an irrigated vineyard with and without shade covering as indicated.

Net carbon balance

The net daily carbon acquisition for whole shoots (*Figure 3.56A*) increased relatively slowly just after budbreak but then increased more rapidly in the exposed vines to reach a maximum rate at about 55 DAB but just after 40 DAB for the shaded vines. It was noteworthy that in both shaded and exposed vines, the maximum rate of carbon acquisition was sustained over 30–40 days but also the maximum rate differed significantly ($P<0.01$) from 1.17 ±0.04 gC sh^{-1} d^{-1} in exposed vines to 0.82 ±0.09 gC sh^{-1} d^{-1} in the shaded vines. The differences were maintained throughout the growing season. In both cases, the rate of carbon acquisition declined from about 90 DAB until about bunch harvest when the rates remained constant. Across the whole growing season, the shoots on exposed vines acquired 103.5 ±5.8 gC sh^{-1} and the shoots on shaded vines 69.2 ±5.9 gC sh^{-1}, some 35% less carbon fixation.

Rates of carbon sequestered into biomass (*Figure 3.56B*) reached a maximum rate within 35 DAB and there was little difference between shaded and exposed leaves and mostly not significant. It was also

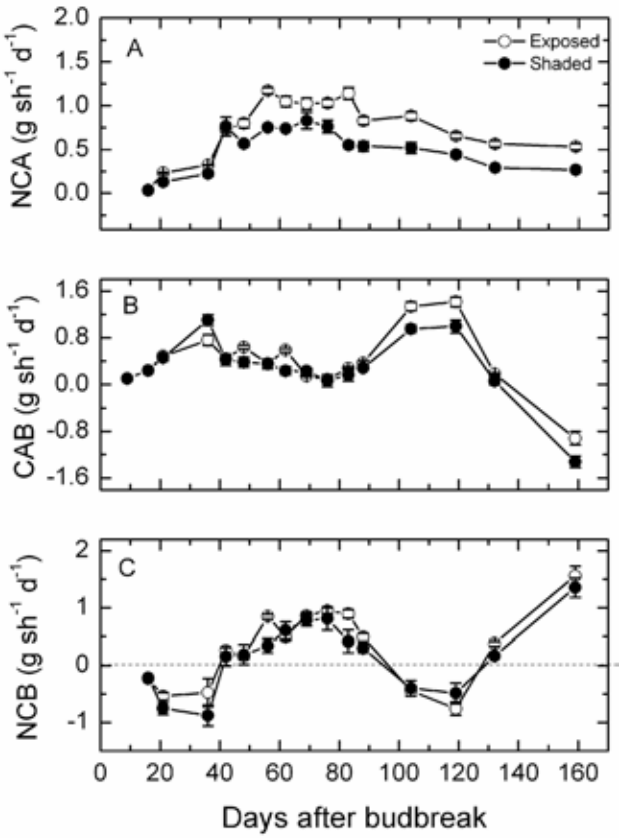


Figure 3.56 Changes (mean ±se, n=8) in the (A) net rate of carbon acquisition (NCA), (B) structural carbon accumulated as biomass (CAB) and (C) the net carbon balance (NCB) of Semillon shoots over the 2008-09 growing season on vines grown in an irrigated vineyard with and without shade covering as indicated.

apparent that the rate of carbon sequestration began declining from this point in the growing season and approached a zero rate at about 75 DAB, coincident with the halt in accumulation of stem and leaf biomass. Thereafter, the rate of carbon sequestration increased again, coincident with bunch growth until 120 DAB when the bunches reached their maximum growth. After harvest of the bunches, the rate of carbon sequestration declined dramatically to reach a negative rate of -0.9 to -1.3 ±0.1 gC sh^{-1} d^{-1}, indicative of loss of carbon from the shoots. In total, the shoots on the vines in exposed conditions sequestered 67.2 ±7.3 gC sh^{-1} over the whole growing season while shoots on shaded vines sequestered 45.4 ±5.3 gC sh^{-1}, again about 32% less than the exposed shoots.

The net carbon balance (*Figure 3.56C*) was negative in both exposed and shaded shoots when growth commenced after budbreak, in keeping with higher rates of carbon sequestration compared to rates of carbon acquisition. The net carbon balance remained negative until about 40 DAB and integration of these data indicated 10.2 ±2.5 and 16.9 ±3.5 gC sh^{-1} for the shoots on exposed and shaded vines, respectively, were required from outside of the shoot to support their growth. After about 45 DAB, the net carbon balance increased to a maximum of about 1.14 ±0.11 gC sh^{-1} d^{-1} at 75 DAB for the shoots on exposed vines and at 0.65 ±0.30 gC sh^{-1} d^{-1} though slightly earlier at 60 DAB for the shoots on shaded vines.

Throughout the bunch ripening period, there was a major demand for carbon with the bunches actively growing, such that a decline in the net carbon balance, which ultimately became slightly negative, occurred until the bunches stopped growing. After the bunches were removed at harvest, the net carbon balance again became strongly positive when carbon demand by the shoot ceased. During the mid season, the net carbon balance was higher in the exposed compared with shaded vines but otherwise there were little to few differences between them for the rest of the growing season. However, the surplus carbon for the whole growing season differed markedly, with the shoots on exposed vines gaining 35.2 ±4.3 gC sh^{-1} surplus while the shoots on shaded vines gained 16.6 ±2.3 gC sh^{-1}, a 53% reduction.

It was apparent from the estimated carbon acquisition in the first 40 days of growth and development, that little net gain in carbon occurred in either treatment confirming the conclusion of Greer and Sicard (2009). After that, however, carbon gain increased rapidly, more so in the exposed than in the shaded vines, as the leaves became fully expanded and photosynthetic rates of the early-emerging leaves became maximal. It was thereafter that the penalty of shade covering on the vines carbon budget became most apparent and, on average, 0.8 gC sh^{-1} d^{-1} (4 gC m^{-2} d^{-1}) was gained throughout the main period of the growing season whereas the exposed vines gained 1.2 gC sh^{-1} d^{-1} (7.7 gC m^{-2} d^{-1}), on average. A similar penalty of shade on carbon gain was also shown in *Alocasia macrorrhiza* (Sims *et al.* 1994). These estimates of carbon gain were, nevertheless, well within the ranges determined for other grapevine varieties including Temperanillo 7 g m^{-2} d^{-1}; (Escalona *et al.* 2003) and Riesling vines 4.3 g m^{-2} d^{-1}; (Weyand and Schultz 2006). The seasonal pattern of change in the carbon acquisition also conformed to that in Sangiovese vines (Palliotti *et al.* 2004). Differences in photosynthesis between the exposed and shaded Semillon leaves clearly accounted for the penalty in carbon acquisition rather than canopy leaf area of the shaded vines.

Later in the growing season, when no further increase in leaf area of the Semillon shoots had occurred and a reduction in the rates of photosynthesis had also occurred, carbon gain in both treatments started to decline progressively from about 80 DAB onwards to low rates. Over the whole growing season, the exposed shoots gained a total of 100 gC sh^{-1} while shaded vines gained at total of 70 gC sh^{-1}. These data strongly confirm the conclusion that reduced PFDs from the shade covering caused a marked reduction in carbon gain. However. these total gains compare well with an estimated 59 gC sh^{-1} for Riesling vines (Downtown and Grant 1992) but contrast with about 280 gC sh^{-1} for fruiting *Actinidia deliciosa* vines (Greer *et al.* 2003).

In concert with the decreased acquisition of carbon by the shaded Semillon vines, sequestration of carbon in biomass was also affected by the shade treatment. However, only small differences in rates of carbon accumulation occurred between vines of both treatments across the growing season. Of more significance, was the rates of carbon accumulation in both cases increased to reach an initial peak of 0.8– 1.1 ±0.9 gC sh^{-1} d^{-1} close to 40 DAB. This coincided with the rapid increase in shoot growth that occurred in the first six weeks after budbreak. After that, the rates of carbon accumulation declined steadily over a 50 day period to approach a rate close to negligible carbon sequestration in concert with

vegetative growth ceasing. However, from about 90 DAB onwards, the rate of carbon accumulation then increased again to peak at 1.4 and 1.0 ±0.9 gC sh^{-1} d^{-1} for the exposed and shaded vines, respectively. Clearly, the flush of bunch growth accounted for this second peak of carbon accumulation. Thus, in vineyard-grown vines, carbon accumulation was bimodal with an initial peak reflecting vegetative growth and a second peak resulting from reproductive growth. Consistent with this, fruiting *Actinidia deliciosa* vines also had a bimodal pattern of carbon accumulation (Greer *et al*. 2003). Across the whole growing season, the exposed Semillon vines sequestered a total of 67 gC sh^{-1} and the shaded vines 45 gC sh^{-1} as biomass compared to 42 gC sh^{-1} for Riesling vines (Downton and Grant 1992) and 32.3 gC sh^{-1} for potted Semillon vines (Greer and Sicard 2009), thus, reasonably comparable given different grapevine varieties and growth conditions.

The relatively slow development of photosynthetic carbon acquisition and the high rates of carbon accumulation in the Semillon vines resulted in a negative net carbon balance over the first 40 days of growth (see also Lakso and Johnson 1990; Wibbe *et al*. 1993), indicative of carbon reserves being consumed to support growth (Goffinet 1994, Bennett *et al*. 2004; Field *et al*. 2009; Holzapfel *et al*. 2010). In total, the shoots of the exposed vines required some 10 gC sh^{-1} while the shaded shoots required nearly 17 gC sh^{-1} of imported carbon during this period of high growth rates. Consistent with this, some 30 g $vine^{-1}$ of starch was lost from roots over a similar time frame in Shiraz vines (Field *et al*. 2009) and a similar amount in Pinot Noir and Merlot vines (Zapata *et al*. 2004), conforming with mobilisation of reserve carbon to supply shoot growth. It was notable that leaf growth rates of the shaded and exposed vines differed little and were maintained at a high rate during this period of heterotrophic shoot growth, suggesting the mobilisation process was unaffected by the shade covering. But when the shoots shifted to an autotrophic state beyond 40 DAB, (see also Zapata *et al*. 2004), leaf growth of the shaded vines declined markedly in keeping with low rates of carbon acquisition.

The net carbon balance was essentially positive once the bunches had been harvested and a strong net gain in carbon ensued and was presumably exported from the shoot. In fact, after harvest some 26 and 21 g sh^{-1} of surplus carbon was accumulated for the exposed and shaded vines respectively, but these would be expected to increase up to leaf fall. Over the whole growing season, a net gain of 35 gC sh^{-1} for the exposed vines and 16.5 gC sh^{-1} for the shaded vines resulted and these compare very well with that estimated for controlled environment-grown Semillon vines (37.2 gC sh^{-1}; Greer and Sicard 2009) and for spur pruned Riesling vines (~17 gC sh^{-1}; Downton and Grant 1992).

Unpublished studies

The data in *Figure 3.42* shows the temperature during the 2008–09 growing season where air and canopy temperatures exceeded 40°C for a sustained period. To put this in context, we analysed the maximum summer (December–February) growing season temperatures over the last decade for the Griffith town ship and this is shown in *Figure 3.57*. This figure shows that one day heat events, where temperatures exceed 40°C, are common in each but not all years and also heat events of two sequential days above 40°C are also common. Three-day heat events are less common, occurring at about one every two-three years and four-day events are uncommon. However, the 2003-04 growing season was marked by two four-day heat events in the same growing season. Heat events longer than 4 days are a rare event and until 2009, the only longer duration heat event occurred in 2005-06 season and lasted seven days. This puts the heat wave of the 2008-09 in an extreme category because it persisted for 14 days in a row and was preceded by one and two 1-day and 2-day heat events also. The highest recorded air temperature at the site was 47°C.

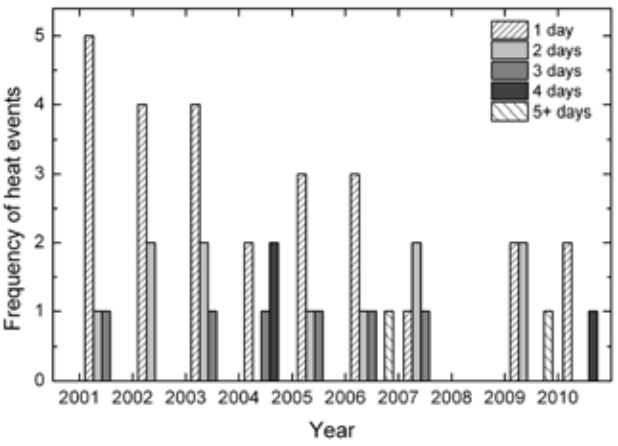


Figure 3.57 Frequency of heat events sustained from 1 to more than 5 days where the mean daily maximum temperatures from December to February of each year exceeded 40°C. These data are were from the Australian Bureau of Meteorology for the Griffith township.

The heat wave in 2008-09 had marked effects, especially on the western sides of the Semillon vines and had over 35% of berries either shrivelled, raisioned or sunburned (*Figure 3.58*).

This heat wave also had a marked impact on berry ripening (*Figure 3.59*) compared with vines protected by the heat event through the use of shade covering. The berries on protected bunches increased ripening in the mid to late stages of sugar accumulation and became riper than berries not protected. This point is reflected in the rates of ripening during the heat wave which averaged 0.86°Brix day^{-1} in the protected bunches and 0.38°Brix day^{-1}. Unfortunately, berry diameters may not have been measured to determine sugar content but as shown earlier (*Figure 3.37*), the sugar content does not increase as a consequence of high temperatures. Furthermore, berry diameter is affected (*Figure 3.35*) and, therefore, an apparent increase in soluble solids concentration in exposed bunches during the 2008-09 heat event may be an artefact of berry shrinkage.



Figure 3.58 Semillon berries on the western side of the canopy with the visible symptoms resulting from the sustained heat wave in Jan–Feb 2009.

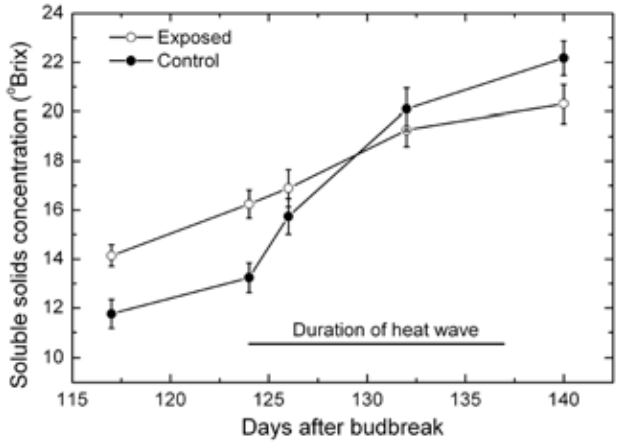


Figure 3.59 Changes in soluble solids concentration (mean ±SE, n=12) in berries of Semillon bunches on vines either protected from a heat event control) compared with those fully exposed to the heat event. The timing of the heat event is shown as a line.

A second component of the heat stress research has been to investigate the role of hydrocooling in protecting vines and bunches from heat events. The precedence for this research comes from the literature where it has been shown to increase berry acidity and colour and soluble solids concentration in several varieties (Kliewer and Schultz 1973). Similarly, Aljibury *et al.* (1975) showed similar results for other varieties when water sprinkling cooled the air, leaf, fruit and soil peak daily temperatures down by 5–10°C. Their results also indicated a much slower rate of ripening in the sprinkler treated vines.

The current hydrocooling project was carried out in the same vineyard in the Riverina over the growing season from 2009–10 to 2010–11 as our previous research. In the first season, two threshold temperatures were set at 35 and 40°C and in the second growing season, a third temperature of 30°C was included. The system was able to maintain temperatures as shown in Figure 3.60.

Although a complete analysis of this part of the project has not been completed, there is evidence to suggest that in the first season the hydrocooling of the vines significantly improved the yield by 30% (11.45 ±0.75 kg vine^{-1}) over that of vines not protected (8.76 ±0.75 kg vine^{-1}). However, in the second season, there was no evidence of an impact of the hydrocooling on the yield and all treatments averaged 11–12 ±0.9 kg vine^{-1}. However, in the second season, a change was made to the hydrocooling system to reduce water consumption and finer sprinklers were used to provide a very fine spray. This was, however,

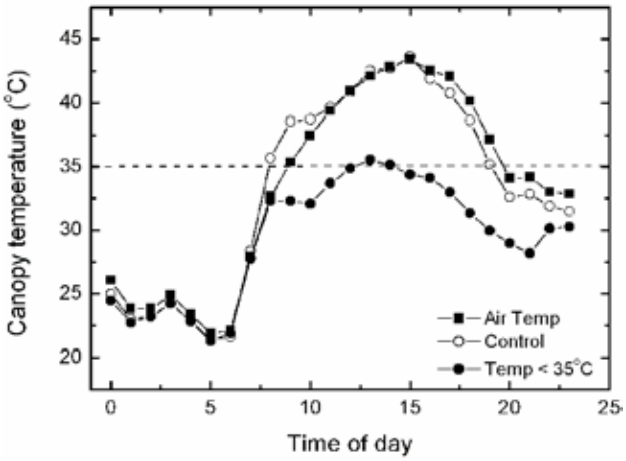


Figure 3.60 Effect of spraying water on Semillon grapevine canopy temperatures in comparison with vines not sprayed. For comparison, the air temperature in included as well.

susceptible to the wind and may have reduced the efficacy of the cooling system. Further evaluation of this system is desirable because no or minimal heat events occurred during the trial. This research is also warranted as a means to prevent heat events impacting on berry ripening as has been shown in these studies to be a major problem.

Conclusions

Covering Semillon vines with shade cloth to reduce exposure to heat had major costs in terms of the carbon budget. Lower incident photon flux densities within the shaded canopy induced leaves with characteristic shade attributes; low light saturated photosynthesis, low light saturation but large leaf areas. Together, these attributes caused a decrease in carbon acquisition which flowed on to reduced allocation to leaf biomass and later on to bunch biomass. Thus, shade had a synergistic effect on the carbon balance of these vines through reductions in carbon acquisition and reductions in biomass allocation and, therefore, was a costly method of protecting vines from high temperature events.

Experiment 3.10
Technetium scintigraphy in plants

Materials and methods

Scintigraphic images were acquired using a gamma camera (Philips Prism 1000, Picker, Cleveland) with high resolution parallel hole collimation (photopeak centred on 140 keV ±15%, 1 min acquisition and 128×128 pixel matrix for the prostrate shoot experiment and a 5 min acquisition and 256×256 pixel matrix for all other images). Images displaying total acquisition counts were processed using a computer (Philips Odyssey VP, Picker, Cleveland) by truncating the count range to span that typically observed in labelled leaves (up to ca. 500 counts). The greyscale range of the image was adjusted to enhance the contrast between labelled plant parts and the image background. Truncated images of suitable contrast were exported after applying a colour palette and areas of radionuclide localisation were confirmed by digitally merging (Merge ver 2.0, www.graphicutils.com) these with a digital photograph taken of the plant during scintigraphic acquisition. Count data reported correspond to images prior to truncation.

Confirming xylem mobility of pertechnetate

$^{99m}TcO_{4^-}$, eluted from a molybdenum-99 generator using 15 mmol L^{-1} NaCl, was provided by a local medical imaging clinic. Doses of the desired radioactivity were obtained by assaying the labelled saline solution in a dose calibrator (Atomlab 100, Biodex Medical Systems, New York).

Plants used in these experiments were *I. alba* grown from directly sown seeds (The Digger's Club, Dromana, Victoria, Australia). Plants were raised in a commercial potting mix in a 2.6 L pot, drip irrigated three times daily and grew as a single shoot trained up a vertical cane placed in the potting mix at the time of seed germination. The plants were maintained in a glasshouse (25/23°C day/night) under natural lighting (decreasing night length) and transferred to the laboratory for labelling and imaging the day prior to experimentation. Plants were approximately 75–100 days old at the time of imaging and many bore reproductive organs at developmental stages ranging from immature floral buds to developing seed capsules.

Six individual, fully-expanded *Ipomoea* leaves (one leaf per plant) were labelled with $^{9m}TcO_{4^-}$ by lightly abrading both sides of a leaf with sandpaper, immersing the leaf in a Petri dish containing 1 GBq of $^{9m}TcO_{4^-}$ for 60 min and air-drying the leaf for 60 min Leaf abrasion was chosen as a treatment because it allows entry of phloem-mobile solutes into leaves (Grignon *et al.* 1989). Each plant was then illuminated with a 100 W lamp for six hours. Three of these labelled leaves were covered in aluminium foil and three were left uncovered. The experiment was repeated with another six leaves omitting the leaf abrasion.

The soil of eight potted *Ipomoea* plants was labelled with 1 GBq of $^{9m}TcO_{4^-}$. The plants were then illuminated with 100 W lamps for four to six hours. The pots were shielded with lead prior to scintigraphic imaging.

The following methods are adapted with minor modifications from Pickard and Hill (1975). Two days prior to labelling, leaves and fruit were removed from the bottom 50 cm of *Ipomoea* shoots that were approximately 80 cm long. To label with $^{9m}TcO_{4^-}$, the shoot was laid prostrate and, while immersing a portion in deionised water in a Petri dish, a longitudinal slit approximately 25 mm long was cut either in the internode immediately below the lowest remaining leaf or the internode between two remnant leaves. 500 MBq of $^{9m}TcO_{4^-}$ was then

added to the deionised water and the labelled shoot was illuminated with three 100 W lamps for 60 min Plants were then positioned on the imaging window of a gamma camera and scintigraphic imaging of the plant approximately 15 cm below the loading point began either while these lights were on (n=2) or immediately after they were turned off (n=4). Lead shielding was used to minimise scatter from the labelling pool to the camera head. Approximately 20 min of imaging in darkness dry ice was applied to the stem acropetal of the labelling point. A further 20 min later dry ice was applied to the stem basipetal of the labelling point and scintigraphic imaging was terminated 20 min later.

Scintigraphic images were acquired using a gamma camera (Philips Prism 1000, Picker, Cleveland) with high resolution parallel hole collimation (photopeak centred on 140 keV ±15%, 1 min acquisition and 128×128 pixel matrix for the prostrate shoot experiment and a 5 min acquisition and 256×256 pixel matrix for all other images). Images displaying total acquisition counts were processed using a computer (Philips Odyssey VP, Picker, Cleveland) by truncating the count range to span that typically observed in labelled leaves (up to ca. 500 counts). The greyscale range of the image was adjusted to enhance the contrast between labelled plant parts and the image background. Truncated images of suitable contrast were exported after applying a colour palette and areas of radionuclide localisation were confirmed by digitally merging (Merge ver 2.0, www.graphicutils.com) these with a digital photograph taken of the plant during scintigraphic acquisition. Count data reported correspond to images prior to truncation.

Results and discussion

The biodistribution of technetium in plants has been widely studied and reported in the literature. The first report of the use of pertechnetate as a tool for the study of plant vascular transport dates back to 1975 (Pickard and Hill, 1975). The researchers were searching for a radiotracer that was mobile in the phloem, the vascular tissue responsible for transporting photosynthates from leaves to developing tissues. Their findings were inconclusive, and they published no further research on technetium after establishing methods for detecting phloem transport of ^{11}C fed to leaves as carbon dioxide (Pickard *et al* 1978). Subsequent research involving technetium and plants focused on the incorporation of environmental ^{99}Tc into the food chain via plants grown in soils polluted by nuclear accidents and nuclear weapons testing and detonation (Bennet and Willey, 2003; Krijer *et al*. 1999).

Pertechnetate (TcO_4^-) is the most stable surface chemical form of technetium and has been reported to be highly mobile in biogeochemical cycles (Tagami *et al*. 2004). TcO_4^- is known to be extracted by plant roots, transported by the xylem, and reduced in the leaves because technetium is not evaporated (Currie and Wheat, 2008). The xylem is the vascular tissue primarily responsible for transporting sap from roots to transpiring organs, such as leaves. In 1999, the role of scintigraphy in the nondestructive quantification of radiotracers in plants was first described (Krijer *et al*. 1999). The paucity of research since then probably reflects the lack of access of plant scientists to scintigraphic equipment and associated expertise, the unfamiliarity of plant physiologists with the imaging capabilities of nuclear medicine, and the limited exposure of nuclear medicine practitioners to research in plant sciences.

To date, tracer studies for plant physiology (radionuclide label or colour dye) have relied on destructive plant sampling. That is, an individual plant (or part thereof) is sacrificed and dissected at a specific time interval for tracer analysis. Consequently, that same plant cannot be used to provide time series or dynamic data and cannot be used in repeat testing. Scintigraphy has several valuable advantages over existing techniques:

1. Sampling is nondestructive; therefore, the plant remains intact for repeat-design experimentation.
2. A single plant can be used to provide contiguous data over time, both reducing the number of plants required and significantly increasing the sampling rate (and thus the accuracy of parameter estimation).
3. Sampling can readily begin at time zero (i.e. application of the radiotracer), offering a broad window of continuous data sampling.
4. Dynamic data permit the quantification of tracer movement on the basis of the region of interest (ROI), improving both the accuracy and the reproducibility of results, especially over those of visual assessment alone.
5. Reductions in costs are achieved through reductions in the number of plants required and tracer quantity. Further reductions in costs are achieved through comparative streamlining of data collection and analysis and reductions in manual sampling and dissection.

In brief, scintigraphy provides significantly improved data quality in a more efficient and reproducible manner for the exploration of time-related changes in plants.

A simple, nondestructive means of introducing a radionuclide to a plant is through root uptake. For hydroponically grown plants, this process is as straightforward as introducing the radionuclide to the hydroponic solution. Unfortunately, radionuclides such as ^{99m}Tc (as pertechnetate) tend to bind with nutrients in the solution, leading to less efficient root uptake. Replacing (after a washing process) the hydroponic solution with tap water improves radionuclide uptake by the root system but only marginally. Distilled (deionized) water is the ideal medium in which to house roots for radionuclide introduction. The same technique can be used for potted plants after the roots are removed from the soil and washed. Care must be taken when transferring and washing the roots because uptake and transport processes can be changed by damage to the roots (microscopic damage to root hairs is sufficient) or air emboli resulting from even brief periods out of solution. The roots should be housed in a container with a volume as small as possible to improve the specific concentration.

For plants grown in potted soil, a radionuclide solution can be added directly to the soil. However, precautions must be taken when applying a radionuclide solution to soil. The radionuclide should be contained in a volume that allows sufficient dilution and diffuse distribution within the soil. Conversely, the specific concentration must be sufficiently high to allow measurable quantities to be taken up by the root system. Generally, this parameter requires the use of a radiation dose much higher than that required for the distilled water method outlined earlier; in turn, a high radiation dose raises concerns about radiation safety and image degradation due to radiation scattered into the field of view of the imaging system. The latter can be managed by ensuring that the soil surface is a sufficient distance from the imaging field of view, washing the solution after surface application or injecting the solution below the surface layer of the soil (>5 cm), and using lead shielding around the soil surface.

Inserting multiple watering spikes into the soil can facilitate improved delivery of the radionuclide more directly to the roots while reducing the risk of contamination, reduce the dilution volume, and improve the efficiency of root uptake. However, this method is inefficient in comparison with methods without soil (described earlier) because variations in radionuclide labelling of soil components decreases root uptake. The level of hydration of the soil (and plant) also has a significant bearing on the efficiency with which a soil-based radionuclide is absorbed. Well-hydrated soils result in slower uptake by the plant, whereas poorly hydrated soils can result in trapping of the radionuclide in the soil solution or rapid physical transit through the soil to the bottom of the pot. Different soil types absorb in different ways; therefore, the efficiency of uptake of radionuclides from soil by roots can vary with soil type. For example, technetium extraction is inhibited in anaerobic soils, particularly those with high concentrations of organic matter, because of the predominance of TcO_2 as opposed to the more familiar form, TcO_4 (Bennet and Willey 2003).

The uptake of a radionuclide by roots is a time-consuming process and results in dilute quantities of the radionuclide in plant structures, particularly in samples from soil. Circumventing delays in root uptake can be achieved with the "cut-shoot" method, in which the shoot of interest is simply cut from the remainder of the plant and introduced to a solution of a radionuclide in distilled water. Care must be taken to avoid the introduction of air into the xylem vessel by, under ideal conditions, cutting the shoot while it is submerged. Failing this, the shoot should be placed in the solution immediately after being cut. Another drawback of this approach is that the excision might result in altered physiology proximal to the cutting site. Generally, this method is considered destructive sampling, prohibiting repeat-design experimentation, although it might provide dynamic data. The principal advantage of this method is that it allows rapid accumulation into plant organs (*Figure 3.61*) and thereby effective evaluation of gross physiology (e.g. relative accumulation in leaves or fruit).

An alternative approach for labelling plant tissues is the "wick" method. In brief, a wetted cotton thread is pulled through a plant organ with a needle (e.g. fruit or stem). One end of the thread is placed in a sealed reservoir of a concentrated radionuclide, and the other end is exposed to air. As evaporation dries the cotton thread, the radionuclide is drawn up the thread and into the plant organ. Care must be taken to prevent the cotton thread from touching any plant structure and risking contamination. The obvious advantage of this approach is that the radionuclide can be introduced at specific locations in the plant.

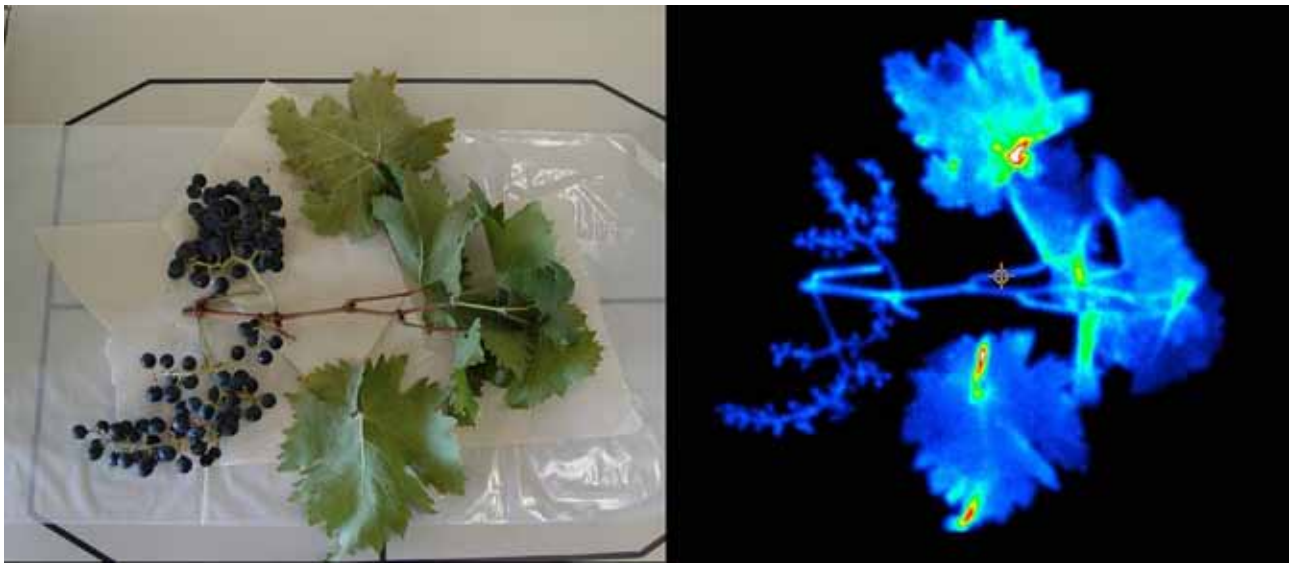


Figure 3.61 Cut-shoot method allows rapid accumulation of radionuclide in plant structures. Scintigraphy of cut shoot reveals accumulation in stem and leaves. Note absence of accumulation in fruit itself. ^{99m}Tc-pertechnetate accumulates in unripe fruit but not in ripe fruit.

The major disadvantage of this method is that the rates of transport and dilution of the concentrated radionuclide within the plant depend on the rate at which the radionuclide is loaded into the xylem. Therefore, a highly concentrated (high-specific-activity) radionuclide is recommended. Another disadvantage of this method is that it ruptures xylem vessels, in turn facilitating the movement of sap away from the wick site. Additionally, the focal increase in the accumulation of the radionuclide at the wick site may impede the evaluation of proximal structures, particularly if transport rates are low. Nonetheless, the method has allowed the demonstration of bidirectional ^{99m}Tc-pertechnetate movement away from the wick site (*Figure 3.62*).

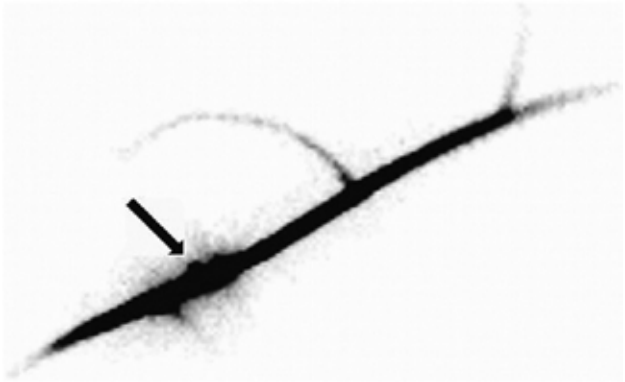


Figure 3.62 Wick method demonstrates bidirectional movement of tracer from wick site (arrow). Distal part of grape stem is at top right of image, and proximal (backflow) part of stem is at bottom left of image.

Infoliarapplication,aradionuclidesolutionisapplied directly to the leaves. In this approach, contamination is a major concern, requiring meticulous attention to technique. Reverse xylem transport must be encouraged by inhibiting transpiration from the labelled leaves. This process is adequately achieved by wrapping the labelled leaves or stem in aluminium foil and encouraging transpiration from the nonlabelled leaves. Unfortunately, radionuclide transport is usually slow because the volume and concentration of radiolabelled water are low. Nonetheless, this technique has been used to successfully demonstrate the movement of ^{99m}Tc-pertechnetate from the leaf back to the plant stem; this finding discounts the previous understanding that ^{99m}Tc-pertechnetate is irreversibly reduced in leaves (Kreijer *et al.* 1999) and indicates movement in a proximal direction (*Figure 3.63*).

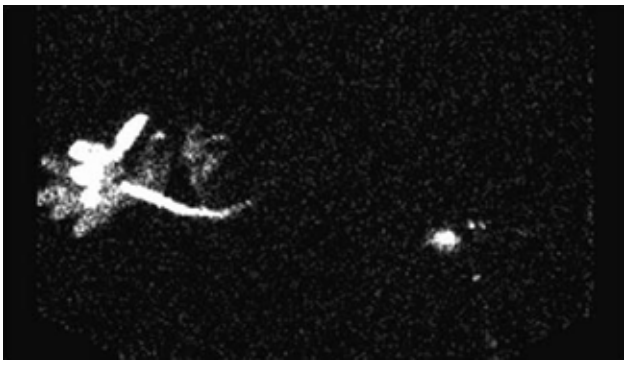


Figure 3.63 Activity applied to leaf (left) migrates down stem. Activity is concentrated at junction of main and branch stems (right).

Immersing specific organs in a radionuclide solution is another labelling method, but it has significant contamination risks. Plant organs such as leaves, fruit, or an individual root can be immersed in a reservoir containing a radionuclide solution

to provide continual exposure to the radioactive solution, leading to uptake and transport of the radionuclide. This method provides better results than foliar application but may not represent true physiologic conditions. An example of this approach that has been found to be useful is the introduction of a radionuclide via a single root. This technique is minimally invasive and allows the functional evaluation of a specific pathway. In this example, a window is cut into the side of a plastic pot containing a plant (*Figure 3.64*). A single root is "dug" out through the window, taking care to minimize damage to the roots. The root is immersed in a container of radionuclide solution and the container is wrapped in foil to eliminate light exposure. It has been observed that individual roots service specific branches of grapevine plants.

Consideration should be given to the use of image merge software, with which a scintigraphic image can be referenced against a photograph for localization and analysis. Traditionally, anatomic localization might be undertaken with a transmission scan to create a silhouette or shadow of the anatomic structure. The photographic fusion approach overcomes the possible limitations of using transmission scanning of very thin and low-density objects and provides a significant improvement in the ability to accurately localize the distribution of activity within a structure. Numerous research studies performed in nuclear medicine departments might be assisted by fusion of planar images with photographs. This technique might be particularly useful, as is the case with plant physiology, if the research involves specialists from outside the nuclear medicine domain. Nonetheless, consideration must be given to alignment errors associated with the merging of an image acquired in a planar fashion (scintigraphy) with an image acquired in a pinhole fashion (photography), particularly toward the periphery of the image (*Figure 3.64*). These difficulties can be overcome with software distortion or simply by maximizing the object-to-aperture distance for the photograph.

The environment in which a standard γ-camera is housed (temperature and lighting) tends to be less than ideal for plant physiology. The γ-camera environment must be modified to induce transpiration; modifications might include artificial lighting, higher temperatures, and fans for air movement. The availability of natural light through windows is an advantage. Plant positioning is also important because movement and too much distance from the



Figure 3.64 Merging of photographic and scintigraphic image data for improved localization. Under ideal circumstances, display would be in colour.

object to the detector can reduce image quality and resolution. Transpiration from individual leaves can be reduced or inhibited if the leaves are positioned too close to the detector or by mechanisms designed to secure the position of the plant. In particular, leaves should not be pressed flat or taped against the surface of the camera during the collection of dynamic data.

Acquisition parameters include the use of an "upright" gantry configuration to image plants vertically. Plants can be placed in a horizontal position for SPECT. Dynamic acquisition at 1 frame per 5–10 min for 3 h and then 1 frame per 30 min up to 24 h is generally used with a 256 matrix. The photopeak should be 15% centered on 144 keV to eliminate scatter events (Currie *et al.* 2008).

One should aim for 100 MBq (2.7 mCi) in 100 mL of solution and a total dose of 400–500 MBq (10.8–13.5 mCi) if roots are to be submersed in water and for foliar applications. Four doses of 100 MBq (2.7 mCi) in 10 mL of solution are best for direct administration to roots from soil (with the aid of several watering spikes), and a dose of 100 MBq (2.7 mCi) mL^{-1} is appropriate for the wick method. In all cases, the uptake period depends on the transpiration rate and soil hydration; however, as a general rule, 2–4 h of accumulation should be used

for physiologic uptake, and 30 min should be used for the cut-shoot application. Sodium chloride tends to be toxic to many plants, albeit at high concentrations; therefore, radionuclide doses should be diluted with deionized water.

Plant imaging presents unique radiation safety issues because the bulk of the radiation dose is not subject to large amounts of attenuation, which might be encountered for internalized human doses. Time, distance, and shielding are particularly important principles to apply during the uptake phase, when a large component of the dose for each plant resides in external containers. Deep soil administration provides some degree of shielding, but the storage of a large volume of plants requires dedicated shielding or an isolated room that still provides an environment conducive to transpiration. The use of radiation in an open delivery system (e.g. spray bottle or open container) involves a substantial contamination risk and requires the use of gloves, gowns, shoe covers, and a generous application of absorbent sheets.

Confirming xylem mobility of pertechnetate

In contrast to clinical, pre-clinical and veterinary nuclear medicine research, in the plant sciences there has been very little exploration of the potential for metastable technetium-99 (^{99m}Tc) to serve as an radiotracer for the study of physiological processes (Desmet 1984). One impediment in this area of research is the lack of a clear understanding of how common forms of Tc, such as pertechnetate (TcO_4^-) and Tc-complexes, are transported in the xylem and phloem of plants.

The focus of this research is ^{99m}Tc transport in the moonflower, *Ipomoea alba* L. This species was chosen because earlier research suggested that it may transport Tc, introduced to the plant in the form of $^{99m}TcO_4^-$, in the phloem. Thirty-five years ago Pickard and Hill (1975) published the first and one of the few papers to explore the usefulness of ^{99m}Tc as a radiotracer in plants. These authors suggested that ^{99m}Tc transport was not driven by the mechanisms responsible for coherent flow in the xylem (hydrostatic pressure driven by processes such as transpiration and osmosis). Rather, they cautiously interpreted their results based on the assumption that the radionuclide was transported in the phloem but could be easily transferred to the apoplast (cell walls and intercellular spaces including xylem vessels and tracheids). This interpretation contrasts with subsequent evidence for the presence of $^{99m}TcO_4^-$ in xylem sap (Cataldo *et al.* 1978; Krijger *et al.* 1999a).

Given the equivocal evidence for the phloem mobility of Tc in *Ipomoea* the aim of this paper is to better understand the long-distance transport of ^{99m}Tc, introduced as $^{99m}TcO_4^-$, in this particular species. Our research is focused on ^{99m}Tc, which emits gamma radiation with a six hour half-life, but is equally applicable to radionuclides of Tc with longer half-lives (^{95}Tc, ^{99}Tc). Because gamma rays have an extremely short wavelength they are highly penetrating, especially with respect to thin plant tissues such as leaves. As demonstrated by Krijger *et al.* (1999b) with experiments on tomato plants, these properties make it possible to quantitatively detect ^{99m}Tc distributions and concentrations in plant tissues, despite their complex geometry, using scintigraphic techniques. Our scintigraphic images of *Ipomoea* plants demonstrate that ^{99m}Tc transport from labelled leaves takes place when these leaves are shaded and identify the sinks for this translocation as other mature leaves. These observations and the presence of trace amounts of ^{99m}Tc in developing pods and immature leaves provide strong evidence that the radionuclide is xylem mobile in *Ipomoea*.

Translocation resulting from labelling of individual leaves

All individual leaves directly labelled with $^{99m}TcO_4^-$ exhibited high concentrations of activity when imaged scintigraphically. Stems and other leaves did not appear in the scintigraphic images when the abrasion treatment of the labelled leaf was not implemented (*Figure 3.65*). Sap exuded from these leaves using a Scholander pressure chamber and collected on absorbent paper did not exhibit counts distinguishable from background when imaged scintigraphically (results not shown). This suggests the radionuclide was not present in the xylem sap of non-abraded leaves. With one exception counts indiscernible from background were present in shoots whose abraded leaf remained uncovered after labelling. The exception was a plant whose labelled leaf wilted, presumably due to damage caused by the leaf abrasion treatment or by heat generated by the artificial light sources. Of the plants with abraded and foil-covered labelled leaves, the first to be imaged exhibited radioactivity extending to the proximal end of its petiole. The shoots of the next two plants exhibited extensive labelling basipetal and acropetal of the labelled leaf (*Figure 3.66*). In these experiments the sinks for the translocated ^{99m}Tc were primarily other fully-expanded leaves but young leaves on shoot

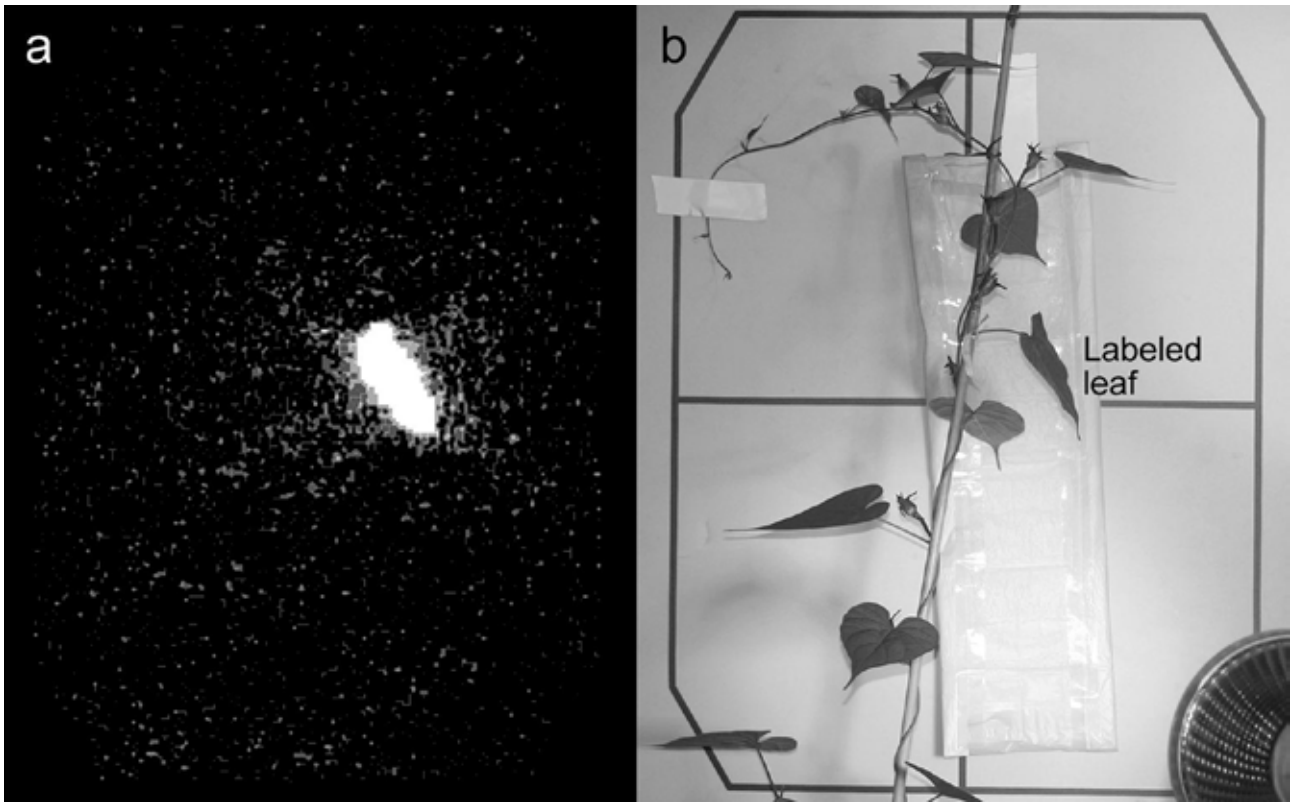


Figure 3.65 Scintigraphic (a) and photographic (b) images of an *Ipomoea* plant after labelling an unabraded leaf with $^{99m}TcO_4^-$. The labelled leaf is indicated in (b). Prior to imaging the leaf was wrapped in aluminium foil and the plant was illuminated with an artificial light source for six hours. The star-shaped distribution of apparent counts surrounding the labelled leaf in (a) is a common scintigraphy artefact resulting from a localized area of high counts and truncation of the count range displayed.

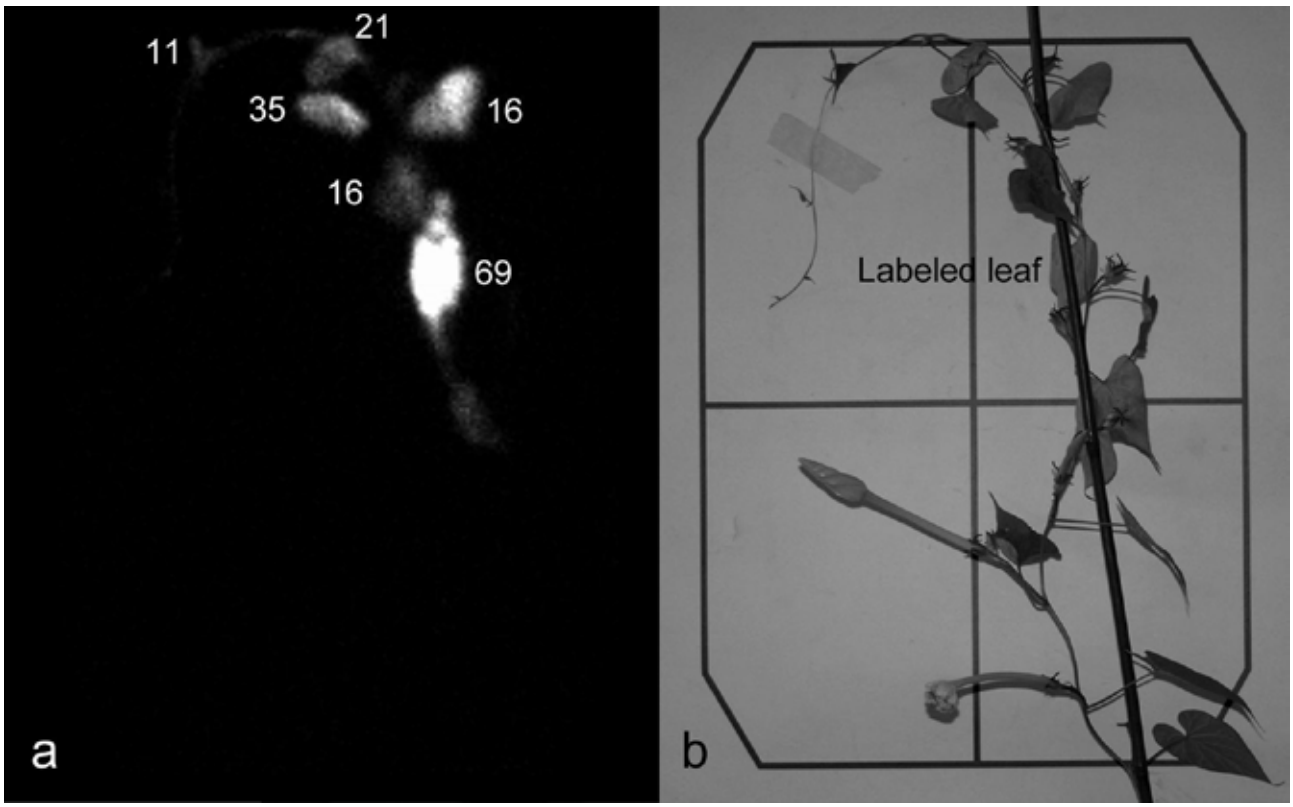


Figure 3.66 Scintigraphic (a) and photographic (b) images of an *Ipomoea* plant after labelling an abraded leaf with $^{99m}TcO_4^-$. The labelled leaf is indicated in (b). Prior to imaging the leaf was wrapped in aluminium foil and the plant was illuminated with an artificial light source for six hours. The numbers in (a) indicate counts per pixel per acquisition. Trace amounts of radioactivity were discernible in the leaf immediately below the labelled leaf and the stem and immature leaves at the shoot apex.

tips were also labelled by translocated radionuclide. ^{99m}Tc was not present in developing flowers.

Pertechnetate uptake from labelled soil

When $^{99m}TcO_4^-$ was added to the soil of potted *Ipomoea* plants nearly all above-ground plant parts were labelled with ^{99m}Tc (e.g. *Figure 3.67*). The relative intensity of ^{99m}Tc labelling in plant organs generally conformed to the trend: well-lit leaves > other leaves > corollas and mature floral buds > immature floral buds and seed capsules (*Table 3.10*).

Table 3.10 The relatively intensity of ^{99m}Tc in organs of *Ipomoea* plants

Organ	Typical range (counts per pixel per 5 min acquisition)[a]
Well-lit leaves	12–15
Other leaves	4–9
Corollas and mature floral buds	5
Immature floral buds and seed capsules	0.5–0.9
Background	0.2–0.5

Note: Labelling was achieved by adding the radionuclide as $^{99m}TcO_4^-$ to the potting media of individual plants.
[a]The values are indicative only because variations before (e.g. efficiency of ^{99m}Tc uptake) and during imaging (e.g. distance from camera face) introduce between-replicate variations in counts.

Translocation resulting from labelling the stem

Of our six attempts to replicate the typical trend reported by Pickard and Hill (1975, their Figure 1) we observed basipetal transport of radiolabel on three occasions. Two of these plants, both of which were imaged in darkness, exhibited radioactivity basipetal of the loading point when imaging began and either a decrease or no change in counts in this region during imaging. In these plants the basipetal transport stopped abruptly at or 2 cm below the node of an excised leaf, respectively and we conclude that the basipetal transport occurred while the shoots were illuminated, prior to scintigraphic imaging. A third plant was imaged in the light, then darkness, and showed no basipetal transport of activity until the acropetal dry ice treatment was applied. This treatment resulted in the immediate and rapid basipetal transport of activity that was halted with the application of the basipetal dry ice treatment (*Figure 3.68*).

Discussion

As observed in other plant species (e.g. Cataldo *et al.* 1984; Myttenaere *et al.* 1984), ^{99m}Tc from $^{99m}TcO_4^-$ labelled soil was rapidly transported to the leaves of *Ipomoea*. This indicates that $^{99m}TcO_4^-$ is highly bioavailable for uptake by *Ipomoea* roots in well-

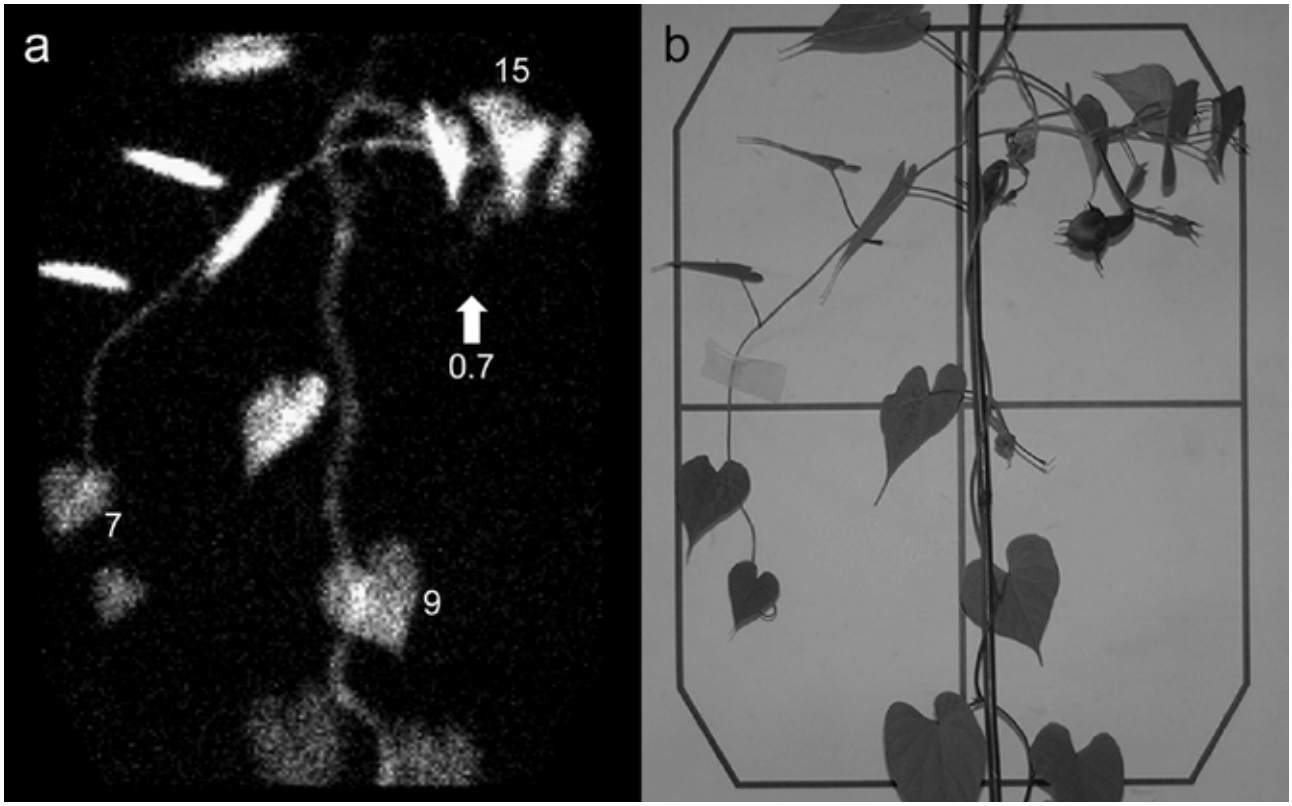


Figure 3.67 Scintigraphic (a) and photographic (b) images of an *Ipomoea* plant labelled with ^{99m}Tc after the addition of $^{99m}TcO_4^-$ to the potting mix of the plant. Numbers in (a) indicate counts per pixel per acquisition. The number in the top right corner of (a) corresponds to the two overlapping leaves seen in (b). The arrow and associated ratio in (a) refers to the seed capsule apparent in (b).

ldrained soil substrates such as commercial potting mix. This observation is in agreement with the high bioavailability of TcO_4^- in field soils under aerobic conditions (Yanagisawa and Muramatsu, 1995).

In this study, translocation of ^{99m}Tc from labelled leaves was highly sensitive to covering leaves with foil. This treatment is expected to reduce transpiration by removing light cues for opening stomatal guard cells (Sharkey and Raschke, 1981) and increasing the resistance of the leaf boundary layer to water vapour diffusion (Monteith, 1965). Because transpiration is the primary mechanism for generating tension in the xylem of plants (Canny, 1995), the covering is expected to have the effect of reducing hydrostatic tension generated by the labelled leaf. The presence of radionuclide in other leaves suggests their transpiration is sufficient to generate the tension necessary for xylem flow out of and away from the labelled leaf. Uncovered leaves also transported ^{99m}Tc to other plant parts but only when the labelled leaf wilted. We suggest that the absence of turgid cells makes the leaf water (and solutes dissolved in it) susceptible to backflow through the xylem. Under both conditions the ^{99m}Tc is redistributed to other sinks for xylem sap, particularly transpiring leaves.

The major sinks for ^{99m}Tc translocated from labelled *Ipomoea* leaves were other fully-expanded leaves. This observation is not consistent with typical models of long-distance phloem transport in which rapidly growing, immature organs are terminal sites in the transport pathway (Canny 1973). Pickard *et al.* (1978) demonstrated that the phloem export of recently acquired photosynthate from illuminated *Ipomoea* leaves should be detectable within minutes after labelling. These authors also demonstrated that shading reduces the phloem export of carbon from source leaves and the transport of carbon to the growing tip (Pickard *et al.* 1978). The sinks for ^{99m}Tc transported from labelled leaves identified here are therefore incompatible with phloem transport. Conversely, they are consistent with ^{99m}Tc being transported according to hydrostatic pressure gradients in the xylem.

The study of dynamic ^{99m}Tc transport in *Ipomoea* shoots lead Pickard and Hill (1975) to equivocally conclude that this species transported the radionuclide in the phloem. Following their methods, upon the application of dry ice we were able to reproduce the basipetal transport typical of their experiments (*Figure 3.68*). We suggest that interpreting the results of such experiments in terms of normal

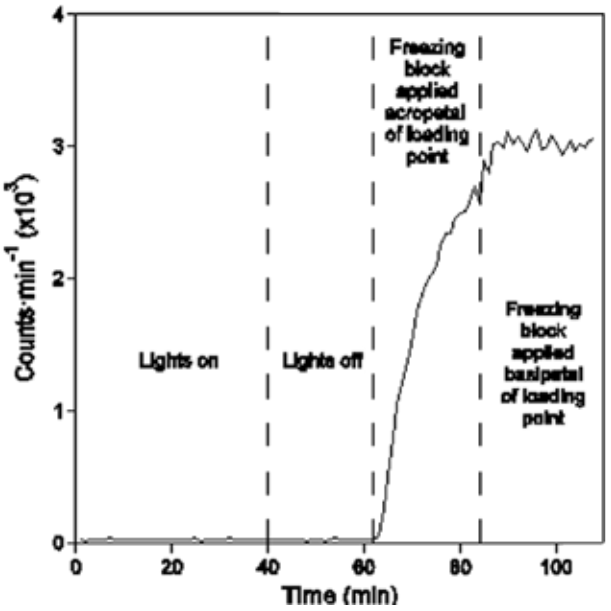


Figure 3.68 Temporal trend in the accumulation of ^{99m}Tc in the stem of an Ipomoea plant basipetal of a loading point following the methods of Pickard and Hill (1975). Counts were acquired in 1 min intervals. As indicated by the labels, data acquisition commenced while the plant was illuminated, the lights were then turned off, 22 min later a dry ice freezing block was applied acropetal of the loading point and a further 23 min later an additional freezing block was applied basipetal of the loading point.

vascular transport processes is problematic. This is because the dry ice effectively isolates the labelling point from major sources and sinks for translocated solutes. Instead, the observations provide insights into how xylem transport processes respond to drastic perturbations. Following the evidence for xylem transport of $^{99m}TcO_4^-$ reported here, we suggest that basipetal transport such as that depicted in *Figure 3.68* reflects the loss of tension in xylem vessels (or tracheids). These conduits transported ^{99m}Tc acropetally until the dry ice froze the xylem sap, eliminating the hydrostatic connection between the acropetal and basipetal portions of the plant. With the hydrostatic tension reduced, the transpiration stream is able to retract basipetally until it is halted by the application of dry ice between the labelling point and detector field. Thus, despite the atypical conditions, such observations are nonetheless explicable in terms of the transport of ^{99m}Tc as a solute in the xylem of *Ipomoea*.

The present research demonstrates that Tc introduced to leaves as $^{99m}TcO_4^-$ can be translocated in the xylem from leaves to other organs. This is in agreement with research that indicates that TcO_4^- remains highly soluble and complexes with few

metabolites (and therefore remains highly mobile) within the first 24 h of leaf labelling (Lembrechts and Desmet 1984; Myttenaere *et al*. 1980; Neel and Onasch 1989). When combined with the versatility with which plant organs can be labelled with ^{99m}Tc (Currie *et al*. 2010), this rapid transport and the limited biological fixation within the first four half-lives of the radionuclide make the scintigraphic detection of ^{99m}Tc a promising method for tracing pathways of xylem transport within plants.

Experiment 3.11
Xylem connections between the bunch and leaves

Materials and methods

The xylem-mobile dye, eosin (eosin yellowish, Chem-Supply, Gillman, SA, Australia) was introduced to the bunch stem of rooted one-bud cuttings of Chardonnay grapevines (clone I10V1) using a cotton wick. The plants (six plants, one bunch per plant) were in their second season of vegetative growth, pruned to two shoots and maintained in 2 L pots in a naturally-lit glasshouse. In the glasshouse, shortly after dawn (6 am), a cotton thread moistened with deionised water was pushed through the distal end of the hypoclade of a pre-veraison bunch with a needle. The hypoclade is the base of the bunch stem proximal to the first bract (often absent in these small bunches) (Pratt 1971). One end of the thread was allowed to hang freely to promote evaporation and the other end was secured in a micro-centrifuge tube containing aqueous eosin (0.1% w/v) and wrapped in aluminium foil. The shoot carrying the labelled bunch was sampled approximately 27 h later. Hand-sections were taken of each internode and of secondary shoots or petioles occurring at each node. The sections were placed on a glass slide, examined using a stereomicroscope (Leica Microsystems, model MZ16) and a digital microphotograph was obtained using transmitted and green light (Leica DSR filter, excitation 545 ±15 nm, barrier 620 ±30 nm). These images were examined for the presence of eosin after digitally merging them using image analysis freeware (Merge 2.0, www.graphicutils.com). Only strong fluorescence was attributed to the dye because the plant tissues exhibited weak autofluorescence under green light.

The above-mentioned wick method was used to label the pre-veraison bunches of potted plants (cv. Shiraz) with pertechnetate ($^{9m}TcO_{4^-}$, 1 GBq, 0.9% saline solution). Pertechnetate is a xylem-mobile, membrane-permeable gamma-ray emitting radiotracer with uptake and accumulation characteristics comparable to a micronutrient (Bennett and Willey 2003). The plants (four, one bunch per plant on a shoot with at least eight nodes) were in their fourth season of vegetative growth, pruned to four shoots and maintained in 40 L pots in a naturally-lit glasshouse. The plants were transferred to the laboratory the day prior to imaging. Prior to inserting the wick, four cuts were made in each primary leaf on the shoot bearing the bunch to be labelled. The cuts extended from each sinus through the lamina to approximately 5 mm from the junction of the five primary veins. The aim of this treatment was to isolate xylem flows arriving via vascular bundles belonging to different leaf traces. Plants used in this experiment were illuminated continuously using 100 W halogen lamps for approximately 28 hr. The labelling commenced approximately 3 h after illumination had begun. The ^{99m}Tc distribution in the plant was detected scintigraphically (20 min acquisitions, 256 × 256 pixel matrix) at the experiment end using a gamma camera (Philips Prism 1000, Picker, Cleveland). Immediately prior to imaging the wick was removed from the labelled bunch.

Digital scintigraphic images (displaying total counts during the acquisition) were processed by digitally truncating counts in the acquired image to span the range typically observed in labelled leaves (up to ca. 500 counts per pixel). If counts indistinguishable from background were observed in regions other than the labelled bunch the image was truncated until the counts in the bunch 'starred out' (a common artefact in scintigraphy that occurs in regions of very high counts). Each time the image was truncated the greyscale range was adjusted to enhance the contrast between labelled regions and the image background. This provided a rapid means of establishing the spatial extremities of ^{99m}Tc translocation. Truncated images of suitable contrast were exported after applying a colour palette then digitally merged (using the above-mentioned freeware) with a digital photograph taken of the plant during scintigraphic acquisition.

Results and discussion

Visual confirmation of the pathway of solute flow through the xylem of plants is commonly undertaken by applying dye or radioisotopes to wounds purposefully made in roots and stems (Postlethwait and Rogers 1958; Larson *et al*. 1994; Sackville Hamilton and Hay 1998). Such experiments typically

demonstrate that the tracers are transported in the transpiration stream and remain confined to a limited number of vessels (Zwieniecki *et al*. 2001) or vascular bundles (Orians *et al*. 2005). The transport pathways are those initially labelled or are connected to these pathways via low resistance apoplastic routes, such as inter-vessel pits (Orians *et al*. 2004; Ellmore *et al*. 2006). This type of transport system is described as 'sectored' and observations such as these are evidence of 'sectoriality': the transport of solutes by vascular bundles in isolation from neighbouring bundles.

The concept of sectoriality was originally used to describe observations of restricted photoassimilate movement within physiological subunits of plants (Watson and Casper 1984). These physiological subunits have boundaries that are commonly defined by morphologically distinguishable subunits, such as leaves related through the 'phyllotaxy' (i.e. leaf arrangement) of the plant (Marshall 1996). In many plants the phyllotaxy is characterised by two or more spirals, each line of which is known as a 'parastichy'. In other plants, such as the grapevine (*Vitis vinifera* L.), leaves are arranged opposite one-another at successive nodes (distichous phyllotaxy). Two 'orthostichies' can be identified in such an arrangement: these are located on opposite sides of the shoot and each consists of leaves (or tendrils and bunches) located directly above each other in a vertical shoot (Beck 2010).

Little is known about transpiration stream sectoriality in the context of non-foliar organs, such as flowers and fruit. Fruits in particular, can have low transpiration rates due to their inherently low conductance to water vapour (*Figure 3.69*) and be strongly reliant on xylem sap for their supply of water and nutrients (Rogiers *et al*. 2001; Windt *et al*. 2009). The successful physiological function of reproductive organs is fundamental to the long-term survival of a species in an ecological context. For this reason it is expected that plants have mechanisms to maximise the effective allocation of xylem resources between foliar and reproductive structures. Sectoriality may be one such mechanism. For example, a sectorial supply of xylem sap is one means of isolating a reproductive structure from other potentially stronger sinks for xylem resources. Thus, sectoriality can conceivably reduce competition for solutes. Alternatively, a sectorial connection with specific leaves could increase the flux of xylem resources, particularly solutes, in the vessels that supply a reproductive structure. A sectorial xylem network that facilitates xylem flow to a reproductive organ may operate in grapevines (Theiler 1973). Another possibility is a reproductive structure with a sectorial supply of xylem sap that is a by-product of a sectorial supply of phloem sap. Xylem and phloem flows with the same degree of sectoriality are to be expected because both vascular tissues originate from a single set of cambial cells. A sectorial phloem supply to a reproductive structure may be the more physiologically transport process given the importance of phloem flow to the growth of these organs (Canny 1973).

The objective of this research is to identify whether there are sectorial xylem connections to the pre-veraison bunch stem and to assess the relationship between these connections and the orthostichies of the *V. vinifera* shoot. This objective is achieved by identifying hydraulic xylem connections between the pre-veraison *V. vinifera* bunch stem and the leaves occurring along the length of the shoot bearing the bunch. Veraison is the transition from hard green berries to soft, pigmented (red and black cultivars), sugar-rich berries (about 55 days after flowering in *Figure 3.69*). *V. vinifera* is an excellent subject for this investigation because there are multiple lines of evidence suggesting that prior to veraison the grape berry is strongly reliant on the xylem for water and solute inputs (Düring *et al*. 1987; Rogiers *et al*. 2000; Tyerman *et al*. 2004; Keller *et al*. 2006; Rogiers *et al*. 2006). Processes of xylem transport such as sectoriality are therefore of physiological significance to the development of the reproductive organ of this species.

Evidence for the flow of xylem sap away from the pre-veraison grape berry (i.e. backflow) helps to identify the location and importance of leaves hydraulically connected to the grape bunch. Greenspan *et al*. (1994) demonstrated that the pre-veraison berry competes with transpiring leaves for xylem sap and that it may be a water source for the transpiring canopy. Other researchers have observed the xylem transport of dye, introduced at the cut stylar end of berries, through the rachis to the shoot internode basipetal to the node carrying the bunch (Tilbrook and Tyerman 2009) and to nearby leaves (Keller *et al*. 2006). This is potentially additional evidence that the pre-veraison berry is a source of water for a transpiring canopy. However, the dye immersion treatment exposes the cells of the cut berry to a dilute solution that they are capable of osmotically absorbing, thereby reducing their osmotic strength and partially satisfying the transpiration demands of the berry cuticle. The treatment may therefore present the canopy with an atypical source

of water held at a relatively low hydrostatic pressure that artificially promotes backflow. Thus, from the evidence for backflow from the grape bunch it seems likely that hydrostatic pressure generated in the vessels that supply xylem water and solutes to pre-veraison berries is effectively communicated with at least some of the vessels that supply xylem sap to leaves on the *V. vinifera* shoot. Importantly, here we clarify the leaves involved in this relationship and demonstrate that these leaves include those occurring on secondary shoots emerging from axillary buds. These observations (1) are used to argue that long-distance xylem transport within the grapevine shoot is sectorial and (2) provide insights into the regulation of xylem solute flow to organs with inherently low transpiration rates in a sectorial vascular system.

Tracing eosin transport from bunches

Eosin was commonly observed in leaves and secondary shoots acropetal of the labelled bunch stem. It was often present in internodes throughout the entire shoot with the exception of some of the most distal internodes (*Figure 3.69*). The primary leaves and secondary shoots most commonly labelled by the dye were in the same orthostichy as the labelled bunch (15 of 17 observations). There were two exceptions to this trend. In one plant, the petiole of the primary leaf located at the same node as the bunch was labelled. The other exception was an instance in which a small portion of a vascular bundle in a secondary shoot occurring at the same node as the bunch was labelled.

In the petiole of primary leaves eosin was observed in a variety of vascular traces. Following the terminology of Fournioux and Bessis (1974), the vascular traces of the dorsal face of the petiole that were stained ranged from the supernumerary bundle through to and including the median bundle. On the ventral face the split bundle (*faisceaux canaliculaire*), lateral bundle, supernumerary and lesser trace adjacent to the median bundle were stained in at least one petiole section. Overall, staining was strongest in the split bundle of both faces and in other traces on the dorsal face.

Tracing technetium transport from bunches

After labelling the hypoclade of a bunch with $^{99m}TcO_4^-$, scintigraphy produced images showing the presence of ^{99m}Tc in primary leaves as well as those of secondary shoots (*Figure 3.70*). Overall, ^{99m}Tc was most often transported to primary leaves and secondary shoots in the same orthostichy as the labelled bunch (again, 15 of 17 observations). Exceptions to this trend involved morphologically abnormal nodes or nodes located large distances (six nodes) from the labelled bunch.

The identification of leaves to which ^{99m}Tc was transported from labelled bunches was aided by characteristic tracer accumulation patterns along the transport pathway. A ubiquitous trend was the presence of ^{99m}Tc in the internodes that separate the bunch from the sink leaf. The transport pathway was further delineated by relatively high concentrations of ^{99m}Tc around nodes. These high concentrations were most evident in the first few centimetres basipetal to the node but also immediately acropetal to the node and at the distal and proximal end of petioles (e.g. *Figure 3.71*).

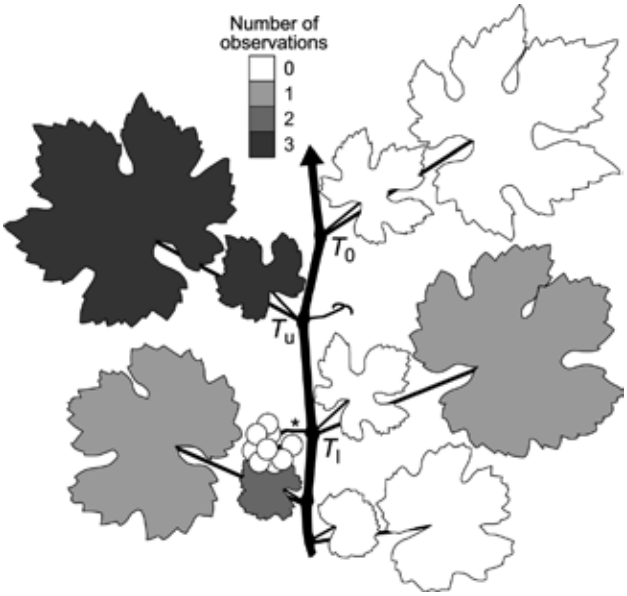


Figure 3.69 Sketch indicating eosin translocation from a cotton wick threaded through the hypoclade of pre-veraison bunches on a rooted Chardonnay cuttings (n=6). Approximate site of the wick is indicated by the asterisk (*). Shading of primary and secondary leaves (large and small leaf at each node, respectively) is grey scale-coded to indicate the number of occasions eosin was observed in their petiole or shoot base, respectively. Lower, upper and no-tendril nodes in the repeating three-node metamer of the *Vitis vinifera* shoot are labelled T_l, T_u, and T_0, respectively. Tendrils are always absent from basal nodes. The shoot above T_0 is not shown because, despite being present in internodes, eosin was not observed in primary leaves or secondary shoots acropetal of this node.



Figure 3.70 Sketch indicating ^{99m}Tc translocation from a cotton wick threaded through the hypoclade of pre-veraison bunches on potted Shiraz plants (n=5). Approximate site of the wick is indicated by the asterisk (*). Nodes are labelled according to the tendril pattern described in *Figure 3.69*. The whole primary leaf at the uppermost T_0 node position is shaded because ^{99m}Tc was observed throughout the leaf–this may be because the lobes were not separated on the particular plant that produced this observation. The observation of ^{99m}Tc in the secondary shoot at the uppermost T_0 node position is potentially atypical because the node gave rise to two primary leaves as if an internode was not present or highly compressed.

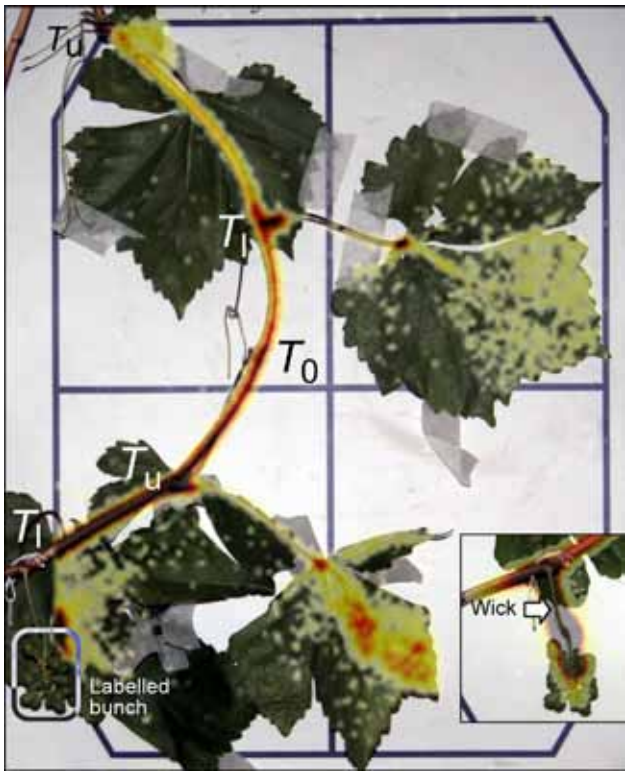


Figure 3.71 Photographic image, overlayed with a scintigraphic image, of a grapevine shoot (referred to in the text as plant C) labelled with pertechnetate introduced via a cotton wick through the hypoclade of the pre-veraison bunch. Nodes are labelled according to the tendril pattern described in Figure 3.69. The inset shows the labelled bunch, which is outside the imaging window in the main scintigraphic image. The arrow indicates the point at which the wick was inserted. Counts radiating out from the labelled bunch in the main image are an artefact resulting from relatively high radioactivity in the vicinity of the wick (removed prior to scintigraphic imaging). The artefact is not evident in the inset because the upper limit of count truncation is higher.

Discussion

Sectorial transport in the xylem of the grapevine shoot

Our results indicate that the xylem transport of solutes in the grapevine shoot is sectorial. Dye was repeatedly transported from a labelled bunch stem to the petioles of primary leaves and base of secondary shoots located within the same orthostichy as the bunch. Similarly, our scintigraphic results indicated that ^{99m}Tc introduced to the bunch stem labels primary and secondary leaves located within the same orthostichy as the bunch. The specific nature of these connections suggests that both membrane and non-membrane permeable solutes are transported in the xylem of the grapevine shoot with minimal transfer between vascular sympodia, at least over the timescale of our observations (ca. 24 h). The term 'sympodia' refers to one of the ten discrete sets of vascular bundles present in the stem and their associated leaf (and bunch/tendril) traces (Esau 1977; Fournioux and Bessis 1979). Further evidence of sectoriality in the xylem of the grapevine shoot comes from the dye experiments of Theiler (1973). This author observed that dye injected into the side of the grapevine shoot remained confined to a limited number of vascular bundles as it was transported apically and that coloured dyes injected into different locations within the same shoot did not mix.

The most repeatable aspect of our dye and radiotracer experiments was translocation from the labelled bunch towards other leaves (primary and

secondary) located within the same orthostichy. However, the nodes at which these sink organs were located varied within both sets of observations. We attribute this variability to between-replicate variation in the vascular bundles of the bunch stem that were labelled with dye or isotope tracer. As illustrated by Fournioux and Bessis (1979), at least four distinct vascular traces are present in the base of the bunch stem, and the sympodia from which these bundles originate have unique trajectories within the vascular network of the grapevine shoot. The location and orientation of the wick can therefore readily produce variations in the vascular traces connected to the xylem vessels labelled in the bunch stem.

We emphasise that the present results do not provide evidence that back- or counter-flow from the bunch to other organs on the grapevine occur under normal physiological conditions. At the site of dye or isotope uptake in the bunch stem, tension in the xylem vessels with a hydraulic connection to the solution supplied by the cotton wick is expected to be close to zero. First, this is because the moistened cotton wick provides access to a water source held under low tension. Second, the hydraulic connection between the conducting xylem vessels and wick solution is likely to be apoplastic (a prerequisite in the case of the membrane-impermeable dye), facilitated by localised damage to the xylem vessels. For this reason, any pre-existing hydrostatic gradient that had been established at the site of tracer uptake is likely to have been eliminated upon insertion of the wick. The insertion and presence of the wick will enhance the hydrostatic gradient between the site of tracer introduction and organs elsewhere on the grapevine shoot generating tension in the xylem: backflow will therefore be artificially enhanced. Despite this caveat, the strength of the wick approach is that it positively identifies hydraulic connections between the xylem vessels of the grape bunch and other organs on the grapevine shoot.

The patterns of sectorial xylem transport documented here have their parallel with previous studies of assimilate transport by phloem flow in the *V. vinifera* shoot. Exposure of primary and secondary leaves to $^{14}CO_2$ typically produces intense autoradiographs of strong assimilate sinks in the same orthostichy as the labelled leaf but is also capable of producing slight but significant autoradiographs of sinks in the opposite orthostichy (Hale and Weaver 1962; Koblet 1969). These patterns of sectorial xylem and phloem flows have an anatomical basis. According to Fournioux and Bessis (1979), the primary vascular network of the grapevine shoots consists of 'unilateral' and 'bilateral' sympodia. There are two sets of three unilateral sympodia arranged in parallel. Each set is confined to one side of the shoot and inter-connect organs (axillary buds, primary leaves and tendrils/bunches) occurring within the same orthostichy. Thus, the unilateral sympodia are responsible for the close correlation between sectorial xylem and phloem flows and the phyllotaxy of the grapevine shoot. The other four vascular sympodia in the grapevine shoot are bilateral: they are also arranged in parallel and primarily link organs in the same orthostichy but they also provide occasional vascular connections to leaves in the opposite orthostichy (Fournioux and Bessis 1979). These bilateral sympodia therefore reinforce the sectorial vascular connections but also provide a link between the opposite halves of the grapevine shoot. It is these bilateral sympodia that are responsible for observations such as the transport of dye from a labelled bunch to the leaf at the same node and the above-mentioned observations of 14C-assimilate transport between orthostichies.

The primary vasculature of the grapevine shoot delineated by Fournioux and Bessis (1979) serves to explain why dye and the radionuclide were typically transported from the bunch stem to primary leaves and secondary shoots located in the same orthostichy. The vascular traces of the bunch stem originate from four of the vascular sympodia in the grapevine shoot. Two of these bunch traces diverge from unilateral sympodia with vascular connections to axillary buds located at the nodes immediately acro- and basipetal of the bunch. The other two bunch traces diverge from sympodia with connections to the primary leaves located at these same nodes. One of these sympodia is unilateral and connected to the median vascular bundle in the primary leaf petiole. The other is bilateral and connected to DORsal vascular bundles in the primary leaf petiole (Fournioux and Bessis 1979). These connections are in agreement with our repeated observations of dye in the median and DORsal vascular bundles of petioles. Thin sections of the petiole-leaf blade junction indicate that these vascular bundles are connected to the median, distal and proximal leaf veins (S.J. Clarke and K. Singh, unpublished). The presence of ^{99m}Tc in the median and proximal lobes of leaves is therefore expected but the paucity of ^{99m}Tc in distal lobes is not. The four sympodia from which the bunch traces originate are repeatedly linked to the same organs (other bunches/tendrils and either axillary buds or primary leaves)

along the length of the shoot (Fournioux and Bessis 1979). These repeated connections enable tracers such as eosin and ^{99m}Tc to label primary leaves and secondary shoots in the same orthostichy recurrently.

The axillary bud (from which the secondary shoot emerges) is connected by unilateral sympodia to tendrils/bunches and other axillary buds in the same orthostichy (Fournioux and Bessis 1979). In agreement with this, our scintigraphic results indicate that xylem-mobile radiotracer was transported from a labelled bunch stem to three leaves occurring on sequential nodes within a secondary shoot, not just those occurring at every second node as seen in the primary shoot. This indicates that the axillary bud unilateral sympodia supply to the secondary shoot bilateral sympodia and/or unilateral sympodia to both orthostichies. The implication is that, within the secondary shoot, there is unlikely to be an anatomical basis for sectoriality in the vascular connections to bunch stems.

Solute supply to the grapevine bunch in a sectorial xylem network

The scintigraphic images identified preferential ^{99m}Tc accumulation near the nodes and at the proximal and distal end of petioles. The most likely explanation for this observation is enhanced uptake and storage of this nutrient analogue by cells located at these regions. Similar xylem-mobile isotope tracer localisation has been observed in the nodes of cereals (McNeil *et al*. 1979; McKay *et al*. 1988; Fujimaki *et al*. 2010). The cells most likely to be responsible for the uptake of ^{99m}Tc are transfer cells. Across a large number of plant genera transfer cells are frequently associated with leaf traces where they diverge from vascular sympodia in the nodal region (Gunning *et al*. 1970). Transfer cells possess wall ingrowths that increase their surface area, making them highly effective at exchanging solutes with intercellular spaces (Gunning and Pate 1969).

Alternative explanations for the localisation of ^{99m}Tc, based upon the hydrostatic or ion exchange characteristics of vessels, are unlikely. For example, it has been emphasised that xylem vessel diameter is slightly narrower in nodes than internodes (Salleo *et al*. 1982). However, if xylem sap is transported through internodes and nodes under the same hydrostatic pressure gradient, then the velocity of flow must be greater and the pressure reduced through the nodes relative to the internodes (Canny *et al*. 2007). The change in velocity would make it less likely that xylem sap would move out of the vessels in nodes driven by hydrostatic pressure. A change in velocity would not effect the diffusion of solutes out of the xylem vessels and their subsequent absorption by cells. Another possible explanation for the high ^{99m}Tc concentrations near nodes is an increase in the number or effectiveness of cation exchange sites in nodal xylem vessels. For example, ^{65}Zn perfused through DORmant grapevine canes preferentially accumulates near the nodes (Hewitt and Gardner 1956). However, for ^{99m}Tc to similarly preferentially accumulate at such sites the isotope must be present in the xylem in the form of a cation, not the pertechnetate anion. This seems unlikely because there is no evidence for a Tc-compound other than TcO_4^- in xylem sap (Krijger *et al*. 1999a). Uptake by xylem-associated cells such as transfer cells is the most parsimonious explanation for the localised accumulation of ^{99m}Tc.

The insights provided by our dye and radionuclide experiments allow us to speculate a model for the regulation of xylem-mobile solute supply to organs with low transpiration rates in a sectorial vascular network. As mentioned above, some of the most significant work in this area was reported by Theiler (1973) – transpiring secondary shoots were observed to promote the labelling of bunch stem xylem vessels with dye. We suggest that this occurred because the transpiring secondary shoots drew dye into xylem vessels that bifurcate to supply the bunch stem. A hydrostatic gradient generated by the transpiration and osmotic pressure of the bunch subsequently drew this local supply of dye-labelled sap into the bunch stem. This observation suggests that transpiration by leaves hydraulically connected to the bunch stem is capable of influencing the flux of solutes in the xylem sap directly accessible by the bunch stem. In isolation, assuming a hypothetical steady flow of constant composition xylem sap, such a process would not increase or change the concentration of solutes accessible by the bunch stem – the concentration of solutes supplied will be the same regardless of the rate of sap flow. The flow induced by leaves with xylem connections to the bunch is important if it operates in conjunction with a storage mechanism capable of temporally dissociating the supply of solutes with their use. This storage function may be filled by the cell populations responsible for the localised accumulation of ^{99m}Tc in nodes identified in the scintigraphic images. The storage of solutes (and their potential metabolism into more physiologically relevant compounds) allows them to be released at times when they are most effective to the bunch.

Over the long term, such a period is pre-veraison berry development when xylem-mobile elements accumulate rapidly (Rogiers *et al*. 2006). In the short term, nutrient supply to the bunch stem would be particularly effective during the night. This is because, although the net xylem flow into the berry may not be particularly rapid at night (Greenspan *et al*. 1994), it is during this period that leaf transpiration is low (Rogiers *et al*. 2009). Under these conditions less of the xylem solutes released by these specialised cells would be supplied to leaves sectorially-linked to the bunch.

Experiment 3.12
Berry oxygen isotope ratios

Materials and methods

Twenty-five well-watered two-year old *Vitis vinifera* cv. Chardonnay (clone V5, own roots) were grown in a glasshouse in 25 L plastic pots. Shoots were established from two buds on two spurs, yielding four shoots per vine. Berry age is expressed as days after flowering estimated (80% capfall) on a bunch specific basis (DAF). Berries from a whole bunch were sampled every two weeks from six randomly selected plants. Twenty representative berries from each sample were crushed in a plastic zip-lock bag. Via a small cut placed in the corner of the bag the juice was collected in a vial for analysis of berry water $^{18}O/^{16}O$ by an isotope ratio mass spectrometer (IRMS) (Micromass PRISM III) following head-space equilibration with CO_2. The remainder of the expressed juice was used to assay total soluble solids (TSS) using a handheld refractometer. An additional 20 berries were dried to a constant weight and ground to a fine powder in a ball mill (Qiagen TissueLyser, Retsch, Germany). The residue was pyrolysed to yield CO in a custom-built furnace (Stuart-Williams *et al*. 2008) for oxygen isotope analysis by an IRMS (Micromass Isochrom, Middlewich, UK). The $^{18}O/^{16}O$ ratio of juice and organic matter samples is expressed in standard delta notation ($\delta^{18}O$) relative to Vienna Standard Mean Ocean Water. Average reproducibility on duplicates was ±0.2‰ for both juice and organic matter samples. Subscripts 'OM' and 'J' are used to denote $\delta^{18}O$ values in berry organic matter and the water in berry juice, respectively.

Nine three-year old plants of *V. vinifera* cv. Merlot (clone D3V14, own roots) were moved into a glasshouse in mid-spring, shortly after bud burst. The plants were well-watered and pruned to four vertically-trained shoots. Samples for $\delta^{18}O$ analysis were taken approximately 20, 35, 60 and 80 DAF. For $\delta^{18}O_{OM}$ and $\delta^{18}O_J$ analysis four and eight berries were sampled from a randomly chosen bunch on each plant, respectively. Residual juice from $\delta^{18}O_J$ samples was assessed for TSS using a handheld refractometer. Throughout the experiment dual and triplicate samples were taken for $\delta^{18}O$ analysis of irrigation water and water vapour (collected over a 24 h period). The samples were analysed as described above.

Gas exchange measurements were obtained using a portable photosynthesis system (Li-6400, LICOR, Nebraska) on leaves every week from the onset of flowering until berry harvest. For each plant leaf gas exchange measurements were obtained on two sun-lit primary leaves located at a node immediately above a bunch and on separate shoots. These measurements were obtained between 11 am and 3 pm. Weather-permitting, an additional set of leaf gas exchange measurements was obtained on a day adjacent to the midday measurements. These measurements sampled the same type of leaves but on a subset of the experiment: one leaf on four randomly chosen plants. These same plants were sampled each week every 90 min from before dawn until after dark to characterise the diurnal trend in leaf gas exchange. For the midday and diurnal time-course measurements the photon flux density was set to 1000 μmol m^{-2} s^{-1} and matched to ambient, respectively. Similarly, the temperature of the gas exchange chamber head was set to within 0.5°C of ambient air temperature and CO_2 concentration was always set to 400 ppm.

The field site for this experiment was the Charles Sturt University, Wagga Wagga, trial block. This block consists of six replicated rows of ten varieties, arranged randomly within rows in three-plant panels. Further information on this block is provided by Rogiers *et al*. (2009). The varieties (and clones) are: Riesling (BV17), Merlot (D3V14), Chardonnay (I10V5), Sauvignon Blanc (F4V6), Shiraz (BVRC12), Sultana (H5), Flame Seedless (K5V8), Pinot Noir (114), Cabernet Sauvignon (SA125) and Semillon (DA16162).

Berries were sampled for TSS and $\delta^{18}O_J$ shortly after veraison, a fortnight later and then in each of the next two weeks, which bracketed 90 DAF for the late and early flowering varieties. Berries were sampled for $\delta^{18}O_{OM}$ and $^{13}C/^{12}C$ (expressed as $\delta^{13}C$ relative to Pee Dee Belemnite) analysis in both of these last two sampling events. Berry samples for isotope analyses were taken from the proximal, mid and distal regions

of six bunches across each panel, immediately placed in a resealable plastic bag and stored on ice for transport to a laboratory for storage at 4°C. $\delta^{18}O$ and TSS assays were performed as described above. $\delta^{13}C$ analysis was performed on CO_2 evolved by combusting samples in an elemental analyser coupled to an IRMS.

Results and discussion

When water diffuses as vapour from a leaf stomatal cavity, isotopic fractionation that discriminates against ^{18}O takes place. The $^{18}O/^{16}O$ ratio of residual water in the stomatal cavity increases as a result. The degree of fractionation depends on environmental factors including the gradient in water vapour concentration between the leaf and atmosphere, as well as the $^{18}O/^{16}O$ of atmospheric water vapour. The two physiological parameters that influence the degree of isotopic enrichment are stomatal conductance and leaf temperature. These two parameters are positively correlated (the leaf is cooled as water becomes vapour) and they drive the $^{18}O/^{16}O$ ratio in the same direction, effectively enhancing the sensitivity of the isotope ratio to stomatal conductance. Across the whole leaf, another process takes place: unfractionated water supplied from the roots via the xylem is mixed with ^{18}O-enriched leaf water. This mixing is sensitive to the transpiration rate. A high transpiration rate reduces the relative contribution of ^{18}O-enriched water at sites of evaporation to the whole leaf water pool. Because transpiration and stomatal conductance are also positively correlated and both reduce the $^{18}O/^{16}O$ ratio of the leaf, this mixing effect further strengthens the stomatal conductance signal in the $^{18}O/^{16}O$ of leaf water. The $^{18}O/^{16}O$ ratio of leaf water is reflected in the isotopic composition of organic molecules synthesised in the leaf. This isotopic character is transferred to the organic matter of organs (such as berries) over the time period they are supplied with photosynthates. Thus, the chief aim of this particular research is to identify leaf $^{18}O/^{16}O$ signals in the organic matter of the grape berry. High fidelity preservation of this isotope ratio in grape berries is expected to provide insights into whole-stomatal conductance.

There is no comparable mechanistic understanding of the environmental and physiological controls of the $^{18}O/^{16}O$ ratio of water in an organ such as the grape berry. A model of $^{18}O/^{16}O$ in grape berries will relate strongly to the proportion of xylem water supplied to the berry directly from the roots (not fractionated) relative to sugar-rich phloem water from the leaves (fractionated by transpiration as described above). A secondary aim of this research is therefore constrain options for modelling the $^{18}O/^{16}O$ of grape berry water. These constraints (or lack thereof) will determine whether useful physiological information can be extracted from the $^{18}O/^{16}O$ ratio of berry water.

Developmental trends in the oxygen isotope ratios of grape berries

This preliminary data set (*Figure 3.72*) indicated that, with respect to elemental oxygen, berry organic matter and juice are isotopically distinct. The $\delta^{18}O_{OM}$ of whole grape berries increased gradually prior to veraison, from approximately 25–30‰. After veraison the $\delta^{18}O_{OM}$ values remained approximately constant. The process or processes responsible for the increase in $\delta^{18}O_{OM}$ is not clear but the stability in the post-veraison values suggests berry $\delta^{18}O_{OM}$ may be a measurement that is not highly sensitive to the date of berry sampling.

The $\delta^{18}O_J$ values ranged from 5–10‰ prior to veraison and steadily increased late in the ripening period. The $\delta^{18}O_J$ values provided no clear evidence of an abrupt shift from xylem to phloem-derived water into the berries as might be expected from phloem-girdling experiments (Greenspan *et al.* 1994). In this experiment xylem water is expected to be approximately –5‰ (based on irrigation water $\delta^{18}O$, results not shown) and phloem-derived water is expected to be far more enriched in ^{18}O, in the vicinity of 15–20‰. One possible explanation for the lack of a clear transition is the length of time taken for berry water to turnover. Based on measurements

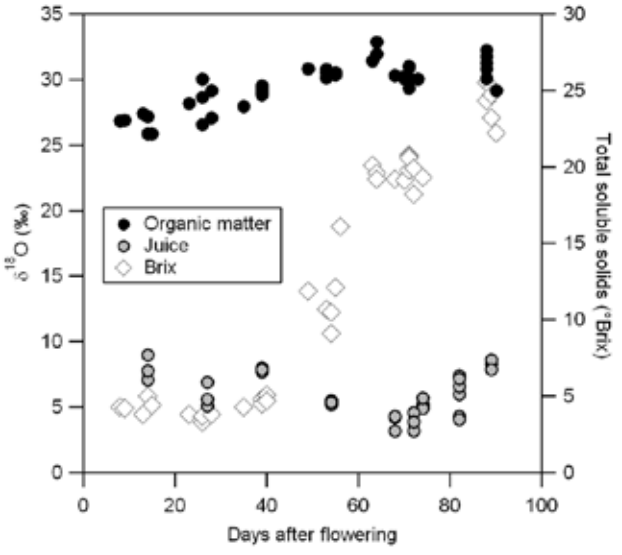


Figure 3.72 Developmental trend in the oxygen isotope ratios of Chardonnay berries from glasshouse-grown plants. Data shown are the $\delta^{18}O$ values of berry organic matter (including seeds) and of juice expressed from berries. For reference, berry total soluble solids are also shown.

on berry transpiration (assuming no backflow and no xylem inflow or outflow) (results not shown), it would take approximately one week of ripening for the equivalent of the berry water content to be transpired. However, water transpired is a mix of resident berry water and incoming phloem-supplied water. Assuming the resident and incoming waters have an equal probability of being transpired, the time taken for isotopic equilibration with the incoming water source will be approximately seven weeks. This gradual process offers a potential explanation for the protracted increase in $\delta^{18}O_J$ observed in the ripening period.

Relating the oxygen isotope ratios of grape berry organic matter to leaf gas exchange processes

This dataset (*Figure 3.74*) provided an opportunity to compare and contrast modelled and observed Merlot berry $\delta^{18}O_{OM}$ values. In contrast to the previous experiment using Chardonnay berries, seeds were removed from the whole berry samples, so the results relate to the accumulation of organic matter in berry pulp and skin. Despite this difference, the developmental pattern of berry $\delta^{18}O_{OM}$ was similar across the Chardonnay (*Figure 3.72*) and Merlot (*Figure 3.73*) datasets. The developmental change in berry $\delta^{18}O_{OM}$ is not due to seasonal shifts in irrigation water or water vapour (which isotopically exchanges with leaves and berries) (*Figure 3.73*).

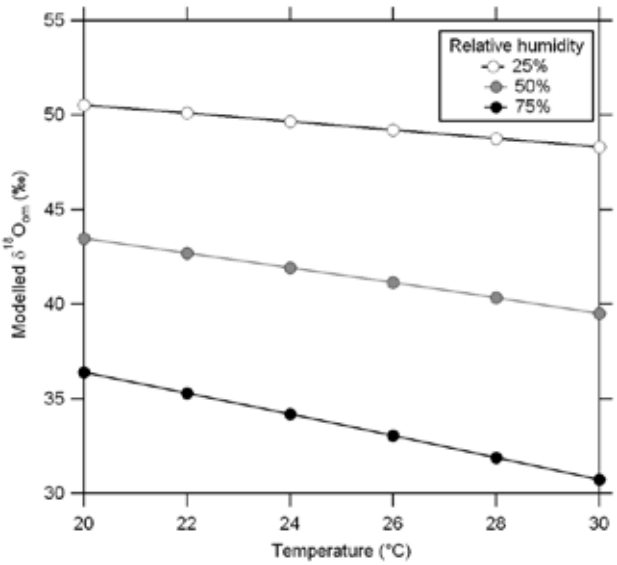


Figure 3.73 Modelled and observed trends in the oxygen isotope ratios of Merlot berries from glasshouse-grown plants. Data shown are the $\delta^{18}O$ values predicted by a model of leaf oxygen isotope fractionation (Barbour *et al.* 2004) and of berry organic matter (excluding seeds), juice expressed from berries, irrigation water and atmospheric water vapour. For reference, berry TSS is also shown.

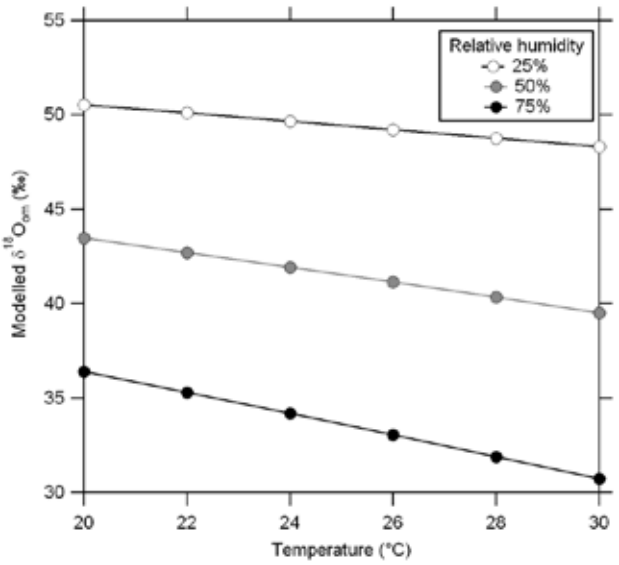


Figure 3.74 The modelled effect of temperature and relative humidity on the $\delta^{18}O$ value of sucrose synthesised in leaves. The model is that of Barbour *et al.* (2004) and inputs were derived from typical midday leaf gas exchange parameters of Merlot plants (T_{leaf}= 0.6 × T + 11°C, g_s=0.11 mol H_2O m^{-2} s^{-1}, E_t = 2 mmol H_2O m^{-2} s^{-1}).

To predict the effect of leaf gas exchange on the $\delta^{18}O$ of sucrose supplied to berries the model of Barbour *et al.* (2004) was used (*Figure 3.73*). This application of the model assumes that the berry organic matter is comprised of sucrose only, and that the accumulated sucrose does not undergo isotopic exchange or fractionation once it has arrived at the berry. The Péclet effect was assumed to be 0.018 m. All other parameters were estimated from midday leaf gas exchange measurements integrated over the course of the growing season. The major contrast between the modelled and observed berry $\delta^{18}O_{OM}$ values occurred prior to veraison (50 days after flowering). During this period the modelled $\delta^{18}O_{OM}$ values consistently exceeded the observed values by approximately 14‰ (*Figure 3.73*). This large contrast suggests that one of the assumptions underlying the application of the model is incorrect. One possibility is that a source in addition to photosynthesising leaves with an isotopic composition less ^{18}O-enriched than that of leaf sucrose contributes carbohydrates to the pre-veraison berries. Such a source may be starch reserves originating from the roots. Sucrose hydrolysed from starch can isotopically exchange oxygen molecules with metabolic water (Gessler *et al.* 2007), which in the roots would be expected to be relatively depleted in ^{18}O (i.e. about –7‰, similar to irrigation water).

The hydrolysis of root starch would supply the berries with sucrose with a $\delta^{18}O$ value of about 20‰, which would imply the supply of sucrose to berry organic matter (30‰) is equally shared between reserves and current photosynthate (40‰) prior to veraison.

During the ripening period, the model over-estimates berry $\delta^{18}O_{OM}$ by about 5‰. One possible reason for this discrepancy is the reliance on 'midday' leaf gas exchange measurements as model inputs. As shown in *Figure 3.74*, modelled $\delta^{18}O_{OM}$ decreases slightly with an increase in temperature, and decreases dramatically with an increase in relative humidity. The latter effect effectively enhances the back-diffusion of atmospheric water vapour (–12‰, *Figure 3.73*) into the leaf, which has the effect of reducing the $\delta^{18}O$ of leaf water and sucrose. From diurnal measurements of leaf gas exchange it is seen that photosynthesis rates are highest mid-morning, prior to the midday sampling period (*Figure 3.75*). Relative humidity in the glasshouse declines during the day (*Figure 3.76*), thus the synthesis of sucrose by the plants is biased towards a period that will supply less ^{18}O-enriched organic matter to grape berries. The 5 ‰ discrepancy between modelled and observed berry $\delta^{18}O_{OM}$ may therefore result from the inability of the midday leaf gas exchange measurements to reflect photosynthesis over an entire day.

The effect of variety on the oxygen isotope ratio in grape berries

Our third set of measurements provided an opportunity to assess:

1. the effect of variety on grape berry $\delta^{18}O$; and
2. the correlation with the carbon isotope composition of grape berry organic matter ($\delta^{13}C_{OM}$).

$\delta^{18}O$ measurements on organic matter were made on berries at their physiological maturity to avoid the changing $\delta^{18}O_{OM}$ values seen prior to veraison in previous experiments (*Figures 3.72* and *3.73*). $\delta^{13}C_{OM}$ measurements were made on a subset of these varieties chosen to span the range of observed $\delta^{18}O_J$ measurements. $\delta^{18}O_J$ measurements were made across the ripening period to provide further insight into the processes controlling the 18O-enrichment of berry water observed in our preliminary set of observations (*Figure 3.72*).

As shown in *Figure 3.77*, across the ten varieties there was a poor correlation between $\delta^{18}O$ measured in berry juice and berry organic matter (sans seeds). If, as suggested above, a first-order approximation of $\delta^{18}O_{OM}$ can be modelled from leaf gas exchange

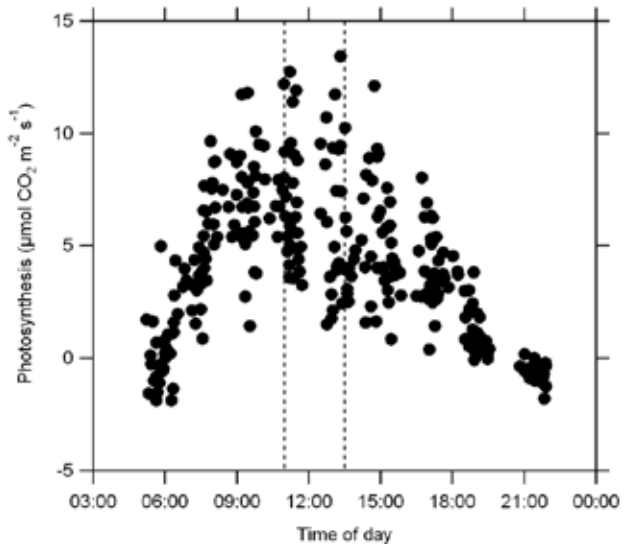


Figure 3.75 The relationship between the rate of photosynthesis of Merlot leaves and the time of day the measurement is taken. Measurements were made on two leaves of four plants nine times per day repeated nine times over the course of the growing season

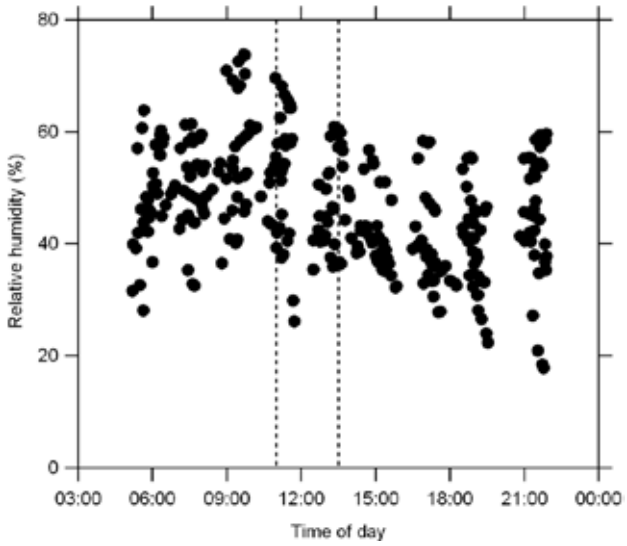


Figure 3.76 The relationship between relative humidity and the time of day the leaf gas exchange measurements are taken. Data sampled as described in Figure 3.75.

parameters, this poor correlation suggests that an alternative process exerts a dominant influence on $\delta^{18}O_J$.

A positive correlation was observed between the $\delta^{18}O_{OM}$ and $\delta^{13}C_{OM}$ values of berries sampled at harvest (*Figure 3.78*). Assuming $\delta^{13}C_{OM}$ is primarily determined by leaf gas exchange processes (Condon *et al.* 2004), this observations supports our suggestion that berry $\delta^{18}O_{OM}$ strongly reflects processes taking place at the site of photosynthesis, at least after veraison. At the leaf scale, less negative $\delta^{13}C$ values are typically associated with more water use efficient plants (H_2O transpired per CO_2 fixed). Thus, it is

noteworthy in *Figure 3.78* that the hot-adapted table grape (Sultana) exhibits the least negative $\delta^{13}C_{OM}$ values and the anisohydric cultivar (Semillon) (Rogiers *et al.* 2009) exhibits the most negative $\delta^{13}C_{OM}$ values. The $\delta^{18}O_{OM}$ and $\delta^{13}C_{OM}$ values are expected to be correlated because both are theoretically predicted to be negatively correlated with stomatal conductance.

A negative correlation was observed between the $\delta^{13}C_{OM}$ and $\delta^{18}O_J$ of berries sampled at harvest (*Figure 3.79*). In the absence of a strong physiological model for interpreting $\delta^{18}O_J$, this correlation is difficult to explain. We observed a strong linear correlation between $\delta^{18}O_J$ and berry total soluble solids across all ten varieties sampled (*Figure 3.80*). Although the slope of this correlation was constant amongst the varieties the *y*-intercept varied with the ripening rate.

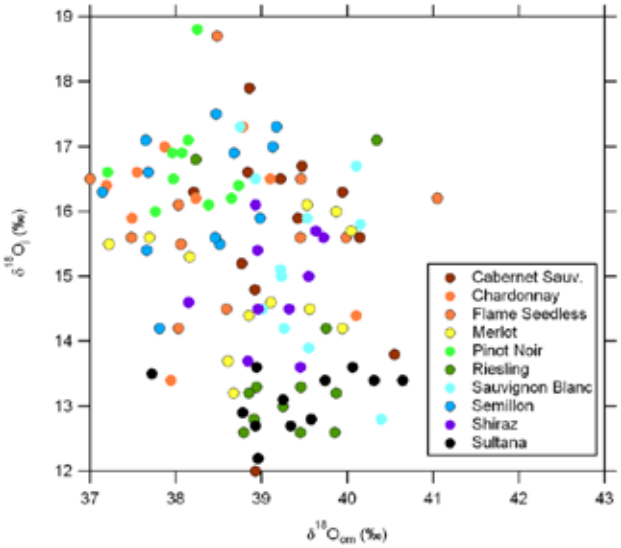


Figure 3.77 Relationship between the oxygen isotope composition of berry organic matter and berry juice across ten varieties.

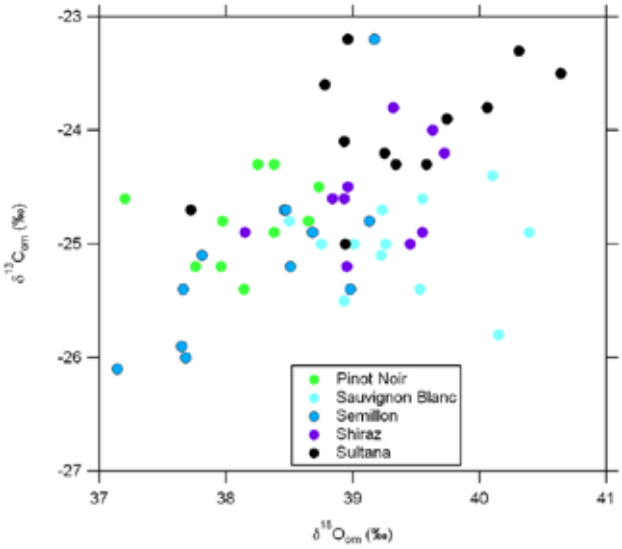


Figure 3.78 Relationship between the carbon and oxygen isotope composition of berry organic matter across five varieties.

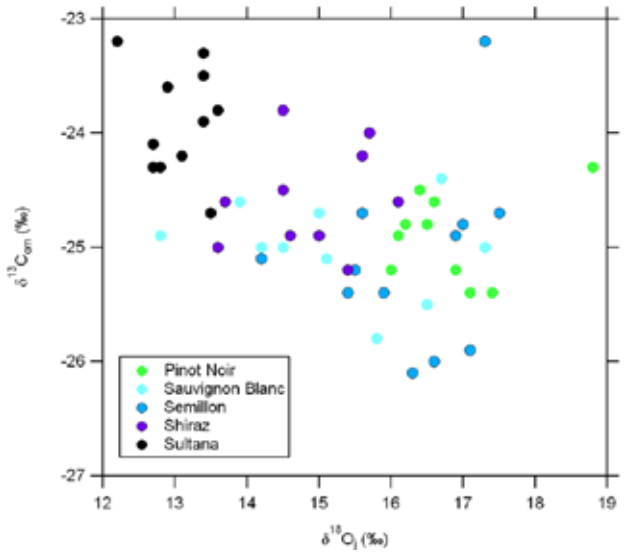


Figure 3.79 Relationship between the carbon isotope composition of berry organic matter and berry juice across five varieties.

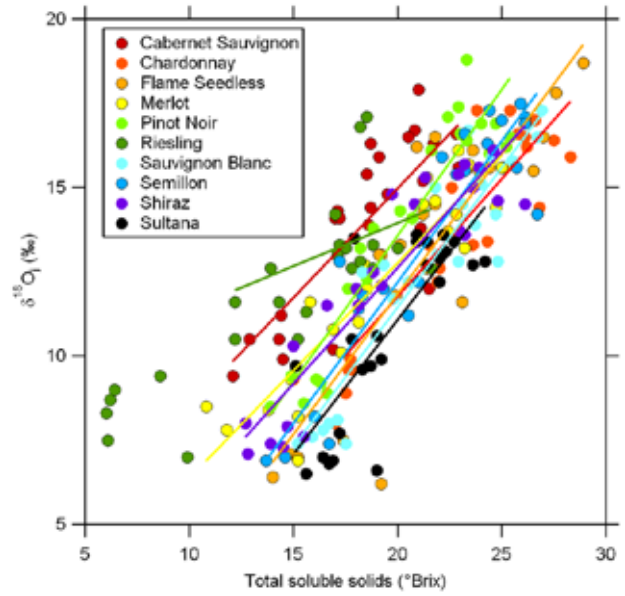


Figure 3.80 Relationship between the oxygen isotope composition of berry juice and berry total soluble solids across ten varieties.

The *y*-intercept was lowest amongst early-ripening varieties such as Chardonnay and the table grapes, and highest amongst late-ripening varieties such as Riesling and Cabernet Sauvignon. This suggests to us that ripening dates, rather than primary physiological mechanisms such as leaf gas exchange, are important determinants of $\delta^{18}O_J$ values. Such an effect has been previously observed in berry oxygen and deuterium isotope ratios (Martin *et al.* 1988; Ingraham and Caldwell 1999). It is likely that vineyard soil water becomes increasingly enriched in $H_2{}^{18}O$ late in the growing season due to the preferential loss of $H_2{}^{16}O$ via soil evaporation. This ^{18}O-enriched water is accessed via grapevine roots and incorporated into leaves and berries via biosynthesis and vascular flows.

However, this soil water effect is not likely to be the sole contributor to the post-veraison increase in $\delta^{18}O_J$. We have observed a post-veraison increase in $\delta^{18}O_J$ amongst well-watered Chardonnay (*Figure 3.72*), Merlot and Semillon (data not shown) plants in the glasshouse. As described above, this is likely to be due to the slow but steady accumulation of ^{18}O-enriched phloem water in the grape berry. The increase in $\delta^{18}O_J$ observed across the varieties during the ripening period is most likely due to the combined effects of vineyard soil water $\delta^{18}O$ and the increase in phloem flow to the berry at veraison.

^{18}O-enriched soil water late in the growing season is also expected to contribute to the accumulation of isotopically-enriched sucrose in grape berries (i.e. $\delta^{18}O_{OM}$). However, the effect is dampened with respect to $\delta^{18}O_{OM}$ because the synthesis of sucrose is also sensitive to the $\delta^{18}O$ of atmospheric water vapour, which is a large, well-mixed and isotopically homogenous source, especially in comparison to vineyard soil water.

Experiment 3.13
Susceptibility to fruit splitting

Materials and methods

This study involved three experiments, each of which used berries from grapevines (*Vitis vinifera* L., cv. Shiraz, clone 1654) either vineyard-grown or grown in 50 L pots for two seasons in a glasshouse or outdoors at the National Wine and Grape Industry Centre, Wagga Wagga, Australia. In each experiment, the developmental stage of berry ripening was characterised in terms of concentration of soluble solids (°Brix), determined by refractometry and days after the onset of ripening (DOR) of source bunches. The onset of ripening was taken as the day 80% of berries in any bunch had begun to change colour.

To determine effects of fruit development on the osmotic (and hence turgor-generating) capacity of berries, as reflected in susceptibility to splitting, berries of similar soluble solids concentration were immersed in solutions of different osmotic potential. At mid-morning on four occasions from January 18, 16 DOR (72 days after anthesis, DAA, i.e. 80% capfall) until 18 February, 2008, two to four bunches were sampled from vineyard-grown plants and taken to the laboratory, where all berries (several hundred) were detached within 30 min of sampling by severing the pedicel a few millimetres from the torus. Grape berries develop asynchronously within bunches, therefore in order to obtain sets of intact berries of similar soluble solids concentration, the berries were classified according to density. Berries were successively placed in a graded series of sucrose solutions (1% increments, in ascending concentration); those that floated in each solution were removed and aggregated according to the procedure described by Nelson *et al.* (1963). Soluble solids concentrations of berries in this experiment were estimated from the linear relationship (least-squares regression, $P<0.001$, $r^2=0.93$) between measured soluble solids concentration of a subset of individual berries (at least three berries per solution), across the range of solutions, and the sucrose concentration of the solution in which they first floated. At each sampling, five berries from each of the two or three most highly populated classes were placed in vials containing 20 mL of 0, 3, 6, 9, 12, 16, 20, 24 or 30% (w/v) aqueous sucrose (after Considine and Kriedemann 1972) to test for developmental changes in the number of berries that split and the time (days) until splitting occurred. The immersed berries were incubated in darkness at 25°C, and inspected daily for splitting for up to 30 days.

In June–July 2008, we examined the rate of water uptake and susceptibility to splitting of berries from 24 glasshouse-grown plants (mean temperature 25/23°C day/night, mean relative humidity 60%). Each plant had several fruit bunches, each of similar size and development. Every seven days for eight weeks (omitting the seventh week to preserve berries and extend the observation period), beginning four days after the onset of bunch ripening, six berries, visually representative (based on size and colour) of the median of the whole berry population, were sampled from a randomly selected plant. Three berries were immersed in 10 mL of deionised water within sealed vials and kept in darkness at 14°C for up to 30 days. The course of water uptake of each berry was determined gravimetrically, following brief removal and careful surface drying, at one- to three-day intervals until the berry split or progressively lost weight. Dry weight was determined by dehydrating berries at 80°C until they reached a constant weight. The other three berries were assayed for cell vitality using nitroblue tetrazolium (NBT) stain as described in the following section. Each sampling was replicated four times on different plants.

Cell vitality was visualised using NBT staining of fresh berry cross sections. Reduction of clear yellow NBT to insoluble blue/purple formazan is an indicator

of oxidative metabolism in living, biological systems (Hauser and Morrison 1964, Altman 1976). The staining method was adapted from that of Krasnow *et al*. (2008) and Tilbrook and Tyerman (2008) for fluorescein diacetate. Berries were first sectioned transversely through the 'brush' region (where the vascular strands of the berry diverge from the torus) to locate the position of seeds. Berries were then bi-sectioned longitudinally between the seeds. One section was analysed for soluble solids concentration by refractometry. The other section was placed cut-surface down in a 20×20 mm cell of a 25-cell clear plastic tray. Each cell contained 750 µL of 0.1% NBT freshly prepared from 1% stock solution and adjusted to within ±0.5°Brix of the sectioned berry using a concentrated sucrose solution. To prevent evaporation, the staining solution in each cell was covered with a thin layer of paraffin oil. The plastic tray was placed in front of a 30 W lamp, shielded by a water-filled glass brick, for approximately 20 h. Stained specimens were hand re-sectioned longitudinally approximately 2 mm below the cut surface, and placed on a microscope slide for observation. The proportion of blue-stained regions, as a percentage of the cut surface area, was estimated from digital photographs using image analysis software (ENVI vs 4.4, ITT Visual Information Solutions, Boulder, Colorado, USA) and confirmed by inspection under a dissecting microscope (Leica MZ8, Heerbrugg, Switzerland).

In January 2009, we examined the route and rate of water uptake through the skin and the pedicels associated with splitting. Berries were sampled from potted, outdoor-grown plants 6 and 20 days after the onset of ripening. On each occasion, 20 berries were sampled; ten berries were immersed in deionised water as in Experiment 2, and ten were cut through the pedicel, which was then end-coated in RTV (room temperature vulcanising) silicon rubber sealant before immersion. All berries were monitored for water uptake as described for Experiment 2. The mean flow rate of water through the pedicel was calculated algebraically from the difference in the flow rate through the sealed and non-sealed berries. The statistical uncertainty was calculated by propagating errors algebraically (Taylor 1982).

Statistical analyses

All statistical analyses for experiments 3.5.10–3.5.14 were performed in JMP IN Ver. 8.0.2 (SAS Institute, Cary, North Carolina, USA). Statistical effects and interactions were tested (=0.05) using a full factorial linear least-squares or nominal logistic model.

Results and discussion

High rainfall events after the onset of ripening commonly cause the skin of grape berries to split (also known as fruit rupture or cracking), and lead to fruit losses through desiccation and/or microbial spoilage. Splitting may occur when swollen berries become tightly adpressed and exert pressure on each other. In the absence of such pressure, splitting is also induced when the rate of water uptake by the berry exceeds water lost through transpiration or backflow to the plant, and the turgor pressure within the berry exceeds the strength of the skin, or more specifically, the cuticle (Considine 1982, Lang and Thorpe 1988, Lang and Düring 1990). The incidence of splitting in both circumstances is driven by osmotic water uptake by pericarp cells and varies considerably between cultivars, between and within bunches and from vineyard site to site. In 2003, unseasonal mid-summer rain across much of southeastern Australia caused widespread splitting of late ripening grape cultivars (e.g. Cabernet Sauvignon, Shiraz, Riesling), while berries of early ripening cultivars, most notably, Chardonnay, generally remained intact (W. J. Hardie, personal observation). These rains occurred before the late ripening cultivars had reached 100 days after anthesis, whereas Chardonnay exceeded that age. Normally, by that developmental age, cells of the grape endocarp have degenerated (Hardie *et al*. 1996), and degeneration of cells of the mesocarp has advanced significantly (Krasnow *et al*. 2008, Tilbrook and Tyerman 2008). These observations indicated a point in berry development beyond which, due to the loss of integrity of cell membranes, little turgor-induced splitting might occur. The possibility of developmentally dependent susceptibility to splitting was first raised by El-Zeftawi and Weste (1972), after El-Zeftawi (1971) found that Zante berries, in which development had been delayed with the application of hormonal treatments (gibberellic acid plus p-chlorophenoxyacetic acid), were more susceptible to rain damage than those left untreated.

Accordingly, we tested the hypothesis that grape berries become less susceptible to turgor-induced splitting during ripening due to loss of cell vitality. In particular, we sought insights to enable better prediction of susceptibility to splitting as a basis of preventative actions, such as cane cutting, irrigation management and pre-emptive, anti-spoilage, chemical applications.

The effect of bunch age and berry ripeness on berry osmotic capacity

At the first sampling of vineyard berries, the range of most common soluble solids concentrations (95% confidence limit) was 16.3–20.6°Brix. At subsequent samplings over the following month the ranges were 21.1–24.9, 18.7–22.3 and 19.5–23.2°Brix, respectively. The samples were taken at 16, 32, 43 and 50 DOR.

Figure 3.81a–d show the number of berries that split when berries, sampled from bunches of different age (DOR) and subsampled according to ripeness (based on soluble solids concentration), were immersed in solutions of different osmotic potential.

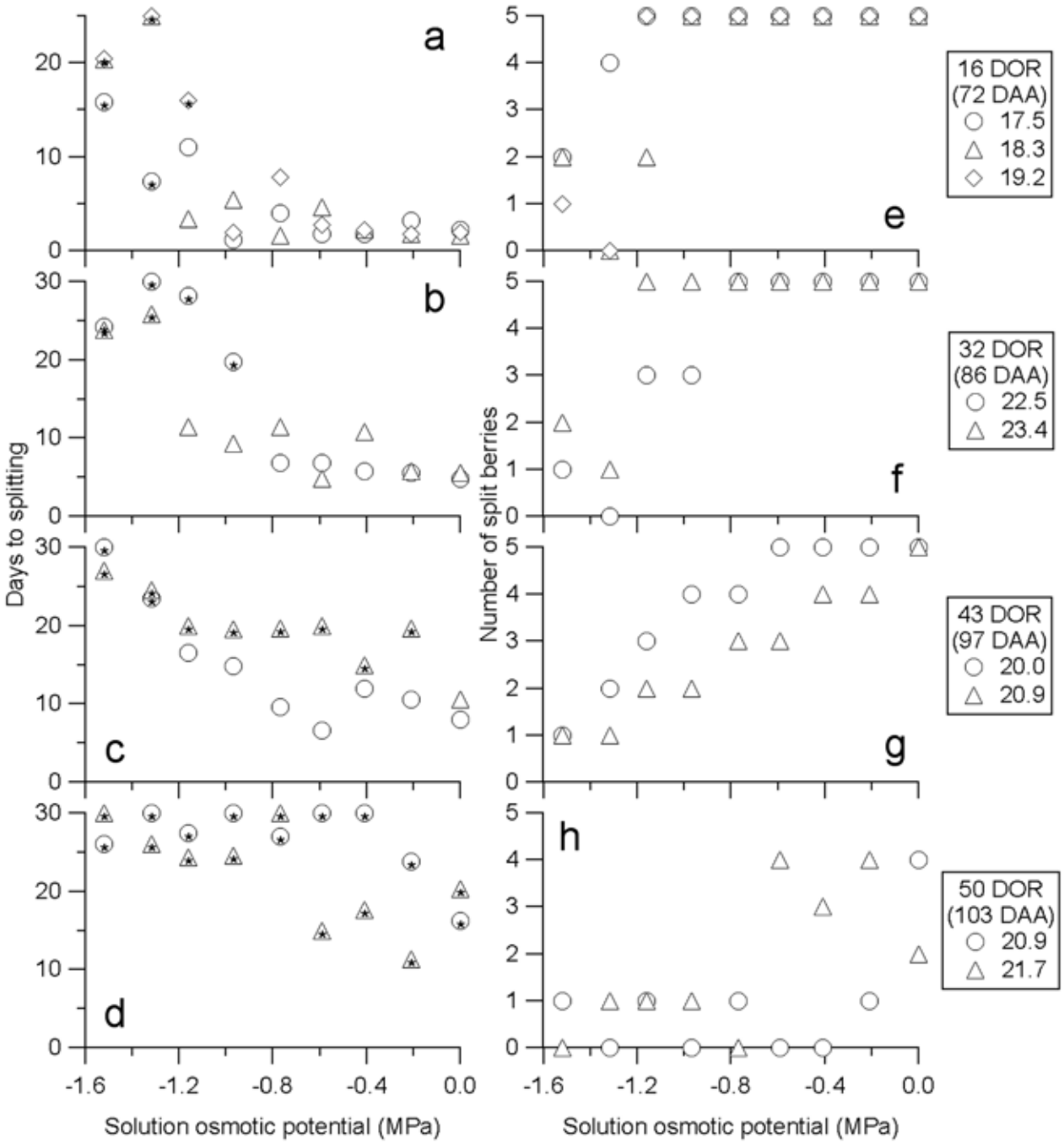


Figure 3.81 Susceptibility to splitting of vineyard-grown Shiraz berries at different ripening stages shown as the number of berries that split (a–d) and the average number of days taken for berries to split (e–h) with respect to the osmotic potential of the sucrose solution in which they were immersed. The number of days of ripening that have elapsed (DOR), the number of days after anthesis (DAA), berry soluble solids concentration (°Brix), and equivalent osmotic potential (MPa) are indicated to the right of each pair of graphs. Shaded symbols in (e–h) indicate that at least one berry in the group had not split at the end of the observation period. In graphs (e–h), each data point represents the average of five berries with the same estimated soluble solids concentration. Observations for the first sample were terminated after 25 days, and those of subsequent samples were terminated after 30 days.

Figure 3.81e–h show the average number of days elapsed before splitting occurred in these conditions. In these figures, the osmotic potential of the sucrose solutions and berries were calculated from the van't Hoff equation and calibration equation associated with *Figure 3.81* of Considine and Kriedemann (1972), respectively.

Whether or not a berry split within the observation period and the number of days it took for a berry to split, for each sampling event and soluble solids combination presented in *Figure 3.81e–h*, were statistically analysed (at the berry level) to identify the effects of (i) the number of days from the onset of ripening (DOR), (ii) berry soluble solids, (iii) the osmotic potential of the immersion solutions, and (iv) interactions between these factors. The osmotic potential of the immersion solution and DOR were significant determinants of whether or not a berry split ($P<0.0001$), and DOR also had a significant effect on the number of days that elapsed before splitting occurred ($P<0.0001$). The interaction between the osmotic potential of the solution and DOR had significant effects on whether a berry split ($P<0.0001$) and the number of days for splitting to occur ($P=0.03$). Generally, as bunches aged, the number of berries that split decreased (*Figure 3.81a–d*), and the time to split increased (*Figure 3.81e–h*), and splitting was more common and rapid in solutions of less negative osmotic potential. Berry soluble solids concentration had a significant effect on the number of days that elapsed before splitting occurred ($P=0.04$), as did the interaction between soluble solids concentration and the osmotic potential of the immersion solution ($P=0.0006$). No other significant interactions were observed. Overall, there was not a strong relationship between soluble solids concentration and susceptibility to splitting principally because changes in soluble solids concentration after 30 days from the onset of ripening were small (*Figure 3.81*). These observations are indicative of osmotic competence within the berry, and are consistent with a progressive loss in osmotic competence and turgor-generating capacity within the berry despite any ongoing sugar accumulation within pericarp cells.

Developmental trends in susceptibility to splitting during ripening

The developmental trend in the susceptibility of glasshouse-grown berries to splitting when immersed in deionised water (maximal osmotic gradients for water transport into the berry) was similar to that observed in the vineyard-grown berries (*Figure 3.82a*). From the onset of bunch ripening until approximately 32 DOR, berries split after six or less days of immersion. Thereafter, the number of days until splitting increased until about 55 DOR, when most berries failed to split and any splitting took place after more than six days of immersion. Visible berry shrivel first occurred at about 40 DOR when mean berry soluble solids concentration was approximately 22°Brix (*Figure 3.82b*). It follows that prior to this point some berries attained their maximum fresh weight. This is evident in *Figure 3.82c*, where data on berry fresh and dry weight is presented. Fresh weight per berry reached a maximum at about 25 DOR, and a minimum at about 55 DOR. Dry weight per berry also reached a maximum 25 DOR and remained approximately constant thereafter. Statistical analysis (at the vine level) of the effects of DOR, soluble solids concentration and vital staining on the average number of days until splitting indicated that DOR ($P=0.02$) and its interaction with vital staining ($P=0.02$) were significant. No other significant effects or interactions were observed. In a similar analysis of these effects on the number of berries that split, only the area of vital cells exhibited a significant effect ($P=0.002$).

Developmental trends in cell vitality during ripening

In a preliminary test, ripening Shiraz berries (20°Brix, n=7) were halved transversely, and one half was frozen by placing it on a metal block cooled with liquid nitrogen. No staining was observed in the treated halves, and partial staining, consistent with our more complete dataset for glasshouse berries, was observed in the controls. As freezing is a means of disrupting membrane integrity (Krasnow *et al.* 2008), this observation validated our use of NBT as a vital stain for ripening grapes.

NBT staining revealed extensive regions of vital pericarp cells (from 100 to approximately 70% of cross-sectional area) during much of the ripening period (0 40 DOR) (*Figure 3.82b*). An example of a fresh berry cross-section stained with NBT is presented in *Figure 3.83a*. *Figure 3.83b* provides a higher magnification view of NBT stained cells near a peripheral vascular bundle. Vital (stained) mesocarp cells are clearly distinguishable from those that are not. The image demonstrates that NBT staining occurs in the cytoplasm, which in ripening grape pericarp cells generally forms a thin, peripheral band. As ripening progressed cells at the stylar end of berries where the central vascular strands branch,

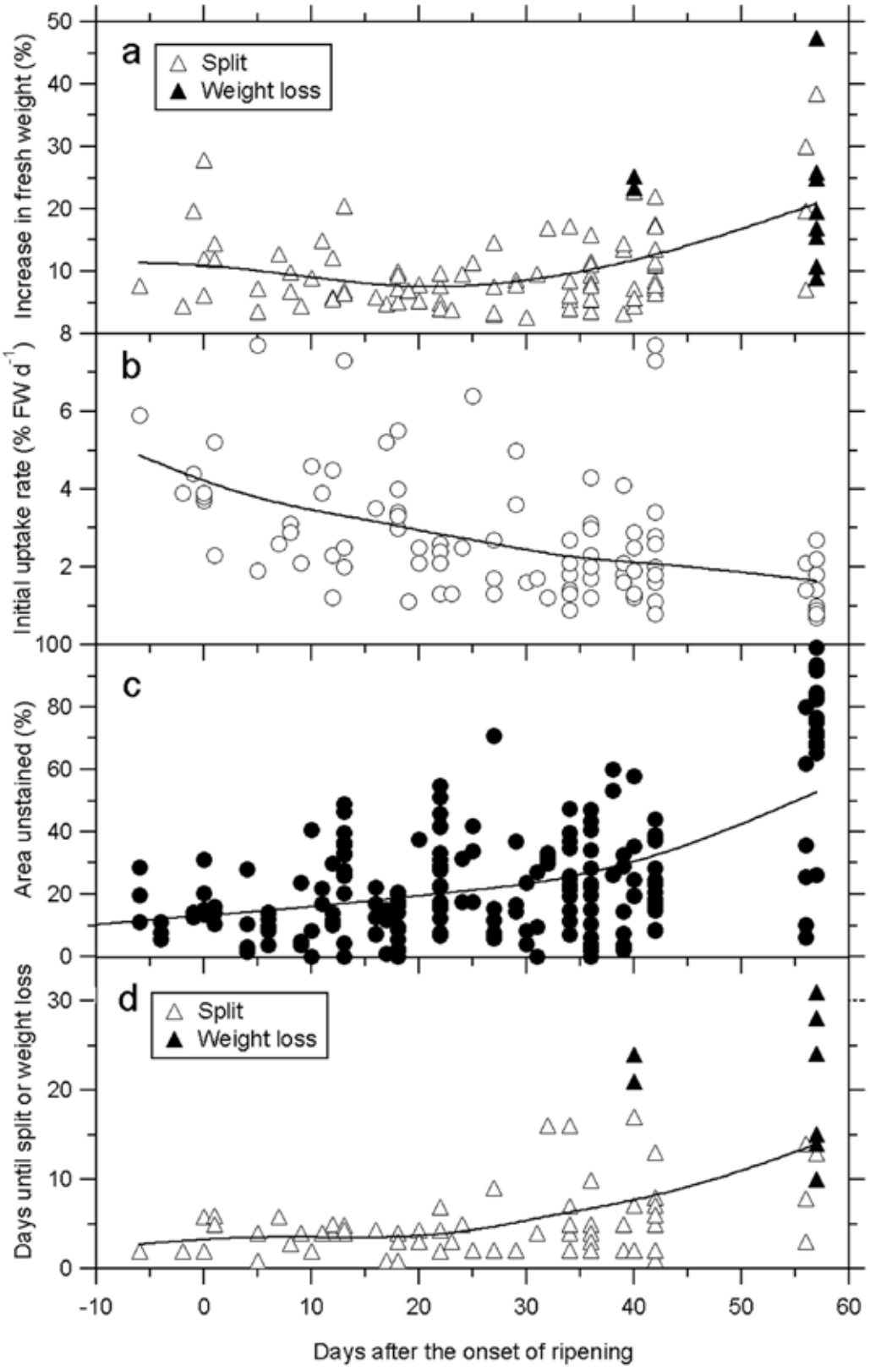


Figure 3.82 Changes in the susceptibility to splitting, soluble solids concentration, cell vitality, berry weight and water uptake during ripening of glasshouse-grown Shiraz grape berries. Berries were detached and immersed in deionised water. Shown are the relationships between days after the onset of ripening and (a) susceptibility of berries immersed in deionised water to splitting expressed as the number of days until splitting or the day at which berry weight ceased to increase, as well as the number of berries that split, (b) soluble solids concentration and loss of cell vitality expressed as the percentage of the area of fresh berry cross-sections not stained with nitroblue tetrazolium, (c) berry fresh and dry weight, and (d) the amount of water taken up at the time of splitting, and the water uptake rate over the first 24 h of immersion expressed as the increase in fresh weight relative to berry dry weight. Each data point represents the mean of berries sampled that week, and the uncertainty bars indicate standard error.

cells near the central vascular strands and those in a small region adjacent to the brush increasingly failed to stain. Subsequently, these unstained regions tended to enlarge and aggregate so that by the time berry shrivel became evident, only remnant areas of vital cells (0–35%) remained (*Figure 3.82b*, >40 DOR). In those berries, staining was mostly confined to cells adjacent to the major peripheral bundles.

Developmental trends in berry water uptake during ripening

Berries sampled from the glasshouse-grown plants all increased in weight when immersed in deionised water (*Figure 3.82d*). Among berries that split, the weight gained up until the time of splitting was typically about 100 µL berry^{-1}. Volumes of 200 µL berry^{-1} or greater were generally not observed until 40 DOR or more (*Figure 3.82d*). A Student's t-test indicated that the mean maximum volume of water absorbed by individual berries that did not split was not significantly different from the mean volume of water absorbed by other berries at the time of splitting.

There was a decline in the rate at which immersed berries absorbed water (over the initial 24 h of observation, expressed relative to dry weight) as bunches developed (*Figure 3.82d*). When immersed in water, berries that were sampled soon after the onset of ripening exhibited initial uptake rates of approximately 35 mL day^{-1} g^{-1}. From this point, the rate of uptake gradually decreased, reaching approximately 10 mL day^{-1} g^{-1} between 30 and 40 DOR, and remained low through to the final observations.

A negative relationship was found between the reciprocal of the initial water uptake rate and the number of days until splitting – the slower a berry increased in weight when immersed in water, the longer it took to split, especially when the uptake rate was less than 15 mL day^{-1} g^{-1} (*Figure 3.84a*). A parabolic curve was used to model the relationship between the total amount of water taken up at the time of splitting and the number of days until splitting so that the x-axis intercept was positive to reflect the expectation that water uptake is necessary to induce splitting (*Figure 3.84b*). The longer a berry was immersed in deionised water, the more water it absorbed up to a maximum of about 0.5 mL berry^{-1}. As expected from the trends in *Figure 3.84*, linear-least squares modelling indicated that the initial uptake rate ($P<0.0002$) and amount of water absorbed ($P=0.01$) had significant effects on the number of days until splitting, as did the interaction between the amount of water absorbed and DOR ($P=0.002$). Other interactions were not significant.

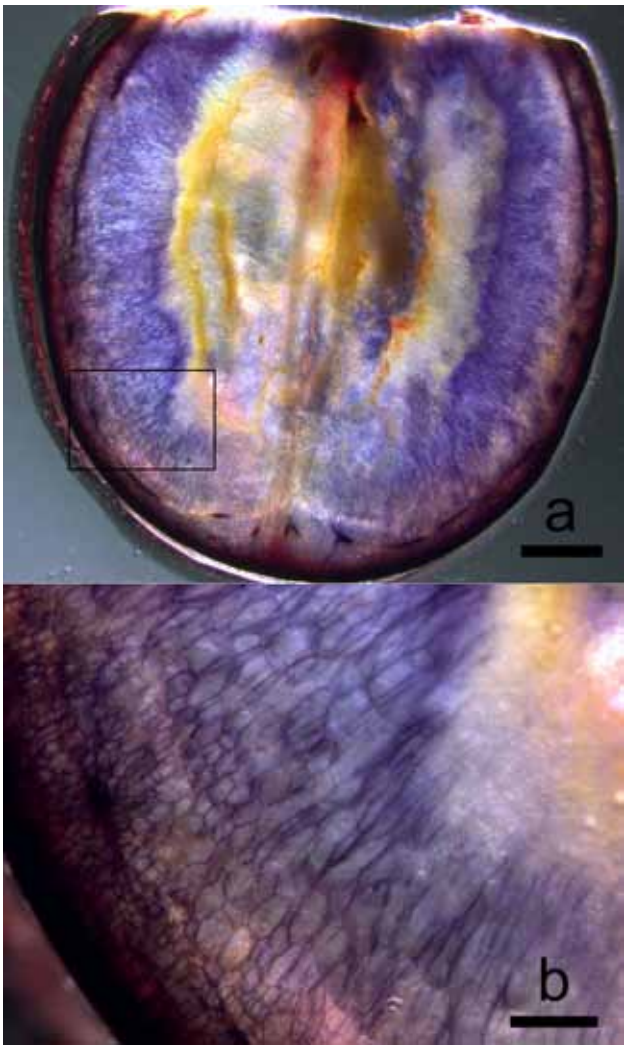


Figure 3.83 An example of nitroblue tetrazolium (NBT) vital staining on a glasshouse-grown Shiraz berry cross-section (a). In panel (b), the region of interest identified in panel (a) is shown. The scale bar length in panels (a) and (b) is 2 and 0.5 mm, respectively. The berry was sampled 74 days after anthesis, 21 days after the onset of ripening and had a soluble solids concentration of 24.2°Brix. Images were obtained using a Leica stereomicroscope (MZ16FA).

Berry water uptake pathways

The mean flow rate of water (expressed relative to fresh weight at the time of sampling) through the berry surface and pedicel combined decreased significantly between 6 and 20 DOR from 6–2.5 day^{-1}. The flow rate of water through the pedicel also decreased across this period (3.0 to 0.9% day^{-1}), as did the flow rate through the skin (2.9 to 1.7% day^{-1}). From the standard error associated with these values (*Table 3.11*), it is inferred that the decrease in flow is likely to be statistically significant for each of these three pathways.

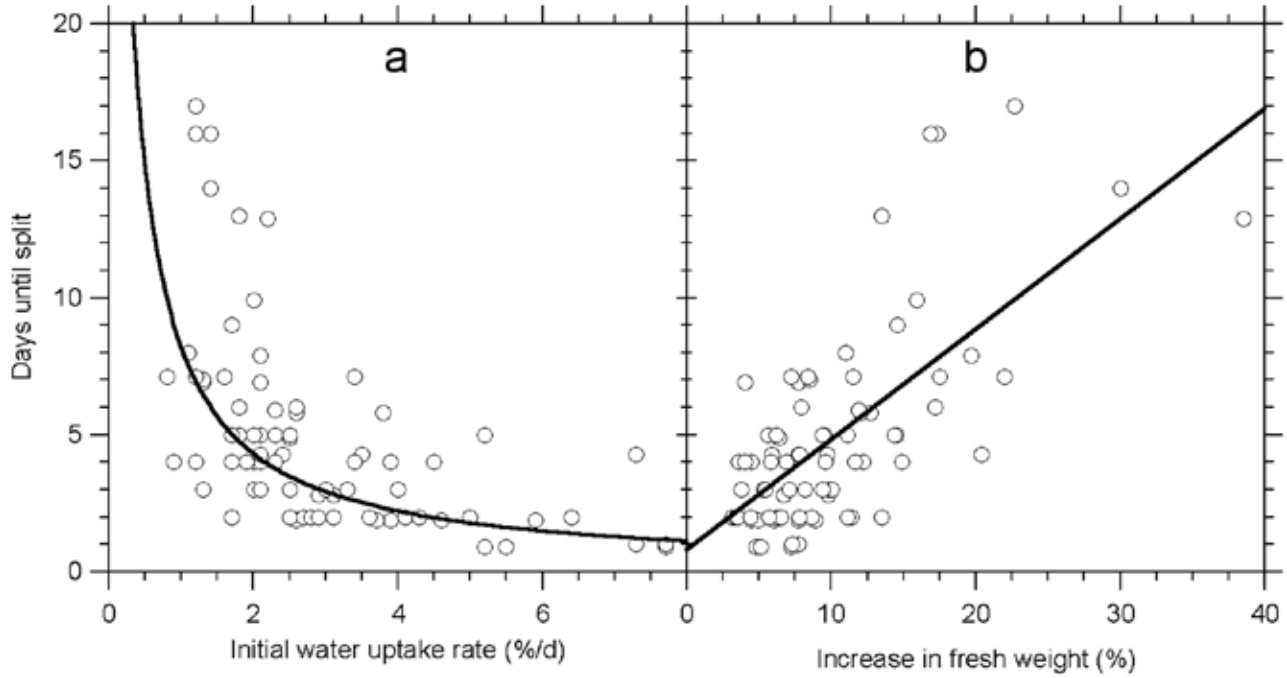


Figure 3.84 Relationships between the days required for glasshouse-grown Shiraz berries immersed in deionised water to split, and (a) the initial rate of water absorption and (b) the increase in berry water content between immersion and splitting. The curvilinear fit in panel (a) is d = 2.0 + 33.7/a, where d=days until splitting and a is the initial rate of water absorption expressed as the amount of water absorbed over the initial 24 h of immersion relative to berry dry weight (mL/day/g). The parabolic fit in panel (b) is $d^2 = -16.7 + 380$ w, where w = the increase in water content calculated from the difference between the fresh weight at the time of sampling and fresh weight at the time of splitting. The r^2 values of these fits are 0.24 and 0.41, respectively. The intercept and slope of each fit is significantly different from zero.

Table 3.11 Initial water uptake rate of Shiraz berries, sampled 6 and 20 days after the onset of ripening, via different uptake pathways.

Days after the onset of ripening	Initial uptake rate (%)		
	Pedicel plus skin	Pedicel	Skin
6	6.0 ± 0.5	3.1 ± 0.6	2.9 ± 0.3
20	2.6 ± 0.2	0.9 ± 0.3	1.7 ± 0.2

The initial uptake rate is expressed as the percentage increase in fresh weight over the first 24 h of immersion in deionised water. The uncertainty terms indicate the standard error.

Discussion

Although previous models of splitting of grape berries (e.g. Considine and Kriedemann 1972, Yamamura and Naito 1985, Lang and Thorpe 1988) have recognised osmotically induced turgor as the driving factor, those models consider the whole berry, enclosed in a semi-permeable skin, as the osmotically functional system. In contrast, the turgor of the whole berry may be more appropriately regarded as the result of the collective osmotic capacity of vital pericarp cells. And thus, as we have shown, loss of osmotic competence that accompanies degeneration of cells within the pericarp during ripening is associated with a large decrease in the susceptibility of grapes to splitting after about 50–55 days from the onset of ripening. From this perspective, exposure of grapevines to rain induces splitting by diluting the concentration of solutes in the apoplast. Diffusion of water through the berry skin, which establishes a hydraulic connection between the apoplasm of the berry and water droplets on the berry surface, would normally contribute to this. Entry of water into the berry renders the osmotic potential of the apoplasm less negative, thus enhancing existing gradients in osmotic potential between the apoplasm and symplasm. Resultant water transport across the cell membrane into the cytoplasm and in turn, across the vacuolar membrane to the vacuole (Tyerman *et al.* 1999), increases the turgor of osmotically functional cells. Splitting occurs when pressure exerted, presumably by the relatively thin, elastic-walled, sugar-rich, parenchymatous cells of the mesocarp onto the thick, less elastic-walled epidermal cells, strains the cuticle beyond its plastic limit, to the point of failure.

Splitting of detached berries following immersion in hypotonic solutions almost certainly follows a similar course to rain-induced splitting, except that hydraulic connection via the xylem of the pedicel

is unlikely to exist until turgor pressure forces the apoplasmic solution to re-fill vessels that filled with air upon release of any tension in the xylem stream at the time of severance. However, even in these circumstances, a pathway of relatively low water conductivity may exist via the parenchyma cells of the pedicel. This perspective accords with the observations of Matthews and Shackel (2005), who reported an increase in the fresh weight and cell turgor of detached pre- and post-veraison berries immersed in tap water for 24 h.

Berry immersion is not a suitable system for quantifying the actual osmotic conditions at which cuticular failure occurs in vivo. This is because flow of apoplasmic solution from the berry in response to increasing turgor within vital pericarp cells is unimpeded by capacitance limits and resistances (e.g. water vapour loss via cuticular and stomatal conductance) within the plant that in vivo (particularly at night and during the wet and low vapour-pressure deficit conditions associated with rain events) limit turgor-mitigating water outflow from the berry and promote splitting. Thus, in vivo, the critical level of turgor within the total plant system at which splitting occurs may be generated at higher (less negative) levels of symplasmic osmotic potential or at a smaller osmotic gradient between the symplasm and the apoplasm than in severed berries. However, such limitations do not affect the suitability of the technique as a means of assessing relative differences in susceptibility to splitting (Considine and Kriedemann 1972).

This study reveals that in the grape cultivar 'Shiraz', susceptibility to splitting, based on the time required for splitting to occur and the number of berries that split after immersion in hypotonic solutions, remains consistently high from the onset of ripening until about 30 days later, and thereafter diminishes greatly. Our unpublished observations of berry splitting in potted Shiraz plants confirm the general applicability of our findings in planta. Under conditions of low vapour pressure deficit (0.8 kPa; 20°C, 65% relative humidity) imposed by a controlled environment chamber, and with wet leaf canopies and bunches, berries from bunches up to 35 DOR split readily. Beyond this stage, a small amount of splitting was confined to compact bunches (>0.2 berries cm^{-3}) where intra-bunch adpression of swollen berries became the causative factor.

The transition in susceptibility to splitting is attributed to an overall decrease in the turgor-generating capacity of the population of cells within the berry as it develops, as inferred from the diminishing effect of solutions of lower osmotic potential. Loss of turgor-generating capacity, despite an increase in the soluble solids concentration of berries, coincided with loss of cell vitality, as determined by vital staining and is attributed principally to that source, although putative increases in osmotic adjustment (Wada *et al*. 2008) may also mitigate to some extent against generation of turgor. It has been shown previously (Tyerman *et al*. 2004), with both cvs. Shiraz and Chardonnay, that berry hydraulic conductance generally decreases during ripening, a result in agreement with the decline in the initial water uptake rates via the pedicel and skin of Shiraz berries observed here. Thus, it is possible that increases in the resistance of water absorption pathways during ripening may also contribute to a progressive decline in the susceptibility of berries to splitting.

Increased capacitance within the berry created by prior shrinkage due to water loss is another factor that may have contributed to the decreased susceptibility to splitting. Increased capacitance over the course of ripening could also be the result of a developmental increase in the ability of the berry cuticle to extend when subjected to stress by an increase in water content. We note, however, that Lustig and Bernstein (1985) found that the strain at the burst point of ripe Dattier berries was less than that of Dattier berries sampled 42 days earlier, soon after the onset of ripening, suggesting that the cuticle had become more susceptible to splitting. In our experiment on glasshouse-grown berries, increased capacitance is evident in the increased volume of water absorbed by berries at the time of splitting. For the berries in this experiment, shrivel was obvious 40 days after the onset of ripening, but may have occurred imperceptibly before that. For example, after 25 DOR, there is an overall decline in berry fresh weight, whereas berry dry weight remains approximately constant. It is therefore possible that imperceptible shrinkage may have increased berry capacitance soon after 25 DOR, immediately preceding the decline in the susceptibility of berries to splitting. A positive correlation between berry hydration and susceptibility to splitting is intuitive, because berry shrinkage and enlargement are expected to be dependent on the proportion of osmotically functional, turgor-inducing pericarp cells. However, increased capacitance alone cannot account for decreased susceptibility to splitting

because even after prolonged immersion and rehydration, many berries did not split.

The response of berries from glasshouse vines sampled at the end of the experiment to immersion was distinct from that of berries sampled in the early stages of ripening (<30 DOR). In particular, berries sampled approximately 40 and 55 DOR exhibited an atypical temporary increase in weight prior to a sustained weight loss (i.e. they were not susceptible to splitting under the imposed treatment). This may have been due to initial diffusion of water into the berry and/or osmotic uptake of water by remnant vital cells. The subsequent decrease in fresh weight is likely to have been due to outward diffusion of solutes and accompanying outflow of water. Another atypical trend late in ripening was an increase in between-berry variability in the number of days of immersion required to produce splitting and the number of split berries. Vital staining and response to immersion in dilute sucrose solutions leads us to suggest that this variability was due to the presence of a small number of berries that retained, for at least as long as 50 DOR, a sufficient proportion of osmotically-competent cells to induce splitting. Despite these contrasts in cell vitality and susceptibility to splitting, all berries sampled at the end of the experiment on glasshouse-grown berries exhibited relatively low initial uptake rates, a trend that is likely to be the result of the decline in the number of vital cells and the concomitant increase in apoplasm volume relative to symplasm volume. Due to the relative increase in apoplasm volume, more water must enter the berry upon the immersion treatment to effect a change in the osmotic gradient between the apoplasm and symplasm.

This research has important implications for understanding the susceptibility of grapes to splitting in vineyard contexts. Our results accord with the field observations that prompted this study insofar as they show that susceptibility of seeded cultivars to splitting is greatly diminished about 100 DAA. Consequently, all other factors being equal, early ripening cultivars are expected to become less susceptible to splitting before later ripening ones. Importantly, our study indicated that bunch age (days after the onset of ripening) is a more reliable indicator of susceptibility to splitting than berry ripeness *per se*, as determined by soluble solids concentration. While both cell degeneration and soluble solids concentration increase with berry age, cell degeneration directly diminishes turgor-generating capacity whereas soluble solids concentration, as measured on whole berry extracts, includes apoplasmic and symplasmic solutes, both of similar concentration from the onset of ripening (Wada *et al*. 2008), and is not directly related to the number of osmotically competent, and hence turgor-generating cells.

Previous studies (Hardie *et al*. 1996, Krasnow *et al*. 2008, Tilbrook and Tyerman 2008), involving a number of different cultivars, have shown that cell degeneration is a general feature of grape ripening. Hardie *et al*. (1996) showed by light microscopy that commencement of degeneration occurs in the endocarp from the inception of ripening. This may be associated with the switch from symplasmic to apoplasmic phloem unloading (Zhang *et al*. 2006), at the onset of ripening, contemporaneous increases in sugars (Brown and Coombe 1985) and decreases in solute potential (Lang and Düring 1991, Wada *et al*. 2008) within the berry apoplasm. The commencement of degeneration of mesocarp cells is not well characterised. Visual evidence of degeneration of those cells presented here and previously (viz. Krasnow *et al*. 2008, Tilbrook and Tyerman 2008), relies on vital staining and pixel analyses at relatively low magnification, and does not allow fine resolution at the cellular level. However, present evidence suggests that after about 30 DOR degeneration of mesocarp cells is generally advanced enough to cause sufficient loss of osmotic capacity to render berries susceptible to water loss (fresh weight loss) and less susceptible to splitting.

Finally, we expect that results obtained with Shiraz will generally apply to seeded grape varieties. We note that Tilbrook and Tyerman (2008) found that late in ripening, cell death in Thompson Seedless, a stenospermocarpic cultivar, did not proceed to the same extent as in seeded cultivars. This cultivar and the parthenocarpic Zante are highly susceptible to splitting, Also, during the rain event that prompted our study, at one site, where the late ripening, seeded variety Sangiovese had an exceptionally high proportion of seedless berries, it was generally only those berries that split (W. J. Hardie personal observation). These observations, together with the coincidence in initiation of cell degeneration in the inner epidermis that surrounds the normally seed-bearing locules and the germinability of seeds at the onset of ripening (Hardie *et al*. 1996), indicate to us that seed development may play a significant role in the inception of degeneration of pericarp cells that enclose them.

Outcomes/conclusions

The changes in nutrient and carbohydrate reserves over the growing season are important for vine growth and development. For grapevines, root and wood reserves are particularly required for early canopy development. We have demonstrated that soil conditions, especially water and soil temperatures, impact on mobilising these reserves for translocation to the aerial parts of vines (Field *et al*. 2009). Several studies have been undertaken in this stream to enhance the knowledge on root dynamics in relation to nutrient uptake and vine carbohydrates.

We assessed the seasonal changes in grapevine partitioning, which was the first study on wine grapes under Australian conditions that determined the carbohydrate and nitrogen dynamics together with the other macro nutrients over an entire growing season. We found that most of the carbohydrate and N reserves are located in the medium to large roots with partitioning of winter reserves below and above ground 75:25 for carbohydrates (Holzapfel *et al*. 2010) and 65:35 for N. The carbohydrate reserves are at their lowest at bloom and highest at DORmancy, with the highest amount on a whole vine basis accumulated at harvest. The most dominant uptake period for N was several weeks prior to bloom and also before veraison, another period of significant uptake was present after harvest. The information on the nutrient accumulation and translocation in the perennial and annual section of the vine is crucial for the understanding of the seasonal nutrient requirements at different stages of vines.

Rootstocks influence vine productivity and the N status of the scion (Holzapfel and Treeby 2007), in this study we were investigating the root dynamics of own rooted Shiraz and Shiraz grafted onto three rootstocks (Ramsey, Schwarzmann and Ruggeri 140). Root activity (total length of white roots) determined using a minirhizotron system was found to be highest at bud-burst to flowering, with the trend not very pronounced in the following two seasons. In the first two seasons a distinct difference in root activity occurred between rootstocks, with Ruggeri 140 the highest and Ramsey showing the lowest activity. It was found that the carbohydrate concentration was often higher in the roots compared to the above ground wood and N concentration was always higher in the roots as compared with the wood. Differences were found between the rootstocks in root carbohydrate and N content and changes during the season. N concentrations declined from bus-burst to harvest, while wood concentrations remained largely unchanged. The carbohydrate concentrations in the root and wood tissue were generally lowest at flowering. At the beginning of the season the lowest carbohydrate concentrations were observed in Ramsey and highest in own root Shiraz, this pattern being generally consistent at other key stages. In contrast, the N reserves at bud-burst were only low in own rooted Shiraz in the first season, and highest in Ramsey and Ruggeri 140. This indicates that rootstocks have a different capacity to supply the early growth with nutrients and carbohydrates, when production of assimilates and uptake of nutrients is low.

Vine management impacts on carbohydrate and N reserves in the perennial structure (Holzapfel and Smith 2011*a*, *b*). This field trial on Shiraz was undertaken to determine the influence of carbohydrate (by leaf removal prior flowering), water and N supply on reserve levels in the root and wood tissues seasonal and seasonal root activity. Root N and carbohydrate concentrations were also higher in the roots compared to the wood, commonly about four times and two times higher respectively. Wood and root carbohydrate levels were generally lowest at flowering. The seasonal changes of N concentration between seasons in the roots were mostly high early in the season and lower towards the end, while seasonal changes in N levels in the wood were inconsistent between seasons. N levels were elevated by the N applications in the roots, while early leaf removal lowered the carbohydrates concentrations in the roots and also in the wood in the last season. Water stress implemented after veraison resulted frequently in reduction of root carbohydrate levels. Despite altered carbohydrate and N reserves in the perennial structure, the treatment effect on root activity was relatively low. The lack of response from the treatments on root dynamics is not clear; however it is likely that the impact of the irrigation treatments was reduced due to seasonal conditions. Overall the work shows the importance of the supply of N and carbohydrate production on the reserves in the perennial structure within a season and between seasons.

N accumulation in the berry is affected by water and N supply (Holzapfel *et al*. 2008), which is important for the fermentation process and the wine produced from the grapes. A pot trial was undertaken to gain a better understanding of the influence of timing of N application under different water regimes. The

five year old Chardonnay vines were supplied with nitrogen (containing 10% of the isotope ^{15}N) during berry development from flowering to harvest. Six groups of eight vines received nitrogen at different times, half in each group received full and the other half the irrigation water. The amount of irrigation water applied and the timing of N application influenced shoot growth, with the impact on berry weights less pronounced. The leaf chlorophyll index was lower in the fully irrigated vines; the timing of N was reflected in the chlorophyll index measured during the period from bloom to harvest. Although the berry ^{15}N content has not been determined at this point of time it appears that N uptakes occur after each application indicated by the chlorophyll index of the leaves during berry growth and maturation. This suggests that fruit N could be elevated later in the season though N application if required, with less impact on acceleration of shoot growth.

The information from several aspects of the project will assist in the development of vineyard management strategies to optimise vine nutrient utilisation for long-term vine performance. The knowledge of the seasonal N reserve dynamics gives better understanding in uptake requirements of vines prior to and during a season. The observed differences in reserves are important findings, giving a better understanding of rootstock and vineyard management on vine scion nutrient status and productivity. In addition, the work will contribute to enhance the timing of N for berry composition and final wine production.

Heat events occur regularly in the Riverina and elsewhere but sustained heat events of five or more sequential days where the temperatures exceed 40°C are uncommon, occurring only twice in the past decade. Therefore, the 14-day heat event in the summer of 2009 was a unique and extreme event that provided such an excellent opportunity to test the hypothesis that heat prevents berries from ripening. The results of the studies show conclusively, both from controlled environment studies and during natural heat events, that indeed sugar accumulation is retarded. Further than that, the potted experiment in the controlled environments was crucial to a wide understanding of heat effects because the sensitivity of the different stages of reproduction to heat were demonstrated. Although the flowering stage was not part of the original objective, the knowledge that this stage is especially sensitive to heat is important because such events do and have occurred at this time (November 2009, Burgess W. pers. comm.) and have had serious consequences for growers. Such knowledge is, therefore, of practical benefit to growers because it facilitates the need to protect the vines during this crucial developmental stage. How to do this is still need to be investigated.

The results of the studies have also revealed that although the sugar ripening process was affected by heat, it was also ascertained that the sugar loading process was not the target of the high temperature stress. In fact, the retarding of berry ripening was an outcome of the carbon balance being perturbed by the heat. Thus, it was the leaf gas exchange processes that incurred the direct impact of the heat event, notably by a stomatal conductance-induced reduction in photosynthesis, at least as shown in the controlled environment study. The field studies provided clear support for the conclusion that heat impacted on the photosynthetic process although the mechanism was different. During the 2009 heat event, photosynthesis was reduced markedly but this was not induced by a stomatal limitation in this case, it was because conductance increased at the same time. This suggests a non-stomatal limitation was affected the photosynthesis process during the heat event. This might include the CO_2 carboxylation process or the regeneration of the substrate Ribulose 1, 5-Bisphosphate, both of which can limit photosynthesis. In fact, the detailed photosynthetic temperature responses outlined above indicated that both these two process co-limited photosynthesis at temperatures above 35°C. Unfortunately no temperature responses were measured during the actual heat event to assess the impact on these processes.

However, these results do have implications for growers as the conclusion that it is the carbon supply process in the leaves that is affected by heat rather than the carbon delivery or loading into the bunch processes that will determine the need for protection. This means that there is less need to protect the bunches compared to the need to protect the leaves. An important distinction must be made, however, about convective heat events where the mass air is heated up such as occurred in the summer 2009 heat event with radiative heat events occurring with bright sun exposure. Warm air is pervasive and will influence all parts of the vine equally through sensible heat gain (see the reduction in photosynthesis in shaded vines). Heat gain will also occur with a high radiant sunlight load but this is not pervasive and there will

be gradients in temperature around the vine through localised shading. However, this radiant heat load did have an extremely marked affect on the exposed vines, especially on the western side, causing a very high incidence of sunburn, shrivel and other berry damage (see *Figure 3.58*) and hence a marked loss in berry quality. Protection from the radiant heating by shade reduced the incidence of this damage.

But this is quite a different impact from the heat-induced retarding of berry ripening discussed above, because there are no visible affects on the berries in this latter case. It was clear from the studies over the three seasons, that this radiant heat load effect interacted strongly with the ambient air temperatures to cause damage. No incidence of damage was noted in the 2006–07 or 2007–08 seasons where heat events were low or absent and a very high incidence of berry damage occurred in concert with the heat event. Clearly, canopy management to keep the bunches well protected by the leaves will protect them when ambient air temperatures interact with the heat event to bring about sunburn and related berry damage. Protection from the heat alone during a high temperature event will require ways to actively reduce the canopy temperature as the principal means by the vine, latent heat loss by transpiration, was shown to be compromised during the heat event. Our study with hydrocooling has shown this method can effectively reduce canopy temperatures and with the smart control system to minimise water use and prevent diseases is a practical means to achieve this. Such an approach has been commercially adopted at the Bellview Estate, Ellerslie, NSW (Farquhar 2010) and frost protection sprinklers have been turned on during the summer heat events in Coonawarra (Loder H. *pers. comm.*).

The use of shade cover in this project was a means to achieve vines with lower temperatures to compare against the ambient temperatures and assess the hypothesis that high temperatures impede sugar accumulation in the berries. The shade cover intercepted 70% of the incident light and did have negative consequences for the vine performance and, therefore, was not intended to be considered as a practical means to manage canopy temperatures. However, the positive impact the this shade cover on canopy temperatures and berry ripening strongly point to canopy management to get maximum shade as insurance against heat events occurring as a practical solution. Nevertheless, some shading of high value wine grapes may be also practical, as it has been widely adopted in the table grape industry Farquhar 2010).

The question of irrigating vines when forewarned of an impending heat event occurring has been widely canvassed by Webb *et al.* (2008). However, there is a paucity of published research into this question and, therefore, became a focus of our studies. Technical difficulties with managing the water status of the vines has meant that this component of the research has not been successfully executed. A further effort to address this question is currently underway.

One outcome of the research was to develop a model to predict climatic events causing heat stress on bunches. Much of the basic information towards developing a model has been achieved through the different measurements undertaken in the field study. To this goal, a modeller has recently been appointed to the NWGIC and plans to develop a grapevine model encompassing this and other research is well underway.

Technetium scintigraphy

Nuclear medicine imaging is a well-established research tool and has broad applications in both research and clinical studies of human and animal populations. Assessing plant physiology with scintigraphy represents an emerging frontier for quantitative plant physiology and is likely to play an important role in agricultural water management. We have demonstrated that the scintigraphic detection of ^{99m}Tc is a powerful tool for the study of xylem transport because $^{99m}TcO_4^-$ behaves as a xylem nutrient analog and the distribution of the radionuclide is amenable to nondestructive visualization and quantification. Our observations of ^{99m}Tc transport in Ipomoea plants are typical: the patterns of (a) the ^{99m}Tc uptake and accumulation from $^{99m}TcO_4^-$ labelled soil and (b) translocation from $^{99m}TcO_4^-$ labelled leaves are consistent with xylem transport of this radionuclide. In particular, ^{99m}Tc primarily accumulated in fully expanded leaves and was not exported from labelled leaves unless they were shaded or wilted. These observations increase confidence in the use of ^{99m}Tc in the form of TcO_4^- as a radionuclide for tracing vascular solute transport in plants.

Xylem connections between the bunch and leaves

Using membrane-impermeable dye and a gamma ray-emitting membrane-permeable nutrient analogue, this research demonstrates there are extensive xylem connections between the *V. vinifera*

bunch and primary and secondary leaves within the same orthostichy as the bunch. Connections between the bunch and the opposing orthostichy were identified but these were relatively uncommon. Xylem flows are therefore strongly sectorial in the grapevine primary shoot, a constraint equally apparent in previous photoassimilate tracing studies and imposed by the vascular anatomy of the grapevine shoot. The observation of nutrient analogue accumulation in nodes, possibly by transfer cells, suggests to us that xylem-associated cells are important for regulating the supply of xylem solutes to the grapevine bunch, an organ that imports xylem nutrients but has an inherently low transpiration rate. Xylem sap flow to these cells is enhanced by the transpiration of leaves sectorially-linked to the grape bunch. These cells would be particularly effective at enhancing the supply of xylem solutes to the grape bunch if they released such solutes when bunch demand for them is high or when leaf transpiration is low.

Berry oxygen isotope ratios

The berry oxygen isotope research has demonstrated that there are consistent developmental trends in the $\delta^{18}O$ values of berry organic matter and juice across varieties and between seasons. $\delta^{18}O_{OM}$ values are likely to yield information on two processes important to the physiology of the grapevine. First of all, root starch mobilisation potentially yields sucrose with a $\delta^{18}O_{OM}$ value distinct from that of sucrose supplied by leaves. This isotopic contrast makes it possible, through $\delta^{18}O_{OM}$ analysis, to assess the relative contribution of these two carbon sources to developing organs, such as the grape bunch. Secondly, it is highly likely that berry $\delta^{18}O_{OM}$ values effectively integrate leaf gas exchange processes spatially across the leaves that supply photosynthate to the bunch and temporally across the growing season. Berry $\delta^{18}O_{OM}$ values may therefore be an important tool in varietal trials, especially when screening cultivars for suitability to hot, dry environments with low soil moisture. In contrast, due to the sensitivity of berry $\delta^{18}O_J$ to the rate of berry ripening, cultivar differences in $\delta^{18}O_J$ are unlikely to yield primary information on important parameters such as plant water use. Overall, $\delta^{18}O_{OM}$ values have the potential to complement and enhance other methods of assessing grapevine physiology, such as carbohydrate analysis, photosynthesis measurements and carbon isotope assays.

Fruit split

The susceptibility of Shiraz grape berries to splitting decreases markedly after about 30 days of ripening and becomes negligible about 30 days later. The decrease in susceptibility is highly correlated with, and is attributable to, progressive degeneration of pericarp cells, which has the effect of reducing the number of those that remain vital and osmotically competent, thereby preventing the generation of turgor-induced berry splitting. During cell degeneration, the capacity of residual live cells to generate turgor required for splitting is likely to be impaired by increased berry capacitance for water due to partial berry dehydration and a possible increase in the resistance of pathways of water entry into the berry. This additional evidence of cell degeneration in developing grape berries is indicative of a process in the physiological development of grapes that warrants specific recognition as the transition from berry ripening to senescence.

Theme outcomes

	Outcome	Achieved
1	Improved understanding by growers of vine nutrient accumulation and the implications for long-term vine performance.	Y
2	Development of vineyard management strategies to help growers optimise vine nutrient utilisation for long-term vine performance.	Y
3	Improved knowledge of the impacts of environmental stresses on bunch development and berry sugar accumulation.	Y
4	Development of vineyard management strategies for growers to ameliorate heat stress on grape bunches.	In progress
5	Development of a model for the grape industry to predict climatic events causing heat stress on bunches and its consequences in subsequent seasons	N*
6	Enhanced understanding of factors affecting transport mechanisms to enable growers to manipulate berry composition and influence wine style.	Y
7	Enhanced industry knowledge of whole vine-environmental interactions on resource allocation and transport on berry quality.	Y

* This model will be completed with a 3rd season of experimental work and growth cabinet studies forming part of the current GWRDC project Sustainable Viticultural Systems

Theme outputs

	Output	Achievement
1	Six refereed publications across the lifetime of the theme	Exceeded: 10 plus 2 in press and 2 submitted
2	Six industry and technical publications on resource allocation, environmental interaction and berry composition	Exceeded: 11 publications
3	Industry presentations at AWITC in 2007 and 2010; and at the NWGIC Annual Symposiums (2007 to 2010).	18 conference proceedings papers and posters
4	Presentations to grower associations in the grape growing regions.	18 presentations
5	Undergraduate, including Honours programs, training of students enrolled in CSU's viticulture and wine science courses	5 lectures developed and presented
6	Short course and certificate programs as part of training at NWGIC and partner organisations in various wine regions.	None developed, but contributions to existing courses (see appendix 3.9.1)
7	Post graduate training of students enrolled in higher degrees at CSU (coursework Masters and research degrees	2 PhD students trained

Theme milestones

	Milestone	Achieved
1	Methods for labelling xylem and phloem developed (June 2008)	Y
2	Preliminary studies on nutrient acquisition and root development conducted (June 2008)	Y
3	Impact of climatic stress on berry sugar accumulation in grape berries and vine performance assessed (September 2009)	Y
4	Impacts of heat stress on crop perenniality and crop load determined (June 2010)	Y
5	Heat stress management strategies to minimise crop damage and yield losses developed (September 2011)	Y
6	Model characterising water and assimilate transport into the berry completed (June 2011)	Y
7	Impacts of vine reserves on vine perenniality established (June 2011)	Y
8	Vineyard management strategies developed to optimise nutrient utilisation (June 2011)	Y

Recommendations

Seasonal nutrient dynamics and vine reserves

The project has achieved further understanding of seasonal nutrient dynamics in the perennial structure and the allocation to different organs of grapevines. This work showed the seasonal nutrient requirement by the annual growth and the importance of the perennial structure to provide nutrients to the early canopy development and, to a lesser extent to the reproductive development. The intra-seasonal changes have been assessed in two Shiraz trials, indicating the variation of the nutrient reserve pool between years. In addition, the work suggests that the nutrient reserves differ between rootstocks and can be altered by water and N supply. The relationship between root dynamics, nutrient accumulation and vine reserves was inconclusive and would require further research.

The findings have identified future research directions and a proportion of the data can be utilised for further work. These existing data on nutrient acquisition and reserve mobilisation can be utilised to enhance the timing and amounts of nutrient application, with the potential of integration into a grapevine model. The ^{15}N study undertaken with potted Chardonnay vines will provide initial information on timing of N for annual shoot and berry development from flowering to harvest. However, the importance of nutrient supply from uptake or storage for early canopy growth and the acquisition of nutrients during berry development on berry composition require further targeted experiments.

The capacity of the vine to take up these nutrients is an important area of research; this would require further studies that determine the role of stored or current assimilates on the root system in relation to root growth, root respiration and nutrient uptake. The methodology for root activity requires enhancement, since the use of minirhizothrons and a root camera did not lead to satisfying results under the conditions in this project. The root activity was variable between the different tubes used to collect the images and was much lower after the initial season, following the installation in autumn the previous season. A refinement of the methodology on a smaller scale field trial, together with studies under more controlled conditions would be most suitable. However, the issue of disturbed and undisturbed soils have to addressed, when root studies are undertaken with potted vines.

The project has further determined the importance of the roots as a storage organ, with its accumulated nutrients showing significant seasonal changes and between seasons. These dynamics are driven by the partitioning of the grapevine and the root environment, with factors such as soil temperature, water and nutrient supply. The understanding of the response of grapevines in relation to nutrient acquisition to the range of vine root environments relevant to current and future climatic trends is crucial. The predicted climatic changes will be reflected in the above and below ground environment and is important to understand the nutrition equitation and utilisation under various conditions for sustainable grape production. The future research on nutrition needs to integrate the soil processes, since they strongly contribute to the availability of nutrients for vine development and ultimately for the characteristics of grapes produced from a particular vineyard in a wine region.

Managing heat stress in vineyards

The research undertaken in this study has demonstrated in one grapevine variety that the vine is unable to protect itself from regularly occurring heat events and vineyard intervention is needed to protect the flowers and berries from the heat. While hydrocooling may provide a solution in some locations, it may not be feasible where water is in short supply and/or expensive. Similarly, the infrastructure for hydrocooling required may also be expensive. However, the value of the crop will be a key determinant of the value of this protection method and wider discussion of this research is warranted. This is a potential priority area for extension, particularly to develop a case study to examine the economics of hydrocooling and potential application in vineyards.

Other practical solutions include interrow planting and a detailed study of the temperature profile in vineyards with and without interrow planting is required. The recent development of infrared radiometers used in this research to monitor canopy temperatures are ideal for a study of the temperature profile in the vineyard and, thus, could be a priority R and D goal for the NWGIC.

The widespread use of, and the vineyard infrastructure to lay out, bird netting may provide a basis for future R and D to find solution to the heat waves. An investigation into vine covering with materials that may confer protection from both birds and heat would be valuable as it may be economic

to cover vines with. Thus, a PhD study of different materials including bird netting, light shade covering of no more than 10 to 30% interception is currently underway to assess the efficacy in reducing canopy temperatures.

Using scintigraphy to better understanding functional connections between leaves and bunches

Scintigraphy is an excellent tool for research into xylem transport through grapevines Because it is non-destructive, scintigraphy provides significantly improved data quality in a more efficient and reproducible manner for the exploration of time-related changes in plants. Currently accessibility to equipment and expertise are factors limiting the wide-spread use of scintigraphy in plant physiology research, however this will be gradually overcome as gamma cameras are placed into plant research facilities.

Experiments using dye and pertechnetate ($^{99m}TcO_4^-$) revealed that bunches bearing unripe berries have strong xylem connections with primary leaves located on the same side of the shoot as the bunch. These connections are also strong with secondary shoots arising from axillary buds on the same side of the stem as the bunch. This research is one of the first to identify functional xylem connections between the grapevine bunch and lateral shoots, a phenomenon that likely affects the development of the bunch. This necessitates modification of current models predicting nutrient exchange between the shoots and bunches of the grapevine. Further research on the nutrient storing cells at nodes within shoots is warranted to understand how and when nutrients are released to the bunch.

Using oxygen isotopes to better understand berry physiology

The analysis of oxygen isotopes in organic matter ($\delta^{18}O_{OM}$) should be considered a potential tool for identifying the relative contribution of root carbohydrate reserves and current photosynthesis to dry matter accumulation in organs such as the pre-veraison grape bunch. The $\delta^{18}O_{OM}$ values of berries at physiological maturity, expressed relative to the same value early in the ripening period (i.e. $\delta^{18}O_{OM}$), should be explored as a proxy measure for between-cultivar comparisons of leaf stomatal conductance. To underpin the application of the technique, future research should confirm the oxygen isotopic composition of important carbohydrate pools, such as sugars hydrolysed from root starch, synthesised by leaves and accumulated by grape berries.

Berry splitting in Shiraz

The decrease in susceptibility of Shiraz berries to splitting was found to diminish after about 100 days after anthesis and this can likely be applied to other seed grape varieties. When predicting the likelihood of splitting, all other factors being equal, early ripening cultivars are expected to become less susceptible to splitting before later ripening ones. Importantly, our study indicated that bunch age (days after the onset of ripening) is a more reliable indicator of susceptibility to splitting than berry ripeness *per se*, as determined by soluble solids concentration.

Appendix 1
Communication

Communication of the results of this research have been three-fold. Firstly, several peer-reviewed journal articles and industry articles have been published and several more have either been submitted or are in advanced stages of writing. Secondly, results have been promulgated at a number of grower and science meetings through oral communication. Thirdly, results are presented to undergraduate student classes at Charles Sturt University. In addition, other communication of results to growers has been undertaken through the NSW WIA Grassroots Solutions Implementation Plan 'Managing heat affected Vineyards'.

Refereed articles

Barlow, K., Bond, W., Holzapfel, B., Smith, J. and Hutton, R. (2009). Nitrogen concentrations in soil solution and surface run-off on irrigated vineyards in Australia. *Australian Journal of Grape and Wine Research* **15**: 131–143.

Clarke, S.J., Hardie, W.J. and Rogiers, S.Y. (2010). Changes in susceptibility of grape berries to splitting are related to impaired osmotic water uptake associated with losses in cell vitality. *Australian Journal of Grape and Wine Research* **16**: 469-476.

Clarke, S.J., Rogiers, S.Y. and Currie, G.M. (2011a). Sectoriality in xylem connections between the bunch and leaves of the grapevine (*Vitis vinifera*) shoot. *Botany* (in review).

Clarke S.J., Rogiers S.Y. and Currie G.M (2011b). Long-distance transport of pertechnetate in the moonflower, *Ipomoea alba* L. *Journal of Environmental Radioactivity* (in press).

Currie, G., Clarke, S.J., Rogiers, S.Y. and Wheat, J. (2010). Scintigraphic evaluation of plant physiology, *Journal of Nuclear Medicine Technology*, **38**: 76–80.

Field, S.T., Smith, J.P., Holzapfel, B.P., Emery, R.J.N. and Hardie, W.J. (2009). Grapevine response to soil temperature: xylem cytokinins and carbohydrate reserve mobilization from budbreak to anthesis. *American Journal of Enology and Viticulture* **60**: 164–172.

Greer D.H. and Sicard S.M. (2009). The net carbon balance in relation to growth and biomass accumulation of grapevines (*Vitis vinifera* cv. Semillon) grown in a controlled environment. *Functional Plant Biology* **36**: 645–653.

Greer, D.H. and Weedon, M. (2011). Modelling photosynthetic responses to temperature of grapevine *Vitis vinifera* cv. Semillon leaves on vines grown in a hot climate. *Plant, Cell and Environment* (submitted).

Greer, D.H., Weedon, M.M. and Weston, C. (2011). Reductions in biomass assimilation, photosynthesis *in situ*, and the net carbon balance are the costs of protecting *Vitis vinifera* cv. Semillon grapevines from heat stress with shade cloth. *AoB Plants* (in press).

Greer, D.H. and Weston, C. (2010*a*). Heat stress affects flowering, berry growth, sugar accumulation and photosynthesis in *Vitis vinifera* cv. Semillon grapevines grown in a controlled environment. *Functional Plant Biology* **37**: 206–214.

Greer, D.H. and Weston, C. (2010*b*). Effects of fruiting on vegetative growth and development dynamics of grapevines (*Vitis vinifera* L. cv. Semillon) can be traced back to events at or before budbreak. *Functional Plant Biology* **37**: 756–766.

Greer, D.H., Weston, C. and Weedon, M. (2010). Shoot architecture, growth and development dynamics of *Vitis vinifera* cv. Semillon vines grown in an irrigated vineyard with and without shade covering. *Functional Plant Biology* **37**: 1061–1070.

Holzapfel, B., Field, S. and Muller, M. (2008). Nitrogen and water management implications on grape production in the Riverina wine grape regions in south eastern Australia. *Le Bulletin de L'OIV* **81**: 17–26.

Holzapfel, B. and Treeby, M. (2007). The effect of nitrogen application on the nitrogen status and juice composition of Shiraz grafted on three rootstocks. *Australian Journal of Grape and Wine Research* **13**: 14–22.

Conference proceedings and industry articles

Clarke, S.J., Rogiers, S.Y. and Currie, G. (2008). Two-dimensional imaging of metastable-technetium xylem transport for the study of grapevine physiology. *In* 'Proceedings of 8th International Symposium on Grapevine Physiology and Biotechnology, Adelaide'. p. 156.

Clarke, S., Rogiers, S. and Hackett, S. (2009). The frustration of fruit splitting. *Australian and New Zealand Grapegrower and Winemaker*. **542**: 37–39.

Clarke, S., Rogiers, S. and Hackett, S. (2010). Fruit splitting. *In* 'Grapevine Management Guide 2010–11'. pp. 16–18.

Clarke, S.J., Rogiers, S.Y. and Hardie, W.J. (2008). Developmental changes in cell vitality, osmotic water uptake and susceptibility to splitting in the post-veraison grape berry. *In* 'Proceedings of 8th International Symposium on Grapevine Physiology and Biotechnology, Adelaide'. p. 155.

Currie, G., Clarke, S. and Rogiers, S. (2008). ^{99m}Tc based approaches to the study of plant vascular transport using scintigraphic imaging. *In* 'Proceedings of Australian and New Zealand Society of Nuclear Medicine Annual Scientific Meeting, Gold Coast, Queensland'.

Currie, G., Clarke, S. and Rogiers, S. (2009). Scintigraphy detection of pertechnetate for the study of plant vascular transport. *In* 'Proceedings of 1st International Plant Phenomics Symposium, Canberra'.

Dean, R.J., Stait-Gardner, T., Clarke, S.J., Rogiers, S. and Price, W. S. (2010). Diffusion tensor imaging (DTI) studies of the grape berry. *In* 'Proceedings of XXIVth International Conference on Magnetic Resonance in Biological Systems, Cairns'. Abstract#429.

Field, S. and Holzapfel, B. (2007). Interactions between nutrient uptake and carbohydrate metabolism in vines. *Poster presentation:* 13th Australian Wine Industry Technical Conference, Adelaide.

Field, S., Smith, J.A., Greer, D., Emery, N. and Holzapfel, B. (2007). Soil temperature effects on reproductive development, starch reserves, partitioning and cytokinin concentration in bleeding sap of Shiraz. *Poster presentation:* 13th Australian Wine Industry Technical Conference, Adelaide.

Field, S.K., Smith, J.P., Greer, D.H., Meunier, M., Holzapfel, B.P. and Emery, N. (2008). Seasonal carbohydrate, nitrogen and cytokinin dynamics and their impact on shoot and root growth. *In* 'Proceedings of 8th International Symposium on Grapevine Physiology and Biotechnology, Adelaide'.

Greer, D.H. (2009). Heat stress in wine grapes. *In* 'Proceedings of IHD Vitilink Technical Conference, Tuscany Wine Estate Resort, Pokolbin, NSW'.

Greer, D.H., Clark, S. and Sicard, S. (2007). Heat stress – does it affect sugar accumulation in Semillon grapes. *Poster presentation:* 13th Australian Wine Industry Technical Conference, Adelaide.

Greer, D.H., Weedon, M. and Weston, C. (2010). High temperature affects on yield and berry composition. *In* 'Proceedings of 14th Australian Wine Industry Technical Conference, Adelaide'.

Holzapfel, B.P., Field, S.K., Hackett, S. and Smith, J.P. (2009). Vine nutrient reserves, rootstocks and root dynamics. *In* 'Proceedings of 16th International Symposium GiESCO. Davis, California, USA'. pp. 71–76.

Holzapfel, B., Müller, M.C., Smith, J., Gourieroux, A. and Field, S. (2007). Effect of N on amino acid profiles. Workshop presentation 'Managing vine nutritional requirements'. *In* 'Proceedings of 13th Australian Wine Industry Technical Conference, Adelaide'.

Holzapfel B.P., Quirk L, Hutton R And Holland J (2009). Wine Grape Nutrition and use of fertilisers and other nutritional supplements to sustain production. *In* 'Water and vine, managing the challenge, Module 15, Technical notes'. 17 pp.

Holzapfel, B., Smith, J. and Field, S. (2009). Vine nutrition and seasonal root dynamics. *In* 'Grapevine Management Guide 2009–10'. pp. 18–20.

Holzapfel, B., Smith, J.P., Hutton, R. and Hackett, S. (2010). Nitrogen management in Chardonnay vineyards in the Riverina. *In* 'Grapevine Management Guide 2010–11'. pp. 25–28.

Holzapfel, B., Smith, J., Hutton, R. and Holland, J. (2010). Nitrogen management in irrigated vineyards in SE Australia. *In* 'Proceedings of International Inter*Vitis* Interfructa Conference, Stuttgart, Germany'.

Müller, M.C., Clark, A. and Holzapfel, B. (2010). Vineyard practices and winery N management. *In* 'Grapevine Management Guide 2010–11'. pp. 29–30.

Müller, M.C., Clark, A., Schultz, H-R. and Holzapfel, B. (2010). Comparison of different vineyard practises and winery N management. *Workshop presentation:* 'Semillon: viticultural management for wine style'. 14th Australian Wine Industry Technical Conference, Adelaide.

Quirk, L.F., Holzapfel, B., Smith, J, Holland, J. and Hutton, R. (2008). Monitoring soil nutrient in irrigated Chardonnay vineyards of the Riverina, NSW. *Australian and New Zealand Grapegrower and Winemaker* **539:** 50–51

Smith, J., and Holzapfel, B. (2008). Seasonal pattern of grapevine root growth: a research update. *In* 'Grapevine Management Guide 2008–09'. pp. 32–34.

Rogiers, S.Y. and Clarke, S. (2010). Vascular transport through grapevines. *In* 'Wagga Wagga Agricultural Institute Update'. pp. 76–77.

Rogiers, S.Y. (2007). The vascular system. The vine's super highway for transport and communication. *Australian and New Zealand GrapeGrower and Winemaker* **524**: 28–30.

Watt, J., Field, S., Sharkey, N., Lamont, R. and Holzapfel, B. (2010). Do rootstocks have different seasonal root and reserve dynamics? *Poster presentation:* 14th Australian Wine Industry Technical Conference, Adelaide.

Watt, J., Hackett, S. and Holzapfel, B. (2010). Root dynamics and carbohydrate reserves in rootstocks. *In* 'Grapevine Management Guide 2010–11'. pp. 33–35.

Seminars, workshops and lectures

Clarke, S.J. (2008). Berry splitting–the importance of cultivar and development. *Presentation:* undergraduate Vine Physiology VIT 301, Wine and Food Industry Training Centre, Wagga Wagga.

Clarke, S.J. (2009) The problem of berry splitting. *Presentation:* Orange Region Vignerons Association.

Clarke, S.J. (2009). The problem of fruit splitting. *Presentation:* undergraduate Vine Physiology VIT 301, Wine and Food Industry Training Centre, Wagga Wagga.

Clarke, S.J. (2010). Understanding the causes of bud necrosis, berry splitting and shrivel. Griffith.

Clarke, S.J. (2010). Understanding the causes of bud necrosis, berry splitting and shrivel. *Presentation*: Canberra-region grape growers, Murrumbateman.

Clarke, S.J. (2010). Scintigraphic detection of water flow through grapevines. *Presentation*: School of Dentistry and Health Sciences, and the National Wine and Grape Industry Centre, Wagga Wagga.

Clarke, S.J. (2010). Scintigraphic detection of solute flow through grapevines. *Presentation*: Vine Physiology VIT 301, CSU Wagga Wagga NSW.

Greer, D.H. (2007). Heat stress in Semillon – how far have we got? *Presentation:* Hunter Valley Vineyard Association/ Winegrowing Futures Steering Committee Workshop, Cessnock NSW.

Greer, D.H. (2008). Canopy temperatures and heat stress in Semillon – what we now know. *Presentation*: North East Victorian Grape Growers and Winemakers Industry /Winegrowing Futures Steering Committee Workshop, Albury NSW.

Greer, D.H. (2009). Heat stress effects on Semillon. *Presentation*: Riverina Field Days Seminar Program, Griffith NSW.

Greer, D.H. (2009). Heat stress in Semillon. GWRDC Climate Change Workshop, Adelaide SA.

Greer, D.H. and Weedon, M. (2011). Heat stress: impacts on grapevine carbon relations and ripening, and remediation by shading and hydrocooling. Industry Showcase Day, NWGIC Wagga Wagga NSW.

Holzapfel, B. (2009). Vine nutrient reserves, rootstocks and root dynamics. *Presentation*: NSW Roadshow, Hunter Valley

Holzapfel, B. (2009). Vine nutrient reserves, rootstocks and root dynamics. *Lecture:* VIT 301, CSU Wagga Wagga NSW.

Holzapfel, B., Field, S., Hutton, R. and Smith, J. (2009). Nitrogen management in vineyards. Root zone management to minimise off-site migration of nutrients and pesticides. *Workshop*: Sunraysia Horticultural Centre, Mildura VIC.

Holzapfel, B.P., Quirk, L., Hutton, R. and Holland, J. (2009). Wine Grape Nutrition and use of fertilisers and other nutritional supplements to sustain production. Water and Vine: managing the challenge, Module 15. Adelaide–March 18, Berri–October 27, Langhorne Creek –November 6, Wangaratta–November 11, Barossa Valley–December 12 (seven national presentations).

Holzapfel, B. and Smith, J. (2008). Rootstock effects on vine partitioning under varied water supply. 2nd National Rootstock Forum, Mildura VIC.

Holzapfel, B., Smith, J., Hutton, R. and Holland, J. (2010). Nitrogen management in Chardonnay vineyards in the Riverina. *Workshop*: Irrigation and nutrition science for Riverina wine production, Griffith NSW.

Müller, M. Clark, A. and Holzapfel, B. (2010). Comparison of different vineyard practises and winery N management. *Workshop*: Irrigation and nutrition science for Riverina wine production, Griffith NSW.

Appendix 2
Intellectual property

Not applicable

Appendix 3
References

Agenbach, W.A. (1977). A study of must nitrogen content in relation to incomplete fermentations, yeast production and fermentation activity. In Proceedings of the South African Society for Enology and Viticulture. E.F. Beukman (Ed.), pp. 66–88. Stellenbosch, South Africa.

Alexander, D.M. (1965). The effect of high temperature regimes or short periods of water stress on development of small fruiting Sultana vines. *Australian Journal of Agricultural Research* **16**: 817–823.

Aljibury, F.K., Brewer, R., Christensen, P. and Kasimatis, A.N. (1975). Grape response to cooling with sprinklers. *American Journal of Enology and Viticulture* **26**: 214–217.

Balasubrahmanyam, V.R., Eifert, J. and Diofasi, L. (1978). Studies on cropping level in grapes. I. Effect of differential cropping level on the organic nutrient reserves in the canes. *Vitis* **17**: 23–29.

Barbour, M.M., Roden, J.S., Farquhar, G.D. and Ehleringer, J.R. (2004). Expressing leaf water and cellulose oxygen isotope ratios as enrichment above source water reveals evidence of a Péclet effect. *Oecologia* **138**: 426–435.

Bates, T., Dunst, R. and Joy. P. (2002). Seasonal dry matter, starch, and nutrient distribution in 'Concord' grapevine roots. *HortScience* **37**: 313–316.

Beck, C.B. (2010). An introduction to plant structure and development: plant anatomy for the twenty-first century. Cambridge University Press: Cambridge.

Bennett, R. and Willey, N. (2003). Soil availability, plant uptake and soil to plant transfer of ^{99}Tc–a review. *Journal of Environmental Radioactivity* **65**: 215–231.

Bennett, J., Jarvis, P., Creasy, G.L. and Trought, M.C.T. (2005). Influence of defoliation on overwintering carbohydrate reserves, return bloom, and yield of mature Chardonnay grapevines. *American Journal of Enology and Viticulture* **56**: 386–393.

Bertamini, M. and Nedunchezhian, N. (2003). Photosynthetic functioning of individual leaves *Vitis vinifera* L. cv. Pinot Noir) during ontogeny in the field. *Vitis* **42**: 13–17.

Bindi, M., Miglietti, F., Gozzini, B., Orlandini, S. and Seghi, L. (1997). A simple model for simulation of growth and development in grapevine *Vitis vinifera* L.) I Model description. *Vitis* **36**: 67–71.

Buttrose, M.S. (1969). Vegetative growth of grapevine varieties under controlled temperature and light intensity. *Vitis* **8**: 280–285.

Candolfi-Vasconcelos, M.C., Candolfi, M.P. and Koblet, W. (1994). Retranslocation of carbon reserves from the woody storage tissues into the fruit as a response to defoliation stress during the ripening period in *Vitis vinifera* L.. *Planta* **192**: 567–573.

Canny, M.J. (1973). Phloem translocation. Cambridge University Press: London.

Canny, M.J. (1995). A new theory for the ascent of sap – cohesion supported by tissue pressure. *Annals of Botany* **75**: 343–357.

Canny, M.J., Sparks, J.P., Huang, C.X. and Roderick, M.L. (2007). Air embolisms exsolving in the transpiration water – the effect of constrictions in the xylem pipes. *Functional Plant Biology* **34**: 95–111.

Cartechini, A. and Palliotti, A. (1995). Effect of shading on vine morphology and productivity and leaf gas exchange characteristics in grapevines in the field. *American Journal of Enology and Viticulture* **46**: 227–234.

Cataldo, D.A., Garland, T.R. and Wildung, R.E. (1984). Plant root absorption and metabolic fate of technetium in plants. *In*: Desmet, G. and Myttenaere, C. (Eds), Technetium in the environment, Elsevier Applied Science Publishers, London. pp. 265–280.

Cataldo, D.A., Wildung, R.E. and Garland, T.R. (1978). Technetium accumulation, fate and behavior in plants. In: Adriano, D.C. and Brisbin, T.L. (Eds), Environmental chemistry and cycling processes, National Technical Information Service, Springfield: pp. 538–549.

Chaumont, M., Morot-Gaudry, J.F. and Foyer, C.H. (1994). Seasonal and diurnal changes in photosynthesis and carbon partitioning in *Vitis vinifera* leaves in vines with and without fruit. *Journal of Experimental Botany* **45**: 1235–1243.

Cheng, L. and Xia, G. (2004). Growth and fruiting of young 'Concord' grapevines in relation to reserve nitrogen and carbohydrates. *Journal of American Society of Horticultural Science* **129**: 660–666.

Cohen, S., Raven, E., Li, Y., Grava, A. and Goldschmidt, E.E. (2005). Physiological responses of leaves, tree growth and fruit yield of grapefruit trees under reflective shade screens. *Scientia Horticulturae* **107**: 27–35.

Comas, L.H., Anderson, L.J., Dunst, R.M., Lakso, A.N. and Eissenstat, D.M. (2005). Canopy and environmental control of root dynamics in a long-term study of Concord grape. *New Phytologist* **167**: 828–840.

Condon, A.G., Richards, R.A., Rebetzke, G.J. and Farquhar, G.D. (2004). Breeding for high water-use efficiency. *Journal of Experimental Botany* **55**: 2447–2460.

Conradie, W.J. (1980). Seasonal uptake of nutrients by Chenin Blanc in sand culture. I. Nitrogen. *South African Journal Enology Viticulture* **1**: 59–65.

Conradie, W.J. (1981). Nutrient consumption by Chenin Blanc grown in sand culture and seasonal changes in chemical composition of leaf blades and petioles. *South African Journal Enology Viticulture* **2**: 15–18.

Conradie, W.J. (1991*a*). Translocation and storage of nitrogen by grapevines as affected by time of application. Proceedings of the International Symposium Nitrogen in Grapes and Wine, American. Society for Enology and Viticulture. Davis, CA. pp. 32–42.

Conradie, W.J. (1991*b*). Distribution and translocation of nitrogen absorbed during early summer by two-year-old grapevines grown in Sand culture. *American Journal of Enology and Viticulture* **42**: 180–190.

Conradie, W.J. (1992). Partitioning of nitrogen in grapevines during autumn and the utilisation of nitrogen reserves during the following growing season. *South African Journal Enology Viticulture* **13**: 45–51.

Conradie, W.J. (2005). Partitioning of mineral nutrients and timing of fertilizer application for optimum efficiency. Proceedings for the Soil Environment and Vine Mineral Nutrition Symposium, American Society for Enology and Viticulture. J.P. Christensen, D.R. Smart (Eds.), pp. 69–81. San Diego, CA.

Considine, J.A. and Kriedemann, P.E. (1972). Fruit splitting in grapes: determination of the critical turgor pressure. *Australian Journal of Agricultural Research* **23**: 17–24.

Coombe, B.G. (1992). Research on development and ripening of the grape berry. *American Journal of Enology and Viticulture* **43**: 101–110.

Coombe, B.G. (1995). Adoption of a system for identifying grapevine growth stages. *Australian Journal of Grape and Wine Research* **1**: 104–110.

Coombe, B.G. and Mc Carthy, M.G. (1997). Identification and naming of the inception of aroma development in ripening grape berries. *Australian Journal of Grape and Wine Research* **3**: 18–20.

Currie, G.M. and Wheat, J.M. (2008). Small angle gamma ray scatter: what is the impact on image quality? *The Internet Journal of Medical Technology* **4**.

Currie, G., Clarke, S.J., Rogiers, S.Y. and Wheat, J. (2010). Techniques for technetium scintigraphy in plants. *Journal of Nuclear Medicine Technology* **38**: 76–80.

De Soyza, A.G. and Kincaid, D.T. (1991). Patterns of leaf morphology and photosynthesis in shoots of Sassafras albidium Lauraceae) *American Journal of Botany* **78**: 89–98.

Desmet, G. (1984). Relevance of the study of technetium accumulation and speciation in plants. Desmet G. and Myttenaere C. (Eds), Technetium in the environment, Elsevier Applied Science Publishers, London: pp. 189–195.

Downton, W.J.S. and Grant, W.J.R. (1992). Photosynthetic physiology of spur pruned and minimal pruned grapevines. *Australian Journal of Plant Physiology* **19**: 309–316.

Düring, H., Lang, A. and Oggionni, F. (1987). Patterns of water flow in Riesling berries in relation to developmental changes in their xylem morphology. *Vitis* **26**: 123–131.

Edson, C.E., Howell, G.S. and Flore, J.A. (1995). Influence of crop load on photosynthesis and dry matter partitioning of Seyval grapevines. II. Seasonal changes in single leaf and whole vine photosynthesis. *American Journal of Enology and Viticulture* **4**: 469–477.

Ellmore, G.S., Zanne, A.E. and Orians, C.M. (2006). Comparative sectoriality in temperate hardwoods: hydraulics and xylem anatomy. *Botanical Journal of the Linnean Society* **150**: 61–71.

El-Zeftawi, B.M. (1971). Effects of GA and CCC on setting, splitting, yield and quality of Zante currants (*Vitis vinifera* var.). *Vitis* **10**: 27–30.

El-Zeftawi, B.M. and Weste, H.L. (1972). Effects of time of application of GA + CCC on yield and splitting of Zante currant *Vitis vinifera* var. *Vitis* **11**: 124–130.

Esau, K. (1977). Anatomy of seed plants. John Wiley and Sons: New York.

Escalona, J.M., Flexas, J., Bota, J. and Medrano, H. (2003). Distribution of leaf photosynthesis and transpiration within grapevine canopies under different drought conditions. *Vitis* **42**: 57–64.

Ferrini, F., Mattii, G.B. and Nicese, F.P. (1995). Effect of temperature on key physiological responses of grapevine leaf. *American Journal of Enology and Viticulture* **46**: 375–379.

Field, S.K., Smith, J.P., Holzapfel, B.P., Hardie, W.J. and Emery, R.J.N. (2009). Grapevine response to soil temperature: xylem cytokinin and carbohydrate reserve mobilisation from budbreak to anthesis. *American Journal of Enology and Viticulture* **60**: 164–172.

Flore, J.A. and Lakso, A.N. (1989). Environmental and physiological regulation of photosynthesis in fruit crops. *Horticultural Reviews* **11**: 111–157.

Foster, T.M., Seleznyova, A.N. and Barnett, A.M. (2002). Independent control of organogenesis and shoot tip abortion are key factors to developmental plasticity in kiwifruit (*Actinidia*). *Annals of Botany* **100**: 471–481.

Fournier, C. and Andrieu, B. (2000). Dynamics of the elongation of internodes in maize *Zea mays* L.). Effects of shade treatment on elongation patterns. *Annals of Botany* **86**: 1127–1134.

Fournioux, J.C. and Bessis. R. (1974). Inégaliés dans la distribution et la différenciation des traces foliaires en rapport avec la dorsiventralité de la tige chez le *Vitis vinifera* L. *Revue Générale de Botanique* **81**: 41–53.

Fournioux, J.C. and Bessis, R. (1979). Etude des relations criblo-vascularies entre les differents organes de la tige de la vigne (*Vitis vinifera* L.). *Connaissance de la Vigne et du Vin* **13**: 91–114.

Freeman, B.F. and Kliewer, W.M. (1984). Grapevine leaf development in relationship to potassium concentration and leaf dry weight and density. *American Journal of Botany* **71**: 294–300.

Fujimaki, S., Suzui, N., Ishioka, N.S., Kawachi, N., Ito, S., Chino, M. and Nakamura, S. (2010). Tracing cadmium from culture to spikelet: non-invasive imaging and quantitative characterization of absorption, transport, and accumulation of cadmium in an intact rice plant. *Plant Physiology* **152**: 1796–1806.

Gerrath, J.M., Posluszny, U. and Dengler, N.G. (2001). Primary vascular patterns in the Vitaceae. *International Journal of Plant Science* **162**: 729–745.

Gessler, A., Peuke, A.D., Keitel, C. and Farquhar, G.D. (2007). Oxygen isotope enrichment of organic matter in *Ricinus communis* during the diel course and as affected by assimilate transport. *New Phytologist* **174**: 600–613.

Givnish, T.J. (1988). Adaptation to sun and shade: a whole plant perspective. *Australian Journal of Plant Physiology* **15**: 63–92.

Glad, C., Farineau,J., Regnard, J.L. and Morot-Gaudry, J.F. (1994). The relative contribution of nitrogen originating from two seasonal ^{15}N supplies to the total nitrogen pool present in the bleeding sap and in whole *Vitis vinifera* cv. Pinot Noir grapevines at bloom time. *American Journal of Enology and Viticulture* **45**: 327–332.

Glad, C., Regnard, J.L., Querou, Y., Brun, O. and Morot-Gaudry, J.F. (1992). Phloem sap exudates as a criterion for sink strength appreciation in *Vitis vinifera* cv. Pinot Noir grapevines. *Vitis* **31**: 131–138.

Goffinet, M.C. (2004). Relation of applied crop stress to inflorescence development, shoot growth characteristics, and cane starch reserves in 'Concord' grapevine. *Acta Horticulturae* **640**: 189–200.

Grassi, G. and Minotta, G. (2000). Influence of nutrient supply on sun-shade acclimation of Picea abies seedlings: effects on foliar morphology, photosynthetic performance and growth. *Tree Physiology* **20**: 645–652.

Greenspan, M.D., Shackel, K.A. and Matthews, M.A. (1994). Developmental changes in the diurnal water budget of the grape berry exposed to water deficits. *Plant, Cell and Environment* **17**: 811–820.

Greer, D.H. (1999). Seasonal and daily changes in carbon acquisition of kiwifruit vines with and without axillary fruit. *New Zealand Journal of Crop and Horticulture* **27**: 23–31.

Greer, D.H. (2001). Photon flux density-dependence of carbon acquisition and demand in relation to growth of kiwifruit Actinidia deliciosa) vines grown in controlled environments. *Australian Journal of Plant Physiology* **28**: 111–120.

Greer, D.H. and Jeffares, D. (1998). Temperature-dependence of carbon acquisition and demand in relation to shoot growth of kiwifruit (*Actinidia deliciosa*) vines grown in controlled environments. *Australian Journal of Plant Physiology* **25**: 843–850.

Greer, D.H. and Sicard, S.M. (2009). The net carbon balance in relation to growth and biomass accumulation of grapevines *Vitis vinifera* cv. Semillon) grown in a controlled environment. *Functional Plant Biology* **36**: 645–653.

Greer, D.H. and Weston, C. (2010*a*). Heat stress affects flowering, berry growth, sugar accumulation and photosynthesis in *Vitis vinifera* cv. Semillon grapevines grown in a controlled environment. *Functional Plant Biology* **37**: 206–214.

Greer, D.H. and Weston, C. (2010*b*). Effects of fruiting on vegetative growth and development dynamics of grapevines (*Vitis vinifera* L. cv. Semillon) can be traced back to events at or before budbreak. *Functional Plant Biology* **37:** 756–766.

Greer, D.H. and Wünsche, J.N. (2003). Late-season temperature effects on the carbon economy and tree performance of 'Royal Gala' apple (*Malus domestica*) trees. *New Zealand Journal of Crop and Horticultural Science* **31**: 235–245.

Greer, D.H., Cirillo, C. and Norling, C.L. (2003). Temperature-dependence of carbon acquisition and demand in relation to shoot and fruit growth of fruiting kiwifruit (*Actinidia deliciosa*) vines grown in controlled environments. *Functional Plant Biology* **30**: 927–937.

Greer, D.H., Weston, C. and Weedon, M. (2010). Shoot architecture, growth and development dynamics of *Vitis vinifera* cv. Semillon vines grown in an irrigated vineyard with and without shade covering. *Functional Plant Biology* **37**: 1061–1070.

Grignon, N., Touraine, B. and Durand, M. (1989). 6(5)Carboxyfluorescein as a tracer of phloem sap translocation. *American Journal of Botany* **76**: 871–877.

Guglielmini, A.C. and Satorre, E.H. (2002). Shading effects on spatial growth and biomass partitioning of *Cynodon dactylon*. *Weed Research* **42**: 123–134.

Gunning, B.E.S. and Pate, J.S. (1969). "Transfer cells". Plant cells with wall ingrowths, specialized in relation to short distance transport of solutes–their occurrence, structure, and development. *Protoplasma* **68**: 107–133.

Gunning, B.E.S., Pate, J.S. and Green, L.W. (1970) Transfer cells in the vascular system of stems: taxonomy, association with nodes, and structure. *Protoplasma* **71**: 147–171.

Hale, C.R. and Weaver, R.J. (1962). The effect of developmental stage on direction of translocation of photosynthate in *Vitis vinifera*. *Hilgardia* **33**: 73–223.

Hale, C.R. and Buttrose, M.S. (1974). Effects of temperature on ontogeny of berries of *Vitis vinifera* L. cv. Cabernet sauvignon. *Journal of the American Society for Horticultural Science* **99**: 390–394.

Hansen, P. (1971). ^{14}C-studies on apple trees. VII. The early seasonal growth in leaves, flowers and shoots as dependent upon current photosynthates and existing reserves. *Physiologia Plantarum* **25**: 469–473.

Hardie, W.J. and Martin, S.R. (2000). Shoot growth on de-fruited grapevines: a physiological indicator for irrigation scheduling. *Australian Journal of Grape and Wine Research* **6**: 52–58.

Hardie, W.J., O'Brien, T.P. and Jaudzems, V.G. (1996). Morphology, anatomy and development of the pericarp after anthesis in grape, *Vitis vinifera* L. *Australian Journal of Grape and Wine Research* **2**: 97–142.

Hewitt, W.M.B. and Gardner, M.E. (1956). Some studies of the adsorption of zinc sulphate in Thompson Seedless grape canes. *Plant Physiology* **31**: 393–399.

Ho, L.C. and Shaw, A.F. (1977). Carbon economy and translocation of ^{14}C in leaflets of the seventh leaf of tomato during leaf expansion. *Annals of Botany* **41**: 833–848.

Holzapfel, B., Field, S. and Müller, M. (2008). Nitrogen and water management implications on grape production in the Riverina wine grape regions in South Eastern Australia. Castellucci, M.F. (Ed.), Le Bulletin de L'OIV 81, 17–26 (paper prepared for XXX World Vine and Wine Congress, Budapest, Hungary, June 10-16, 2007).

Holzapfel, B. and Smith, J. (2011*a*). The influence of various management practices on nitrogen reserves of the perennial structure in Shiraz grapevines in south-eastern Australia. Proceedings XVIIth International Symposium GiESCO, Asti – Alba, Italy, August 29–September 2, 427–430.

Holzapfel, B.P. and Smith, J.P. (2011*b*). Developmental stage and climatic factors impact more on carbohydrate reserve dynamics of Shiraz than cultural practice. *American Journal of Enology and Viticulture* (submitted).

Holzapfel, B.P., Smith, J.P., Field, S.K. and Hardie, W.J. (2010). Dynamics of carbohydrate reserves in cultivated grapevines. *Horticulture Reviews* **37**: 143–211.

Holzapfel, B. and Treeby, M. (2007). The effect of nitrogen application on the nitrogen status and juice composition of Shiraz grafted on three rootstocks. *Australian Journal of Grape and Wine Research* **13**: 14–22.

Ingledew, W.M. and Kunkee, R.E. (1985). Factors influencing sluggish fermentations of grape juice. *American Journal of Enology and Viticulture* **36**: 65–76.

Ingraham, N.L. and Caldwell, E.A. (1999). Influence of weather on the stable isotopic ratios of wines: tools for weather/climatic reconstruction? *Journal of Geophysical Research* **104**: 2185–2194.

Jones, K.S., Paroschy, J., McKersie, B.D. and Bowley, S.R. (1999). Carbohydrate composition and freezing Tolerance of canes and buds in *Vitis vinifera*. *Journal Plant Physiology* **155**: 101–106.

Keller, M., Smith, J.P. and Bondada, B.R. (2006). Ripening berries remain hydraulically connected to the shoot. *Journal of Experimental Botany* **57**: 2577–2587.

Keller, M. (2010). The science of Grapevines: anatomy and physiology. Elsevier Inc., Amsterdam.

Kliewer, W.M. (1977*a*). Effect of high temperatures during the bloom-set period on fruit-set, ovule fertility, and berry growth of several grape cultivars. *American Journal of Enology and Viticulture* **28**: 215–222.

Kliewer, W.M. (1977*b*). Influence of temperature, solar radiation and nitrogen on coloration and composition of Emperor grapes. *American Journal of Enology and Viticulture* **28**: 96–103.

Kliewer, W.M. (1991). Methods for determining the nitrogen status of vineyards. pp. 133–147. J.M. Rantz (ed.), Proceedings Int. Symp. Nitrogen in Grapes and Wine, ASEV, Seattle, USA.

Kliewer, W.M. and Schultz, H.B. (1973). Effect of sprinkler cooling of grapevines on fruit growth and composition. *American Journal of Enology and Viticulture* **24**: 17–26.

Koblet, W. (1969). Translocation of photosynthate in vine shoots and influence of leaf area on quantity and quality of the grapes. *Die Wein-Wissenschaft* **24**: 277–319.

Koblet, W., Candolfi-Vasconcelos, M.C. and Keller, M. (1996). Stress und Stressbewältigung bei Weinreben. Bot. Helv. **106**: 73–84.

Krasnow, M., Matthews, M.A. and Shackel, K.A. (2008). Evidence for substantial maintenance of membrane integrity and cell viability in normally developing grape (*Vitis vinifera* L.) berries throughout development. *Journal of Experimental Botany* **59**: 849–859.

Kriedemann, P.R., Kliewer, W.M. and Harris, J.M. (1970). Leaf age and photosynthesis of *Vitis vinifera* L. *Vitis* **9**: 97–140.

Krijger, G.C., Van Vliet, P.M. and Wolterbeek, H.T. (1999*a*). Metal speciation in xylem exudate of Lycopersicon esculentum Mill - technetium. *Plant and Soil* **212:** 165–173.

Krijger, G.C., Verburg, T.G., Den Hollander, W., Hermans, P.M.J.A., De Goeij, J.J.M. and Wolterbeek, H. (1999*b*). Approaches for nondestructive spatial distribution measurements in whole plants using radionuclides. *Journal of Plant Physiology* **155:** 165–172.

Lakso, A.N. and Johnson, R.S. (1990). A simplified dry matter production model for apple using an automated programming simulation software. *Acta Horticulturae* **276:** 141–148.

Lambers, H., Scheurwater, I. and Atkin, O.K. (1995). Respiratory patterns in roots in relation to their functioning. In Plant roots. The hidden half. Waisel Y., Eshel A. Kafkafi U. (Eds.). pp. 323–362. Marcel Dekker Inc. – New York/Basel/Hong Kong.

Lang, A. and Düring, H. (1990). Grape berry splitting and some mechanical properties of the skin. *Vitis* **29:** 61–70.

Lang, A. and Thorpe, M.R. (1988). Why do grape berries split? In: R.E. Smart, R.J. Thornton, S.B. Rodriguez and J.E. Young (Eds). Proceedings of the Second International Cool Climate Viticulture and Oenology Symposium, 11-15 January, 1988. Auckland, New Zealand: New Zealand Society for Viticulture and Oenology, 69–71.

Larson, D.W., Doubt, J. and Matthes-Sears, U. (1994). Radially sectored hydraulic pathways in the xylem of Thuja occidentalis as revealed by the use of dyes. *International Journal of Plant Sciences* **155:** 569–582.

Lebon, E., Pellegrino, A., Tardieu, F. and Lecoeur, J. (2004). Shoot development in grapevine *Vitis vinifera*) is affected by the modular branching pattern of the stem and intra- and inter-shoot trophic competition. *Annals of Botany* **93:** 263–274.

Lembrechts, J.F.M.M. and Desmet, G.M. (1984). Accumulation of Tc-bio-organic complexes in spinach plants in relation to growth. In: Desmet G., and Myttenaere C. (Eds), Technetium in the environment, Elsevier Applied Science Publishers, London: pp. 295–300.

Liu, Y., Schieving, F., Stuefer, J.F. and Anten, N.P.R. (2007). The effects of mechanical stress and spectral shading on the growth and allocation of ten genotypes of a stoloniferous plant. *Annals of Botany* **99:** 121–130.

Loescher, W.H., McCamant, T. and Keller, J.D. (1990). Carbohydrate reserves, translocation, and storage in woody plant roots. *HortScience* **25**: 274–281.

Löhnertz, O., Schaller, K. and Mengel, K. (1989). Nährstoffdynamik in Reben III. Mitteilung: Stickstoffkonzentration und Verlauf der Aufnahme in der Vegetation. Vitic. Enol. Sci. 44:192–204

Lopes, C. and Pinto, P.A. (2005). Easy and accurate estimation of grapevine leaf area with simple mathematical models. *Vitis* **44:** 55–61.

Louarn, G., Guedon, Y., Lacoeur, J. and Lebon, E. (2007). Quantitative analysis of the phenotypic variability of shoot architecture in two grapevine *Vitis vinifera*) cultivars. *Annals of Botany* **99:** 425–437.

Lugassi-Ben-Hamo, M., Kitron, M., Bustan, A. and Zaccai, M. (2010). Effects of shade regime on flower development, yield and quality in lisianthus. *Scientia Horticulturae* **124:** 248–253.

Lustig, I. and Bernstein, Z. (1985). Determination of the mechanical properties of the grape berry skin by hydraulic measurements. *Scientia Horticulturae* **25:** 279–285.

Luykk, F. (1984). Technetium discharges into the environment. Desmet G., and Myttenaere C. (Eds), Technetium in the environment, Elsevier Applied Science Publishers, London: pp. 21–27.

Maillard, P., Deléens, E., Daudet, F.A., Lacointe, A. and Frossard, J.S. (1994). Carbon economy in walnut seedlings during the acquisition of autotrophy studied by long-term labelling with $^{14}CO_2$. *Physiologia Plantarum* **91:** 359–368.

Marshall, C. (1996). Sectoriality and physiological organisation in herbaceous plants: an overview. *Vegetation* **127:** 9–16.

Martin, G.J., Guillou, C., Martin, M.L., Cabanis, M.-T., Tep, Y. and Aerny, J. (1988). Natural factors of isotope fractionation and the characterization of wines. *Journal of Agriculture and Food Chemistry* **36:** 316–322.

Matsui, A., Ryugo, K. and Kliewer, W.M. (1986). Growth inhibition of Thompson Seedless and Napa Gamay berries by heat stress and its partial reversibility by applications of growth regulators. *American Journal of Enology and Viticulture* **37:** 67–71.

Matsui, A., Ryugo, K. and Kliewer, W.M. (1991). Lowered berry quality due to heat stress at the early ripening stage of berry growth in a seeded grapevine, *Vitis vinifera* L. *Research Bulletin of Faculty of Agriculture. Gifa University* **56:** 139–145.

Matthews, M.A. and Shackel, K.A. (2005). Growth and water transport in fleshy fruit. Vascular Transport in Plants. Eds N.M. Holbrook and M.A. Zwieniecki (Elsevier Academic Press: Amsterdam) pp. 181–197.

Matthews, M.A., Anderson, M.M. and Schultz, H.R. (1987). Phenologic and growth responses to early and late season water deficits in Cabernet franc. *Vitis* **26:** 147–160.

May, P. (1994). Using Grapevine Rootstocks: The Australian Perspective. Winetitles, Adelaide, p. 62.

May, P. (2000). From bud to berry, with special reference to inflorescence and bunch morphology. *Australian Journal of Grape and Wine Research* **6:** 82–98.

McCarthy, M.G. (1999). Weight loss from ripening berries of Shiraz grapevines (*Vitis vinifera* L. cv. Shiraz). *Australian Journal of Grape and Wine Research* **5:** 10–16.

McKay, R.M.L., Palmer, G.R., Ma, X.P., Layzell, D.B. and McKee, B.T.A. (1988). The use of positron emission tomography for studies of long-distance transport in plants: uptake and transport of 18F. *Plant, Cell and Environment* **11:** 851–861.

McKenry, M. (1984). Grape root phenology relative to control of parasitic nematodes. *American Journal of Enology and Viticulture* **35:** 206–211.

McNeil, D.L., Atkins, C.A. and Pate, J.S. (1979). Uptake and utilization of xylem-borne amino compounds by shoot organs of a legume. *Plant Physiology* **63:** 1076–1081.

Mengel, K. and Kirkby, E.A. (2001). Principles of plant nutrition. Kluwer Academic Publishers – Dordrecht/ Boston/London

Meynhardt, J.T. (1964). A histological study of berry-splitting in some grape cultivars. *South African Journal of Agricultural Science* **7:** 707–716.

Miller, D.P., Howell, G.S. and Flore, J.A. (1997). Influence of shoot numbers and crop load on potted Chambourcin grapevines. II. Whole-vine vs. single-leaf photosynthesis. *Vitis* **36:** 109–114.

Moncur, M.W., Rattigan, K., MacKenzie, D.H. and Mcintyre, G.N. (1989). Base temperature for budbreak and leaf appearance of grapevines. *American Journal of Enology and Viticulture* **40:** 21–26.

Monteiro, F. and Bisson, L.F. (1991). Amino acid utilisation and urea formation during vinification fermentations. *American Journal of Enology and Viticulture* **42:** 199–208.

Monteith, J.L. (1965). Evaporation and environment. *Symposia of the Society for Experimental Biology* **19:** 205–234.

Morrell, A.M., Wample, R.L., Mink, G.I. and Ku, M.S.B. (1997). Heat shock protein expression in leaves of Cabernet sauvignon. *American Journal of Enology and Viticulture* **48:** 459–464.

Mullins, M.G., Bouquet, A. and Williams, L.E. (1992). Biology of the Grapevine. Cambridge Univ. Press, Cambridge. p. 239

Myttenaere, C., Daoust, C. and Roucoux, P. (1980). Leaching of technetium from foliage by simulated rain. *Environmental and Experimental Botany* **20:** 415–419.

Myttenaere, C., Vandecasteele, C.M., Roucoux, P., Lietart, E.A., Itschert, A. and Mousny, J. (1984). Processus biologiques responsables de l'accumulation du Tc-99 par les Végétaux. In: Desmet G., and Myttenaere C. (Eds), Technetium in the environment, Elsevier Applied Science Publishers, London: pp. 281–294.

Neel, J.W. and Onasch, M.A. (1989). Cytological effects of Tc on young soybean plants. *Health Physics* **57:** 289–298.

Orians, C.M., Smith, S.D.P. and Sack, L. (2005). How are leaves plumbed inside a branch? Differences in leaf-to-leaf hydraulic sectoriality among six temperate tree species. *Journal of Experimental Botany* **56:** 2267–2273.

Orians, C.M., van Vuuren, M.M.I., Harris, N.L., Babst, B.A. and Elmore, G.S. (2004). Differential sectoriality in long-distance transport in temperate tree species: evidence from dye flow, 15N transport, and vessel element pitting. *Trees* **18:** 501–509.

Pallas, B., Christophe, A., Cournède, P-H. and Lecoeur, J. (2009). Using a mathematical model to evaluate the trophic and non-trophic determinants of axis development in grapevines. *Functional Plant Biology* **36:** 156–170.

Pallas, B., Louarn, G., Christophe, A., Lebon, E. and Lecoeur, J. (2008). Influence of intra-shoot trophic competition on shoot development in two grapevine cultivars (*Vitis vinifera*). *Physiologia Plantarum* **134:** 49–63.

Palliotti, A., Cartechini, A., Nasini, L., Silvestroni, O., Mattioli, S. and Neri, D. (2004). Seasonal carbon balance of 'Sangiovese' grapevines in two different Central Italy environments. *Acta Horticulturae* **652:** 183–190.

Peñalosa, J. (1983). Shoot dynamics and adaptive morphology of Ipomoea phillomega Vell.) House Convolvulaceae), a tropical rainforest liana. *Annals of Botany* **52:** 737–754.

Petrie, P.R., Trought, M.C.T. and Howell, G.S. (2000). Growth and dry matter partitioning of Pinot Noir *Vitis vinifera* L.) in relation to leaf area and crop load. *Australian Journal of Grape and Wine Research* **6:** 40–45.

Petrie, P.R., Trought, M.C.T., Howell, G.S. and Buchan, G.D. (2003). The effect of leaf removal and canopy height on whole-vine gas exchange and fruit development of *Vitis vinifera* L. Sauvignon Blanc. *Functional Plant Biology* **30:** 711–717.

Pickard, W.F. and Hill, R.L. (1975). An application of gamma-scintigraphy to the observation of basipetal transport in moonflower. *Planta* **125:** 289–301.

Pickard, W.F., Minchin P.E.H. and Troughton, J.H. (1978). Real time studies of carbon-II translocation in moonflower. I. The effects of cold blocks. *Journal of Experimental Botany* **29:** 993–1001.

Poni, S. and Giachino, E. (2000). Growth, photosynthesis and cropping of potted grapevines *Vitis vinifera* L. cv. Cabernet Sauvignon) in relation to trimming. *Australian Journal of Grape and Wine Research* **6:** 216–226.

Postlethwait, S.N. and Rogers, B. (1958). Tracing the path of the transpiration stream in trees by the use of radioactive isotopes. *American Journal of Botany* **45:** 753–757.

Pradubsuk, S. and Davenport, J.R. (2010). Seasonal uptake and partitioning of macronutrients in mature 'Concord' grape. *Journal of American Society of Horticultural Science* **135:** 474–483.

Pratt, C. (1971). Reproductive anatomy in cultivated grapes – a review. *American Journal of Enology and Viticulture* **22:** 9–109.

Procter, J.T.A., Watson, R.L. and Lansberg, J.J. (1976). The carbon budget of a young apple tree. *Journal of the American Society for Horticultural Science* **101:** 579–582.

Radoglou, K. and Teskey, R.O. (1997). Changes in rates of photosynthesis and respiration during needle development of loblolly pine. *Tree Physiology* **17:** 485–488.

Rana, G., Katerji, N., Introna, M. and Hammami, A. (2004). Microclimate and plant water relationship of the 'overhead' table grape vineyard managed with three different covering techniques. *Scientia Horticulturae* **102:** 105–120.

Roberts, D. and R. Blazer. (1993). Clonal influence on Merlot vine and wine characteristics. American Journal of Enology and Viticulture **44**:339.

Rogiers, S.Y., Greer, D.H., Hatfield, J.M., Orchard, B.A. and Keller, M. (2006). Mineral sinks within ripening berries (*Vitis vinifera* L.). *Vitis* **45:** 115–123.

Rogiers, S.Y., Greer, D.H., Hutton, R.J. and Landsberg, J.J. (2009). Does night-time transpiration contribute to anisohydric behaviour in a *Vitis vinifera* cultivar? *Journal of Experimental Botany* **60:** 3751–3763.

Rogiers, S.Y., Keller, M., Holzapfel, B.P. and Virgona, J.M. (2000). Accumulation of potassium and calcium by ripening berries on field vines of *Vitis vinifera* (L) cv. Shiraz. *Australian Journal of Grape and Wine Research* **6:** 240–243.

Rogiers, S.Y., Smith, J.A., White, R., Keller, M., Holzapfel, B.P. and Virgona, J.M. (2001). Vascular function in berries of *Vitis vinifera* (L) cv. Shiraz. *Australian Journal of Grape and Wine Research* **7:** 47–51.

Sackville Hamilton, N.R. and Hay, M.J.M. (1998). Vascular architecture of a large-leafed genotype of Trifolium repens. *Annals of Botany* **81:** 441–448.

Sadras, V.O., Collins, M. and Soar, C.J. (2008). Modelling variety-dependent dynamics of soluble solids and water in berries of *Vitis vinifera*. *Australian Journal of Grape and Wine Research* **14:** 250–259.

Salleo, S., Rosso, R. and Lo Gullo, M.A. (1982). Hydraulic architecture of *Vitis vinifera* L. and Populus deltoides Bartr. 1-year old twigs: II - The nodal regions as 'constriction zones' of the xylem system. *Giornale Botanico Italiano* **116:** 29–40.

Sanchez, L.A. and Dokoozlian, N.K. (2005). Bud microclimate and fruitfulness in *Vitis vinifera* L. *American Journal of Enology and Viticulture* **56:** 319–329.

Sanchez-Alonso, F. and Lachia, M. (1987). Seasonal trends in the elemental content of sweet cherry leaves. *Communications in Soil Science Plant Analysis* **18**: 17–29.

Schaller, K., Löhnertz, O. and Geiben, R. (1990). N-Stoffwechsel von Reben. II Mitteilung: N- und Aminosäuredynamik in vegetativen und generativen Teilen der Müller-Thurgau-Rebe im Verlaufe einer Vegetationsperiode. *Vitic. Enol. Sci.* **45:** 160–166.

Schreiner, R.P., Scagel, C.F. and Baham, J. (2006). Nutrient uptake and distribution in a mature 'Pinot Noir' vineyard. *HortScience* **41:** 336–345.

Schultz, H. (1992). An empirical model for the simulation of leaf appearance and leaf area development of primary shoots of several grapevine *Vitis vinifera* L.) canopy-systems. *Scientia Horticulturae* **52:** 179–200.

Schultz, H.R., Keifer, W. and Gruppe, W. (1996). Photosynthetic duration, carboxylation efficiency and stomatal limitation of sun and shade leaves of different ages in field-grown grapevine *Vitis vinifera* L.). *Vitis* **35:** 169–176.

Seiwa, K. (1999). Changes in leaf phenology are dependent on tree height in Acer mono, a deciduous broad-leaves tree. *Annals of Botany* **83:** 355–361.

Seleznyova, A.N. and Greer, D.H. (2001). Effects of temperature and leaf position on leaf area expansion of kiwifruit Actinidia deliciosa) shoots: Development of a modelling framework. *Annals of Botany* **88:** 605–615.

Seleznyova, A.N., Thorp, T.G., Barnett, A.M. and Costes, E. (2002). Quantitative analysis of shoot development and branching patterns in Actinidia. *Annals of Botany* **89:** 471–482.

Sepúlveda, G.R. and Kliewer, W.M. (1983). Estimation of leaf area of two grapevine cultivars *Vitis vinifera* L.) using lamina linear measurements and fresh weight. *American Journal of Enology and Viticulture* **34:** 221–226.

Sepúlveda, G. and Kliewer, W.M. (1986*a*). Effect of high temperature on grapevines (*Vitis vinifera* L.). II Distribution of soluble sugars. *American Journal of Enology and Viticulture* **37:** 20–25.

Sepúlveda, G. and Kliewer, W.M. (1986*b*). Stomatal response of three grapevine cultivars (*Vitis vinifera* L.) to high temperature. *American Journal of Enology and Viticulture* **37:** 44–52.

Sepúlveda, G., Kliewer, W.M. and Ryugo, K. (1986). Effect of high temperature on grapevines (*Vitis vinifera* L.). I. Translocation of 14C-photosynthates. *American Journal of Enology and Viticulture* **37:** 13–19.

Sharkey, T.D. and Raschke, K. (1981). Separation and measurement of direct and indirect effects of light on stomata. *Plant Physiology* **68:** 33–40.

Sims, D.A., Gebauer, R.L.E. and Pearcy, R.W. (1994). Scaling sun and shade photosynthetic acclimation of Alocasia macrorrhiza to whole-plant performance- II. Simulation of carbon balance and growth at different photon flux densities. *Plant, Cell and Environment* **17:** 889–900.

Smart RE, Coombe BG 1983. Water relations of grapevines. In 'Water deficits and plant growth. Volume VII. Additional woody crop plants' Ed. TT Kozlowski) pp. 137–196. Academic Press: London)

Smith, J.P. (2004). Investigations into the mechanisms underlying grapevine rootstock effects on scion growth and yield. Thesis, Charles Sturt University, Wagga Wagga, p. 196.

Smith, J.P. and Holzapfel, B.P. (2009). Cumulative response of grapevine (*Vitis vinifera* L.) to late season perturbation of carbohydrate reserve status. *American Journal of Enology and Viticulture* **60:** 461–470.

Soar, C.J., Collins, M.J. and Sadras, V.O. (2009). Irrigated Shiraz vines (*Vitis vinifera*) upregulate gas exchange and maintain berry growth in response to short spells of high maximum temperature in the field. *Functional Plant Biology* **36:** 801–814.

Sommer, K.J. and Clingeleffer, P.R. (1996). Vine canopy development and carbohydrate partitioning as influenced by pruning. p. 123–127. In: C.S. Stockley, A.N. Sas, R.S. Johnstone, and T.H. Lee (eds.), Proceedings 9th AWTC, Winetitles, Adelaide.

Sommer, K.J., Islam, M.T. and Clingeleffer, P.R. (2000). Light and temperature effects on shoot fruitfulness in *Vitis vinifera* L. cv. Sultana: Influence of trellis type and grafting. *Australian Journal of Grape and Wine Research* **6:** 99–108.

Spann, T.M., Beede, R.H. and Dejong, T.M. (2007). Preformation in vegetative buds of pistachio Pistacia vera): relationship to shoot morphology, crown structure and rootstock vigor. *Tree Physiology* **27:** 1189–1196.

Stuart-Williams, H., Wong, S.C., Farquhar, G.D., Keitel, C. and Clayton, S. (2008). An innovative molybdenum column liner for oxygen and hydrogyen stable isotope analysis by pyrolysis. *Rapid Communications in Mass Spectrometry* **22:** 1117–1126.

Tagami, K. and Uchida, S. (2004). Comparison of transfer and distribution of technetium and rhenium in radish plants from nutrient solution. *Applied Radiation and Isotopes* **61:** 1203–1210.

Theiler, R. (1973). Anordnung der Leitbündel in einjährigen Trieben und ihren Organen, *Vitis vinifera* L. *Die Wein-Wissenschaft* **5:** 260–277.

Tilbrook, J. and Tyerman, S.D. (2008) Cell death in grape berries: varietal differences linked to xylem pressure and berry weight loss. *Functional Plant Biology* **35:** 173–184.

Tilbrook, J. and Tyerman, S.D. (2009). Hydraulic connection of grape berries to the vine: varietal differences in water conductance into and out of berries, and potential for backflow. *Functional Plant Biology* **36:** 541–550.

Treeby, M.T. and Wheatley, D.M. (2006). Effect of nitrogen fertiliser on nitrogen partitioning and pool sizes in irrigated Sultana grapevines. *Australian Journal of Experimental Agriculture* **46:** 1207–1215.

Tromp, J. (1983). Nutrient reserves in fruit trees, in particular carbohydrates and nitrogen. *Plant and Soil* **71:** 401–413

Tyerman, S.D., Bohnert, H.J., Maurel, C., Steudle, E. and Smith, J.A.C. (1999) Plant aquaporins: their molecular biology, biophysics and significance for plant water relations. *Journal of Experimental Botany* **50:** 1055–1071.

Tyerman, S.D., Tilbrook, J., Pardo, C., Kotula, L., Sullivan, W. and Steudle, E. (2004). Direct measurement of hydraulic properties in developing berries of *Vitis vinifera* L. cv Shiraz and Chardonnay. *Australian Journal of Grape and Wine Research* **10:** 170–181.

Uys, D.C. and Orffer, C.J. (1983). Changes in carbohydrates in nursery-grown grapevine rootstocks. *South African Journal of Enology and Viticulture* **4:** 13–19.

Van Zyl, J.L. (1984). Response of Colombar grapevines to irrigation as regards quality aspects and growth. South African Journal of Enology and Viticulture **5:** 19–28.

Wade, J.A., Holzapfel, B., DeGaris, K., Williams, D. and Keller, M. (2004). Nitrogen and water strategies for wine grape quality. *Acta Horticulturae* **640:** 61–67.

Walton, E.F. and Fowke, P.J. (1995). Estimation of the annual cost of kiwifruit vine growth and maintenance. *Annals of Botany* **76:** 617–623.

Wample, R.L., Schnabel, B. and Ahmedullah, M. (1987). Leaf area and conductance, internode length and root structure of five cultivars of *Vitis vinifera* treated with Paclobutrazol. *American Journal of Enology and Viticulture* **38:** 255–259.

Watson, M.A. and Casper, B.B. (1984). Morphogenetic constraints on patterns of carbon distribution in plants. *Annual Review of Ecology and Systematics* **15:** 233–258.

Webb, L., Watt, A., Hill, T., Whiting, J., Wigg, F., Dunn, G., Needs, S. and Barlow, S. (2010). Extreme heat: Managing grapevine response. University of Melbourne Report 54 pp.

Weyand, K.M. and Schultz, H.R. (2006). Light interception, gas exchange and carbon balance of different canopies of minimally and cane-pruned field-grown Riesling grapevines. *Vitis* **45:** 105–114.

Whiting, J.R. (2004). Grapevine Rootstocks. pp. 167–188. In: P.R. Dry, and B.G. Coombe (eds.), Viticulture. Volume 1. Resources. Winetitles, Adelaide.

Wibbe, M.L., Blanke, M.M. and Lenz, F. (1993). Effect of fruiting on carbon budgets of apple tree canopies. *Trees* **8:** 56–60.

Williams, L.E. and Smith, R.J. (1991). The effect of rootstock on the partitioning of dry weight, nitrogen and potassium, and root distribution of Cabernet Sauvignon grapevines. *American Journal of Enology and Viticulture* **42:** 118–122.

Windt, C.W., Gerkema, E. and Van As, H. (2009). Most water in the tomato truss is imported through the xylem, not the phloem: A nuclear magnetic resonance flow imaging study. *Plant Physiology* **151;** 830–842.

Wolf, T.K. and Pool, R.M. (1988). Effect of rootstocks and nitrogen fertilisation on the growth and yield of Chardonnay grapevines in New York. *American Journal of Enology and Viticulture* **39:** 29–32.

Wullschleger, S.D., Norby, R.J., Love, J.C. and Runck, C. (1997). Energetic costs of tissue construction in Yellow-poplar and White Oak trees exposed to long-term CO_2 enrichment. *Annals of Botany* **80:** 289–297.

Wullschleger, S.D. and Oosterhuis, D.M. (1990). Photosynthesis of individual field-grown cotton leaves during ontogeny. *Photosynthesis Research* **23:** 163–170.

Yamamura, H. and Naito, R. (1985). Susceptibility to berry splitting in several grape cultivars. *Journal of the Japanese Society for Horticultural Science* **53:** 390–395.

Yanagisawa, K. and Muramatsu, Y. (1995). Transfer of technetium from soil to paddy and upland rice. *Journal of Radiation Research* **36:** 171–178.

Yang, Y.-S. and Hori, Y. (1979). Studies on retranslocation of accumulated assimilates in "Delaware" grapevines. I. Retranslocation of C-assimilates in the following spring after ^{14}C feeding in summer and autumn. *Tohoku Journal Agricricultural Research* **30:** 43–56.

Zapata, C., Deléens, E., Chaillou, S. and Magné, C. (2004). Mobilisation and distribution of starch and total N in two grapevine cultivars differing in their sensitivity to shedding. *Functional Plant Biology* **31:** 1127–1135.

Zapata, C., Deléens, E., Chaillou, S. and Magné, C. (2004). Partitioning and mobilisation of starch and N reserves in grapevine (*Vitis vinifera* L.). *Journal of Plant Physiology* **161:** 1031–1040.

Zwieniecki, M.A., Melcher, P.J. and Holbrook, N.M. (2001). Hydraulic properties of individual xylem vessels of *Fraxinus americana*. *Journal of Experimental Botany* **52:** 257–264.

Appendix4
Staff

Investigators

Dr Suzy Rogiers

Dr Simon Clarke

Dr Bruno Holzapfel

Dr Jason Smith

Dr Dennis Greer

Mr Stewart Field (PhD candidate)

Ms Jaqui Watt

Dr Marc Thomas

Professor Jim Hardie

Technical Support

Ms Edwina Blackney

Mr Ned Sharkey

Ms Kirstina Lamont

Mr Peter Carey

Mr Sebastian Holzapfel

Mr Rob Lamont

Ms Sylvie Sicard

Mr Chris Weston

Mr Mark Weedon

Mrs Helen Pan

Ms Laura Chisdall

Ms Kylie Singh

Mr Markus Müller (PhD candidate)

Mr Col Lamont

Mr Michel Meunier

Mr Campbell Meeks

Ms Helen Pan

Mr Andrew Drumm (CSU winemaker).

Collaborators

Dr Geoff Currie (Senior Lecturer, Charles Sturt University, Macquarie University)

Dr David Wheeler (University of Wollongong)

Dr Hilary Stuart-Williams (The Australian National University)

Dr Linda Barry (Australian Nuclear Science and Technology Organisation)

Students

Mr Thomas Decker (Charles Sturt University)

Ms Samantha Stevenson (Charles Sturt University)

Administrative support

Ms Barbara Dyer

Appendix 5
Other relevant material

Not applicable

Appendix 6
Budget reconciliation

See *Winegrowing Futures Final Report, Theme 1*